EVALUATION OF SELF-CONSOLIDATING CONCRETE FOR USE IN PRESTRESSED GIRDER APPLICATIONS

Except where reference is made to the work of others, the work described in this thesis is my own or was done in collaboration with my advisory committee. This thesis does not include proprietary or classified information.

____

James Benson Roberts

Certificate of Approval:

G. Ed Ramey Professor Civil Engineering	Anton K. Schindler, Chair Gottlieb Assistant Professor Civil Engineering
Robert W. Barnes Associate Professor Civil Engineering	Stephen L. McFarland Dean Graduate School

EVALUATION OF SELF-CONSOLIDATING CONCRETE FOR USE IN PRESTRESSED GIRDER APPLICATIONS

James Benson Roberts

A Thesis

Submitted to

the Graduate Faculty of

Auburn University

in Partial Fulfillment of the

Requirements for the

Degree of

Master of Science

Auburn, Alabama
December 16, 2005

EVALUATION OF SELF-CONSOLIDATING CONCRETE FOR USE IN

PRESTRESSED GIRDER APPLICATIONS

James Benson Roberts

____
Signature of Author

____
Date

VITA

James Benson Roberts, son of Bennie Franklin and Anna (Bowman) Roberts, was born April 24, 1981, in Macon, Georgia. He graduated from First Presbyterian Day School (FPD) as an honor graduate in 1999. He enrolled at Auburn University in the fall of 1999 and graduated cum laude with a B.C.E. in December, 2003. He entered Graduate School at Auburn University in January of 2004 where he worked as a Research Assistant until December of 2005.

THESIS ABSTRACT

EVALUATION OF SELF-CONSOLIDATING CONCRETE FOR USE IN PRESTRESSED GIRDER APPLICATIONS

James Benson Roberts

Master of Science, December 16, 2005
(B.C.E., Auburn University, 2003)

290 Typed Pages

Directed by Anton K. Schindler

Self-consolidating concrete (SCC) is a highly flowable, yet cohesive, concrete that is able to fill formwork and completely encapsulate any reinforcement without the need for external vibration. The use of SCC may help prestress plants to produce high-quality prestressed concrete elements at reduced labor costs. An evaluation of SCC mixtures for use in prestressed concrete applications is presented in this thesis. Twenty-one SCC mixtures were made with varying water-to-powder ratios of 0.28, 0.32, 0.36, and 0.40, varying sand-to-aggregate ratios of 0.38, 0.42, and 0.46, and different powder combinations that included Type III cement, Class C fly ash, ground granular blast-furnace (GGBF) slag, and silica fume. The inverted slump flow, VSI, T-50, J-Ring, and L-Box were used to evaluate the fresh properties of the twenty-one SCC mixtures.

Cylinders were match-cured to a time-temperature profile that is typical of prestressing operations. SCC mixture properties were compared to those of two conventional-slump prestressed concrete mixtures. The SCC mixtures achieved 18-hour (prestress transfer) compressive strengths between 5,470 and 9,530 psi. Compressive strengths at prestress transfer and at later ages were not sensitive to changes in the sand-to-aggregate ratio. All SCC mixtures had lower 18-hour moduli of elasticity than the control mixture with a water-to-powder ratio of 0.37. The moduli of elasticity at prestress transfer and at later ages were not significantly affected by changes in the sand-to-aggregate ratio. The moduli of elasticity of the SCC mixtures are in reasonable agreement with the elastic stiffness assumed during the design of conventional-slump concrete structures. The AASHTO LRFD formulation generally underestimates the modulus of elasticity of the SCC mixtures. The ACI 363 formulation also underestimates the modulus of elasticity for SCC mixtures but on a higher order of magnitude than the AASHTO LRFD formulation. The 112-day drying shrinkage strain for all the SCC mixtures are of the same order of magnitude or less than those measured for the control mixtures. A change in sand-to-aggregate ratio from 0.38 to 0.46 had no significant effect on the 112-day drying shrinkage strain of the SCC mixtures. At later ages of 56 and 112 days, the AASHTO LRFD procedure overestimated the measured drying shrinkage of the SCC mixtures, while the ACI 209 procedure corresponded reasonably well with the measured drying shrinkage of the SCC mixtures. The use of SCC in prestressed applications appears favorable and full-scale evaluations of the mixtures developed in this study should be undertaken.

ACKNOWLEDGMENTS

I would like to thank my advisor Dr. Anton Schindler. Your guidance, advice, and time have been greatly appreciated and will not be forgotten. I would also like to thank Dr. Robert Barnes for his assistance and valuable input on this project. Much appreciation goes out to the following graduate and undergraduate students who helped with this project: Kelly Levy, Forest Walker, Jason Stough, Jason Meadows, Shane Swords, Robbie Strong, Seth Green and Zack Thomas. The assistance of Mr. Billy Wilson, the concrete laboratory technician, is also appreciated. Without your help none of this would have been possible.

Funding for this study was provided by the Alabama Department of Transportation (ALDOT). The funding, cooperation, and assistance of ALDOT are gratefully acknowledged, particularly the guidance provided by Fred Conway and Larry Lockett. The assistance of Dwain Hamby, Paul Gustafson, and Rickey Swancey is gratefully acknowledged.

I would like to thank my mother and father. Your guidance and lessons that you have taught me over the years have made me who I am today. Thank you for instilling in me a hard work ethic. I would also like to thank you for your support and encouragement throughout this time, as well as the financial support you have given me over the last 24 years. Hang in there; it is almost over, except for Clayton.

Finally, I would like to thank God for giving me this opportunity. Without You, nothing is possible.

Style manual or journal used Chicago Manual of Style

Computer software used Microsoft® Word, Microsoft® Excel

TABLE OF CONTENTS

LIST OF TABLES xv

LIST OF FIGURES xvii

CHAPTER 1: INTRODUCTION 1

1.1 BACKGROUND 1

1.2 PROJECT OBJECTIVES 2

1.3 RESEARCH APPROACH 3

1.4 REPORT OUTLINE 5

CHAPTER 2: SELF-CONSOLIDATING CONCRETE 6

2.1 INTRODUCTION 6

2.2 SCC TESTING PROCEDURES 8

2.2.1 Slump Flow Test 9

2.2.2 L- Box Test 17

2.2.3 J-Ring Test 19

2.3 MATERIALS AND MIXTURE DESIGN OF SCC 21

2.3.1 Available Methods for Designing SCC Mixtures 24

2.3.2 Powder Properties 27

2.3.3 Fine and Coarse Aggregate Characteristics 33

2.3.4 Chemical Admixtures 37

2.4 FRESH CONCRETE PROPERTIES 40
2.4.1RHEOLOGY. 40
2.4.2 WORKABILITY 42
2.5 HARDENED CONCRETE PROPERTIES 50
2.5.1 MICROSTRUCTURE 51
2.5.2 COMPRESSIVE STRENGTH 52
2.5.3 MODULUS OF ELASTICITY 54
2.5.4 DRYING SHRINKAGE 56
2.5.5 CREEP 59
2.6 PRODUCTION, QUALITY CONTROL, AND QUALITY ASSURANCE 60
2.6.1 PRODUCTION 60
2.6.2 QUALITY CONTROL AND QUALITY ASSURANCE 70
2.7 MODULUS OF ELASTICITY AND DRYING
SHRINKAGE PREDICTIONS 76
2.7.1 PREDICTION OF MODULUS OF ELASTICITY 76
2.7.2 PREDICTION OF SHRINKAGE 77
2.8 SUMMARY 85
CHAPTER 3: EXPERIMENTAL TESTING PROGRAM AND MATERIALS 87
3.1 INTRODUCTION 87
3.2 EXPERIMENTAL TESTING PROGRAM 88
3.2.1 REQUIREMENTS FOR SCC MIXTURES 89
3.2.2 EXPERIMENTAL TEST FACTORIAL 90
3.2.3 TESTING PROGRAM 95

3.3 EXPERIMENTAL PROCEDURES 95
3.3.1 BATCHING 95
3.3.2 MIXING PROCEDURE 97
3.3.3 FRESH CONCRETE TEST PROCEDURES 99
3.3.4 SPECIMEN PREPARATION AND CURING 104
3.3.5 HARDENED CONCRETE TEST PROCEDURES 110
3.4 MATERIALS 113
3.4.1 POWDERS 113
3.4.2 CHEMICAL ADMIXTURES 116
3.4.3 COARSE AGGREGATE 118
3.4.4 FINE AGGREGATE 119
CHAPTER 4 PRESENTATION AND ANALYSIS OF RESULTS 121
4.1 FRESH PROPERTIES 121
4.1.1 SLUMP FLOW 123
4.1.2 T-50 126
4.1.3 VISUAL STABILITY INDEX (VSI) 128
4.1.4 AIR CONTENT 128
4.1.5 J-RING 131
4.1.6 L-BOX 132
4.1.7 UNIT WEIGHT 133
4.2 MECHANICAL PROPERTIES 133
4.2.1 COMPRESSIVE STRENGTH 138
4.2.2 MODULUS OF ELASTICITY 154

4.2.3 DRYING SHRINKAGE 171

4.3 SUMMARY OF RESULTS 186

4.3.1 SUMMARY OF FRESH PROPERTIES 186

4.3.2 SUMMARY OF MECHANICAL PROPERTIES 187

CHAPTER 5: CONCLUSIONS AND RECOMMENDATIONS 189

5.1 SUMMARY OF LABORATORY WORK 189

5.2 CONCLUSIONS 190

5.2.1 SCC'S FRESH PROPERTIES 190

5.2.2 SCC'S HARDENED PROPERTIES 191

5.2.3 PRODUCTION, QUALITY ASSURANCE, AND QUALITY CONTROL OF SCC 192

5.3 RECOMMENDATIONS FOR FUTURE RESEARCH 193

5.4 RECOMMENDATIONS FOR IMPLEMENTATION 194

REFERNECES 195

APPENDICES 208

APPENDIX A: TEST PROCEDURES FOR FRESH PROPERTIES 209

A.1 SLUMP FLOW TEST 209

A.1.1 APPARATUS 209

A.1.2 PROCEDURE 209

A.2 L-BOX TEST 210

A.2.1 APPARATUS 210

A.2.2 PROCEDURE 210

A.3 J-RING TEST 211

A.3.1 APPARATUS 211

A.3.2 PROCEDURE 211

APPENDIX B: SUMMARY OF COMPRESSIVE STRENGTH RESULTS 213

B.1 MATCH-CURED CYLINDERS 213

B.2 MOIST-CURED CYLINDERS 213

APPENDIX C: SUMMARY OF MODULUS OF ELASTICITY RESULTS 223

C.1 MATCH-CURED CYLINDERS 223

C.2 MOIST-CURED CYLINDERS 223

APPENDIX D: SUMMARY OF DRYING SHRINKAGE STRAIN RESULTS 242

D.1 7-DAY MOIST-CURED PRISMS 242

D.2 28-DAY MOIST-CURED PRISMS 242

LIST OF TABLES

Table 2-1 Overview of Test Methods Used for This Research 8

Table 2-2 Visual Stability Index (VSI) Rating 13

Table 2-3 Passing Ability Rating 21

Table 2-4 Typical Chemical Composition of Fly Ash 29

Table 2-5 Typical Chemical Composition of Silica Fume 30

Table 2-6 Typical Chemical Composition of GGBF Slag 31

Table 2-7 Recommended Additions of SCMs 32

Table 2-8 Grading Limits for Coarse Aggregates 35

Table 2-9 Grading Limits of Fine Aggregate 36

Table 2-10 Grading Limits of Coarse Aggregates Used in Alabama 36

Table 2-11 Total Air Content in Percent by Volume 40

Table 2-12 Placement Techniques and Discharge Characteristics 66

Table 2-13 Slump Flow Parameter Determination 72

Table 2-14 T-50 Parameter Determination 73

Table 2-15 L-Box Blocking Ratio (%) Parameter Determination 74

Table 2-16 J-Ring Value (mm) Determination 75

Table 3-1 Experimental Mixture Plan and Mixture Specifications 92

Table 3-2 Mixture Proportions 94

Table 3-3 Chemical Composition of all Powders ... 115

Table 3-4 Gradation of No. 78 Crushed Limestone ... 119

Table 3-5 Gradation of Fine Aggregate ... 119

Table 4-1 Summary of SCC and Conventional-Slump Concrete Fresh Properties and Admixture Dosages ... 121

Table 4-2 Fresh Properties of Small-Scale Prestressed Elements ... 122

Table 4-3 Compressive Strengths and Modulus of Elasticity Results ... 134

Table 4-4 Compressive Strengths and Modulus of Elasticity Results for Small-Scale Prestressed Elements ... 135

Table 4-5 Drying Shrinkage Strain (7-Day Moist Curing) ... 136

Table 4-6 Drying Shrinkage Strain (28-Day Moist Curing) ... 137

Table B-1 Complete Summary of Compressive Strength Results ... 214

Table C-1 Complete Summary of Modulus of Elasticity Results ... 225

Table D-1 Summary of Drying Shrinkage for all Mixtures {7}. Results Not Available for Ternary SCC Mixtures ... 244

Table D-2 Summary of Drying Shrinkage for all Mixtures {28}. Results Not Available for Ternary SCC Mixtures ... 245

LIST OF FIGURES

Figure 2-1 Inverted Slump Cone 11

Figure 2-.2 Upright Slump Cone..11

Figure 2-.3 Typical Visual Stability Index Rating of 0 14

Figure 2-4 Typical Visual Stability Index Rating of 0.5 14

Figure 2-5 Typical Visual Stability Index Rating of 1.0 15

Figure 2-6 Typical Visual Stability Index Rating of 1.0 15

Figure 2-7 Typical Visual Stability Index Rating of 1.5 16

Figure 2-8 Typical Visual Stability Index Rating of 2.0 16

Figure 2-9 Typical Visual Stability Index Rating of 2.0 17

Figure 2-10 Typical Visual Stability Index Rating of 3.0 17

Figure 2-11 Diagram of L-Box Test Apparatus 19

Figure 2-12 Typical J-Ring Apparatus 20

Figure 2-.13 General Approach to Proportioning SCC 22

Figure 2-14 Effect of Added Water on the Viscosity of SCC 26

Figure 2-15 Strength Development of Cement and SCM Blends 33

Figure 2-16 Bingham Fluid Model...42

Figure 2-17 Mechanism of Blocking...48

Figure 2-18 Basic Workability Requirements and Typical Actions Taken to Achieve These Requirements 50

Figure 2-19 Strength Versus Cement-to-Water Ratio 53

Figure 2-20 Elastic Modulus Versus Sand-to-Aggregate Ratio 56

Figure 2-21 Influence of *w/c* and Aggregate Content on Shrinkage................................57

Figure 2-22 Effects of Different Types of Aggregates on Creep.....................................60

Figure 2-23 SCC Being Pumped into Formwork by Means of a Bifurcating Pipe Hose 64

Figure 2-24 Single Pump Operator Casting a Bridge Pier Foundation............................65

Figure 2-25 Average Annual Relative Humidity in Percent for the United States and Canada...83

Figure 3-1 Overview of Experimental Work Performed With SCC 88

Figure 3-2 12-ft^3 Concrete Mixer Used for this Project 97

Figure 3-3 Testing Equipment for Slump Flow Test 100

Figure 3-4 J-Ring Used for this Research 102

Figure 3-5 Dimensions of the L-Box Used for this Project...103

Figure 3-6 L-Box Used for this Project 103

Figure 3-7 Match-Curing Mold 106

Figure 3-8 Shrinkage Prism Mold 107

Figure 3-9 Target Time-Temperature Profile Versus Measured Time-Temperature Profile 109

Figure 3-10 Forney Compression Machine 111

Figure 3-11 Compressometers Used to Determine the Modulus of Elasticity 112

Figure 3-12 Length Comparator 113

Figure 4-1 Summary of HRWR Admixture Dosages for the SCC Mixtures 124

Figure 4-2 Summary of T-50 Times 126
Figure 4-3 Summary of Required Air-Entraining Admixture Dosage for all SCC Mixtures 129
Figure 4-4 Effect of *s/agg* on the 18-hr Compressive Strength for Fly Ash Mixtures 139
Figure 4-5 Effect of *s/agg* on the 18-hr Compressive Strength for Slag Mixtures 139
Figure 4-6 Effect of *s/agg* on the 18-hr Compressive Strength for Ternary Mixtures 140
Figure 4-7 Effect of *s/agg* on the 56-day Compressive Strength for Fly Ash Mixtures.. 140
Figure 4-8 Effect of *s/agg* on the 56-day Compressive Strength for Slag Mixtures 141
Figure 4-9 Effect of *s/agg* on the 56-day Compressive Strength for Ternary Mixtures 141
Figure 4-10 Effect of *w/p* on the 18-hr Compressive Strength for Fly Ash Mixtures .. 143
Figure 4-11 Effect of *w/p* on the 18-hr Compressive Strength for Slag Mixtures 143
Figure 4-12 Effect of *w/p* on the 18-hr Compressive Strength for Ternary Mixtures .. 144
Figure 4-13 Effect of *w/p* on the 56-day Compressive Strength for Fly Ash Mixtures 144
Figure 4-14 Effect of *w/p* on the 56-day Compressive Strength for Slag Mixtures 145
Figure 4-15 Effect of *w/p* on the 56-day Compressive Strength for Ternary Mixtures 145

Figure 4-16 Effect of Different Powder Combinations on the 18-hr Compressive Strengths 148
Figure 4-17 Effect of Different Powder Combinations on the 56-day Compressive Strengths 149
Figure 4-18 18-hr to 28-day Strength Gain (%) for Match-Cured Cylinders 151
Figure 4-19 3-day to 56-day Strength Gain (%) for Moist-Cured Cylinders 152
Figure 4-20 Effect of *s/agg* on the 18-hr Modulus of Elasticity for Fly Ash Mixtures 154
Figure 4-21 Effect of *s/agg* on the 18-hr Modulus of Elasticity for Slag Mixtures 154
Figure 4-22 Effect of *s/agg* on the 18-hr Modulus of Elasticity for Ternary Mixtures 155
Figure 4-23 Effect of *s/agg* on the 56-day Modulus of Elasticity for Fly Ash Mixtures 155
Figure 4-24 Effect of *s/agg* on the 56-day Modulus of Elasticity for Slag Mixtures 156
Figure 4-25 Effect of *s/agg* on the 56-day Modulus of Elasticity for Ternary Mixtures 156
Figure 4-26 Effect of *w/p* on the 18-hr Modulus of Elasticity for Fly Ash Mixtures 158
Figure 4-27 Effect of *w/p* on the 18-hr Modulus of Elasticity for Slag Mixtures 159
Figure 4-28 Effect of *w/p* on the 18-hr Modulus of Elasticity for Ternary Mixtures 159
Figure 4-29 Effect of *w/p* on the 56-day Modulus of Elasticity for Fly Ash Mixtures 160
Figure 4-30 Effect of *w/p* on the 56-day Modulus of Elasticity for Slag Mixtures 160

Figure 4-31 Effect of *w/p* on the 56-day Modulus of Elasticity for Ternary Mixtures 161
Figure 4-32 Effect of Different Powder Combinations on the 18-hr Modulus of Elasticity 163
Figure 4-33 Effect of Different Powder Combinations on the 56-day Modulus of Elasticity 164
Figure 4-34 AASHTO LRFD Estimate of the Modulus of Elasticity 167
Figure 4-35 ACI 363 Estimate of the Modulus of Elasticity 168
Figure 4-36 Effect of *s/agg* on the *32*-week Drying Shrinkge for Fly Ash Mixtures 170
Figure 4-37 Effect of *s/agg* on the *32*-week Drying Shrinkge for Slag Mixtures 171
Figure 4-38 Effect of *s/agg* on the *16*-week Drying Shrinkge for Ternary Mixtures 171
Figure 4-39 Effect of *w/p* on the *32*-week Drying Shrinkge for Fly Ash Mixtures 173
Figure 4-40 Effect of *w/p* on the *32*-week Drying Shrinkge for Slag Mixtures 173
Figure 4-41 Effect of *w/p* on the *16*-week Drying Shrinkge for Ternary Mixtures 174
Figure 4-42 Effects of Different Powder Combinations on the *16*-week Drying Shrinkage 177
Figure 4-43 Measured Versus Estimated Drying Shrinkage Strain Using the ACI 209 Procedure 181
Figure 4-44 Measure Versus Estimated Drying Shrinkage Strain Using the AASHTO LRFD Procedure 182
Figure 4-45 Measured Versus Estimated Drying Shrinkage Strain Using the NCHRP 496 Procedure 183

Figure B-1 Effect of *s/agg* on 28-day Compressive Strength for Fly Ash Mixtures {4x8} 215
Figure B-2 Effect of *s/agg* on 28-day Compressive Strength for Slag Mixtures {4x8} 215
Figure B-3 Effect of *s/agg* on 28-day Compressive Strength for Ternary Mixtures {4x8} 216
Figure B-4 Effect of *s/agg* on 28-day Compressive Strength for Fly Ash Mixtures {6x12} 216
Figure B-5 Effect of *s/agg* on 28-day Compressive Strength for Slag Mixtures {6x12} 217
Figure B-6 Effect of *s/agg* on 28-day Compressive Strength for Ternary Mixtures {6x12} 217
Figure B-7 Effect of *w/p* on 28-day Compressive Strength for Fly Ash Mixtures {4x8} 218
Figure B-8 Effect of *w/p* on 28-day Compressive Strength for Slag Mixtures {4x8} 218
Figure B-9 Effect of *w/p* on 28-day Compressive Strength for Ternary Mixtures {4x8} 219
Figure B-10 Effect of *w/p* on 28-day Compressive Strength for Fly Ash Mixtures {6x12} 219
Figure B-11 Effect of *w/p* on 28-day Compressive Strength for Slag Mixtures {6x12} 220

Figure B-12 Effect of *w/p* on 28-day Compressive Strength for Ternary Mixtures {6x12} 220
Figure B-13 Effect of Different Powder Combinations on the 28-day Compressive Strength {4x8} 221

Figure B-14 Effect of Different Powder Combinations on the 28-day Compressive Strength {6x12} 222
Figure C-1 Effect of *s/agg* on the 28-day Modulus of Elasticity for Fly Ash Mixtures {4x8} 226
Figure C-2 Effect of *s/agg* on the 28-day Modulus of Elasticity for Slag Mixtures {4x8} 226
Figure C-3 Effect of *s/agg* on the 28-day Modulus of Elasticity for Ternary Mixtures {4x8} 227
Figure C-4 Effect of *s/agg* on the 28-day Modulus of Elasticity for Fly Ash Mixtures {6x12} 227
Figure C-5 Effect of *s/agg* on the 28-day Modulus of Elasticity for Slag Mixtures {6x12} 228
Figure C-6 Effect of *s/agg* on the 28-day Modulus of Elasticity for Ternary Mixtures {6x12} 228
Figure C-7 Effect of *w/p* on the 28-day Modulus of Elasticity for Fly Ash Mixtures {4x8} 229
Figure C-8 Effect of *w/p* on the 28-day Modulus of Elasticity for Slag Mixtures {4x8} 229

Figure C-9 Effect of *w/p* on the 28-day Modulus of Elasticity for Ternary Mixtures {4x8} 230
Figure C-10 Effect of *w/p* on the 28-day Modulus of Elasticity for Fly Ash Mixtures {6x12} 230
Figure C-11 Effect of *w/p* on the 28-day Modulus of Elasticity for Slag Mixtures {6x12} 231
Figure C-12 Effect of *w/p* on the 28-day Modulus of Elasticity for Ternary Mixtures {6x12} 231
Figure C-13 Effect of Different Powder Combinations on the 28-day Modulus of Elasticity {4x8} 232
Figure C-14 Effect of Different Powder Combinations on the 28-day Modulus of Elasticity {6x12} 233
Figure C-15 AASHTO LRFD Prediction of the 18-hour Modulus of Elasticity {4x8} 234
Figure C-16 AASHTO LRFD Prediction of the 21-hour Modulus of Elasticity {4x8} 234
Figure C-17 AASHTO LRFD Prediction of the 3-day Modulus of Elasticity {6x12} 235
Figure C-18 AASHTO LRFD Prediction of the 7-day Modulus of Elasticity {4x8} 235
Figure C-19 AASHTO LRFD Prediction of the 7-day Modulus of Elasticity {6x12} ..236
Figure C-20 AASHTO LRFD Prediction of the 28-day Modulus of Elasticity {4x8} ..236
Figure C-21 AASHTO LRFD Prediction of the 28-day Modulus of Elasticity {6x12} 237

Figure C-22 AASHTO LRFD Prediction of the 56-day Modulus of Elasticity {6x12} 237
Figure C-23 ACI 363 Prediction of the 18-hour Modulus of Elasticity {4x8} 238
Figure C-24 ACI 363 Prediction of the 21-hour Modulus of Elasticity {4x8} 238
Figure C-25 ACI 363 Prediction of the 3-day Modulus of Elasticity {6x12} 239
Figure C-26 ACI 363 Prediction of the 7-day Modulus of Elasticity {4x8} 239
Figure C-27 ACI 363 Prediction of the 7-day Modulus of Elasticity {6x12} 240
Figure C-28 ACI 363 Prediction of the 28-day Modulus of Elasticity {4x8} 240
Figure C-29 ACI 363 Prediction of the 28-day Modulus of Elasticity {6x12} 241
Figure C-30 ACI 363 Prediction of the 56-day Modulus of Elasticity {6x12} 241
Figure D-1 Effect of *s/agg* on *32*-week drying shrinkage for Fly Ash Mixtures {28} 246
Figure D-2 Effect of *s/agg* on *32*-week drying shrinkage for Slag Mixtures {28} 246
Figure D-3 Effect of *s/agg* on *16*-week drying shrinkage for Ternary Mixtures {28} 247
Figure D-4 Effect of *w/p* on *32*-week Drying Shrinkage for Fly Ash Mixtures {28} 247
Figure D-5 Effect of *w/p* on *32*-week Drying Shrinkage for Slag Mixtures {28} 248
Figure D-6 Effect of *w/p* on *16*-week Drying Shrinkage for Ternary Mixtures {28} 248
Figure D-7 Effects of Different Powder Combinations on *16*-week Drying Shrinkage {28} 249

Figure D-8 Measured Versus Estimated Drying Shrinkage Strain Using the ACI 209 Procedure 250
Figure D-9 Measured Versus Estimated Drying Shrinkage Strain Using the AASHTO LRFD Procedure 251
Figure D-10 Measured Versus Estimated Drying Shrinkage Strain Using the NCHRP 496 Procedure 252
Figure D-11 Shrinkage Development of Fly Ash Mixtures with a *w/p* of 0.28 253
Figure D-12 Shrinkage Development of Fly Ash Mixtures with a *w/p* of 0.32 253
Figure D-13 Shrinkage Development of Fly Ash Mixtures with a *w/p* of 0.36 254
Figure D-14 Shrinkage Development of Slag Mixtures with a *w/p* of 0.28 254
Figure D-15 Shrinkage Development of Slag Mixtures with a *w/p* of 0.32 255
Figure D-16 Shrinkage Development of Slag Mixtures with a *w/p* of 0.36 255
Figure D-17 Shrinkage Development of Ternary Mixtures with a *w/p* of 0.32 256
Figure D-18 Shrinkage Development of Ternary Mixtures with a *w/p* of 0.36 256
Figure D-19 Shrinkage Development of Ternary Mixtures with a *w/p* of 0.40 257
Figure D-20 Shrinkage Development of Fly Ash Mixtures with a *w/p* of 0.28 257
Figure D-21 Shrinkage Development of Fly Ash Mixtures with a *w/p* of 0.32 258
Figure D-22 Shrinkage Development of Fly Ash Mixtures with a *w/p* of 0.36 258
Figure D-23 Shrinkage Development of Slag Mixtures with a *w/p* of 0.28 259
Figure D-24 Shrinkage Development of Slag Mixtures with a *w/p* of 0.32 259
Figure D-25 Shrinkage Development of Slag Mixtures with a *w/p* of 0.36 260
Figure D-26 Shrinkage Development of Ternary Mixtures with a *w/p* of 0.32 260
Figure D-27 Shrinkage Development of Ternary Mixtures with a *w/p* of 0.36 261

Figure D-28 Shrinkage Development of Ternary Mixtures with a *w/p* of 0.40 261
Figure D-29 Shrinkage Development of Fly Ash Mixtures Versus AASHTO Prediction 262
Figure D-30 Shrinkage Development of Slag Mixtures Versus AASHTO Prediction 262
Figure D-31 Shrinkage Development of Ternary Mixtures Versus AASHTO Prediction 263
Figure D-32 Shrinkage Development of Fly Ash Mixtures Versus AASHTO Prediction 263
Figure D-33 Shrinkage Development of Slag Mixtures Versus AASHTO Prediction 264
Figure D-34 Shrinkage Development of Ternary Mixtures Versus AASHTO Prediction 264

CHAPTER 1

INTRODUCTION

1.1 BACKGROUND

Self-consolidating concrete (SCC) is a highly fluid concrete that is able to deform under its own weight and completely encapsulate any reinforcement in the absence of vibration without exhibiting defects due to segregation or bleeding (Khayat 1999). To date, the use of SCC, specifically prestressed applications, has been limited in the United States because of uncertainties about its long-term performance, especially creep and shrinkage properties.

SCC differs significantly from conventional-slump concrete that is traditionally used for prestressed applications. SCC has a higher fine aggregate content (thus increasing the sand-to-aggregate ratio) and a smaller coarse aggregate size. SCC requires a higher content of high range water reducing (HRWR) admixture than does conventional-slump concrete. SCC also incorporates a higher volume of powder(s) than conventional-slump concrete in order to provide the concrete with the cohesiveness necessary for successful casting (Ghezal, Khayat, and Beaupre 2003; Khayat, Hu, and Monty 1999).

SCC offers many benefits over conventional-slump concrete including better productivity, improved working environment, and better aesthetics (Persson 2001; Skarendahl 2000b). SCC also has the potential to significantly reduce the overall cost because of a reduction in the labor required to place the concrete (Ozyildirim and Lane

2003; Fang, Jianxiong, and Changhui 1999). While the use of SCC can be very beneficial, there are concerns that must be answered prior to widescale implementation in the concrete industry.

At this time, there are no standard specifications available to concrete producers for SCC. The Precast/Prestressed Concrete Institute (PCI) has published a set of "interim guidelines" for the use of SCC (PCI 2003). The National Cooperative Highway Research Program (NCHRP) started a research project in the summer of 2004 to develop guidelines for the use of self-consolidating concrete in precast, prestressed concrete bridge elements; it will be completed in the summer of 2007 (NCHRP 2005). Some state DOT's have formulated their own guidelines as well.

The Alabama Department of Transportation (ALDOT) is interested in the possibilities of using SCC for prestressed girder applications. While literature has shown that SCC exhibits sufficient hardened properties such as compressive strengths, modulus of elasticity, freeze-thaw characteristics, and low permeability, the use of SCC has been restricted mainly because of a lack of standardized test procedures and performance data, as well as uncertainty regarding the applicability of current design procedures to elements made with SCC.

1.2 PROJECT OBJECTIVES

Limited research has been done to date to evaluate the long-term performance of SCC and the effect of the use of SCC in prestressed girders. The research described in this thesis was performed to address the following primary objectives:

- Develop and evaluate SCC mixtures for use in prestressed applications

- Compare and analyze the performance of the SCC mixtures to conventional-slump concrete mixtures used in prestress applications
- Evaluate the effect of SCC on the strength and modulus of elasticity at prestress transfer and long-term ages
- Evaluate the long-term shrinkage behavior of various SCC mixtures
- Develop recommendations for ALDOT for possible implementation of SCC for prestressed concrete girder applications

The study addressed the following secondary objectives:

- Evaluate the effects of sand-to-aggregate ratio (*s/agg*), water-to-powder ratio (*w/p*), and different powder combinations on the fresh and hardened properties of the SCC mixtures
- Evaluate the correlation between the modulus of elasticity and compressive strength compared to the predictive equations of the *AASHTO LRFD Bridge Design Specifications* (2004) and ACI 318 (2005), as well as ACI 363 (1997)
- Compare the drying shrinkage of the SCC mixtures to values estimated by applying the predictive models of the *AASHTO LRFD Bridge Design Specifications* (2004), ACI 209 (1997), and the National Cooperative Highway Research Program (NCHRP) Report 496 (Tadros et al. 2003).

1.3 RESEARCH APPROACH

The research team met in February 2004 with representatives of ALDOT, FHWA, the precast/prestressed concrete industry, and the chemical admixture industry to develop the best possible project work plan to achieve the objectives outlined in Section 1.2. From this meeting, a consensus work plan was outlined. This plan included the production of various SCC mixtures with varying *s/agg*, *w/p*, and supplementary cementing materials (SCMs) as well as the testing of their fresh and hardened properties as they relate to prestress girder applications. Two conventional-slump concrete mixtures typically used in the local precast/prestressed concrete industry were also prepared for comparison to the SCC mixtures. All constituents used in the production of these concrete mixtures were obtained from sources routinely used in the Alabama concrete industry.

Because of a lack of standardized test procedures, available literature was reviewed to determine the most appropriate test methods and procedures to assess the fresh properties of SCC. To simulate increased temperatures associated with the steam-curing or radiant-curing process used in the precast/prestressed concrete industry in the southeastern United States, several SCC specimens from each mixture were match-cured to a time-temperature profile. The hardened properties that may affect the performance of prestressed elements were evaluated for all mixtures at times corresponding to prestress transfer as well as later ages. Shrinkage prisms were also prepared for all mixtures to measure the early-age and long-term drying shrinkage characteristics associated with the control and SCC mixtures.

After the development and testing of SCC mixtures, future tasks include the testing of small-scale prestressed elements made with SCC, the testing of full-scale prestressed girders made with SCC, and a final report assessing the possible implementation of SCC into the precast/prestressed industry.

1.4 REPORT OUTLINE

Published literature on SCC was reviewed for this research project. Chapter 2 of this report contains an introduction to SCC, factors that influence the fresh and hardened properties of SCC, procedures for testing SCC's fresh properties, and materials and mixture design for SCC. Production, quality control, and quality assurance procedures for SCC can also be found in Chapter 2.

Chapter 3 discusses the experimental testing program used to assess the fresh and hardened properties of SCC mixtures including specimen preparation, curing procedures, and the materials used in the production of the SCC mixtures. Chapter 4 presents an analysis of the fresh and hardened properties of the SCC mixtures as well as the conventional-slump concrete mixtures. Results of the fresh and hardened properties of the small-scale prestressed elements created in Phase II of the study are also given in Chapter 4.

Chapter 5 summarizes all of the overall laboratory work performed for this project. Conclusions and recommendations are also provided in Chapter 5.

CHAPTER 2

SELF-CONSOLIDATING CONCRETE

2.1 INTRODUCTION

Okamura and Ouchi (1999) report that, in the early 1980's, Japan's construction industry suffered from a noticeable decline in the number of skilled workers, which in turn directly affected the quality of construction. Skilled workers were required to provide sufficient concrete compaction to ensure durable concrete structures. The lack of durability in the resulting structures became a major problem. Hajime Okamura, professor at Kocki University of Technology, pioneered an innovative type of concrete that was less sensitive to the quality of construction labor. The result was self-consolidating concrete, now commonly referred to as SCC. SCC arrived on the construction scene in 1988 in Japan, and has since been used in a variety of construction applications in various parts of the world (Okamura and Ouchi 1999).

Self-consolidating concrete offers many advantages attributable to its ability to fill formwork and encapsulate reinforcement while maintaining its homogeneity (Skarendahl 2000a). SCC can be used in most applications. Its functions range from backfill to highly reinforced structures, and it is equally applicable for on-site construction as well as precast operations (Skarendahl 2000a). To qualify as "self-consolidating", a concrete mixture must exhibit three distinct qualities in the fresh state. RILEM Report 23 (Skarendahl 2000a) defines these three characteristics:

1. *Filling Ability*: Ability to completely fill the formwork and encapsulate any reinforcement with a homogeneous concrete. Substantial horizontal and vertical movement of the concrete within the formwork is allowed making use of the inherent flow properties of the material.
2. *Resistance to Segregation*: The ability of the particle suspension (in the fresh state) to maintain homogeneity throughout the mixing, transportation, and casting process.
3. *Passing Ability*: The ability of the concrete to go around obstacles such as closely spaced reinforcement and pass through narrow sections without getting blocked by interlocking of aggregate particles.

While SCC has more widespread use on other continents, the acceptance of SCC in North America is taking a more holistic approach (Khayat and Daczko 2003). The reason for this type of approach can be attributed to the amount of interest from different parties. Engineers and architects are more concerned with the properties of SCC in the hardened state; contractors' and precast producers' concerns are with mixture cost versus constructability. Owners are concerned with in-service value and construction timetables. Once standardized methods for testing and evaluation of the fresh, as well as hardened, states become available for self-consolidating concrete, it has the potential to revolutionize the concrete industry (Khayat and Daczko 2003).

2.2 TESTING PROCEDURES

As previously stated in Section 2.1, there are three main requirements for classification as "self-consolidating". It is important to understand that these three properties are not always independent but are often interrelated. For this reason, several of the available tests for SCC offer viable information about two or three characteristics. There are a variety of tests that have been developed to evaluate SCC, but only a limited number of these are necessary to characterize SCC. For this reason, this literature will focus on the tests that can be used for quality control and quality assurance purposes. The described test methods have not been accepted as standard procedures, although it is anticipated that ASTM and ACI committees will develop consensus standards for SCC testing in the near future (PCI 2003).

This research focused on three specific test procedures that were used to assess the fresh properties of the concrete mixtures: the slump flow test, the J-Ring test, and the L-Box test. Table 2-1 illustrates which of the three required characteristics are evaluated with each test method. These tests are discussed in detail in the following sections.

Table 2-1: Overview of test methods used for this research.

SCC Characteristic	Slump Flow Test	J-Ring Test	L-Box Test
Passing Ability		✓	✓
Filling Ability	✓	✓	✓
Resistance to Segregation	✓	✓	✓

2.2.1 Slump Flow Test

Although none of the test methods associated with SCC have been standardized, probably the most accepted method available for the evaluation of SCC's fresh properties is the slump flow test. Ramsburg (2003) is confident that the slump flow test "will be the first test method for SCC to be published by ASTM International". The slump flow test yields three results: the slump flow, the visual stability index (VSI), and the T-50. The slump flow is a measure of the deformation capacity, or how far the concrete will flow into the formwork. The T-50 is the time that it takes the concrete to flow 20 inches and provides an indication of the viscosity of the mixture. The VSI is a visual classification according to any segregation that may have occurred after the slump flow test has been completed.

The actual slump flow is the average of two perpendicular measurements of the final diameter of the slump patty. A higher slump flow indicates that the mixture will have a greater ability to fill the formwork. As of now, there are no accepted tolerances for a specified value although PCI (2003) states that ±2 inches may be appropriate. Suggested slump flow values vary depending on the mixture's application. Table 2-13 in Section 2.6.2 lists slump flow ranges for various purposes.

The T-50 is the time it takes the concrete to reach the 20-inch (50-cm) diameter circle. The time begins with the initial movement of the slump cone in the vertical direction, and the time ends as soon as any part of the concrete reaches the 20-inch (50-cm) diameter circle (PCI 2003). As previously stated, the T-50 time is often used as an indication of the viscosity of the mixture. However, it is important to note that the slump flow affects the T-50. A higher slump flow will yield a lower T-50, while the opposite is true for a smaller slump flow. Takada and Tangtermsirikul (2000) state that the T-50 is unable to estimate the viscosity of the mixture independently of the deformation capacity; only when the slump flow remains constant may the T-50 be used to evaluate the viscosity of SCC. However, this test should not be used to reject a batch of SCC, but rather as a quality control analytical test (PCI 2003). Often, there is operator error associated with the visual timing of the test; therefore, the PCI (2003) recommends that one person lift the slump cone while the other person operates the stopwatch. Typical T-50 values can be found in Table 2-14 in Section 2.6.2. These values are based on the characteristics of the formwork and the amount of reinforcement.

The slump flow test can be used to assess the filling ability and the resistance to segregation and can be performed in one of two ways: upright or inverted. The only difference in procedure between these two tests is that when performing the inverted slump flow test, the slump cone is positioned so that the concrete is poured into the larger-diameter end as illustrated in Figure 2-1. The main reason for inverting the slump cone is that the test can be conducted by one operator, while the upright technique usually requires two operators. The slump cone is also much easier to fill with SCC when it is in the inverted position. The upright position can be seen in Figure 2-2.

Ramsburg (2003) reports that recent studies of the two methods show that the slump flow value was not affected by the method selected. Even when aggregate more dense than the average concrete constituents, as well as lightweight aggregate, were used to evaluate the two test configurations, there was no difference in the variability of the test results. While both methods are acceptable, the operator(s) should refrain from switching back and forth between the two. The method selected should be used consistently in the quality control of SCC (Ramsburg 2003).

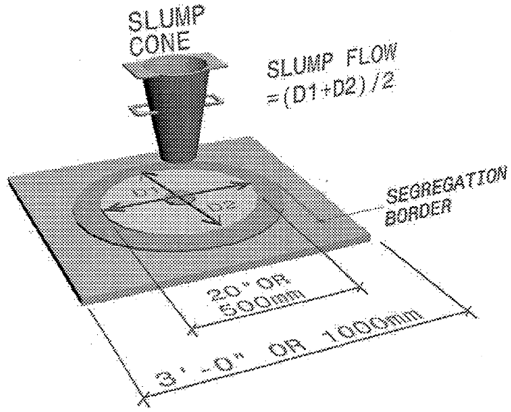

Figure 2-1: Inverted slump cone (PCI 2003)

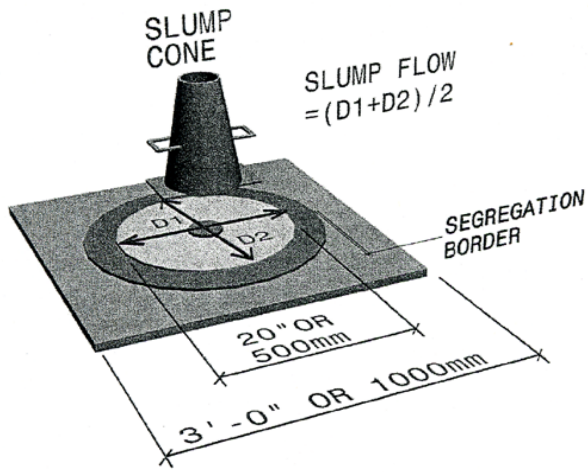

Figure 2-2: Upright slump cone (PCI 2003)

It has been noted that there is no significant difference in the final slump flow between the upright method and the inverted method. However, there is an increase in T-50 times when performed using the inverted slump cone method. This can be attributed to the fact that the concrete exits a 4-inch diameter hole rather than an 8-inch diameter hole. Further testing may determine whether a value could be added to the T-50 to correlate the two methods (Ramsburg 2003).

The slump flow test also allows the producer to evaluate the stability of the mixture by visually observing the slump flow patty. After the concrete has completely stopped flowing, a visual stability index (VSI) can be assigned. The VSI is a numerical value from 0 to 3 in increments of 0.5. If the inverted slump cone method is used, the aggregate may have a tendency to pile up in the middle of the slump patty, which is why this method is considered to be a more stringent evaluation of the resistance to segregation (Ramsburg 2003). The slump flow patty is not the only concrete that should be used to assign a VSI to the SCC. The PCI (2003) concludes, "Because the slump flow patty has no significant depth through which settlement of aggregate can occur, a visual inspection of the concrete in the wheelbarrow or mixer should be part of the process in determining the VSI rating". Table 2-2 and Figures 2-3 through 2-10 should be used as a guideline for rating the stability of SCC.

Table 2-2: Visual stability index (VSI) rating (Khayat, Assaad, and Daczko 2004)

VSI Rating	Criteria
0	No evidence of segregation in slump flow patty, mixer drum, or wheelbarrow
1	No mortar halo in slump flow patty, but some slight bleeding on surface of concrete in mixer drum and/or wheelbarrow
2	Slight mortar halo (< 10 mm) in slump flow patty and noticeable layer of mortar on surface of testing concrete in mixer drum and wheelbarrow
3	Clearly segregating by evidence of large mortar halo (>10 mm) and thick layer of mortar and/or bleed water on surface of testing concrete in mixer drum or wheelbarrow

The PCI (2003) gives additional definitions for VSI ratings of 0.5 and 1.5 as follows:

- **A VSI rating of 0.5:** Indicates no mortar halo or aggregate pile in the slump flow patty, but very slight evidence of bleed or air popping on the surface of the SCC in the mixer drum or sampling wheelbarrow.
- **A VSI rating of 1.5**: Indicates just noticeable mortar halo and/or a just noticeable aggregate pile in the slump flow patty and noticeable bleeding in the mixer drum and sampling wheelbarrow.

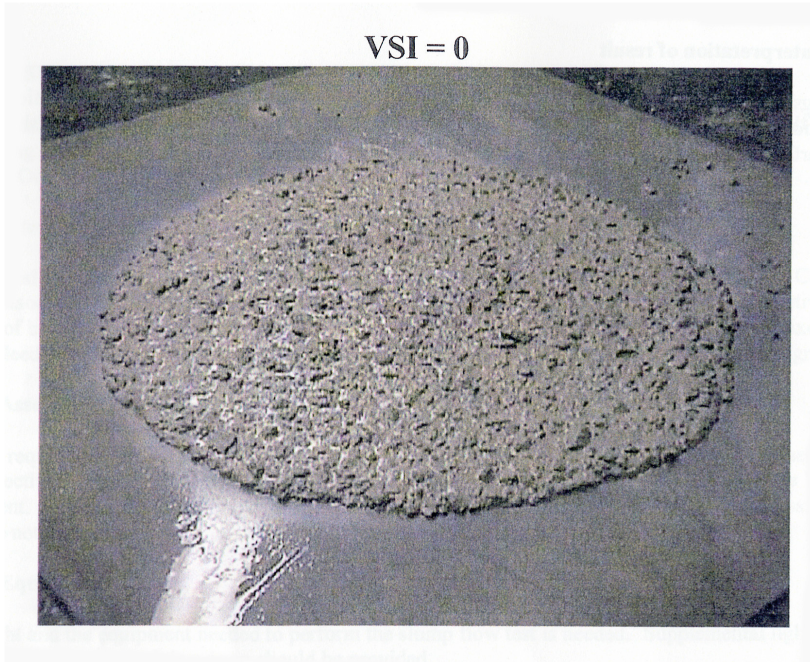

Figure 2-3: Typical visual stability index rating of 0 (PCI 2003)

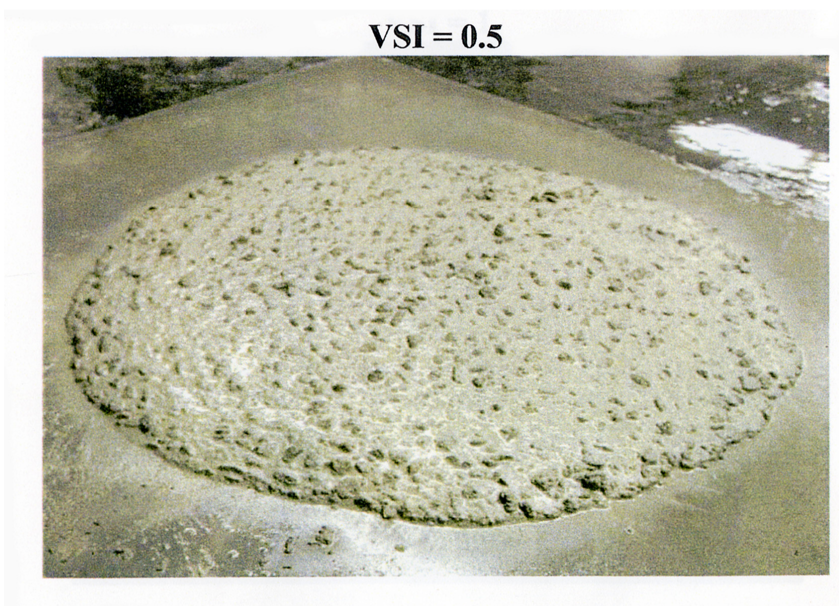

Figure 2-4: Typical visual stability index rating of 0.5 (PCI 2003)

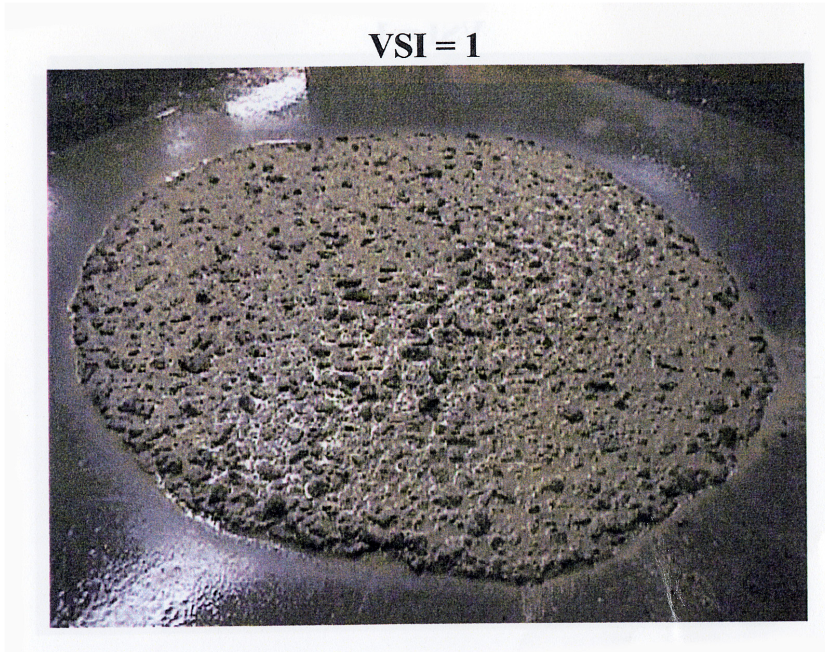

Figure 2-5: Typical visual stability index rating of 1.0 (PCI 2003)

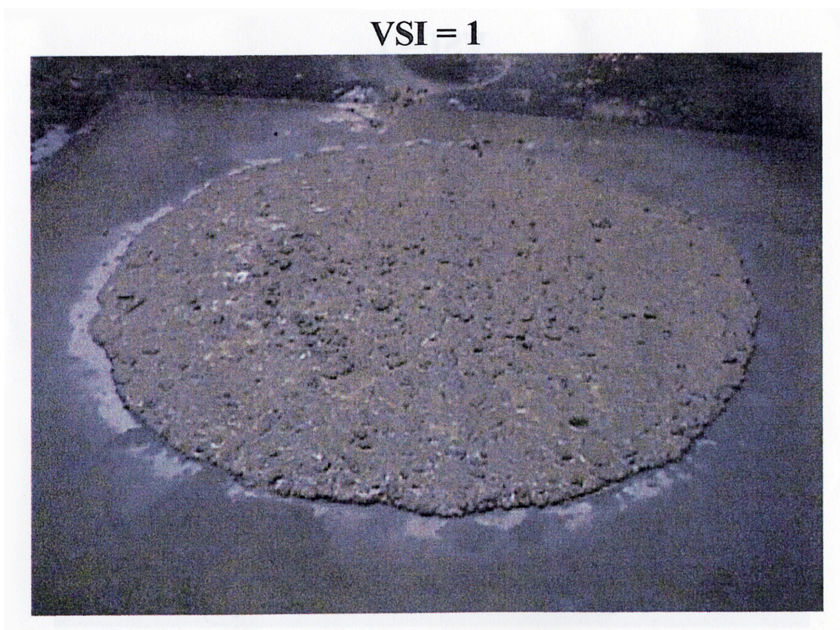

Figure 2-6: Typical visual stability index rating of 1.0 (PCI 2003)

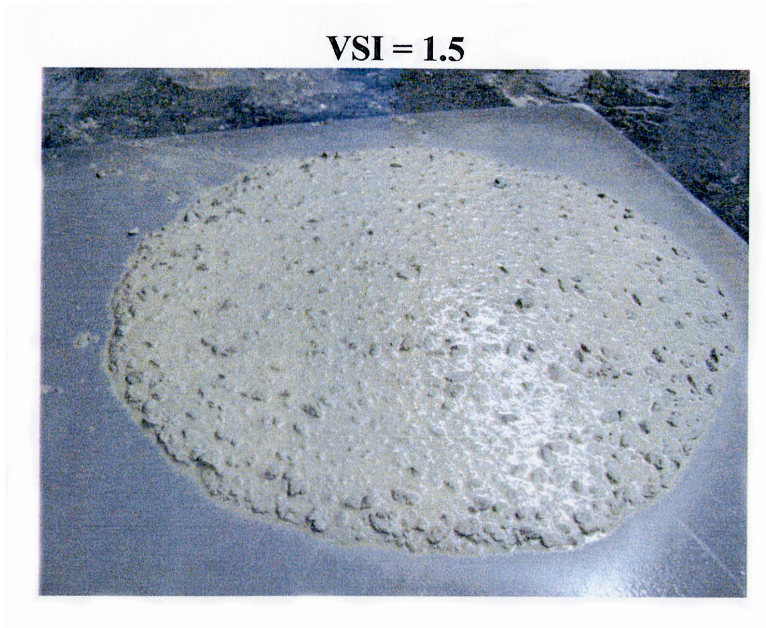

Figure 2-7: Typical visual stability index rating of 1.5 (PCI 2003)

Figure 2-8: Typical visual stability index rating of 2.0 (PCI 2003)

Figure 2-9: Typical visual stability index rating of 2.0 (PCI 2003)

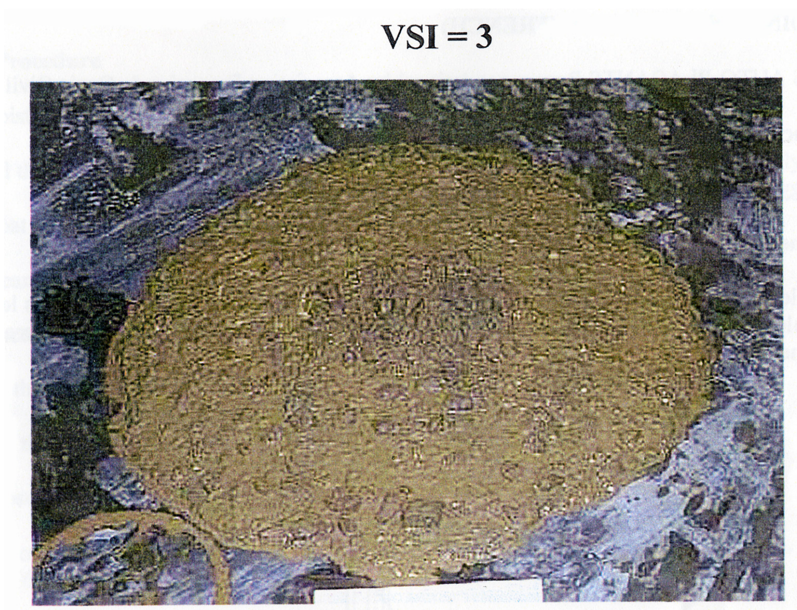

Figure 2-10: Typical visual stability index rating of 3 (PCI 2003)

2.2.2 L-Box Test

The L-Box test, based on a design created in Japan for evaluating underwater SCC, was developed to assess its passing and filling ability. However, a certain degree of instability can be detected visually, although one should not rely solely on this test to evaluate SCC's resistance to segregation (PCI 2003; Khayat, Assaad, and Daczko 2004). Named for its "L" shape, the L-Box consists of vertical and horizontal portions separated by a movable gate as shown in Figure 2-11. Directly behind the moveable gate, in the vertical portion of the box, vertical reinforcement bars are inserted to restrict the flow of the SCC.

There is no set standard for the size of reinforcement to be used. However PCI (2003) states, "The sections of reinforcing bar can be of different diameters and spaced at different intervals: in accordance with normal reinforcement considerations, three times the maximum aggregate size might be appropriate". The spacing of the bars can be used to impose a degree of severity on the passing ability of the mixture. The closer the reinforcement bars are spaced, the more difficult it becomes for the SCC to pass without blockage occurring.

The test value obtained from performing the L-Box test is called the "blocking ratio", which is defined the ratio of H_2/H_1. H_1 and H_2 are shown in Figure 2-11. The closer this value is to 1.0, the better passing ability of the SCC. According to Petersson (2000), an acceptable range for the blocking ratio is 0.80 to 1.00.

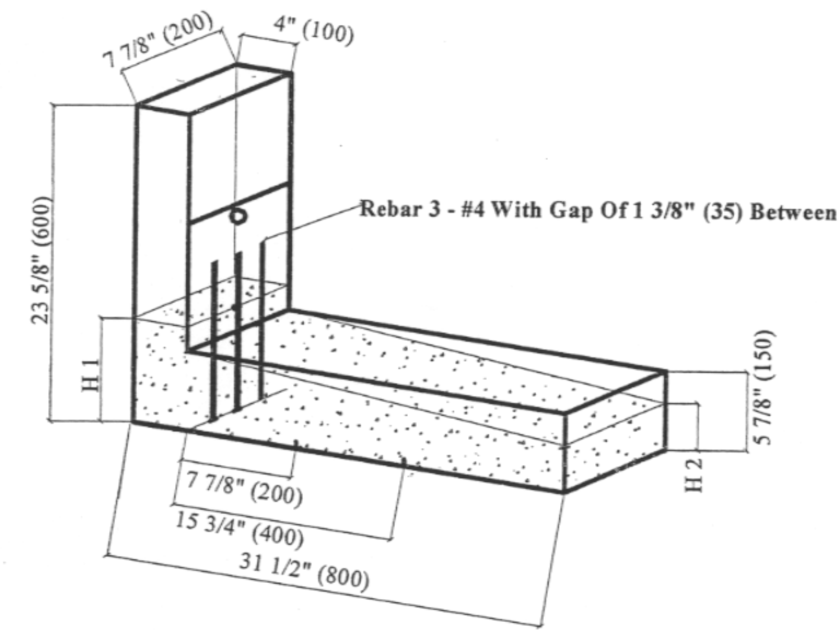

Figure 2-11: Diagram of L-Box test apparatus (PCI 2003)

2.2.3 J-RING TEST

Like the L-Box test, the J-Ring test was also developed to assess the passing ability of SCC. Figure 2-12 is representative of a typical J-Ring. The J-Ring consists of an open steel circular ring, or similar material, that has been drilled vertically with holes to accept threaded sections of reinforcement (PCI 2003). The J-Ring is attached to the slump table. PCI (2003) states, "These sections of bar can be of different diameters and spaced at different intervals: in accordance with normal reinforcement considerations, three times the maximum aggregate size might be appropriate".

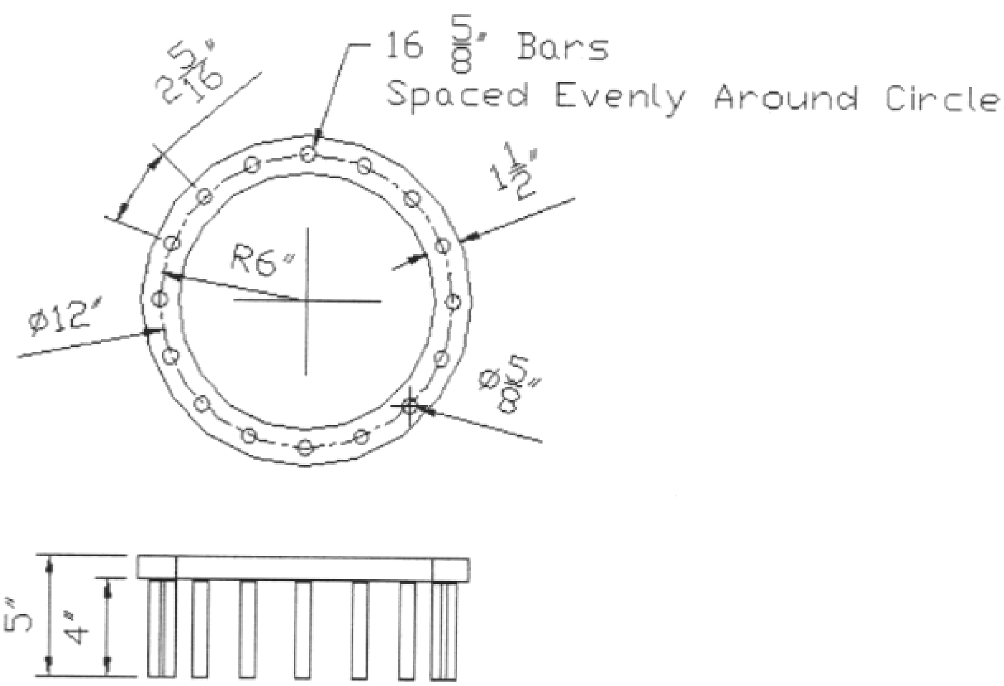

Figure 2-12: Typical J-Ring apparatus (ASTM Draft 2004)

The J-Ring test is performed in conjunction with the slump flow test. The J-Ring and slump flow tests should be performed the same way: either inverted or upright. However, if the slump cone is used in the upright position, the tabs at the base of the slump cone must be removed so that the slump cone is able to fit inside the J-Ring. While the slump flow test provides information about the flowing ability and stability of the mixture, the passing ability can be evaluated from the flow measured with the J-Ring in place. The J-Ring flow is measured in the exact same way as the slump flow. The difference in spread between the slump flow test and the J-Ring test provides a measure of the concrete's passing ability. Table 2-3 can be used to rate the passing ability of a given mixture. According to German SCC guidelines, the difference in flow should not exceed 50 mm

(2 in.), although this limit was reduced to 10 mm (0.4 in.) by the European Federation for Specialist Construction Chemicals and Concrete Systems (Khayat, Assaad, and Daczko 2004).

Table 2-3: Passing ability rating (ASTM 2004)

Difference between Slump Flow and J-Ring Flow, X	Passing Ability Rating	Remarks
$0 \leq X \leq 1$ inch	0	No visible blocking
$1 < X \leq 2$ inches	1	Minimal to noticeable blocking
$X > 2$ inches	2	Noticeable to extreme blocking

2.3 MATERIALS AND MIXTURE DESIGN OF SCC

There are many parameters that can be adjusted during the development of SCC mixture proportions. It is clear that there is no single solution for any specific application, and any number of mixture variations could provide satisfactory performance. While it is impossible to produce universal SCC mixtures because of the variation and availability of materials in different locations, a satisfactory mixture design should produce mixtures that satisfy a wide variety of performance requirements while using locally available materials (Domone 2000).

When designing a SCC mixture, the ultimate goal is to obtain a mixture with excellent deformability and adequate resistance to segregation‑enabling flow around obstructions without blockage and ensuring high filling capacity (Khayat 1999). With such contradicting properties involved, a balance must be obtained. Often this balance is achieved by *carefully* applying three common tactics: limiting the coarse aggregate content, lowering the water-to-powder ratio, and using a superplasticizer (Ambroise and Pera 2003; Domone 2000; Khayat 1999; Okamura and Ouchi 1999). Figure 2-13 is a representation of how these tactics assist in reaching the defining properties of SCC.

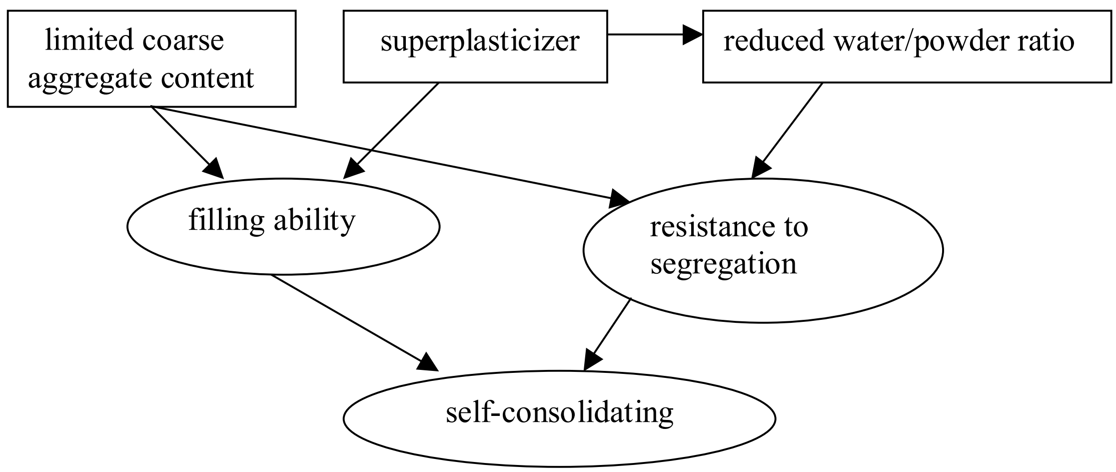

Figure 2-13: General approach to proportioning SCC (Domone 2000)

- ***Reduced Coarse Aggregate Content*:** In order to get the workability required for SCC, and at the same time avoid obstruction of closely spaced reinforcement, SCC is designed with limits not only on the amount of aggregate, but also on its nominal maximum size (Ozyildirim and Lane 2003; Tangtermsirikul and Khayat 2000). The passing ability is increased because, when the coarse aggregate is reduced, there is a reduction in the amount of collisions between the aggregate particles (Domone 2000; Khayat, Assaad, and Daczko 2004). Frequently, this path necessitates the use of a higher volume of cement (Khayat 1999). However, since a higher volume of cement leads to an increase in cost, temperature, and shrinkage, SCC contains high-volume replacements of fine powders to enhance the cohesiveness and fluidity of the mixtures (Khayat 1999; Domone 2000). Examples of some of these fine powders are: silica fume, fly ash, ground-granulated blast-furnace (GGBF) slag, limestone filler, or stone dust (Khayat 1999). Khayat (1999) adds that, "The incorporation of one or more powder materials having different morphology and grain-size distribution can improve particle packing density and reduce interparticle friction and viscosity, hence improving deformability, self-compactability, and stability". These particles are easier to keep in suspension as large aggregate particles are more likely to settle than smaller particles (Bonen and Shah 2003).

- ***Lowering the Water-to-Powder Ratio*:** Lowering the water-to-powder ratio (*w/p)* will enhance the cohesiveness of the mixtures as well as provide resistance to segregation (Domone 2000). When the *w/p* ratio is too high, the increase of interparticle distance can lead to segregation (Khayat, Assaad, and Daczko 2004). In most cases, some type of viscosity-modifying admixture (VMA) is used to increase the stability of the mixtures (Khayat 1999; Lachemi et. al 2004; Domone 2000).
- ***Superplasticizer*:** The use of a superplasticizer is essential in all SCC mixtures. Superplasticizers, also referred to as high-range water-reducing (HRWR) admixtures, are what give SCC its high deformability (Domone 2000; Khayat 1999). If more water were added, it would reduce the yield value and the viscosity, but the incorporation of a HRWR admixture will mostly reduce the

yield value with only a slight decrease in viscosity. Thus, a highly flowable and stable mixture can be achieved (Tangtermsirikul and Khayat 2000).

2.3.1 Available Methods for Designing SCC Mixtures

There have been a number of SCC mixture design methods developed employing a variety of factorial design models (Domone 20000). This approach takes into account several mixture parameters, such as the *w/p*, the concentration of VMA, the concentration of HRWR admixture, the volume of coarse aggregate, and the content of cementitious materials (Khayat, Ghezal, and Hadriche 1999). Often, tailoring the concrete mixture to have the required fresh properties may require special software (Khayat, Ghezal, and Hadriche 1999). Adequate stability is the most important aspect of SCC, especially when the concrete must flow through densely reinforced elements (Khayat, Hu, and Monty 1999). To avoid segregation, which can lead to blockage of flow, SCC must demonstrate sufficient cohesion to secure uniform deformation of all the constituents through limited spacing (Khayat, Hu, and Monty 1999). There are three basic methods to ensure the stability of SCC in the fresh state: reduction in free water content, incorporation of a viscosity-modifying admixture, and a combination of both approaches.

2.3.1.1 Reduction in Free Water Content Approach

The first approach involves using a large content of very fine powders to limit the amount of total aggregate volume and using low water content to limit unnecessary free water. Khayat, Hu, and Monty (1999) define free water as “the total mixture’s water minus water that is physically and chemically retained by the aggregate and powder materials as well as any water bound by chemical admixtures, such as water-retaining admixtures”. The reduction of free water decreases friction between solid particles and allows better deformability through narrow spaces, while the high content of powder enhances both the stability and deformability (Khayat, Hu, and Monty 1999). For this research, fine powders include: Type III cement, Grade 120 GGBF slag, silica fume, and Class C fly ash. Khayat, Hu, and Monty (1999) state that the powders are "combined to enhance the grain-size distribution, packing density, and reduce interparticle friction to lower the water demand necessary to attain a given viscosity".

In general, this approach will typically result in stable SCC mixtures with high slump flow values. The dosage of HRWR admixture required for this method is considered high. This higher dosage of HRWR admixture is required because of the reduction in water content and the increase in cementitious materials (Khayat, Hu, and Monty 1999).

2.3.1.2 Incorporation of Viscosity-Modifying Admixture (VMA) Approach

For this method, the *w/p* can remain at a value that will provide the necessary strength and durability requirements, and a modest dosage of VMA (or viscosity-enhancing admixture VEA) is used to ensure adequate stability (Khayat, Hu, and Monty 1999). The use of a VMA is also important because of SCC's moisture sensitivity. Berke et al. (2003) explain that SCC's sensitivity to uncontrolled moisture in the aggregate can often lead to an unstable mixture. This is extremely important when controlling the moisture of the mixture becomes difficult. The effect of added water on SCC's viscosity is shown in Figure 2-14. When VMA is present, added water results in less of an effect (shown by the decreased slope). The use of a VMA has proven valuable in overcoming deficiencies due to uncontrolled moisture. Not only will VMA provide better stability, reduced bleeding and segregation, but it also allows for deficiencies in the amount of moisture within the mixture (Berke et al. 2003).

The use of a HRWR admixture is also used in this method. The combination of a VMA and a HRWR admixture will yield high deformability and sufficient stability providing a greater filling capacity (Khayat, Hu, and Monty 1999). Khayat, Hu, and Monty (1999) add that "higher resistance to segregation over a wide range of fluidity, and better flowability through narrow spaces can be obtained when a suitable dosage of VEA is incorporated".

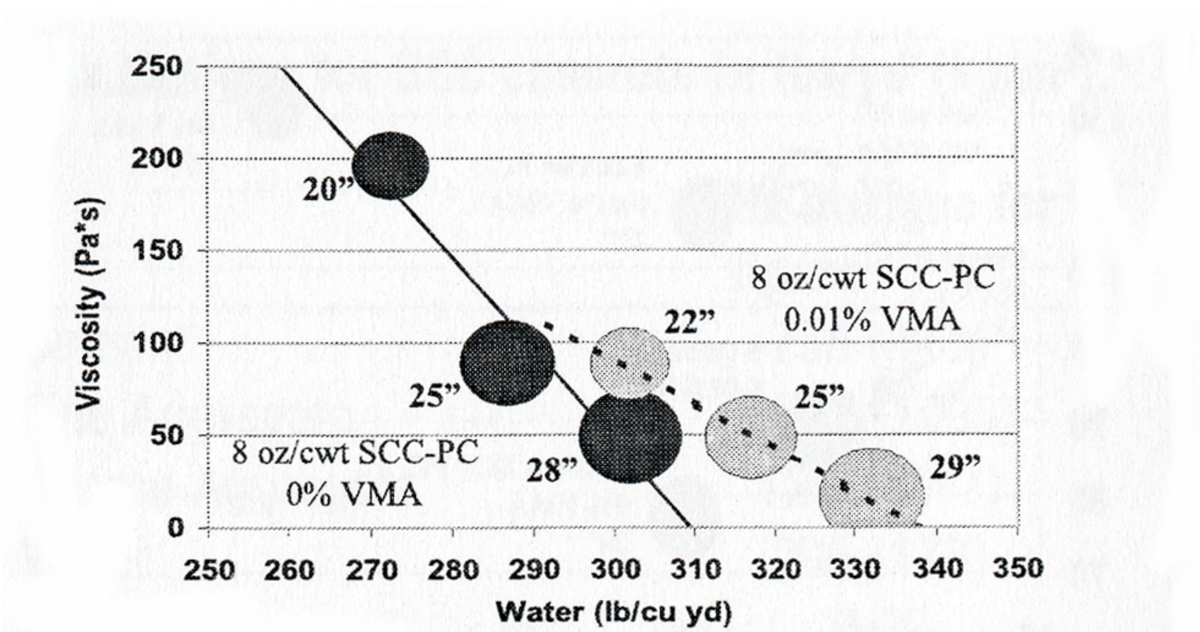

The effect of uncontrolled water on plastic viscosity. The middle point in each series is at the designed water, the extremes are at ± 5% water. Solid circles, SCCPC; Hashed circles SCC-PC + VMA

Figure 2-14: Effect of added water on the viscosity of SCC (Berke et al. 2003)

2.3.1.3 Combination Approach

This method uses low concentrations of VMA with a limited water content in the mixture. Khayat, Hu, and Monty (1999) explain that the VMA "is mainly used here to reduce the variability of the SCC that can arise from changes in material properties and placement conditions". The VMA controls the amount of bleeding and gives the concrete more body, while the low water content provides the mixtures with the necessary viscosity (Khayat, Hu, and Monty 1999).

2.3.2 Powder Properties

Often, supplementary cementing materials (SCMs) are used to reduce the amount of cement that is required in SCC. Several SCMs were incorporated during the course of this research. The incorporation of SCMs in concrete is used extensively for the improvement of durability properties, such as improved sulfate resistance, reduction in chloride diffusion, control of the alkali-silica reaction, and reduction in efflorescence and leaching (Mindess, Young, and Darwin 2003). The three SCMs used in this research were silica fume, fly ash, and ground-granulated blast-furnace (GGBF) slag. The characteristics of these SCMs, as well as the cement used, are discussed below.

2.3.2.1 Type III Cement

There are five types of portland cements recognized by ASTM, designated Type I through Type V, which differ in fineness and chemical composition. The most common type of cement used in general construction is ASTM Type I (Mindess, Young, and Darwin 2003). For this project, ASTM Type III cement was used because it provides the most rapid increase in early-age strength gain and is consistent with what is being used in the precast industry today.

Type III cement is ground finer than the other four cement types, which increases its surface area, thus increasing the amount of contact with water to produce faster hydration and strength development. It is not uncommon for concrete made with Type III cement to exhibit twice the strength in the first 24 hours as concrete made with Type I cement (Mindess, Young, and Darwin 2003).

2.3.2.2 Fly Ash

Fly ash is the most extensively used SCM and is defined by Mindess, Young, and Darwin (2003) as “the inorganic, noncombustible residue of powdered coal after burning in power plants”. There are two main classes of fly ashes, Class F and Class C; these designations reflect the composition of their inorganic fractions (Mindess, Young, and Darwin 2003). Class F fly ashes are commonly found in states east of the Mississippi river and are produced from bituminous and sub-bituminous coals, while Class C fly ashes are found mainly in western states from the ashes of lignitic coals. For this research, a Class C fly ash was used as its strength gain characteristics are more conducive to the rapid construction process used in the precast industry.

Fly ash is considered to be a type of pozzolan. Committee ACI 116R (2000) defines a pozzolan as, “A siliceous or siliceous and aluminous material, which in itself possesses little or no cementitious value but will, in finely divided form and in the presence of moisture, chemically react with calcium hydroxide at ordinary temperatures to form compounds possessing cementitious properties”. Calcium hydroxide is a hydration product formed when portland cement reacts with water.

The use of fly ash offers several benefits to concrete including reduced permeability to water and aggressive chemicals, reduced heat of hydration, improved workability, reduced expansion due to alkali-silica reaction, and contributions to the long-term strength of hardened concrete (Neville 1996; ACI 232 1996). Fly ash is also the cheapest of the three SCMs used; its cost is about half the cost of portland cement (ACI 232 1996). Table 2-4 shows variations in the chemical composition of several types of fly ash.

Table 2-4: Typical chemical composition of fly ash (ACI 232 1996)

	Bituminous	Subbituminous	Northern Lignite	Southern Lignite
SiO_2, percent	45.9	31.3	44.6	52.9
Al_2O_3, percent	24.2	22.5	15.5	17.9
Fe_2O_3, percent	4.7	5.0	7.7	9.0
CaO, percent	3.7	28.0	20.9	9.6
SO_3, percent	0.4	2.3	1.5	0.9
MgO, percent	0.0	4.3	6.1	1.7
Alkalies,* percent	0.2	1.6	0.9	0.6
LOI, percent	3.0	0.3	0.4	0.4
Air permeability fineness, m^2/kg	40.3	393	329	256
45 μm sieve retention, percent	18.2	17.0	21.6	23.8
Density, Mg/m^3	2.3	2.7	2.54	2.43
* Available alkalies expressed as Na_2O equivalent.				

2.3.2.3 Silica Fume

Silica fume is also considered to be a pozzolan and is the by-product in the production of silicon metal and alloys (Mindess, Young, and Darwin 2003). Silica fume is also an important SCM for improving the properties of concrete. Silica fume is one of the most common SCMs used for the production of super-high-strength concrete (Mindess, Young, and Darwin 2003; Fang, Jianxiong, and Changhui 1999). ACI Committee 234 (2000) and Neville (1996) list several benefits of using silica fume: reduced bleeding, greater cohesiveness, increased resistance to segregation, reduction in permeability, improved resistance to chemical attack, and improvement in long-term durability of the concrete. Silica fume also provides excellent resistance to freeze-thaw cycling (Bilodeau and Carette 1989). It should be noted that silica fume absorbs a lot of water because of its large surface area. Therefore, a HRWR admixture is needed in every mixture containing silica fume (ACI 234 2000; Mindess, Young, and Darwin 2003; Neville 1996). Table 2-5 shows variations in the chemical composition of typical silica fumes, used for the production of concrete, from silicon furnaces in North America as well as Norway.

Table 2-5: Typical chemical composition of silica fume (ACI 234 2001)

Silicon alloy type	Si (1)		FeSi-75 percent (1)		Si and FeSi-75 percent blend (2)		FeSi-75 percent (3)		Si (4)	
Number of samples (n)	42		42		32		6		28	
	Mean	Standard Deviation	Mean	Standard Deviation	Mean	Standard Deviation	Mean	Standard Deviation	Mean	Standard Deviation
SiO_2	93.65	3.84	93.22	1.71	92.10	1.29	91.40	0.92	94.22	0.34
Al_2O_3	0.28	0.13	0.31	0.20	0.25	0.12	0.57	0.03	0.36	0.04
Fe_2O_3	0.58	2.26	1.12	0.86	0.79	0.70	3.86	0.41	0.10	0.01
CaO	0.27	0.07	0.44	0.34	0.38	0.11	0.73	0.08	0.27	0.05
MgO	0.25	0.26	1.08	0.29	0.35	0.10	0.44	0.05	0.20	0.02
Na_2O	0.02	0.02	0.10	0.06	0.17	0.04	0.20	0.02	-	-
K_2O	0.49	0.24	1.37	0.45	0.96	0.22	1.06	0.05	-	-
S	0.20 (5)	0.16 (5)	0.22 (5)	0.06 (5)	-	-	-	-	-	-
SO_3	-	-	-	-	0.36	0.10	0.36 (6)	0.16 (6)	-	-
C	3.62 (5)	0.96 (5)	1.92 (5)	1.15 (5)	-	-	-	-	3.05	0.25
LOI	4.36 (5)	1.48 (5)	3.10 (5)	0.90 (5)	3.20	0.45	2.62 (6)	0.42 (6)	3.60	0.33

Note:
(1) From Nebesar and Carette, 1986
(2) From Pistilli, Rau, and Cechner, 1984
(3) From Pistillo, Wintersteen, and Cechner, 1984
(4) From Luther, 1989a
(5) n = 24
(6) n = 30

2.3.2.4 Ground-Granulated Blast-Furnace (GGBF) Slag

ACI Committee 116 (2000) defines ground-granulated blast-furnace (GGBF) slag as "the nonmetallic product, consisting essentially of silicates and aluminosilicates of calcium and of other bases that is developed in a molten condition simultaneously with iron in a blast furnace". GGBF slag is not considered a pozzolan, but is considered a cementitious material even though it may require an activator (Philleo 1989).

Like fly ash and silica fume, the use of GGBF slag also benefits the properties of concrete. The incorporation of GGBF slag into a concrete mixture will improve workability, enhance sulfate resistance, improve overall durability, and greatly reduce the permeability of the concrete (ACI 233 2000; Neville 1996). It has also been reported that the use of GGBF slag reduces the bleeding of concrete when the slag is ground to a high fineness (Neville 1996; ACI 233 2000). GGBF slag will yield lower strengths in the first few days (1-3) but will increase strength at seven days and beyond (Neville 1996; ACI Committee 233). Table 2-6 indicates typical chemical composition ranges of GGBF slag in the U.S. and Canada.

Table 2-6: Typical chemical composition of GGBF slag (ACI 233 2000)

Chemical constituents (as oxides)*	Range of composition percent by mass
SiO_2	32-42
Al_2O_3	7-16
CaO	32-45
MgO	5-15
S	0.7-2.2
Fe_2O_3	0.1-1.5
MnO	0.2-1.0

*Except for sulfur.

2.3.2.5 Strength Enhancement with SCMs

While each of the SCMs enhance certain properties of the concrete, they all assist in the development of strength when properly cured. Table 2-7 and Figure 2-15 show some recommended additions of the SCMs (by mass) and the development of strength over time respectively. From Table 2-7, it is apparent that GGBF slag can replace more cement by mass than both fly ash and silica fume, which can replace only 5 to 15% of cement by mass. According to Figure 2-15, when silica fume is incorporated into the mixture, it will provide the highest early-age strength; however, a high replacement percentage of GGBF slag will provide the highest long-term strength (of the SCMs used for this research).

Table 2-7: Recommended additions of SCMs (Mindess, Young, and Darwin 2003)

Admixture	*Replacement Level (mass %)*	*Remarks*
Fly ash—Class F*	15–25	Ignition loss ≤ 3%
Fly ash—Class C*	20–35	
Ignition loss ≤ 3%		
Blast furnace slag	25–65	
Natural pozzolans	15–40	
Silica fume	5–15	Requires higher levels of superplasticizers

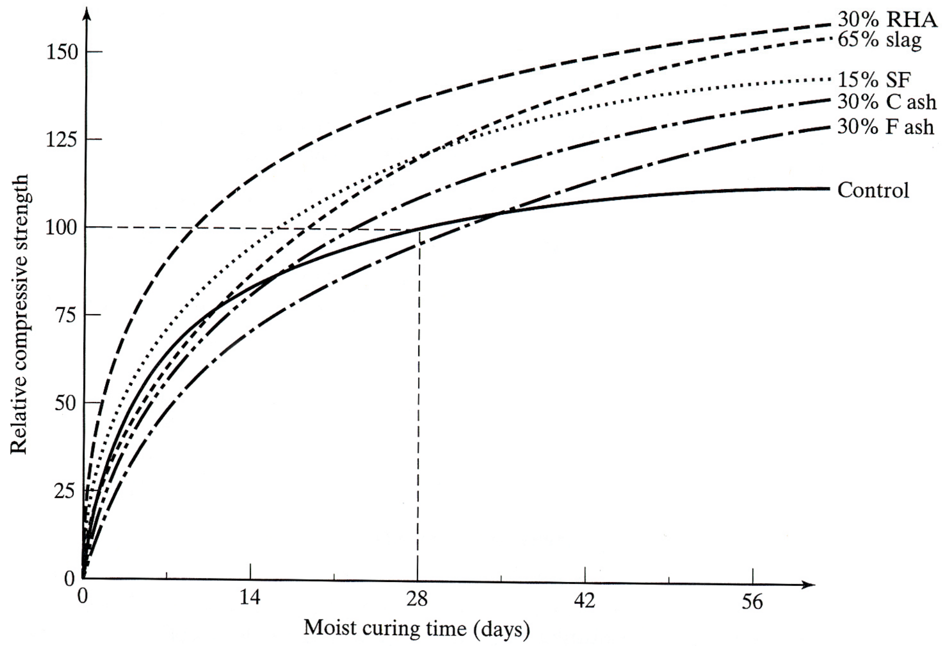

(RHA = rice husk ash; SF = silica fume; C ash = Class C fly ash; F ash = Class F fly ash).

Figure 2-15: Strength development of cement and SCM blends (Mindess, Young, and Darwin 2003)

2.3.3 Fine and Coarse Aggregate Characteristics

The selection of aggregates is important in the development of SCC to help ensure that the desired fresh properties are realized. Researchers have consistently selected a well-graded sand, either quartzite or siliceous in nature, as the fine aggregate (Khayat, Assaad, and Daczko 2004; Khayat and Assaad 2002; Beaupre, Lacombe, and Khayat 1999; Sonebi and Bartos 2002; Khayat, Ghezal, and Hadriche 1999; Sonebi 2004). The same literature recorded bulk specific gravities for their fine aggregate ranging from 2.56 to 2.72.

A continuously graded crushed aggregate with a nominal maximum size of either 14 mm ($\frac{9}{16}$ in.) or 20 mm (0.8 in.) was a common choice for the coarse aggregate. While the most common coarse aggregate type was limestone, basalt and granite have also been used (Khayat, Assaad, and Daczko 2004; Khayat and Assaad 2002; Beaupre, Lacombe, and Khayat 1999; Sonebi and Bartos 2002; Khayat, Ghezal, and Hadriche 1999; Sonebi 2004). The specific gravities ranged from 2.62 to 2.90 for the coarse aggregates used in these studies.

Tables 2-8 and 2-9 define the AASHTO grading limits for coarse and fine aggregate respectively. The coarse aggregate grading requirements specified by ALDOT are also provided in Table 2-10 (ALDOT 2002).

Table 2-8: Grading limits for coarse aggregates (AASHTO M43 2003)

Size Number	Nominal Size, Square Openings	Amounts Finer Than Each Laboratory Sieve (Square Openings), Mass, percent														
		100 mm (4 in.)	90 mm ($3^1/_2$ in.)	75 mm (3 in.)	63 mm ($2^1/_2$ in.)	50 mm (2 in.)	37.5 mm ($1^1/_2$ in.)	25.0 mm (1 in.)	19.0 mm ($^3/_4$ in.)	12.5 mm ($^1/_2$ in.)	9.5 mm ($^3/_8$ in.)	4.75 mm (No. 4)	2.36 mm (No. 8)	1.18 mm (No. 16)	300 µm (No. 50)	150 µm (No. 100)
1	90 to 37.5 mm ($3\,^1/_2$ to $1\,^1/_2$ in.)	100	90 to 100	—	25 to 60	—	0 to 15	—	0 to 5	—	—	—	—	—	—	—
2	63 to 37.5 mm ($2\,^1/_2$ to $1\,^1/_2$ in.)	—	—	100	90 to 100	35 to 70	0 to 15	—	0 to 5	—	—	—	—	—	—	—
24	63 to 19.0 mm ($2\,^1/_2$ to $^3/_4$ in.)	—	—	100	90 to 100	—	25 to 60	—	0 to 10	0 to 5	—	—	—	—	—	—
3	50 to 25.0 mm (2 to 1 in.)	—	—	—	100	90 to 100	35 to 70	0 to 15	—	0 to 5	—	—	—	—	—	—
357	50 to 4.75 mm (2 in. to No. 4)	—	—	—	100	95 to 100	—	35 to 70	—	10 to 30	—	0 to 5	—	—	—	—
4	37.5 to 19.0 mm ($1\,^1/_2$ to $^3/_4$ in.)	—	—	—	—	100	90 to 100	20 to 55	0 to 15	—	0 to 5	—	—	—	—	—
467	37.5 to 4.75 mm ($1\,^1/_2$ to No. 4)	—	—	—	—	100	95 to 100	—	35 to 70	—	10 to 30	0 to 5	—	—	—	—
5	25.0 to 12.5 mm (1 to $^1/_2$ in.)	—	—	—	—	—	100	90 to 100	20 to 55	0 to 10	0 to 5	—	—	—	—	—
56	25.0 to 9.5 mm (1 to $^3/_8$ in.)	—	—	—	—	—	100	90 to 100	40 to 85	10 to 40	0 to 15	0 to 5	—	—	—	—
57	25.0 to 4.75 mm (1 to No. 4)	—	—	—	—	—	100	95 to 100	—	25 to 60	—	0 to 10	0 to 5	—	—	—
6	19.0 to 9.5 mm ($^3/_4$ to $^3/_8$ in.)	—	—	—	—	—	—	100	90 to 100	20 to 55	0 to 15	0 to 5	—	—	—	—
67	19.0 to 4.75 mm ($^3/_4$ to No. 4)	—	—	—	—	—	—	100	90 to 100	—	20 to 55	0 to 10	0 to 5	—	—	—
68	19.0 to 2.36 mm ($^3/_4$ to No. 8)	—	—	—	—	—	—	100	90 to 100	—	30 to 65	5 to 25	0 to 10	0 to 5	—	—
7	12.5 to 4.75 mm ($^1/_2$ to No. 4)	—	—	—	—	—	—	—	100	90 to 100	40 to 70	0 to 15	0 to 5	—	—	—
78	12.5 to 2.36 mm ($^1/_2$ to No. 8)	—	—	—	—	—	—	—	100	90 to 100	40 to 75	5 to 25	0 to 10	0 to 5	—	—
8	9.5 to 2.36 mm ($^3/_8$ to No. 8)	—	—	—	—	—	—	—	—	100	85 to 100	10 to 30	0 to 10	0 to 5	—	—
89	9.5 to 1.18 mm ($^3/_8$ to No. 16)	—	—	—	—	—	—	—	—	100	90 to 100	20 to 55	5 to 30	0 to 10	0 to 5	—
9	4.75 to 1.18 mm (No. 4 to No. 16)	—	—	—	—	—	—	—	—	—	100	85 to 100	10 to 40	0 to 10	0 to 5	—
10	4.75 mm (No. 4 to 0)[a]	—	—	—	—	—	—	—	—	—	100	85 to 100	—	—	—	10 to 30

[a] Screening.

Table 2-9: Grading limits of fine aggregate (AASHTO M6 2003)

Sieve Size	Mass, Percent Passing
9.5 mm (3/8 in.)	100
4.75 mm (No. 4)	95 to 100
2.36 mm (No. 8)	80 to 100
1.18 mm (No.16)	50 to 85
600 μm (No. 30)	25 to 60
300 μm (No. 50)	10 to 30
150 μm (No. 100)	2 to 10

Table 2-10: Grading limits of coarse aggregates used in Alabama (ALDOT 2002)

TABLE OF ALDOT COARSE AGGREGATE SIZES *

PERCENT PASSING BY WEIGHT {MASS}, EACH LABORATORY SIEVE (U.S.A. STANDARD SERIES)

Size > / Number v	4 inch {100 mm}	3.5 inch {90 mm}	3 inch {75 mm}	2.5 inch {63 mm}	2 inch {50 mm}	1.5 inch {37.5 mm}	1 inch {25.0 mm}	3/4 inch {19.0 mm}	1/2 inch {12.5 mm}	3/8 inch {9.5 mm}	# 4 {4.75 mm}	# 8 {2.36 mm}	# 16 {1.18 mm}	# 50 {300 μm}	# 100 {150 μm}	# 200 {75 μm}
1	100	90-100		25-60		0-15		0-5								
2			100	90-100	35-70	0-15		0-5								
24			100	90-100		25-60		0-10	0-5							
3				100	90-100	35-70	0-15		0-5							
357				100	95-100		35-70		10-30		0-5					
4					100	90-100	20-55	0-15		0-5						
467					100	95-100		35-70		10-30	0-5					
410					100	85-100	60-85		30-60		18-30	11-20	8-15	5-9		2-6
5						100	90-100	20-55	0-10	0-5						
56						100	90-100	40-85	10-40	0-15	0-5					
57						100	95-100		25-60		0-10	0-5				
6							100	90-100	20-55	0-15	0-5					
67							100	90-100		20-55	0-10	0-5				
68							100	90-100		30-65	5-25	0-10	0-5			
610							100	90-100		25-60		7-30		0-15		
7								100	90-100	40-70	0-15	0-5				
78								100	90-100	40-75	5-25	0-10	0-5			
710								100	90-100	50-85		12-35		0-15		
8									100	85-100	10-30	0-10	0-5			
89									100	90-100	20-55	5-30	0-10	0-5		
810									100		70-90	50-74	38-62	20-42		9-24
8910									100	90-100	60-85	40-70		10-25		1-5
9										100	85-100	10-40	0-10	0-5		
10										100	85-100				10-30	

2.3.4 CHEMICAL ADMIXTURES

Chemical admixtures are used to improve workability, reduce the *w/p* ratio, and decrease cement contents (Mindess, Young, and Darwin 2003). Chemical admixtures commonly used in the production of SCC are high-range water-reducing (HRWR) admixtures, viscosity-modifying admixtures (VMA), and air-entraining admixtures (AEA). These will thus be discussed in detail.

2.3.4.1 High Range Water Reducing Admixture

High-range water-reducing (HRWR) admixtures, or superplasticizers as they are commonly called, are the most important chemical admixtures used to create SCC. Sonebi and Bartos (2002) state that "the use of superplasticizer can disperse cement grains and reduce inter-particle friction and enable the reduction in water content while maintaining the required levels of flowability and viscosity". Neville (1996) reports that the use of a HRWR admixture can reduce the water content by approximately 25-35% for a given workability. While providing high early strength and improved workability, the use of a HRWR admixture also increases the cohesiveness and improves the resistance to bleeding and segregation (Neville 1996). However, Mindess, Young, and Darwin (2003) point out that overdosing with a HRWR admixture can result in severe segregation.

The HRWR admixtures used today are unlike the traditional HRWR admixtures of the past. While traditional HRWR admixtures were a blend of high-quality raw materials, the new HRWR admixtures are manufactured at the molecular level (Bury and Christensen 2003). The most common type of HRWR admixture used today is polycarboxylate-based (Sugamata, Edamatsu, and Ouchi 2003). Bury and Christensen (2003) further state that "this new technology breakthrough allows for the development of admixtures possessing a wide range of premier performance attributes, such as controlled setting time, controlled slump retention, unmatched water-reduction with linear dosage response, enhanced concrete stability, enhanced pumpability, enhanced finishability, superior response to vibration and superior strength development". Traditional HRWR admixtures cannot provide the fresh property characteristics required for SCC (Bury and Christensen 2003).

2.3.4.2 Viscosity-Modifying Admixture

Viscosity-modifying admixtures (VMA) increase the cohesiveness of the fresh concrete and improve its resistance to bleeding and segregation (Mindess, Young, and Darwin 2003). As stated in Section 2.3.1.3, the use of a VMA greatly enhances the mixture's stability. It is also important to note that the use of a VMA can improve the thixotropy of the mixtures, thereby increasing the viscosity after casting, which further enhances the stability (Khayat 1999). PCI (2003) defines thixotropic behavior as "the property of a material that will allow it to exhibit a low viscosity while being mechanically agitated, but stiffen after a short period at rest".

Khayat (1995) classifies the water-soluble viscosity-modifying admixtures into three categories: natural polymers, semi-synthetic polymers, and synthetic polymers. VMAs that are classified as natural polymers are often referred to as organic or mineral VMAs, while VMAs falling into the semi-synthetic and synthetic polymer categories are referred to as chemical VMAs. Decomposed starch and its derivatives, cellulose-ether derivatives, and electrolytes are types of semi-synthetic polymers, while synthetic polymers include those based on ethylene and vinyl. Mineral VMAs, such as welan gum, are more potent than chemical VMAs. However, this type of VMA is more costly, and it also requires a higher dosage of HRWR admixture. While mineral VMAs are more powerful than chemical VMAs, both types will control bleeding and segregation while rendering the mixture more robust when properly used with a HRWR admixture (Felekoglu, Yardimci, and Baradan 2003).

2.3.4.3 Air-Entraining Admixture

Research conducted on concrete durability has recognized that the best protection for concrete against the harsh effects of freezing and thawing cycles and deicing salts comes from an appropriate air void system in the hardened cement paste. Difficulties can arise in attempting to provide a stable air-void system when a mixture contains a high cementitious materials content and a HRWR admixture is used (Mindess, Young, and Darwin 2003; Ozyildirium and Lane 2003).

The major drawback to using an air-entraining admixture is that it has a negative effect on strength. There is an approximate 5% loss in compressive strength for each 1% increase in total air content. With the high cementitious contents associated with high-strength concretes, a loss in strength is inevitable with the addition of entrained air. (Mindess, Young, and Darwin 2003)

While the amount of total air content will vary from state to state, PCI (2003) gives recommendations for the total air content based on the nominal maximum size of aggregate shown in Table 2-11. For concretes possessing a compressive strength greater than 5,000 psi, a reduction of total air content in Table 2-11 by 1% shall be permitted.

Table 2-11: Total air content in percent by volume (PCI 2003)

Nominal maximum size of aggregate in. (mm)	**Total air content, percent by volume.**	
	Severe Exposure	Moderate Exposure
Less than 3/8 (9)	9.0 %	7.0 %
3/8 (9)	7.5 %	6.0 %
1/2 (13)	7.0 %	5.5 %
3/4 (19)	6.0 %	5.0 %
1 (25)	6.0 %	5.0 %
1-1/2 (38)	5.5 %	4.5 %

2.4 FRESH CONCRETE PROPERTIES

It has been mentioned that SCC must exhibit adequate filling and passing ability while resisting segregation in the fresh state. Before discussing these three properties of SCC, it is important to understand that rheological behavior influences the performance of SCC in the fresh state. Thus, rheology is a property at the focal point of SCC development (Tangtermsirikul and Khayat 2000).

2.4.1 RHEOLOGY

To better understand the mechanics of SCC, it is important to examine a few principles of rheology, which Mindess, Young, and Darwin (2003) define as "the science dealing with deformation and flow of materials under stress".

Fresh concrete can be described as particles in suspension. It is a complex suspension with the variety of particle sizes as well as the time-dependent properties associated with chemical reactions. The suspension might be considered as sand particles in a liquid paste (phase consisting of water, cement, and other powder-sized particles), or coarse aggregates in a liquid mortar (phase consisting of water, fine particles, and cement). Rheology of concrete, mortar, and paste is valuable in understanding a mixture's behavior (Tangtermsirikul and Khayat 2000).

Rheology of concrete in the fresh state is most often characterized through the yield stress and plastic viscosity. The Bingham Model Equation, Equation 2-1 (Mindess, Young, and Darwin 2003), can be used to define the behavior of SCC, where τ is the shear stress in psi, τ_o is the yield stress in psi, μ is the plastic viscosity in psi $\cdot$ s, and γ is the shear rate in 1/s.

$$\tau = \tau_o + \mu * \gamma \qquad \textit{(Equation 2-1)}$$

Shown in Figure 2-16, fresh concrete has a definite yield stress, τ_o, which must be exceeded before flow can occur followed by increasing strain rate, caused by increasing shear stress (Tangtermsirikul and Khayat 2000; Mindess, Young, and Darwin 2003). This is known as the Bingham Fluid Model. The ideal rheological properties for SCC are a low yield stress (high flowability) coupled with an adequate plastic viscosity (Tangtermsirikul and Khayat 2000).

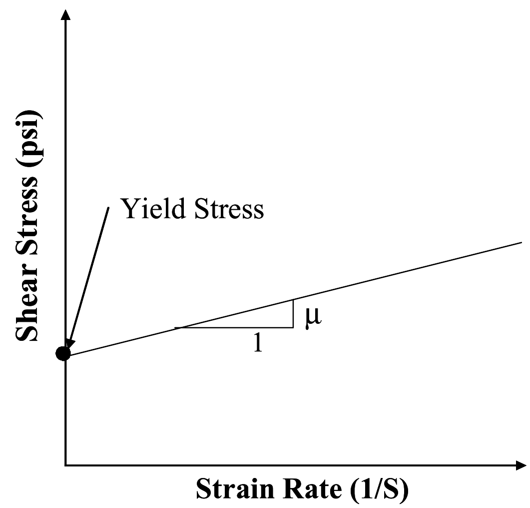

Figure 2-16: Bingham Fluid Model (Mindess, Young, and Darwin 2003)

The two parameters measured by different rheology methods are the initial yield stress and the plastic viscosity, and according to Emborg (1999), many believe that rheometers are the most accurate way to describe the real behavior of the fresh concrete. While there are a number of different rheometers available for testing fresh concrete, they are based on different measurement principles, and thus measurements with different types of equipment cannot be compared easily (Tangtermsirikul and Khayat 2000). Another drawback for rheology methods is that they are not practical for use at the construction site; in addition, they can be rather time consuming and expensive (Emborg 1999).

2.4.2 Workability

In mechanical terms, the self-consolidating ability of concrete is related to the rheology of the fresh concrete, while it is related to workability parameters in terms of handling in practice. In workability terms, “self-consolidating” signifies the ability of concrete to flow under its own self-weight and fill formwork, while adequately surrounding any reinforcement within the formwork, all while maintaining a uniform-quality concrete. As a fresh state property, self-consolidating can be characterized by its three essential requirements (see definitions in Section 2.1): filling ability, resistance to segregation, and passing ability (Tangtermsirikul and Khayat 2000).

2.4.2.1 Filling Ability

Self-consolidating concrete must be able to deform very well under the influence of gravity alone. The filling ability of SCC has two major components:

1. Deformation Capacity: How far can the concrete flow from the discharge point?
2. Velocity of Deformation: Speed with which the concrete flows. When evaluating the deformation capacity, this can be thought of as the time it takes the concrete to reach a certain deformation (Tangtermsirikul and Khayat 2000).

To acquire good filling ability, the concrete must have low inter-particle friction and paste with excellent deformability. To make the concrete deform well, friction must be reduced between the solid particles. Included in the solid particles are: coarse aggregate, fine aggregate, and all powders. Three different types of friction occur when casting SCC (Tangtermsirikul and Khayat 2000):

1. Aggregate-to-Aggregate friction
2. Powder-to-Powder friction
3. Aggregate-to-Powder friction

One way to achieve a reduction in the aggregate-to-aggregate friction is by increasing the inter-particle distance by limiting the amount of aggregate content, thereby increasing the paste content. However, this method cannot be used to reduce the powder-to-powder friction because it would increase the water content, which in turn leads to segregation and undesirable hardened properties. Typically, HRWR admixtures are used to disperse the fine powder particles. Reducing the aggregate-to-powder friction usually results in a lower resistance to segregation. Therefore, it is more effective to increase the viscosity of the mixtures rather than the deformability (Tangtermsirikul and Khayat 2000).

The other prerequisite for having a mixture with good filling ability is a paste with excellent deformability. Reducing the friction of the solid phase is not sufficient, the paste has to deform well too (Tangtermsirikul and Khayat 2000). It is very important to ensure a low yield stress (high flowability) and high resistance to segregation (reasonable viscosity) to achieve a high quality SCC mixture. As mentioned in Section 2.3, this can be accomplished with the use of a HRWR admixture. Tangtermsirikul and Khayat (2000) agree that unlike the addition of water, which leads to a reduction in the yield stress and the viscosity, the use of a HRWR admixture will reduce the yield stress with only a slight decrease in viscosity. A low *w/p* can reduce the deformation of the paste, and thus has to be controlled so that it is not too high or too small. A mixture with a low *w/p*, that has incorporated the use of a HRWR admixture, tends to have a high deformation capacity but low velocity of deformation, and the *w/p* needs to be balanced with various fillers and cementitious materials to attain sufficient deformability and deformation velocity (Tangtermsirikul and Khayat 2000). The following actions should be taken to achieve satisfactory filling ability (Tangtermsirikul and Khayat 2000).

1. Reduce inter-particle friction
    - Use an optimum-graded powder relative to the cement and aggregates
    - Lower the coarse aggregate content
2. Increase the deformability of the paste
    - Use a HRWR admixture (superplasticizer)
    - Use a balanced water-to-powder ratio

2.4.2.2 Resistance to Segregation

The production of prestressed elements requires the use of self-consolidating concrete that must have adequate dynamic and static stabilities. The dynamic stability refers to the resistance to segregation during transport and placement, while the static stability describes the resistance to segregation of the fresh concrete after placement (Assaad, Khayat, and Daczko 2004). Tangtermsirikul and Khayat (2000) stress that SCC should exhibit little or none of the following types of segregation during the static or dynamic phases:

- Bleeding of water
- Paste and aggregate segregation
- Coarse aggregate segregation leading to blocking
- Non uniformity in air-void distribution

In order to avoid segregation between water and solid particles, the amount of free water in the mixture needs to be reduced. The free water tends to "bleed" when heavy solid constituents settle and the water is displaced to the surface, although it can remain in "bleed channels" within the concrete (Sonebi and Bartos 2002). Lowering the free water is often done by lowering the *w/p*. Another way of reducing the amount of free water in a given mixture is to use powder materials with a high surface area enabling more water retention (Tangtermsirikul and Khayat 2000). The segregation resistance between water and solid phases can also be controlled by the use of a VMA (Tangtermsirikul and Khayat 2000; Khayat, Assaad, and Daczko 2004; Khayat 1999). The use of a viscosity agent increases the ability of the mixture to retain water. Khayat (1999) explains that, "Higher resistance to segregation over a wide range of fluidity levels can be obtained when a suitable dosage of VEA (viscosity enhancing admixture) is incorporated".

The other categories of segregation can be reduced by increasing the phase-to-phase interaction force, which is considered to be composed of friction and cohesion (Tangtermsirikul and Khayat 2000). Tangtermsirikul and Khayat (2000) further state that since inter-particle friction can lead to blockage, increasing the phase-to-phase cohesion is most beneficial. Typically, the cohesion of the paste is increased by lowering the *w/p* and using a VMA, which will increase the paste's capacity for suspending solid particles (Khayat, Assaad, and Daczko 2004; Bonen and Shah 2004).

The segregation of coarse aggregate seems to be the decisive factor when SCC is being cast into forms of highly congested members (Tangtermsirikul and Khayat 2000). Bonen and Shah (2004) agree: "the actual size of aggregate controls the ability to flow through confined spaces and adjacent rebars, but also has to be taken into account because of segregation considerations as coarser aggregate settle down more rapidly than finer one".

There must also be sufficient resistance to segregation in the static state. Bonen and Shah (2004) used Stocks' Law to help evaluate the segregation of coarser aggregates in the static state. Stocks' Law is defined as follows, "in a static state the sedimentation velocity is proportional to the square size of the particle, the difference in the densities of the particles and suspension, and inversely related to the viscosity of the suspension" (Bonen and Shah 2004). Although Stocks' Law does not apply to concentrated suspensions like concrete, it is useful for determining the tendency of the solid particles to segregate. Bonen and Shah (2004) concluded that for a constant viscosity and aggregates with a constant density, larger aggregates will settle much faster than smaller ones assuming aggregate particles do not interact with each other.

Tangtermsirikul and Khayat (2000) suggest the following actions be taken to ensure adequate resistance to segregation:

1. Reduce separation of solid particles
    - Limit the aggregate content
    - Reduce the maximum size aggregate
    - Use a low *w/p*
    - Incorporate a viscosity-modifying admixture
2. Minimize the amount of free water (bleeding)
    - Lower the amount of water
    - Use a low *w/p*
    - Incorporate a viscosity-modifying admixture
    - Use powders with high surface area

Bonen and Shah (2004) also suggest a low *w/c* and high content of fines or implementation of viscosity-modifying admixture.

2.4.2.3 Passing Ability

One of the most appealing properties of SCC is its ability to pass through narrow openings or areas of highly congested reinforcement. This ability of SCC to maneuver through these types of areas without the blocking or segregation of coarse aggregate is what makes it unique. For a SCC mixture to have sufficient passing ability, there must be a balance between the size and amount of large solid particles and the spacing between reinforcement and openings in the formwork that it must flow through (Tangtermsirikul and Khayat 2000). When the nominal maximum size of the aggregate is too large or the content of coarse aggregate is too high, the passing ability of the mixture is compromised (Khayat, Assaad, and Daczko 2004).

Figure 2-17 illustrates how blocking occurs. Low cohesiveness increases the risk of segregation. Segregation promotes blockage which causes insufficient passing ability. In order for the concrete to flow through openings and around reinforcement, the aggregate particles must change their flow path, resulting in collision and contact of the particles near the opening (Tangtermsirikul and Khayat 2000). When these aggregate particles begin colliding with each other, an arch will tend to form at the opening, which is developed easily when the amount and size of aggregate is increased (Tangtermsirikul and Khayat 2000). If the first two conditions of SCC are met (good filling ability and resistance to segregation) and blockage is still occurring, then the maximum size aggregate is too large or the coarse aggregate content is too high.

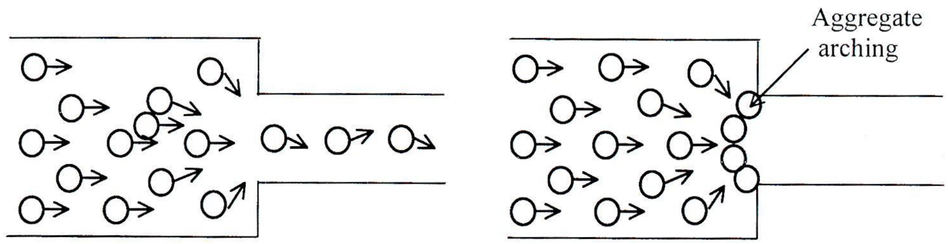

Figure 2-17: Mechanism of blocking (Tangtermsirikul and Khayat 2000)

Even if the maximum size of aggregate is not excessively large, blockage will occur when the aggregate segregates. Larger size reinforcement can also lead to blockage of adequate aggregate materials because it provides more stable support for the arch to form. The following actions should be taken to reduce the possibility of blocking and ensure adequate passing ability (Tangtermsirikul and Khayat 2000).

1. Enhance the cohesiveness to lower segregation of aggregate
    - Use a low *w/p*
    - Incorporate a viscosity-modifying admixture
2. Improve compatability between clear spacing and coarse aggregate characteristics
    - Reduce the maximum size of aggregates
    - Use a low coarse aggregate volume

While it is essential to have all three workability requirements for SCC to be successful, one can see that several actions improve more than one of the defined fresh properties. Figure 2-18 below is an overview of all three of the essential properties and typical remedies for achieving these properties. Excellent deformability, good stability, and low risk of blockage are equivalent to filling ability, resistance to segregation, and passing ability respectively.

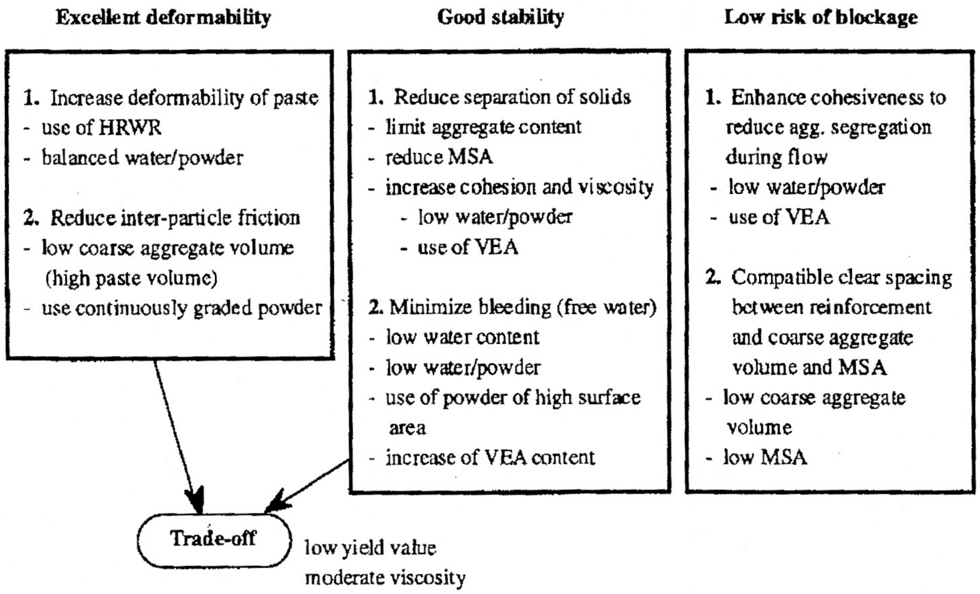

Figure 2-18: Basic workability requirements and typical actions taken to achieve these requirements (Khayat 1999)

2.5 HARDENED CONCRETE PROPERTIES

Designers and engineers value numerous properties of concrete in the hardened state: compressive and tensile strength, modulus of elasticity, creep, shrinkage, permeability, durability, and attractiveness. Even though properties of SCC vary according to their various constituents, studies have shown that the mechanical properties of SCC are in some cases comparable if not better than the corresponding properties of conventional-slump concrete (Bonen and Shah 2004). The work documented in this thesis focuses on compressive strength, modulus of elasticity, and drying shrinkage. The attractiveness (or how the surface finishes) and creep characteristics will be discussed briefly.

2.5.1 MICROSTRUCTURE

The microstructure of the hydrated cement paste is important in the development of the desired hardened properties. First, it is important to note that the microstructure of the hydrated cement paste in the immediate vicinity of the interface zone, which can occupy as much as one-half of the total volume of hardened cement paste, differs from the majority of the cement paste (Neville 1996). The interface zone, or interfacial transition zone (ITZ), is the interface between the coarse aggregate and the surrounding mortar (Neville 1996; Tragardh 1999). According to Neville (1996), the difference in microstructure between the ITZ and the bulk of the cement paste is that, during mixing, some of the dry cement particles do not become closely packed with the large aggregate particles. When concrete requires vibration, water tends to concentrate on the surfaces of the larger aggregates causing significant porous and weak interfacial zones to form (Skarendahl 2000c; Tragardh 1999). On the other hand, if the fresh concrete is homogenously mixed, resists segregation, and is placed without any vibration, a very small amount of interfacial transition zones is likely to develop (Skarendahl 2000c). This is important because microcracking is initiated at the ITZ, and the typical cracking pattern includes the interface (Neville 1996).

Since SCC does not require any external vibration and has increased powder content and improved water retention properties, its microstructure is expected to be tighter and more homogenous than that of conventional vibrated concrete (Skarendahl 2000c). Research conducted by Tragardh (1999) reported that SCC containing high amounts of limestone fillers had a denser microstructure than that of conventional concrete with the same *w/c*. The improvement in the microstructure of SCC should result in enhanced hardened properties (Skarendahl 2000c).

2.5.2 COMPRESSIVE STRENGTH

Strength of concrete is commonly considered its most valuable property. The strength of the concrete will generally give a good idea of its quality because it reflects the structure of the hydrated cement (Neville 1996). Many factors influence the strength of concrete such as cement type, type of HRWR admixture, curing conditions, size and shape of coarse aggregates, *w/p,* air content, and the type of pozzolans. However, when the same type of powders, admixtures, and aggregates have been used along with the same mixing, curing, and testing conditions, the most influential factor affecting concrete's strength is the *w/p* (Neville 1996; Bonen and Shah 2004).

Neville (1996) states "*in practice* the water-to-cement ratio is the largest single factor in the strength of fully compacted concrete". When concrete is fully compacted, i.e. the hardened concrete contains approximately 1% air voids, its strength is found to be inversely proportional to the *w/c*. While the strength of the concrete increases with lower *w/c*, it does so at a progressively decreasing rate as shown in Figure 2-19. From this figure, it is clear that the increase in strength is significant as the *w/c* nears 0.38, but as the *w/c* becomes smaller, the strength gain increases at a smaller rate (Neville 1996).

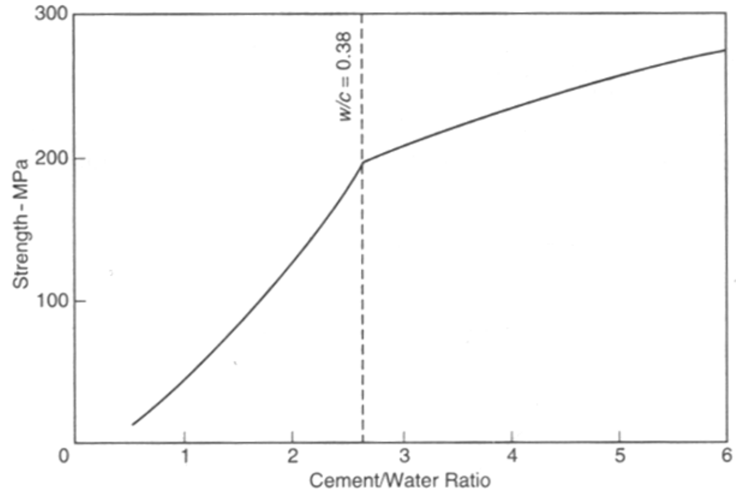

Figure 2-19: Strength versus cement-to-water ratio (Neville 1996).

In a study conducted by Attiogbe, See, and Daczko (2003), the compressive strength of SCC mixtures (slump flow of 26 to 27 in.) was evaluated and compared with the compressive strength of conventional-slump concrete mixtures (8 to 9 in. slump). Two SCC mixtures having a *w/p* of 0.37 and a sand-to-aggregate ratio (*s/agg*) of 0.53 (by mass) were evaluated and compared with two conventional-slump concretes having the same *w/p* but a *s/agg* of 0.44 (by mass). Two different polycarboxylate-based HRWR admixtures were used in conjunction with a VMA. Both of the conventional-slump concrete mixtures and one of the SCC mixtures were made with the normal-set HRWR (NS HRWR) admixture, while the second SCC mixture was made with a high early strength HRWR (HES HRWR) admixture. The SCC mixture made with the NS HRWR admixture was steam-cured and compared with the conventional-slump concrete mixture that was also steam-cured. The remaining SCC mixture, made with the HES HRWR admixture, was air-cured and compared with the conventional-slump concrete mixture that was also air-cured.

The results showed that both the 1-day and 28-day compressive strengths of the steam-cured SCC mixture were comparable to the 1-day and 28-day compressive strengths of the steam-cured conventional-slump concrete mixture. However, the 1-day and 28-day compressive strengths of the air-cured SCC mixture exceeded the same-day compressive strengths of the air-cured conventional-slump concrete mixture (Attiogbe, See, and Daczko 2003). This is not surprising due to the difference in the type of HRWR admixture used for the respective air-cured mixtures.

2.5.3 Modulus of Elasticity

The modulus of elasticity, E_c, is an important parameter for structural design, specifically prestress applications. The modulus of elasticity at transfer, E_{ci}, is needed in order to determine the member camber and elastic shortening at the time of prestress release, while E_c at later ages is used to compute transformed section properties for composite sections. The modulus of elasticity is also used to predict the deflections and prestress losses of members at later ages. Accurately determining the value of E_c helps the designers and producers provide a superior product (Huo, Al-Omaishi, and Tadros 2001).

While there is no doubt that the modulus of elasticity increases with an increase in compressive strength, there are other factors that clearly affect the E_c as well, most notably the aggregate content and the properties of those aggregates (Neville 1996; Huo, Al-Omaishi, and Tadros 2001; Bonen and Shah 2004). As the total volume of aggregate and its modulus of elasticity increase, the modulus of elasticity of the concrete increases (Bonen and Shah 2004). Since SCC typically has a lower coarse aggregate content than conventional-slump concrete, E_c will be lower for SCC than for normal concrete of the same strength (Bonen and Shah 2004). Therefore, it is important to evaluate E_{ci} for SCC to be used in prestressed applications.

Su et al. (2002) conducted research on how different sand-to-aggregate (*s/agg*) ratios would affect the modulus of elasticity of SCC. In Su et al.'s (2002) research, 6 different *s/agg* (0.3, 0.4, 0.45, 0.475, 0.5, 0.525, and 0.55) were considered in the mixture proportions. A constant aggregate volume fraction of 0.6 was kept for all mixtures as was a *w/p* of 0.4. By keeping a constant *w/p* and aggregate volume fraction, the only variable influencing the modulus of elasticity was the *s/agg*. The influence of the elastic modulus of the fine and coarse aggregate on the modulus of elasticity was also investigated. Su et al. (2002) concluded that when the fine and coarse aggregate have comparable elastic moduli, and the total volume of aggregate is held constant, the sand-to-aggregate ratio does not significantly affect the modulus of elasticity of the concrete. This is illustrated in Figure 2-20.

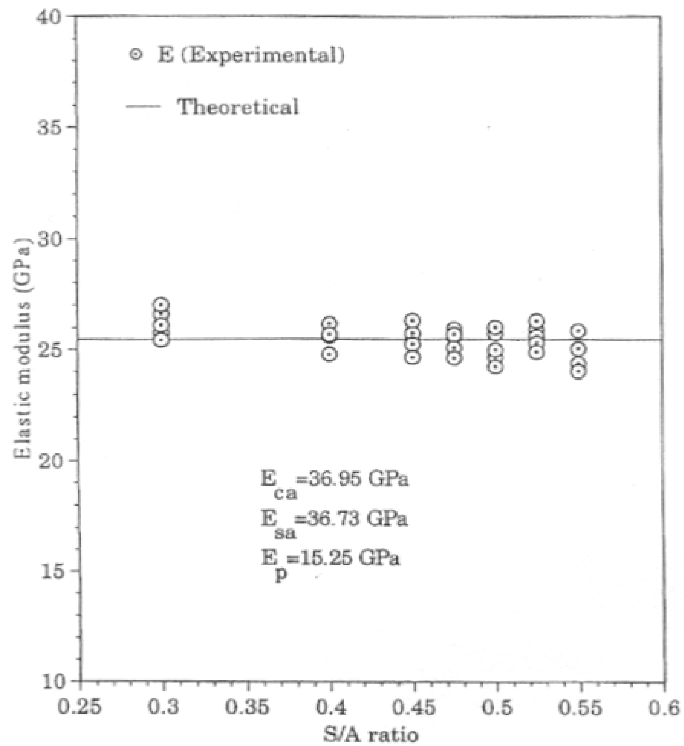

Figure 2-20: Elastic modulus versus sand-to-aggregate ratio (Su et al. 2002)

2.5.4 Drying Shrinkage

Shrinkage is an important aspect in the design of concrete elements. As Mindess, Young, and Darwin (2003) state "inadequate allowance for the effects of drying shrinkage in concrete design and construction can lead to cracking or warping of elements of the structure due to restraints present during shrinkage". Much of the prestress losses and some of the long-term deflection experienced by prestressed concrete members are the direct result of shrinkage (Huo, Al-Omaishi, and Tadros 2001). As water evaporates from concrete, the concrete contracts (Mindess, Young, and Darwin 2003). This contraction due to the loss of water is known as drying shrinkage.

Shrinkage is a paste property, and the aggregate is the most influential restraining influence on the change in volume within the paste (Neville 1996; Mindess, Young, and Darwin 2003). At a constant water-to-cement ratio, shrinkage increases with an increase in cement content because of the increasing volume of hydrated cement paste (Neville 1996). In turn, if the water content is held constant and the cement content is increased (low *w/c*), the amount of shrinkage can be reduced because the higher strength paste is more able to resist shrinkage (Neville 1996). Figure 2-21 shows how the water-to-cement ratio and the total aggregate content (by volume) influence the shrinkage strain. From Figure 2-21, it can be seen that at any water-to-cement ratio, an increase in the total aggregate content will reduce the amount of shrinkage.

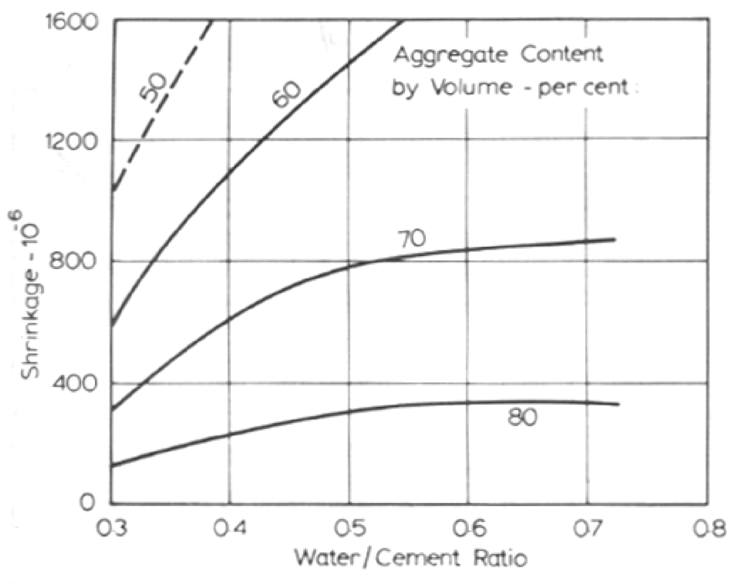

Figure 2-21: Influence of *w/c* and aggregate content on shrinkage (Neville 1996)

Neville (1996) also states that while the size and grading of the aggregate do not have significant influence on the shrinkage, increasing the maximum size of aggregate allows for a leaner mixture, thus reducing the amount of shrinkage. However, increasing the nominal maximum size aggregate used in SCC will prevent it from achieving its desired fresh properties. Prediction equations adopted by ACI Committee 209 (1997), which will be discussed in detail in Section 2.7.2.1, use the sand-to-aggregate ratio as a factor in determining the amount of shrinkage. According to ACI Committee 209 (1997), as the sand-to-aggregate ratio increases, so does the amount of drying shrinkage. Equations 2-7 and 2-8, found in Section 2.7.2.1, show how an increasing *s/agg* increases the fine aggregate correction factor, which will in turn increase the amount of drying shrinkage. When the *s/agg* is increased from 0.40 to 0.50, the amount of drying shrinkage is increased by 16%.

A high *w/c* and a small amount of coarse aggregate (or a large sand-to-aggregate ratio) will cause an increase in the amount of shrinkage. It has already been established that SCC needs a higher sand-to-aggregate ratio when compared to conventional concrete so that it meets its workability requirements. However, the shrinkage resulting from its higher sand-to-aggregate ratio might be countered by the use of a lower water-to-cement ratio.

Hindy et al. (1994) states that curing conditions have a significant effect on drying shrinkage. Air-cured specimens showed a pronounced increase in drying shrinkage compared with specimens that had been sealed. The research conducted by Hindy et al. (1994) showed that in any case, the longer the specimens were cured, the lower the drying shrinkage would be.

Raghavan, Sarma, and Chattopadhyay (2003) performed a study on the amount of drying shrinkage in conventional-slump concrete versus the amount of drying shrinkage in SCC. The SCC had more powder than the conventional-slump concrete, while the conventional-slump concrete had more coarse aggregate. The water contents were the same for each mix. The researchers found that the conventional-slump concrete had 25% more drying shrinkage than the SCC at 28 days. This can be attributed to the fact that the SCC had a lower *w/p* giving it a higher strength paste.

2.5.5 Creep

Naaman (2004) defines creep as "the time-dependent strain in excess of elastic strain induced in a material subjected to a sustained stress". Creep, like shrinkage, is a paste property; it too is dependent on many parameters, most notably the aggregate content and the aggregate modulus (Mindess, Young, and Darwin 2003). The role of the aggregate in creep is the same as it is in shrinkage, as it acts as a restraint to reduce potential deformations. Figure 2-22 shows how different types of aggregates affect creep. From Figure 2-22, it can be seen that limestone has the least amount of creep at early and later ages when compared to sandstone, gravel, and granite.

Creep also plays a vital role in the design of prestressed concrete elements. An accurate estimate of the amount of creep to be expected is important because the shortening strain in the concrete leads to a loss of prestress in the tendons (Naaman 2004). In the study conducted by Raghavan, Sarma, and Chattopadhyay (2003) mentioned previously, creep in SCC mixtures and conventional-slump concrete mixtures was compared. It was concluded that the initial elastic deformation is larger for SCC, but the final overall strain induced by creep is less in SCC than in conventional-slump concrete.

Circumstances prevented creep testing during the portion of the study reported in this thesis. However, research is being performed to obtain SCC's creep properties and will be published in the future.

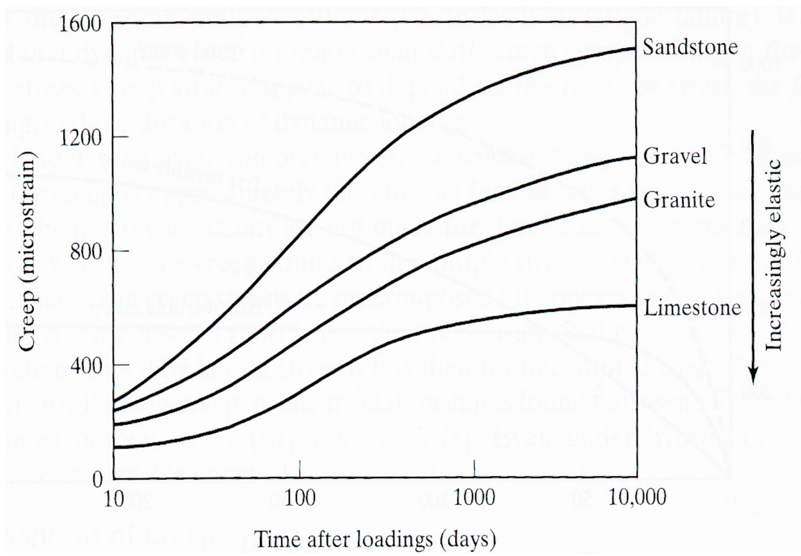

Figure 2-22: Effects of different types of aggregates on creep (Mindess, Young, and Darwin 2003)

2.6 PRODUCTION, QUALITY CONTROL, AND QUALITY ASSURANCE

2.6.1 PRODUCTION

In a continuous effort to improve economy and performance, improvement in concrete production is crucial, whether the applications are simple or the most advanced and demanding structures. One of SCC's most attractive assets is that it can improve the productivity of the concrete placement process. By eliminating the need for mechanical consolidation, the speed of construction is increased and the overall cost is reduced thus improving the overall productivity. The use of SCC will play a major role in increasing the competitiveness in the concrete industry and will also increase the performance for customers (Skarendahl 2000b).

2.6.1.1 Batching Accuracy

PCI (2003) stresses that the batching of SCC's constituents needs to be done with the highest amount of accuracy possible, because fluctuations in batching can significantly affect both fluidity and stability. SCC mixtures are far more sensitive to constituent material consistency and quantity variations during production. Variations in materials, such as gradations and moisture contents, can significantly affect a SCC mixture's stability. Fluctuation in the amount of mixture water will have a more pronounced affect on SCC mixtures than on conventional-slump and typical high-strength concretes (PCI 2003).

2.6.1.2 Mixing Sequence

Mixing sequences reviewed by the author varied greatly. For this reason, several different mixing sequences are outlined below. Methods A, B, and D are believed to be performed under laboratory conditions because the author of the relevant reports specified that the mixing was done in either a rotating-drum mixer or an open-pan mixer. Method C was conducted under laboratory conditions.

Method A: (Proposed by Khayat, Ghezal, and Hadriche 1999)

1. Homogenize the sand and coarse aggregate for 30 seconds.
2. Add 75% of the mixing water and all of the HRWR admixture that is not in the VMA-HRWR dispersion and mix for 30 seconds.

3. Add the cement and mix for one minute.
4. Add the remaining mixing water plus the VMA-HRWR dispersion and set retarder.
5. Mix for 3 minutes. Allow to rest for 2 minutes and then mix again for 2 additional minutes.

Method B: (Proposed by Khayat, Assaad, and Daczko 2004)

1. Homogenize the sand and coarse aggregate for 1 minute.
2. Introduce 1/3 of the mixing water.
3. Add cement, HRWR admixture, and another 1/3 of the mixing water and mix for 3 minutes.
4. Add the VMA, diluted in the remaining mixing water, and the set-retarding agent and mix for additional 2 minutes.

Method C: (Proposed by Sonebi and Bartos 2002)

1. Mix the sand and coarse aggregate, then add 25% of the mixing water.
2. Add any cementitious materials, the remaining mixing water, the HRWR admixture, and mix for 3 minutes.
3. After a 1-minute rest period, mix the concrete for an additional 2 minutes.

Method D: (Proposed by Khayat and Assaad 2002)

1. Homogenize the sand and cementitious materials for 1 minute before introducing 1/2 of the mixing water and 75% of the HRWR admixture.
2. Add the coarse aggregate, followed by the AEA and the remaining HRWR admixture.

3. Mix for 3 minutes then add the set-retarding admixture (if required) and the VMA diluted in the second half of the mixing water.
4. Keep the concrete at rest for 1 minute before mixing for an additional 2 minutes.

The mixing procedures outlined above are presented with as much detail as possible based on the information presented in the cited sources. From these four different mixing procedures, one can see that there is no universal mixing procedure for SCC.

2.6.1.3 Transportation

Productivity can also be improved by the method of transportation. It has been well established that the dynamic and static stability of SCC is of great importance. Because of the risk of segregation involved with transportation from the production site to the building site, agitator trucks are the most common means of transportation (Takada 2000). The quality of SCC in its fresh state depends on the amount of time elapsed after mixing. The SCC's filling ability will change over a short period of time as the effectiveness of the HRWR admixture is reduced. For this reason, the transportation time should be as short as possible, and in most cases, it should not exceed 60 minutes (Takada 2000). For high-strength prestressed concrete mixtures, this time is reduced to 30 minutes. Other means of transporting SCC at the jobsite are discussed in Section 2.6.1.4.

2.6.1.4 Placement

Two main production issues that will affect the fresh properties of SCC are the type of placement and the intricacy of the element being cast (PCI 2003). Several types of placement are available such as a truck, pump, crane and bucket, or an auger. SCC's fluidity has created the development of new pumping and formwork procedures thus resulting in new casting processes (Skarendahl 2000b). The force required to pump SCC depends on its viscosity; the higher the viscosity, the higher the pump pressure required (Takada 2000). SCC with a low viscosity will require approximately the same pump pressure as normal concrete (Takada 2000). Pumping the SCC also affects its fresh properties. Takada (2000) reported that, for the most part, slump flow values decreased after pumping. Figure 2-23 (Skarendahl 2000b) illustrates the pumping of SCC into formwork while Figure 2-24 (Skarendahl 2000b) shows the casting of SCC performed by a single operator.

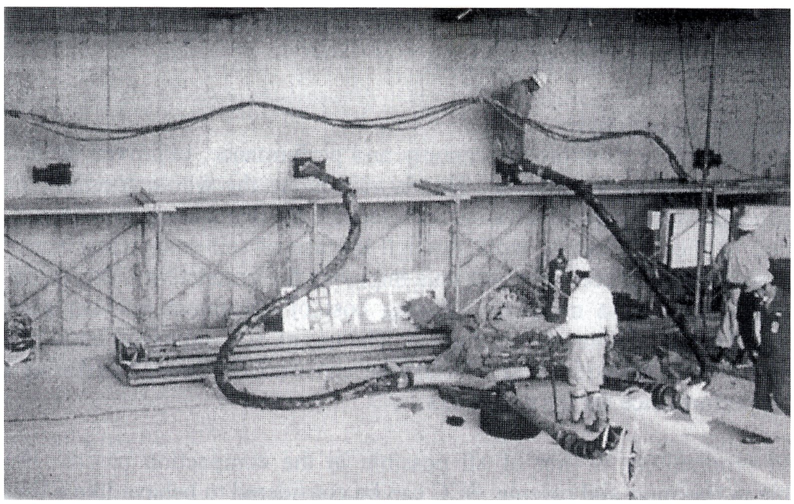

Figure 2-23: SCC being pumped into formwork by means of a bifurcating pipe hose (Skarendahl 2000b)

Figure 2-24: Single pump operator casting a bridge pier foundation (Skarendahl 2000b)

When a ready-mix truck is used, the mixture will have increased flowing distances and improved filling capacities because the speed of discharge and the volume of concrete is high and continuous (Bury and Buhler 2003). A hopper/bucket is slower and more discontinuous as compared to the truck. For this reason, the mixture may have to have a higher slump flow. Bury and Buhler (2003) report that “SCC users find that it is advantageous in their precast/prestress operations to switch to larger volume transport vehicles such as ready-mixture trucks rather than Tuckerbuilt transporters”. This allows producers to cast entire members from one batch and avoid a situation where the batching of the concrete might not be able to keep up with the speed of placement (Bury and Buhler 2003). Table 2-12 summarizes the various placement techniques and their discharge characteristics as presented by PCI (2003).

Table 2-12: Placement techniques and discharge characteristics (PCI 2003)

Placement Technique	Discharge Rate	Discharge Type	Single Discharge Volume	Relative Energy Delivered
Truck Discharge	High	Continuous	High	High
Pumping	Medium/High	Continuous	Medium	High/Medium
Crane and Bucket	High	Discontinuous	Low	Medium
Auger Discharge	Low/Medium	Continuous	Medium	Low/Medium

Other concerns with the placement of SCC are the height from which the concrete must be dropped and the distance that it must flow. While the distance from the surface to the mouth of the discharge pipe is usually controlled to be between 0-5 m (0-16 ft), it has been reported that a distance of 8 m (26 ft) has given sufficient results, although casting SCC directly onto the surface after passing through reinforcement can lead to the separation of coarse aggregates from the paste (Takada 2000). PCI (2003) agrees that properly designed and qualified SCC mixtures can fall from heights in excess of 10 ft without segregating, but that segregation is a possibility when falling through reinforcement. Permitting the direct free-fall of SCC is not agreed upon by everyone. Bury and Buhler (2003) recommend avoiding direct free-fall of SCC altogether.

Takada (2000) discusses the importance of the distance that the concrete must flow. This distance is controlled not only by the mixture proportion of the concrete, but also by the boundary conditions of the formwork, i.e. the shape and arrangement of reinforcement. Based on Japanese research, it has been reported that if the mixture is properly designed, segregation will not occur if the horizontal distance does not exceed 10 m (33 ft). In most cases, the distance has been restricted not to exceed 3-10 m (10-33 ft). Therefore, casting points need to be set so that intervals do not exceed 6-20 m (20-66 ft). The casting rate is also significant. If the casting rate exceeds the rate of self-weight flowing, air is entrapped and honeycombs form on the surface of the concrete (Takada 2000).

2.6.1.5 Formwork Issues

Other main factors affecting the production of SCC are the intricacy of the formwork and the lateral pressure exerted on the formwork by the concrete. As the complexity of the formwork increases, there is a decrease in the mixture's ability to fill the formwork sufficiently without any voids or honeycombs internally or on the formed surface (PCI 2003; Bury and Buhler 2003). There are seven element characteristics to consider in the production of SCC (PCI 2003). These characteristics are:

1. **Reinforcement Level**: This characteristic involves the minimum clear spacing between between reinforcement as well as the spacing between the form walls and the reinforcement. As the reinforcement level increases, so does the possibility for segregation and blocking to occur. A high level of reinforcement will require a higher slump flow with adequate passing ability (PCI 2003).
2. **Element Shape Intricacy**: How difficult will it be for the mixture to fill the formwork without leaving significant voids on the surface as well as internally? As the intricacy level increases, so does the requirement for a higher slump flow (PCI 2003).

3. **Element Depth**: This refers to the depth at which the fresh concrete will be placed. As the depth increases, requirements for the dynamic and static stabilities of the mixture will also increase (PCI 2003).
4. **Surface Finish Importance**: This depends on the necessity of having a superior surface finish. In general, improved surface appearance is obtained with higher levels of fluidity with controlled viscosity (PCI 2003).
5. **Element Length**: How far must the SCC flow from the discharge point to completely fill the formwork? Element length must be taken into consideration when determining required levels of fluidity and dynamic stability (PCI 2003).
6. **Coarse Aggregate Content**: This characteristic was created to cover the application of having an exposed aggregate finish. To achieve this visual effect, higher volumes of coarse aggregate may be required. Since coarse aggregate content is a major issue in controlling a SCC mixture's passing ability, the effects of a higher volume of coarse aggregate must be taken into consideration (PCI 2003).
7. **Wall Thickness**: Wall spacing within the formwork will affect the ability of the SCC mixture to fill the element. The ability of entrapped voids to escape without leaving surface defects will also be affected. Generally speaking, thin walls will require a higher slump flow.

Before the concrete is placed, considerable attention needs to be given to the amount of pressure that will be exerted on the forms. The shape and dimension of the structure, temperature, casting rate, proportioning of the mixture, and still other factors control the lateral pressure that SCC places on the formwork (Takada 2000; Khayat, Assaad, and Mesbah 2003).

Khayat, Assaad, and Mesbah (2003) explain that, independent from other factors, the lateral pressure tends to increase as the casting rate increases. Due to the fact that the lateral pressure is directly related to the shear strength of the plastic concrete, a lower casting rate allows the concrete more time to build up shear strength which results in slightly lower lateral pressures. One of the main factors affecting the lateral pressures on the formwork appears to be the mixture's thixotropy (see Section 2.3.4.2) (Khayat, Assaad, and Mesbah 2003).

After the concrete has come to rest in the form, there is an initial drop in lateral pressure which can be attributed to the reversible effect of the thixotropy (shear recovery) which allows the material to re-gain its shear strength properties (internal friction and cohesion). This causes a "restructuring" of the concrete and an increase in rigidity. Research has indicated that mixtures with higher thixotropy developed lower initial lateral pressure and also exhibited a faster drop in pressure after casting was complete (Khayat, Assaad, and Mesbah 2003).

While lateral pressures will decrease with increasing thixotropy and decreasing casting rates, producers need a simple, concise way to design their forms. It has been reported in Japan that the lateral pressure on the forms is approximately 80-95% of the fluid pressure, which is taken to be the unit weight of the concrete times the covering height of the placed concrete (Takada 2000). For safety purposes, Takada (2000) recommends that formwork be designed to endure the full liquid pressure.

2.6.1.6 Working Environment

The use of SCC also improves the working environment, thereby increasing the total cost efficiency of concrete construction. Improvement of working conditions enables companies to retain experienced and valuable staff while reducing societal health-care costs. The use of SCC creates a quieter workplace with limited physical work, and with no transformers, cables, or vibrators (handheld, surface, or form) to hinder the work. This allows the worker to focus his attention on the quality of concrete placement. The reduction in noise is beneficial not only to the workers but for the neighbors of the concrete plant as well (Skarendahl 2000b).

In Sweden, SCC has already been used for highway and dwelling applications. Persson (2000) states that not only has there been a 60% increase in productivity, but that by using SCC, both the conditions for the worker and for the surroundings have been improved by lowering the noise level of construction and diminishing the effects on the environment.

2.6.2 Quality Control and Quality Assurance

Mindess, Young, and Darwin (2003) define quality assurance as "all of the steps taken to ensure adequate confidence that the concrete will perform satisfactorily in service" while they define quality control as "each action used to measure the properties of the concrete, or its components, and to control them within the established specifications". To ensure mixture design qualification during development, each SCC mixture should undergo production-based confirmation, assessing both the fresh and hardened states (PCI 2003).

One important qualification procedure for SCC mixtures is to make trial batches from production mixers and adjust the mixture as necessary to achieve the desired properties

(PCI 2003). This is essential because often there are considerable differences in the fresh performance of SCC that was mixed in a small lab mixer when compared to the same mixture created in a production mixer at a plant. Once mixture designs have been finalized, appropriate test methods should be identified. An optimum combination of test methods to assess SCC in the fresh state has yet to be defined; however, the PCI (2003) suggests that quality-control testing should be no less for SCC than for conventional-slump concrete.

It is the producer's responsibility to select the appropriate test method(s) for qualification of his SCC mixture depending on the mixture's applications (PCI 2003). Therefore, one can assume that different test methods may be appropriate for different mixture applications. The PCI (2003) goes on to say that the "concrete supplier and precast producer (if different) should, therefore, agree on a procedure for acceptance/compliance at the start of a contract". This agreement should also include a procedure for action to be taken if the concrete should be rejected (PCI 2003). During the acceptance inspection of the fresh properties of SCC, the quality should be verified to satisfy the expected range of values (Takada 2000). Target control values may vary according to the materials used, the mixture proportions, and the intricacy of the formwork (Takada 2000). Tables 2-13 through 2-16 give guidance for what typical values might be for different applications. The dark blocks represent potential problem areas. For example, in Table 2-13, if the reinforcement level is medium, but the element shape intricacy is high, a slump flow greater than 26 in. is suggested.

Table 2-13: Slump flow parameter determination (PCI 2003)

			Slump flow		
			<22"	22-26"	>26"
Member Characteristics	Reinforcement Level	Low			
		Medium	■		
		High	■		
	Element Shape Intricacy	Low			
		Medium	■		
		High	■	■	
	Element Depth	Low			
		Medium			
		High			
	Surface Finish Importance	Low			
		Medium	■		
		High	■	■	
	Element Length	Low			
		Medium	■		
		High	■	■	
	Wall Thickness	Low	■	■	
		Medium	■		
		High			
	Coarse Aggregate Content	Low			
		Medium			
		High			
	Placement Energy	Low	■	■	
		Medium	■		
		High			

Dark blocks represent potential problem areas.

Table 2-14: T-50 time parameter determination (PCI 2003)

			T 50 time		
			<3 sec	3-5 sec	>5 sec
Member Characteristics	Reinforcement Level	Low			
		Medium	■		
		High	■		
	Element Shape Intricacy	Low			
		Medium			■
		High			■
	Element Depth	Low			
		Medium			
		High	■		
	Surface Finish Importance	Low			
		Medium			■
		High			■
	Element Length	Low			
		Medium			
		High	■		
	Wall Thickness	Low			■
		Medium			
		High			
	Coarse Aggregate Content	Low			
		Medium			
		High			
	Placement Energy	Low			
		Medium			
		High	■		

Dark blocks represent potential problem areas.

Table 2-15: L-Box blocking ratio (%) parameter determination (PCI 2003)

			L-Box		
			<75	75-90	>90
Member Characteristics	Reinforcement Level	Low			
		Medium	■		
		High	■		
	Element Shape Intricacy	Low			
		Medium			
		High			
	Element Depth	Low			
		Medium			
		High			
	Surface Finish Importance	Low			
		Medium			
		High			
	Element Length	Low			
		Medium	■		
		High	■	■	
	Wall Thickness	Low	■		
		Medium			
		High			
	Coarse Aggregate Content	Low			
		Medium			
		High			■
	Placement Energy	Low	■		
		Medium			
		High			

Dark blocks represent potential problem areas.

Table 2-16: J-Ring value (mm) determination (PCI 2003)

J-Ring and Inverted Slump Cone Test Parameter Determination		Passing Ability: Excellent [<15]	Passing Ability: Good [10 – 15]	Passing Ability: Poor [>10]
Reinforcement Level	Low			
	Medium			■
	High		■	■
Element Shape Intricacy	Low			
	Medium			
	High		■	■
Element Depth	Low			
	Medium			■
	High		■	■
Surface Finish	Low			
	Medium			
	High			
Element Length	Low			
	Medium			■
	High		■	■
Wall Thickness	Low			
	Medium			
	High			
Coarse Aggregate Content	Low			
	Medium			■
	High		■	■
Placement Energy	Low		■	■
	Medium			■
	High			

Dark blocks represent potential problem areas.

***NOTE:** *Excellent* should read [<10] and *Poor* should read [>15].

To verify quality confirmation of hardened SCC, the same tests and procedures that have been used for conventional-slump concrete should also be used for SCC. If shrinkage and creep characteristics are important design parameters (i.e. if limits have been specified), tests need to be performed to ensure these limits have not been exceeded (PCI 2003).

When planning their quality assurance programs, PCI producers have long relied on a successful history of concrete mixture design and constituent material performance. However, this history will not be initially available with SCC to guide the growth of efficient and economical quality assurance programs. Thus, until this background has been developed within the industry (including producer plants), quality-control inspectors must be properly trained in the various testing procedures and methods and know how to evaluate those results (PCI 2003).

2.7 MODULUS OF ELASTICITY AND DRYING SHRINKAGE PREDICTIONS

2.7.1 PREDICTION OF MODULUS OF ELASTICITY

According to the *AASHTO LRFD Bridge Design Specifications* and ACI 318 (2005), the modulus of elasticity can be estimated from the compressive strength and unit weight using Equation 2-2.

$$E_c = 33\, w_c^{1.5} \sqrt{f'_c} \qquad \textit{(Equation 2-2)}$$

In Equation 2-2, E_c represents the modulus of elasticity in psi, w_c is the unit weight of the concrete in lb/ft^3, and f'_c is the compressive strength in psi. ACI 318 (2005) recommends that this equation be used for concretes with a w_c between 90 and 150 lb/ft^3 and compressive strengths up to 6000 psi. ACI Committee 363 (1997) concludes that Equation 2-2 overestimates the modulus of elasticity for concretes with compressive strengths greater than 6,000 psi. For this reason, ACI Committee 363 (1997) developed another equation for determining the value of E_c for high-strength concretes. According to ACI Committee 363 (1997), Equation 2-3 is valid for normal-weight concretes with compressive strengths ranging from 3,000 to 12,000 psi.

$$E_c = 40{,}000\sqrt{f'_c} + 1{,}000{,}000 \qquad \textit{(Equation 2-3)}$$

In Equation 2-3, E_c and f'_c are in psi and represent the modulus of elasticity and the compressive strength respectively.

Research has also been carried out to see how accurately these equations estimate measured values of E_c. Huo, Al-Omaishi, and Tadros (2001) report that research conducted at the University of Minnesota found the ACI 318 equation to overestimate the modulus of elasticity for high-strength concrete. These results are not surprising due to the fact that ACI Committee 363 (1997) formulated Equation 2-3 to more accurately predict the modulus of elasticity for higher-strength concretes. However, researchers from the University of Texas at Austin showed that using a higher content of coarse aggregate with a smaller maximum size made it possible to achieve higher values of E_c. After comparison of these test results with ACI 318 values, it was concluded that the ACI 318 equation underestimates the modulus, especially at early ages (Huo, Al-Omaishi, and Tadros 2001).

ACI Committee 363 (1997) reports that various researchers have found Equation 2-3 to underestimate values of E_c for high-strength concrete. While opinions on the prediction equations for the modulus of elasticity vary, the best way to obtain the value of E_c is to perform the modulus of elasticity test prescribed in ASTM C 469 (1998) (Huo, Al-Omaishi, and Tadros 2001).

2.7.2 Prediction of Shrinkage

There are several methods available for predicting the ultimate shrinkage strain of conventional and/or high-strength concrete. However, there is no universally accepted method for SCC. Three of the most common methods available are summarized below.

2.7.2.1 ACI 209

The ACI 209 Committee Report (1997) was devised to create a unified approach for predicting shrinkage and creep for concrete. All of the equations presented on shrinkage in the ACI 209 Committee Report (1997) are simplified expressions resulting from lab testing under steady environmental conditions. The committee stresses that "no prediction method can yield better results than testing actual materials under environmental and loading conditions similar to those expected in the field" (ACI 209 1997).

ACI Committee 209 (1997) uses an ultimate shrinkage coefficient for predicting the shrinkage strain. This coefficient is adjusted by various correction factors to account for a variety of environmental conditions and design aspects. It also uses a time-rate function to obtain the shrinkage at different ages after curing. The correction factors used in predicting the shrinkage account for variability in humidity, volume-to-surface ratio (V/S), fine aggregate percentage, slump, cement content, air content, curing period, and curing method.

The fine aggregate percentage, air content, slump, and cement content usually do not greatly affect the estimate and can therefore be neglected (ACI 209 1997). Neglecting these factors is advantageous for a designer since this information is not usually known at the design stage. For the purposes of this project, all of these factors were taken into account since they were known.

The following equations are used by ACI 209 to modify the ultimate drying shrinkage:

$$(\varepsilon_{sh})_u=(\gamma_{sh})780*10^{-6}\ in./in. \qquad \textit{(Equation 2-4)}$$

where $(\varepsilon_{sh})_u$ is the ultimate drying shrinkage strain and $\gamma_{sh} = (\gamma_\lambda*\gamma_{vs}*\gamma_\psi*\gamma_s*\gamma_c*\gamma_a*\gamma_{cp})$ is the ultimate drying shrinkage correction factor.

γ_λ is the humidity correction factor:

$$\gamma_\lambda=1.40-.010H, for\ 40 \leq H \leq 80 \qquad \textit{(Equation 2-5)}$$

where H is relative humidity in percent.

γ_{vs} is the volume-to-surface ratio correction factor:

$$\gamma_{vs}=1.2\ exp(-0.12\ V/S) \qquad \textit{(Equaiton 2-6)}$$

where V/S is the volume to surface ratio in inches.

γ_ψ is the fine aggregate percentage correction factor:

$$\gamma_\psi=0.30 + .014\Psi,\ for\ \Psi \leq 50\ percent \qquad \textit{(Equation 2-7)}$$

$$\gamma_\psi=0.90 + .002\Psi,\ for\ \Psi > 50\ percent \qquad \textit{(Equation 2-8)}$$

where Ψ is the ratio of the fine aggregate to total aggregate by weight expressed as a percentage.

γ_s is the slump correction factor:

$$\gamma_s=0.89 + 0.041s \qquad \textit{(Equation 2-9)}$$

where s is the observed slump in inches.

γ_c is the cement content correction factor:

$$\gamma_c = 0.75 + 0.00036c \qquad \text{(Equation 2-10)}$$

where c is the cement content in pounds per cubic yard.

γ_a is the air content correction factor:

$$\gamma_a = 0.95 + 0.008a \qquad \text{(Equation 2-11)}$$

where a is the air content in percent.

γ_{cp} is the curing period factor:

$$\gamma_{cp(28)} = 0.86 \qquad \text{(Equation 2-12)}$$

where $\gamma_{cp(28)}$ is constant for 28-day moist curing, or

$$\gamma_{cp(7)} = 1.00 \qquad \text{(Equation 2-13)}$$

where $\gamma_{cp(7)}$ is constant for 7-day moist curing.

γ_t is the concrete age adjustment function:

$$\gamma_t = \frac{t}{35 + t} \qquad \text{(Equation 2-14)}$$

where t is the length of time the concrete has been exposed to the air in days (after the curing period has ended). The age adjustment function coupled with the ultimate shrinkage coefficient will yield the shrinkage at any time.

$$\varepsilon_{sh}(t) = (\varepsilon_{sh})_u * \gamma_t \qquad \text{(Equation 2-15)}$$

The ultimate shrinkage strain is the predicted infinite-age shrinkage strain in in./in. The age adjustment factor, which is subject to change depending on the day in question, enables the designer to obtain a prediction at different time intervals (i.e. 7 days, 14 days, 32 weeks, etc.). However, care should be taken when this coefficient is used. The amount of shrinkage from Day 7 to Day 28 (after cessation of moist curing), can be determined by taking the 28-day factor and subtracting the 7-day factor before multiplying the difference by the ultimate shrinkage strain.

2.7.2.2 AASHTO LRFD Bridge Design Specifications

The *AASHTO LRFD Bridge Design Specification*s (hereafter referred to as AASHTO LRFD) is intended for the design of bridge and retaining wall components constructed of normal-weight or lightweight concrete and reinforced with steel bars, welded wire reinforcement, and/or prestressing strands, bars, or wires. These provisions are based on the concrete having a compressive strength between 2.4 ksi and 10.0 ksi, unless higher strengths are allowed.

The shrinkage values obtained through the use of the AASHTO LRFD can be used to determine the effects of shrinkage on the loss of prestressing force in the structure in question. While AASHTO acknowledges that shrinkage can be attributed to aggregate characteristics and proportions, average humidity at the bridge site, water-to-cement ratio, type of curing, *V/S*, and drying period, its ultimate shrinkage coefficient only takes into account *V/S*, type of curing, humidity, and drying age.

AASHTO LRFD uses the following equation and related factors to predict the drying shrinkage strain for moist-cured concrete:

Drying shrinkage strain:

$$(\varepsilon_{sh})_u = -k_s k_h \left(\frac{t}{35+t}\right) 0.51*10^{-3} \qquad \text{(Equation 2-16)}$$

where $(\varepsilon_{sh})_u$ is the drying shrinkage strain and t is the drying time in days.

k_s is the size adjustment factor:

$$k_s = \left[\frac{\dfrac{t}{26e^{0.36(V/S)} + t}}{\dfrac{t}{45 + t}} \right] \left[\frac{1064 - 94(V/S)}{923} \right] \qquad \textit{(Equation 2-17)}$$

where *V/S* is the volume-to-surface ratio including only the surface area that is exposed to the atmospheric drying, and *t* is the drying time in days.

k_h is the humidity correction factor:

$$k_h = \frac{140 - H}{70}, \textit{ for } H < 80\% \qquad \textit{(Equation 2-18)}$$

$$k_h = \frac{3(100 - H)}{70}, \textit{ for } H \geq 80\% \qquad \textit{(Equation 2-19)}$$

where *H* is the relative humidity in percent.

2.7.2.3 NCHRP 496

Tadros et al. (2003) compiled NCHRP Report 496 in an effort to develop design guidelines, consistent in form with existing formulas, for predicting prestress losses in high-strength pretensioned concrete girder bridges. Two areas of particular concern that account for prestress losses are creep and shrinkage.

The proposed formula for ultimate shrinkage strain is similar in approach to the shrinkage formulas found in the ACI 209 Committee Report and AASHTO LRFD. Since the AASHTO LRFD and the ACI 209 methods overestimate the ultimate drying shrinkage of high-strength concrete, Tadros et al. made modifications to account for the drying shrinkage associated with these higher concrete strengths.

The NCHRP Report 496 (Tadros et al. 2003) uses an ultimate shrinkage strain for predicting the shrinkage losses. This strain is modified by various correction factors to account for environmental conditions and design aspects. This method also uses a time-development correction factor to estimate the effects of shrinkage at different drying times. The correction factors used to predict the shrinkage account for changes in humidity, volume-to-surface ratio (*V/S*), concrete strength, and drying age (Tadros et al. 2003).

The ultimate shrinkage strain is computed using Equation 2-20 and the associated correction factors:

$$(\varepsilon_{sh})_u=(\gamma_{sh})480*10^{-6} \text{ in./in.} \qquad \text{(Equation 2-20)}$$

where $(\varepsilon_{sh})_u$ is the ultimate drying shrinkage, and $\gamma_{sh} = k_s*k_{hs}*k_f$, where γ_{sh} is the ultimate drying shrinkage correction coefficient.

k_{hs} is the relative humidity correction factor:

$$k_{hs} = 2.00-0.0143*H \qquad \text{(Equation 2-21)}$$

where *H* is the relative humidity in percent. Figure 2-25, adopted from AASHTO LRFD, shows the average annual relative humidity in percent for the United States and Canada.

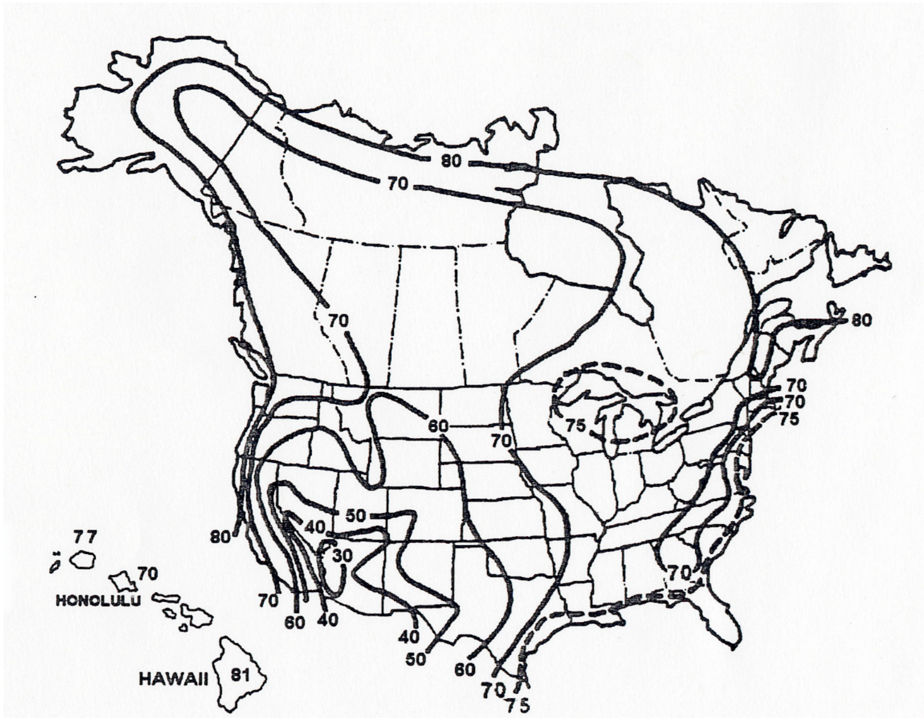

Figure 2-25: Average annual relative humidity in percent for the United States and Canada (Tadros et al. 2003)

k_s is the volume-to-surface ratio correction factor:

$$k_s = \frac{1064 - 94(V/S)}{735} \qquad \textit{(Equation 2-22)}$$

where *V/S* is taken as the ratio of cross-sectional area to the perimeter exposed to the environment.

k_f is the concrete strength correction factor:

$$k_f = \frac{5}{1 + f'_{ci}} \qquad \textit{(Equation 2-23)}$$

where f'_{ci} is the specified compressive strength at prestress transfer for prestressed members or 80% of the strength at service for non-prestressed members in ksi.

There is also a time-development correction factor, k_{td}:

$$k_{td} = \frac{t}{61 - 4f'_{ci} + t} \qquad \textit{(Equation 2-24)}$$

where t is the age of concrete in days after the curing period has ended. The time-development factor coupled with the ultimate shrinkage strain will yield the shrinkage at any time.

$$\varepsilon_{sh}(t) = (\varepsilon_{sh})_u * k_{td} \qquad \textit{(Equation 2-25)}$$

The time-development correction factor specified by Tadros et al. (2003) in NCHRP Report 496 is intended to account for increasing concrete strength over time; the higher-strength concretes tend to have accelerated shrinkage at early ages. This specific factor was one of the limitations of the AASHTO LRFD and ACI 209 predictions for ultimate shrinkage strain (Tadros et al. 2003).

Other factors, such as fine aggregate ratio, air and cement content, and slump were disregarded in the formulation of the shrinkage strain coefficient because of their reported minor effects (Tadros et al. 2003).

2.8 SUMMARY

Based on the literature reviewed for this report, the following main points are summarized for emphasis:

- SCC is a highly flowable, yet cohesive, concrete that is able to fill formwork and completely encapsulate any reinforcement without any external vibration.
- SCC has three fresh property requirements: adequate filling ability, adequate passing ability, and resistance to segregation.

- There must be enough tests available at the production facility and placement location to assess all three of these requirements.
- Because there are a variety of different mixture constituents, proportions, and mixing procedures, it is recommended that trial batches be produced to assess both the fresh and hardened states of the SCC mixture.
- While there are many different types of raw materials that may be used to produce SCC, particular attention needs to be given to the nominal maximum size of aggregate and the amount of moisture already contained in the raw materials.
- The use of a HRWR admixture based on polycarboxylate chemistry is a necessity for every SCC mixture.
- Before mixing, it is important to know the characteristics of the formwork and reinforcement details so that the mixture can be adjusted accordingly.
- If the mixture does not satisfly any of the three fresh property requirements, the concrete producer can try any of the approaches outlined in Sections 2.3.1.1 through 2.3.1.3.

CHAPTER 3

EXPERIMENTAL TESTING PROGRAM AND MATERIALS

3.1 INTRODUCTION

An objective of this study was to develop SCC mixtures with fresh and hardened properties to perform well in prestressed concrete applications. As with the development of any new product, the performance criteria and testing procedures had to be outlined before the research could begin. An in-depth discussion about the research was held in a meeting on February 4, 2004, at the Alabama Department of Transportation (ALDOT) Bridge Division, located in Montgomery, AL. Members of the research team, along with representatives from FHWA, ALDOT, the chemical admixture industry, and the precast/prestressed industry discussed the specifics of how the research should be conducted and which materials should be used.

Each party had expertise related to different aspects of the project. All facets of the project were reviewed including the experimental testing program, test procedures, and the selection of the raw materials. Each party voiced its concerns and opinions on how the research was to be conducted. From this meeting, the types of fine and coarse aggregates to be used were selected as well as the types of supplementary cementing materials (SCMs). A complete experimental testing program was outlined as well as how to perform all of the tests to assess the SCC mixtures' fresh properties.

3.2 EXPERIMENTAL TESTING PROGRAM

An overview of the experimental work involving SCC is outlined in Figure 3-1. The experimental testing program for this research consisted of two phases. The first phase involved the testing and evaluation of each SCC mixture in its fresh state while the second phase focused on the testing and assessment of each SCC mixture's hardened properties. the majority of the work documented in this project will refer to Phase I unless stated otherwise. The author was solely responsible for Phase I and assisted in the completion of Phase II. The conventional slump mixture and the four SCC mixtures used for Phase II were a direct result from the work the test results obtained from Phase I.

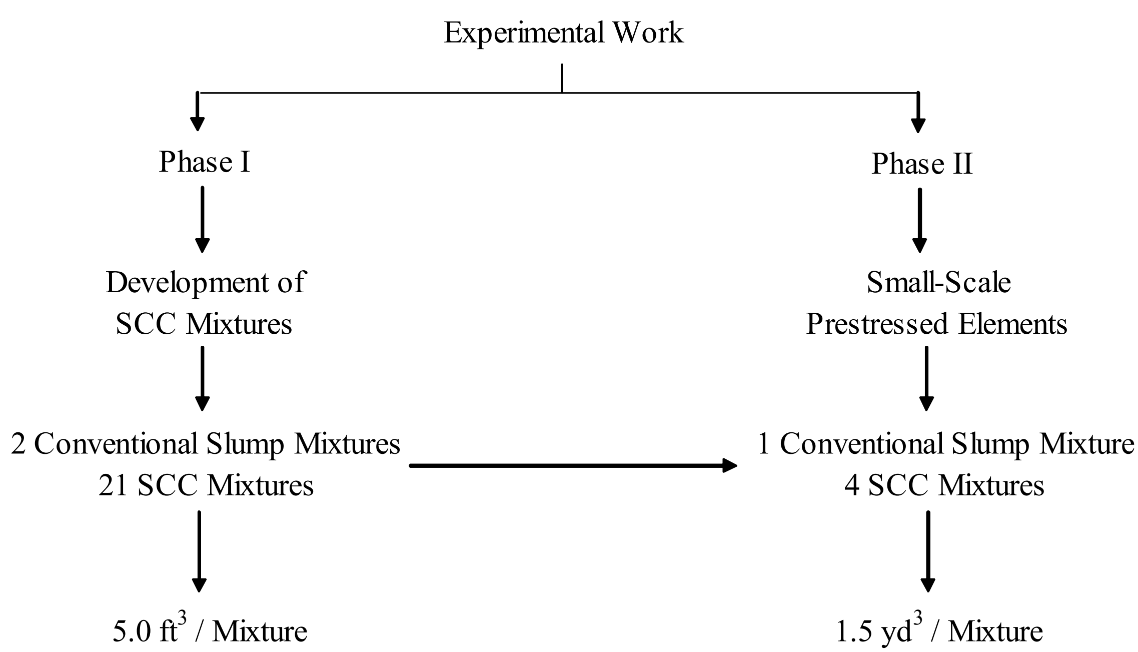

Figure 3-1: Overview of experimental work performed with SCC

It was decided that the slump flow, VSI, T-50, unit weight, temperature, and air content would be tested for every mixture. Running all of these tests, along with inspecting the mixing drum, gave a good indication on whether or not the mixture would have adequate filling ability, passing ability, and resistance to segregation. Although no test was used that directly tests the passing ability, segregation can give a good indication of the passing ability because segregation promotes blockage which leads to insufficient passing ability. The L-Box and J-Ring tests were also used, in addition to all of the other tests previously mentioned, when extra workers were available. However, both of these tests were used to evaluate the fresh properties of the SCC mixtures that were selected for creating the small-scale prestressed elements in Phase II.

3.2.1 Requirements for SCC Mixtures

All of the following requirements were based on discussions from the meeting held in Montgomery, AL. These requirements were considered to be representative of published literature on SCC at the time of the meeting except for the total air content requirement, which varies from state to state.

3.2.1.1 Fresh Properties

For each mixture's fresh properties, it was decided that the slump flow should be 27 in. ± 3 in. This range allows for some variability in materials, weather conditions, and inherent variability of this test method. The VSI rating should be below 2.0. In Table 2-2, it is stated that a mixture with a VSI of 2.0 will have a noticeable layer of mortar on the surface of the concrete in the mixer and a mortar halo on the slump patty. The air content should be 4% ± 1%, which is the range required by the ALDOT 2002 Standard Specification. If any of these parameters were not met, the mixture was subjected to rejection depending on how extreme its variation was (e.g. a mixture with a slump flow of 27 in., a VSI rating of 1.5, and an air content of 5.2% would not be discarded). The temperature, unit weight, T-50, blocking ratio (L-Box), and passing ability rating (J-Ring) were recorded but not used as a source of rejection.

3.2.1.2 Hardened Properties

An average compressive strength at release (f'_{ci}) that is used in the Alabama prestressed industry is approximately 6,500 psi (45 MPa). It was determined that SCC mixtures for this study should be evaluated that have a f'_{ci} range of 5,000 to 9,000 psi (34 to 62 MPa) at a release age of 18 hours. This specified range will be for cylinders that have been exposed to elevated curing temperatures to simulate the steam curing conditions commonly used in prestressing plants. There were no guidelines for what the modulus of elasticity should be, nor were there limitations on the amount of allowable shrinkage. Therefore, the modulus of elasticity and drying shrinkage results of the SCC mixtures will be compared to those obtained from two conventional-slump concrete mixtures and those obtained from current design formulas.

3.2.2 Experimental Test Factorial

A total of 21 SCC mixtures and 2 conventional-slump concrete mixtures were produced for this research. Table 3-1 indicates all of the SCC mixtures' identification numbers as well as their water-to-powder ratios (*w/p*) by mass, sand-to-aggregate ratios (*s/agg*) by volume, and powder combinations. The powder combinations shown in Table 3-1 shows how much SCM (in percent) was used to replace Type III cement. For example, SCC1:0.28-0.38-FA, would have a *w/p* of 0.28, a *s/agg* of 0.38, and its powder combination would consist of Type III cement and Class C fly ash. Upon further observation, one can see that of the 929 lbs/yd^3 used for this particular SCC mixture, 70% would be Type III cement and 30% would be Class C fly ash. All powder combinations contain Type III cement. S represents Grade 120 GGBF slag, while ternary consists of silica fume and Class C fly ash. The exact mixture proportions for all of these mixtures are shown in Table 3-2. The fine and coarse aggregate weights are in terms of saturated surface dry condition.

Initially the *w/p* varied between 0.28, 0.32, and 0.36. While most documents' *w/p* ranges fell closer to 0.32 and 0.36, a ratio of 0.28 was selected because this low *w/p* was required to obtain 9,000 psi release strengths. Bonen and Shah (2003) experimented with SCC mixtures having a *w/p* ranging from 0.25 to 0.50, while Sonebi (2004) produced valid mixtures with a *w/p* ranging from 0.38 to 0.72. A higher *w/p* of 0.40 was used for mixtures containing silica fume to determine if the minimum prestress strength transfer requirements could be met and if the mixture would have adequate fresh properties. Also, a higher *w/p* (at a constant water content) would reduce the overall cost of the mixture. The effects of varying the *w/p* on the fresh and hardened properties of the SCC mixtures are analyzed in Chapter 4.

Table 3-1: Experimental mixture plan and mixture identification

Powder Combination	Sand/Aggregate Ratio	Water-to-Powder Ratio			
		0.28	**0.32**	**0.36**	**0.40**
		powder = 929 pcy	powder = 828 pcy	powder = 750 pcy	powder = 688 pcy
	(by volume)	water = 260 pcy	water =265 pcy	water = 270 pcy	water = 275 pcy
Type III cement + 30% Class C fly ash	0.38	SCC1:0.28-0.38-FA	SCC2:0.32-0.38-FA	SCC3:0.36-0.38-FA	
	0.42	SCC4:0.28-0.42-FA	SCC5:0.32-0.42-FA	SCC6:0.36-0.42-FA	
	0.46	SCC7:0.28-0.46-FA	SCC8:0.32-0.46-FA	SCC9:0.36-0.46-FA	
Type III cement + *x* % Grade 120 GGBF Slag		*(30% Slag)*	*(40% Slag)*	*(50% Slag)*	
	0.42	SCC10:0.28-0.42-S	SCC11:0.32-0.42-S	SCC12:0.36-0.42-S	
	0.46	SCC13:0.28-0.46-S	SCC14:0.32-0.46-S	SCC15:0.36-0.46-S	
Type III cement + 22% Class C ash + 8% Silica Fume	0.42		SCC16:0.32-0.42-Ternary	SCC17:0.36-0.42-Ternary	SCC18:0.40-0.42-Ternary
	0.46		SCC19:0.32-0.46-Ternary	SCC20:0.36-0.46-Ternary	SCC21:0.40-0.46-Ternary

The sand-to-aggregate ratios considered are also comparable to the values reported in the literature reviewed. When Su et. al (2002) published their work on the effects of different sand-to-aggregate ratios in SCC, their *s/agg* ranged from 0.30 to 0.55 (Su et. al 2002). The effects of the varying sand-to-aggregate ratios on the fresh and hardened properties of the SCC mixtures are analyzed in Chapter 4.

Three different supplementary cementing materials (SCMs) were selected for this research and are discussed later in Section 3.4. The powder combinations used for this project fall within the range of the recommended additions of SCMs displayed in Table 2-7**.** The effects of varying the powder type and their dosages have been analyzed and can be found in Chapter 4.

Table 3-2: Mixture proportions

Mixture ID	Water (pcy)	Cement (pcy)	Fly Ash (pcy)	GGBF Slag (pcy)	Silica Fume (pcy)	Coarse Agg. (pcy)	Fine Agg. (pcy)	AEA (oz/cwt)	Mid-Range WRA (oz/cwt)	HRWR Admixture (oz/cwt)	VMA (oz/cwt)
CTRL-1	260	705	0	0	0	1,942	1,102	3.00	4.0	6.0	0.0
CTRL-2	270	640	0	0	0	1,964	1,114	0.33	4.0	5.0	0.0
SCC-1	260	650	279	0	0	1,756	1,035	0.80	4.0	5.0	2.0
SCC-2	265	580	248	0	0	1,807	1,065	0.30	4.0	5.0	2.0
SCC-3	270	525	225	0	0	1,848	1,089	0.35	4.0	5.5	2.0
SCC-4	260	650	279	0	0	1,643	1,143	0.80	4.0	6.0	2.0
SCC-5	265	580	248	0	0	1,690	1,177	0.35	4.0	5.5	2.0
SCC-6	270	525	225	0	0	1,726	1,201	0.00	4.0	7.5	2.0
SCC-7	260	650	279	0	0	1,529	1,252	0.80	4.0	6.0	2.0
SCC-8	265	580	248	0	0	1,574	1,289	0.35	4.0	6.0	2.0
SCC-9	270	525	225	0	0	1,607	1,316	0.40	4.0	6.0	2.0
SCC-10	260	650	0	279	0	1,659	1,155	3.25	6.0	7.5	2.0
SCC-11	265	497	0	331	0	1,702	1,185	2.25	6.0	5.5	2.0
SCC-12	270	375	0	375	0	1,733	1,206	1.50	6.0	5.5	2.0
SCC-13	260	650	0	279	0	1,544	1,265	3.75	6.0	7.0	2.0
SCC-14	265	497	0	331	0	1,584	1,297	2.30	6.0	5.5	2.0
SCC-15	270	375	0	375	0	1,613	1,321	1.50	6.0	5.5	2.0
SCC-16	265	580	182	0	66	1,686	1,173	0.10	6.0	8.5	0.0
SCC-17	270	525	165	0	60	1,721	1,198	0.04	6.0	8.5	0.0
SCC-18	275	482	151	0	55	1,748	1,217	0.00	7.5	7.0	0.0
SCC-19	265	580	182	0	66	1,569	1,285	0.10	6.0	8.5	0.0
SCC-20	270	525	165	0	60	1,603	1,312	0.02	6.0	9.0	0.0
SCC-21	275	482	151	0	55	1,627	1,333	0.00	10.0	5.0	0.0

Note: AEA = Air-Entraining Admixture, WRA = Water-Reducing Admixture, VMA = Viscosity-Modifying Admixture

3.2.3 Testing Program

The testing program required testing each SCC mixture in its fresh and hardened states. The fresh concrete tests were performed in accordance with the guidelines provided in Appendix A, while the hardened concrete tests will be discussed in detail in Section 3.3.5.

For every mixture (SCC and conventional slump concrete), there were 20 cylinders and six shrinkage prisms made. Eight of the 20 cylinders were 4 in. x 8 in. These cylinders were match-cured according to a temperature profile representative of that found in a prestressing plant. The compressive strength and modulus of elasticity were tested on these cylinders at 18 hours, 21 hours, 7 days, and 28 days. The remaining cylinders were 6 in. x 12 in. moist-cured cylinders. These cylinders were also tested for their compressive strength and modulus of elasticity at ages of 3, 7, 28, and 56 days.

The six shrinkage prisms were divided into two groups. One group would be moist-cured for seven days before being exposed to drying conditions, while the other group would be moist-cured for 28 days before being exposed to drying conditions. After the onset of drying, readings were taken at 1, 2, 3, 4, 7, 14, and 28 days, as well as 8, 16, 32, and 64 weeks.

3.3 EXPERIMENTAL PROCEDURES

3.3.1 Batching

Before the mixing began, all of the necessary raw materials were batched. The type and amount of raw materials depended on what mixture was being made (see Table 3-1).

3.3.1.1 Collection of Materials

All of the aggregates used for this project were obtained from Alabama quarries, and they are commonly used in the prestressed concrete industry. These materials were ordered and stored at a local ready-mix company (Twin City Concrete) in Auburn. Aggregates were then transported to Auburn University's Structural Research Laboratory and stored in sealed 55-gallon drums. For this research, a well-graded siliceous sand and a continuously graded crushed limestone were chosen. These agree with the requirement for aggregates used to make SCC that are reviewed in Section 2.3.3.

The various powders (Type III cement, Grade 120 GGBF slag, Class C fly ash, and silica fume) were also stored in the laboratory, either in sealed 55-gallon drums, or in the bags in which they were received. The powders were free from any moisture until time of mixing.

3.3.1.2 Moisture Corrections

Because SCC mixtures are so sensitive to water, moisture corrections were performed to see how much water was already contained in the aggregates. Moisture corrections were made to ensure that the total free water content of each mixture is as designed. The fine and coarse aggregates were thoroughly mixed (separately from one another) as to create a homogeneous sample. A sample weighing approximately 550 g was then heated until all the moisture was evaporated and its weight remained constant. These weights (before and after the addition of heat) were used to calculate the new amounts of water, fine aggregate, and coarse aggregate.

3.3.2 Mixing Procedure

All mixtures created in the course of this study were mixed in an air-conditioned mixing room. The temperature within this room was controlled to be within a 70 to 76º F range.

3.3.2.1 Buttering the Mixer

The only task left to complete before mixing started, was to “butter” the mixer. This consists of mixing a couple of pounds of cement and sand together, turning on the mixer, and then adding just enough water to create a mortar. This practice is performed to coat the wall of the mixer before the actual mixture is mixed. The 12-ft^3 mixer used for this project is shown in Figure 3-2.

Figure 3-2: 12-ft^3 concrete mixer used for this project

3.3.2.2 Mixing Sequence

After the moisture corrections have been performed and the mixer has been buttered, the mixing process can begin. The mixing procedure used for most of the mixtures is outlined below.

1. Add 80% of mixing water.
2. Add all fine and coarse aggregates by alternating the five gallon buckets containing the materials.
3. Mix for 1 minute.
4. While mixing, add any air-entraining admixture onto the aggregates.
5. Stop mixing.
6. Add all powder materials.
7. Add all remaining mixing water.
8. Cover the opening of the mixer.
9. Mix concrete for 2 minutes.
10. Run mixer for 3 minutes.
11. While mixing, add VMA (if necessary).
12. While mixing, add any water reducing admixtures.
13. Stop mixing and rest for 3 minutes.
14. Run mixer for 3 minutes.
15. Stop mixing. Test the slump flow, VSI, and T-50. If the slump flow is too low, add more HRWR admixture. Run mixer for 1 minute and test again. Continue this process until the target slump flow has been reached.
16. Once the slump flow has been reached, continue to perform the remaining fresh concrete QC tests: J-Ring, L-Box, Air, Temperature, and Unit Weight.
17. Return all unused concrete to mixer and mix for 1 minute.
18. Proceed to make all specimens for testing hardened properties.

The procedure outlined above was the general mixing procedure used for this research with a few exceptions, when GGBF slag and ternary mixtures were produced.

Modification for GGBF slag mixtures

When using Grade 120 GGBF slag, Step 13's resting time was increased to five minutes to allow the water reducing admixtures time to take effect. Without this prolonged pause, the effectiveness of the HRWR admixture was significantly reduced.

Modifications for ternary mixtures

When incorporating silica fume into the mixture design, the mixing procedure was slightly changed in the beginning. Initially, add 80% of the mixing water, all of the coarse aggregate, and the silica fume and mix for 5 minutes to disperse the silica fume particles. Next, add the fine aggregate and mix for one minute. While mixing, add any air-entraining admixture. Now continue as usual with Step 6. This mixing procedure was recommended by the Silica Fume Association. This modification was effective in eliminating problems encountered with high air contents.

3.3.2.3 Mixture Adjustments to Meet QC Requirements

As discussed in Section 2.6.2, trial batches should be performed in order to assess the fresh properties of the mixture. From these trial batches, adjustments to the following mixture's proportions can be made to alleviate any problems with the fresh properties. The literature provided in Chapter 2, Sections 2.4.2.1 throguh 2.4.2.3, should be used to correct any one of the three major fresh state requirements of SCC.

3.3.3 FRESH CONCRETE TEST PROCEDURES

3.3.3.1 Slump Flow

While this test has not been standardized, it is probably the most common test used to evaluate SCC. This test gives an indication of the SCC mixture's filling ability and insight on its resistance to segregation. This method is discussed in detail in Section 2.2.1. The exact test procedure used for this research is outlined in Appendix A.1. For this research, the slump flow test was performed with the slump cone in the *inverted* position. If the slump flow exceeded the upper slump flow limit of 30 in., the mixture was discarded and modifications were made to the dosage of HRWR admixture. However, if the slump flow was less than the lower slump flow limit of 24 in., additional HRWR admixture was used to reach the desired slump flow. Figure 3-3 shows the components of the apparatus used for this test.

Figure 3-3: Testing equipment for slump flow test

3.3.3.2 Visual Stability Index (VSI)

The VSI rating is a subjective result directly obtained after evaluating the slump flow patty. Once the concrete has completely come to rest on the slump table, the VSI is evaluated. Guidelines for rating the VSI of the slump flow patty are given in Table 2-2. However, the mixer should also be inspected in order to properly evaluate the mixture's stability. This test method is discussed in detail in Section 2.2.1.

3.3.3.3 T-50

The T-50 is carried out in conjunction with the slump flow test and is also discussed in Section 2.2.1. When performing the slump flow test as described in Appendix A.1, the T-50 is measured. As stated in Section 2.2.1, this is the time it takes the concrete to flow 20 inches, and it is an indication of the mixture's viscosity.

3.3.3.4 J-Ring

The J-Ring test is also unique to SCC. This test has yet to be standardized, but it is a valuable test method to determine a mixture's passing ability. The J-Ring test is discussed in detail in Section 2.2.3, while the procedure used to perform the J-Ring test is outlined in Appendix A.3. Figure 3-4 shows the J-Ring used for this research. The J-Ring apparatus consists of a steel ring measuring 12 inches in diameter at the center of the ring and 1 inch in thickness, and 16 – 5/8 in. diameter smooth steel rods 4 inches in length spaced evenly at $2\frac{5}{16}$ inches around the ring. Figure 2-12 gives a plan view and side views of these dimensions.

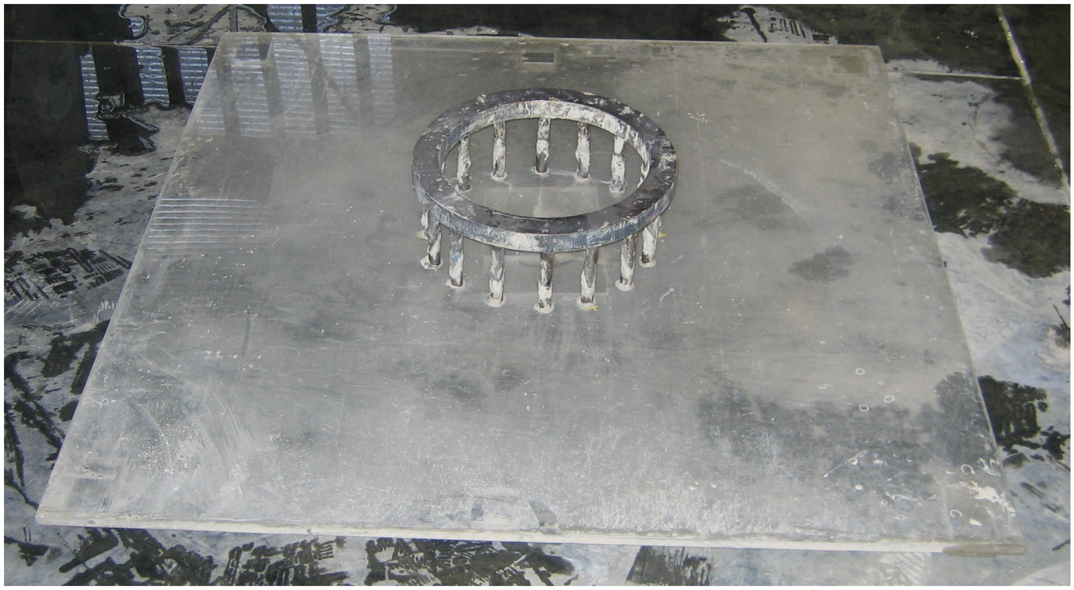

Figure 3-4: J-Ring used for this research

3.3.3.5 L-Box

The L-Box test procedure is discussed in Section 2.2.2. This test method is used to evaluate SCC's filling ability as well as passing ability, while a certain degree of instability can also be detected (PCI 2003; Khayat, Assaad, and Daczko 2004). The procedure used to perform this test is defined in Appendix A.2. Figure 3-5 is a schematic of the dimensions of the L-Box used for this project, while Figure 3-6 is a picture of the actual L-Box.

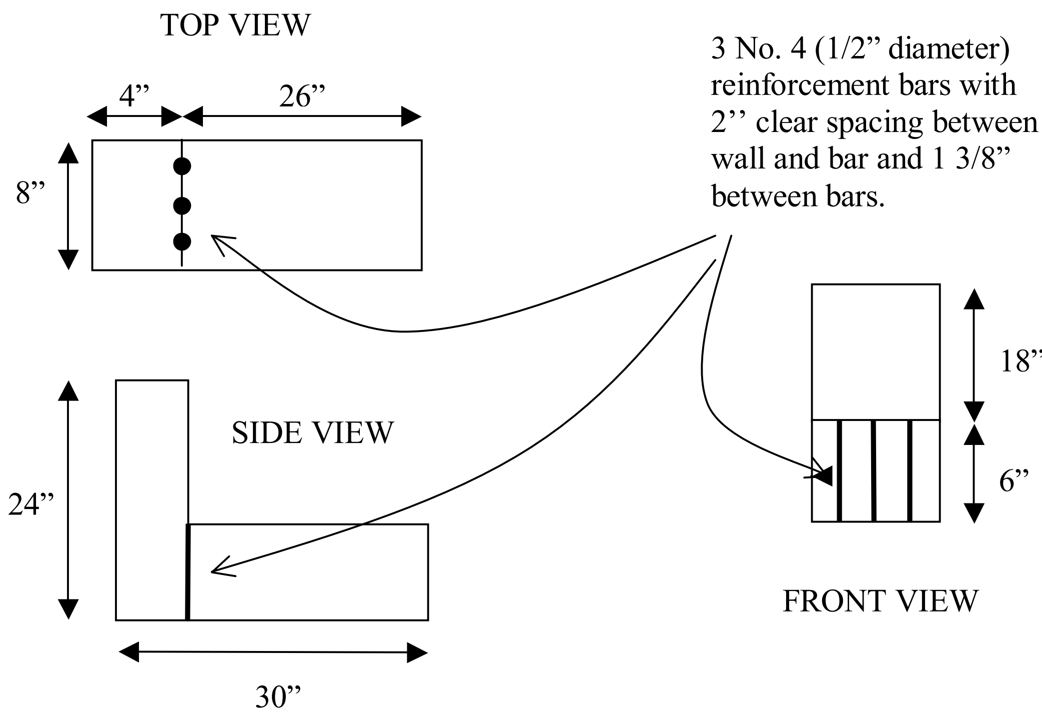

Figure 3-5: Dimensions of the L-Box used for this project

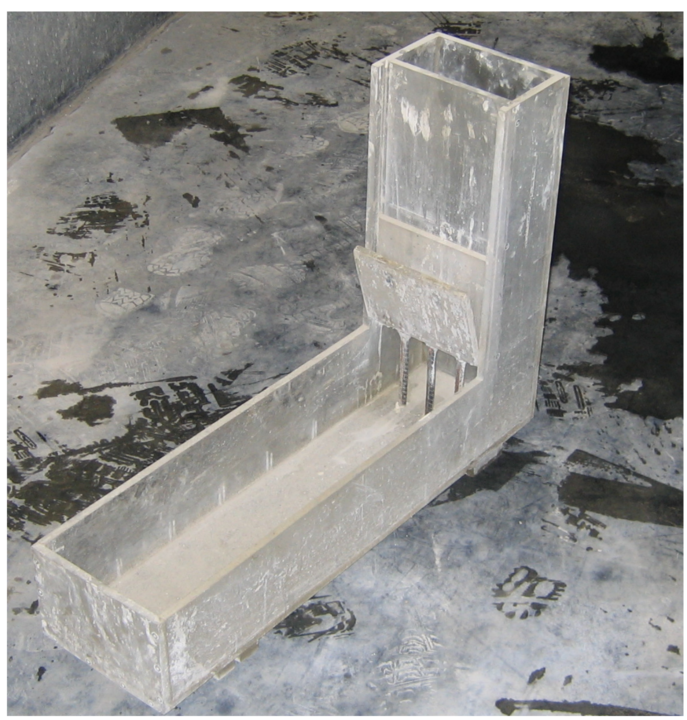

Figure 3-6: L-Box used for this project

3.3.3.6 Air Content (Pressure Meter) and Unit Weight

The air content and unit weight was determined for all SCC mixtures according to the procedures outlined in AASHTO T 121 (2003) with the exception of the following modifications:

- The concrete was placed in 3 equal layers, however there was no rodding.
- After each layer was placed, the container was then lightly tamped 10 to 12 times.

Tamping was applied to the container to reduce the amount of air pockets that might have been trapped on the walls rather than an effort to help consolidation.

As mentioned earlier, the total air content was specified to be between 3% and 5%. This test was used to reject any concrete that was *significantly* out of this range. However, the unit weight was only measured and recorded for quality assessment purposes.

3.3.3.7 Fresh Concrete Temperature

The fresh concrete temperature for all SCC mixtures was determined according to the procedure outlined in AASHTO T 309 (2003). The temperature of the SCC mixtures was not required to meet any specifications. It was simply tested and recorded to check the consistency of the mixing environment.

3.3.4 SPECIMEN PREPARATION AND CURING

As stated earlier, there were a total of 26 specimens made with every mixture. This included 12 cylinders with dimensions of 6 in. x 12 in., 8 cylinders with dimensions of 4 in. x 8 in., and 6 shrinkage prisms with dimensions of 3 in. x 3 in. x 11.25 in. All cylinders were prepared in accordance with AASHTO T 126 (2003) with a few modifications specific to SCC, while all shrinkage prisms were prepared and stored in accordance with AASHTO T 126 (2003) with a few adjustments particular to SCC. These modifications are discussed in the following sections.

3.3.4.1 Specimen Consolidation

The procedure described in AASHTO T 126 (2003) was followed as closely as possible with the following exceptions:

- All 6 in. x 12 in. cylinders were placed in 3 equal layers without any rodding.
- After each layer was placed, each cylinder was lightly tapped 10 to 12 times in an effort to reduce the amount of entrapped air bubbles along the sides of the cylinder molds.

The 4 in. x 8 in. cylinders, which were match-cured to a time-temperature profile, were also prepared as closely to AASHTO T 126 (2003) as possible with the following alterations:

- The 4 in. x 8 in. match-curing molds (often referred to as 4 in. x 8 in. cylinders) were placed in 2 equal layers with no rodding.
- After each layer was poured, the surfaces of the match-curing molds were tapped 10 to 12 times in an effort to diminish any air pockets along the sides of the molds.

Figure 3-7 is a picture of one of the eight match-curing molds used for this research.

Figure 3-7: Match-curing mold

The remaining six specimens made for this research were drying shrinkage prisms. These specimens were made in accordance with AASHTO T 160 (2003) with the following modifications:

- Each prism was placed in two equal layers without any rodding; the concrete was not manipulated around the gage studs.
- After each layer was placed, the sides of the prism were lightly tapped with a mallet approximately 8 to 10 times.
- Since these specimens were the last to be completed (approximately 30 minutes after the water was added to the mixture), it was not unusual for the SCC mixture to lose most of its fluidity. When this occurred, the sides of the prism were firmly tapped so that the prisms were completely filled. Other researchers state that *some* mechanical consolidation might be required to

ensure the complete filling of the formwork (Khayat, Assaad, and Daczko 2004).

Figure 3-8 shows a picture of one of the six shrinkage prism molds used for this research.

Figure 3-8: Shrinkage prism mold

3.3.4.2 Curing Conditions

All 6 in. x 12 in. specimens were cured according to the guidelines in AASHTO T 126 (2003). Each cylinder was sealed with a nonabsorptive, nonreactive plastic cap. For the first 24 hours, the specimens remained approximately six feet away from where they were made. After 24 hours in the air conditioned mixing room, specimens were removed from their molds and stored in a curing environment in accordance with AASHTO T 126 (2003) until the time of testing.

The 4 in. x 8 in. cylinders were cured according to a time-temperature profile representative of curing conditions typically experienced in a prestressing plant. Upon completion, the molds were covered with wet burlap, which was covered with a sheet of plastic to prevent loss of moisture. The burlap was kept moist until all specimens had been removed as best as possible. At approximately 18 and 21 hours, two specimens were tested. This left a total of four specimens remaining in the match-curing molds at the end of 24 hours. At this time, the four remaining 4 in. x 8 in. specimens were stored in a curing environment in agreement with AASHTO T 126 (2003) until the time of testing.

Figure 3-9 shows the time-temperature profile that the specimens were to follow and their actual time-temperature profile. It is impossible for the temperature to instantaneously drop from 150º F to 73º F. For this reason, the remaining 4 specimens were simply removed and placed in the curing room at the end of 24 hours. It is important to note that the 4 in. x 8 in. cylinders that were match-cured for Phase II followed the natural temperature history of the 4 in. x 4 in. x 10 ft. small-scale prestressed elements that were cured under 68 to 76 °F conditions.

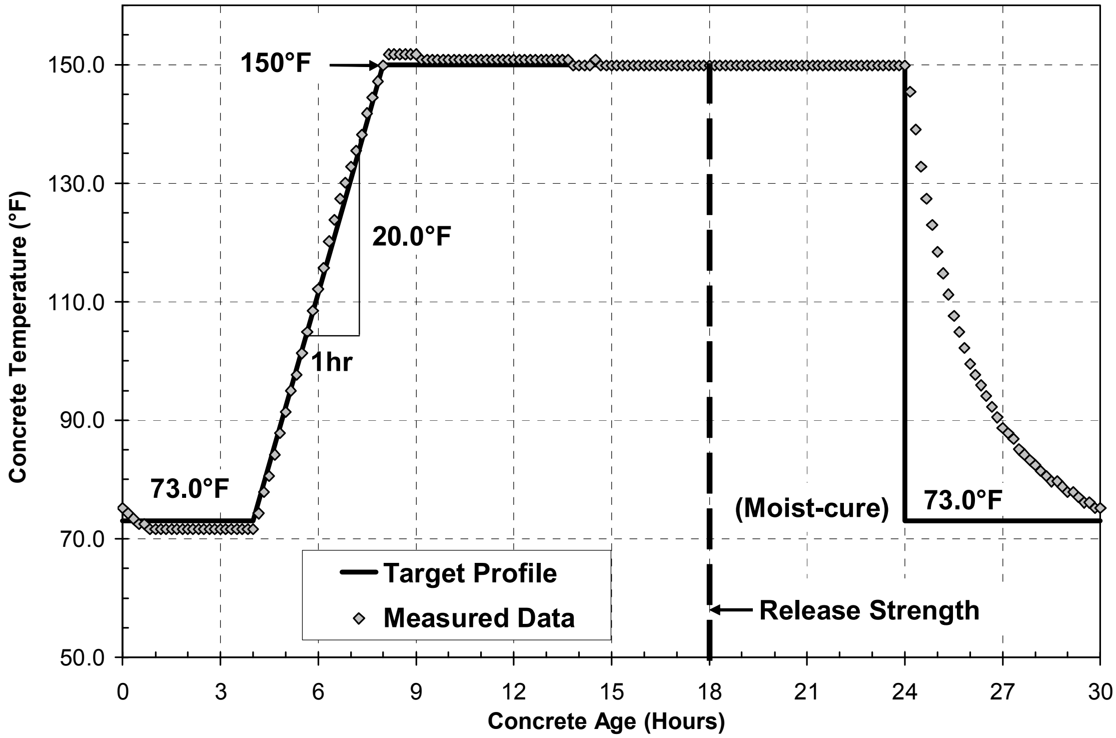

Figure 3-9: Target time-temperature profile versus measured time-temperature profile.

All of the shrinkage prisms were cured following the methods stated in AASHTO T 160 (2003). Upon striking off the excess concrete, the prisms were transported to the curing room with as little vibration as possible, whereby they were covered with moistened burlap. The burlap was then covered with plastic to completely prevent them from exposure to any dripping water. The specimens were then removed from their molds and stored in a lime-saturated water bath in agreement with AASHTO T 160 (2003).

The shrinkage prisms were separated into two groups. Three specimens were cured in the lime bath for seven days while the remaining three specimens were cured for 28 days. At the end of their respective curing durations, they were exposed to drying conditions in accordance with AASHTO T 160 (2003) for as long as they were tested.

3.3.5 Hardened Concrete Test Procedures

3.3.5.1 Compressive Strength

The compressive strength was tested on all cylinder specimens, whether match-cured or moist-cured, in accordance with AASHTO T 22 (2003). All of the equipment used met the specifications set forth in AASHTO T 22 (2003). Unbonded neoprene pads with a durometer of 70 were used to cap all the cylinders. The neoprene pads and the steel retaining ring in which they were placed met the standards specified in ASTM C 1231 (2000). The neoprene pads were replaced after no more than 50 tests. The load rate used when testing the compressive strength for the 6 in. x 12 in. cylinders was 60,000 lbs/min., and 26,000 lbs/min. for the 4 in. x 8 in. cylinders. Each cylinder was tested in a Forney compression machine, like the one shown in Figure 3-10, which had a capacity of 600 kips.

The compressive strength results and how they were affected by the different constituents are presented in Chapter 4.

Figure 3-10: Forney compression machine

3.3.5.2 Modulus of Elasticity

Since no AASHTO specification exists for determining the modulus of elasticity, each modulus of elasticity value was obtained in accordance with ASTM C 469 (2002). All equipment met the requirements listed in ASTM C 469. For this test, the unbonded neoprene pads, as described in Section 3.3.5.1, were used. When performing this test on 6 in. x 12 in. cylinders, the first cylinder was loaded until failure in agreement with AASHTO T 22 (2003). The remaining two cylinders' moduli of elasticity were obtained following ASTM C 469 (2002) guidelines using 40% of the first cylinder's ultimate compressive strength as the upper limit of the testing range.

For the 4 in. x 8 in. cylinders, only two cylinders were tested at time. Therefore, the author had to make an educated estimate of 40% of the compressive strength. After running the modulus of elasticity and compressive strength tests on the first cylinder, the second cylinder was tested using 40% of the first cylinder's strength. Figure 3-11 is a picture of the compressometers used to conduct these tests.

The modulus of elasticity results and how they were affected by the different constituents are presented in Chapter 4.

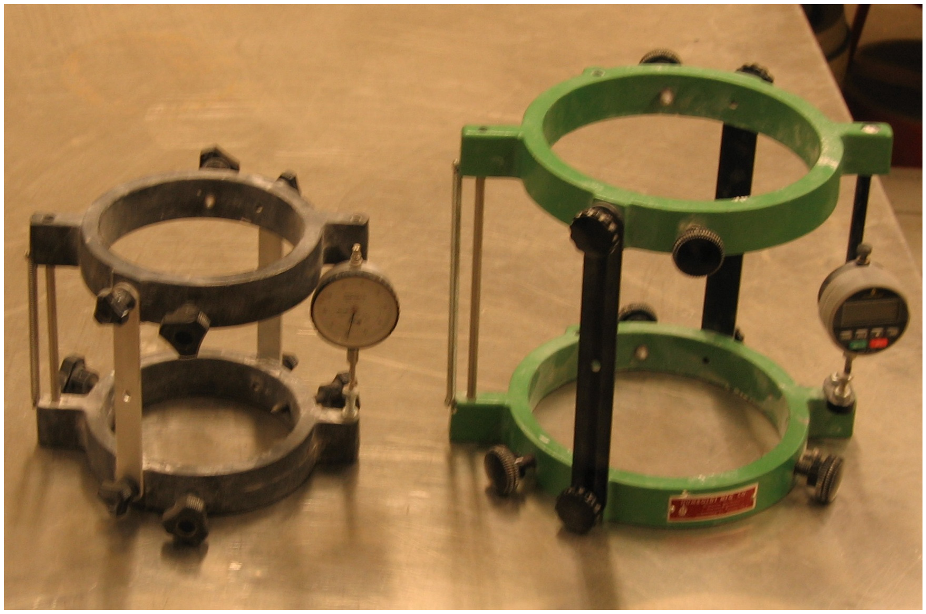

Figure 3-11: Compressometers used to determine the modulus of elasticity

3.3.5.3 Drying Shrinkage

All six shrinkage prisms were tested in accordance with AASHTO T 160 (2003). The equipment used for performing shrinkage testing met the requirements of AASHTO T 160. The length change of the specimens was tested at periods specified in AASHTO T 160 (2003). Additional length change readings were recorded at ages of 1, 2, and 3 days after being exposed to drying conditions. Figure 3-12 is a picture of the length comparator used for measuring the change in length.

The drying shrinkage results along with their predictions are presented in Chapter 4.

Figure 3-12: Length comparator

3.4 MATERIALS

3.4.1 POWDERS

For this research, four types of powders were used in different combinations. The term powder collectively refers to Type III cement, Grade 120 GGBF slag, Class C fly ash, and silica fume. The use of different types of powders provided the necessary data to compare and contrast how each powder combination affected the SCC's properties. Nine mixtures used a combination of Type III cement and Class C fly ash, six mixtures used a combination of Grade 120 GGBF slag, and the final six SCC mixtures consisted of a ternary blend using Type III cement, silica fume, and Class C fly ash. Fly ash, GGBF slag, and silica fume are commonly referred to as supplementary cementing materials (SCMs). Table 2-7 gives recommendations on the additions of these SCMs by mass of cement that they replace.

3.4.1.1 Type III Cement

Type III cement was chosen because it provides a rapid increase in early-age strength and is consistent with what is being used in the precast industry. The Type III cement used for this research was manufactured by Cemex at their Demopolis, AL plant. The physical characteristics of concrete made with Type III cement are found in Section 2.3.2.1. The chemical composition of the Type III cement used for this research is shown in Table 3-3.

3.4.1.2 Class C Fly Ash

Of the different types of fly ash available, Class C fly ash was chosen because its strength gain characteristics are more desirable for the rapid construction process used in the precast industry. The Class C fly ash used for this project was acquired from Holcim (US), Inc. located in Birmingham, AL. The effects of fly ash on the mechanical properties of concrete are explained in Section 2.3.2.2, and the typical chemical composition of Class C fly ash is shown in Table 2-4. The chemical composition of Class C fly ash used for this research can be found in Table 3-3. The chemical composition of the Class C fly ash used for this research meets the requirements of Table 2-4.

Table 3-3: Chemical composition of all powders

Parameter	Type III Portland Cement	Class C Fly Ash	GGBF Slag	Silica Fume
Silicon dioxide, SiO_2 (%)	20.01	37.59	32.68	95.57
Aluminum oxide, Al_2O_3 (%)	5.25	18.87	9.67	0.02
Iron oxide, Fe_2O_3 (%)	3.88	6.06	1.12	0.05
Calcium oxide, CaO (%)	62.69	24.12	45.32	0.41
Magnesium oxide, MgO (%)	0.90	5.71	7.40	0.43
Alkalies (Na_2O + 0.658K_2O) (%)	0.27	2.29	-	0.77
Sulfur trioxide, SO_3 (%)	4.27	1.38	1.66	0.1
Loss on ignition, LOI (%)	2.02	0.31	0.84	2.43
Tricalcium silicate, C_3S (%)	50.16	-	-	-
Dicalcium silicate, C_2S (%)	19.52	-	-	-
Tricalcium aluminate, C_3A (%)	7.34	-	-	-
Tetracalcium aluminoferrite, C_4AF (%)	11.81	-	-	-
Specific surface area (m^2/kg)	567	409	547	1204
Specific gravity	3.15	2.63	2.91	2.3

3.4.1.3 Silica Fume

The selection of silica fume to be used as a SCM for this research was made because it is considered to be essential for the production of very high strength concrete (Mindess, Young, and Darwin 2003). It was also thought that silica fume would increase the viscosity of the SCC, which would increase its stability. The silica fume used for this project was obtained from Simcala, Inc. located in Mt. Meigs, AL. The effects of silica fume on the mechanical properties of concrete are explained in Section 2.3.2.3, and its typical chemical composition is shown in Table 2-5. The chemical composition of silica fume used in the production of SCC for this research is shown in Table 3-3, and it is in agreement with the requirements given in Table 2-5.

3.4.1.4 Ground-Granular Blast-Furnace (GGBF) Slag

Like fly ash and silica fume, ground granular blast furnace (GGBF) slag can also improve some of the properties of concrete. The GGBF slag used for this research was a Grade 120 purchased from Lone Star Industries, Inc. out of New Orleans, LA. This GGBF slag had a smaller fineness than the Type III cement used in this project. The decreased particle size distribution of the GGBF slag is expected to increase the viscosity of the SCC, which should increase its stability. The effects of GGBF slag on the mechanical properties of concrete are discussed in Section 2.3.2.4, and its typical chemical composition is given in Table 2-6. The chemical composition of GGBF slag used for this research is shown in Table 3-3, and it meets the ranges given in Table 2-6.

3.4.2 Chemical Admixtures

Four different types of chemical admixtures were used during this research. The selected admixtures were used to help achieve the desired fresh properties (some enhanced hardened properties) of SCC. Two types of water-reducing admixtures, an air-entraining admixture (AEA), and a viscosity-modifying admixture (VMA) were used to achieve the desired fresh and hardened properties. These four admixtures are discussed below.

3.4.2.1 High-Range Water-Reducing (HRWR) Admixture

The effects of incorporating a HRWR admixture are discussed in Section 2.3.4.1. Without the use of a HRWR admixture, the production of SCC would not be possible. Two types of HRWR admixtures were used for this research, and they are based on polycarboxylate chemistry: Glenium 3200 HES and Polyheed 1025. These admixtures were obtained from Degussa Admixtures, Inc. Glenium 3200 HES's water reducing capacity is more pronounced than that of Polyheed 1025. While Polyheed 1025 is generally referred to as a mid-range water-reducer (MRWR), it meets the requirements of ASTM C 494 Type A and Type F admixtures (Degussa Admixtures, Inc. 2005). Degussa Admixtures, Inc. (2005) recommends a dosage of 2 to 14 fl oz/cwt of powder and 3 to 12 fl oz/cwt of powder for Glenium 3200 and Polyheed 1025 respectively, although dosages outside this range may be required due to the variability in concrete materials (Degussa Admixtures, Inc. 2005).

3.4.2.2 Viscosity-Modifying Admixture (VMA)

The effects of using a VMA are discussed in Section 2.3.4.2. The VMA used for this research was Rheomac VMA 362, also purchased from Degussa Admixtures, Inc. This is a synthetic type of VMA. This VMA was primarily used to decrease the SCC's sensitivity to fluctuations in the free water content. The recommended dosage of Rheomac VMA 362 is 2 to 14 fl oz/cwt of powder, although dosages outside of this range may be required due to the variability in concrete materials (Degussa Admixtures, Inc. 2005).

3.4.2.3 Air-Entraining Admixture (AEA)

Air had to be entrained into almost all of the SCC mixtures to meet the total air requirements of the Alabama Department of Transportation. Reasons for using an air-entraining admixture are discussed in Section 2.3.4.3. The AEA used for this research was Micro Air, obtained from Degussa Admixtures, Inc. There is no set dosage for Micro Air because of interactions caused by various concrete materials and ambient conditions. A dosage of 1/8 to $1\frac{1}{2}$ fl oz/cwt of powder is a recommended starting point when performing trial batches. An AEA other than Micro Air was used in one instance.

MB AE 90, also obtained from Degussa Admixtures, Inc., was used for CTRL1:0.37. A dosage of ¼ to 4 fl oz/cwt of powder is a recommended starting point when performing trial batches containing MB AE 90 (Degussa Admixtures, Inc. 2005).

3.4.3 Coarse Aggregate

The coarse aggregate used for this research was a No. 78 crushed limestone (AASHTO M 43). This was the only coarse aggregate used throughout the course of this project. The selection of this aggregate agrees with the findings reviewed in Section 2.3.3. The coarse aggregate was obtained from Vulcan Materials Company located in Calera, AL. The gradation of the No. 78 crushed limestone, along with the specification requirements of AASHTO M 43 (found in Table 2-8) are shown in Table 3-4. It may be seen that the coarse aggregate used for this project satisfies all the requirements for a No. 78 gradation. The bulk specific gravity was 2.72, the saturated surface dry specific gravity was 2.73, and the absorption capacity was 0.40%.

3.4.4 Fine Aggregate

The fine aggregate used for this research was a siliceous sand from Superior Products, Inc. located in Jemison, AL. The use of a siliceous sand is in agreement with the literature reviewed in Section 2.3.3. This fine aggregate was incorporated into every mixture. The gradation of the fine aggregate, along with the specification requirements of AASHTO M 6 (found in Table 2-9) are shown in Table 3-5. The bulk specific gravity was 2.58, the saturated surface dry specific gravity was 2.60, and the absorption capacity was 1.00%.

Table 3-4: Gradation of No. 78 crushed limestone

Sieve Size	Percent Passing	AASHTO M 43 Specification of Percent Passing (%)
3/4"	100	100
1/2"	97.3	90-100
3/8"	72.6	40-75
#4	10.1	5-25
#8	0.9	0-10
#16	0.3	0-5

Table 3-5: Gradation of fine aggregate

Sieve	Percent Passing (%)	AASHTO M 6 Specification of Percent Passing (%)
No. 4	96.6	95-100
No. 8	85	80-100
No. 16	76.46	50-85
No. 30	56.2	25-60
No. 50	18.98	10-30
No. 100	3.48	2-10

CHAPTER 4

PRESENTATION AND ANALYSIS OF RESULTS

All of the fresh and hardened properties of the 21 SCC mixtures and two conventional-slump concrete mixtures are presented in this chapter. The fresh properties are presented and discussed in Section 4.1, while the hardened properties are presented and discussed in Section 4.2. Effects of the *w/p*, *s/agg*, and the different powder combinations had on the fresh or hardened properties are also discussed. A summary of the fresh and hardened properties for the small-scale prestressed elements created in Phase II is also given. A summary of the conclusions regarding SCC's fresh and hardened properties that can be drawn based on this research is presented in Section 4.3.

4.1 FRESH PROPERTIES

All of the fresh properties determined for the SCC and control mixtures are summarized in Table 4-1. The dosage of air-entraining admixture, mid-range WR admixture, and HRWR admixture are also provided. There are no J-Ring or L-Box results for the 21 SCC mixtures made for Phase I of this research. However, both of these tests were performed for the four SCC mixtures selected for production of the small-scale prestressed elements. These results, along with the other fresh properties measured for the small-scale prestressed elements, are provided in Table 4-2.

Table 4-1: Summary of SCC and conventional-slump concrete fresh properties and admixture dosages

Mixture ID	Slump Flow	T-50	VSI	Total air	Unit Weight	Temp.	AEA	Mid-Range WRA	HRWR Admixture	VMA
	(in.)	(sec)		(%)	(lb/ft^3)	(ºF)	(oz/cwt)	(oz/cwt)	(oz/cwt)	(oz/cwt)
CTRL1: 0.37	9.5*	-	-	3.0	151.48	76	3**	4.0	6.0	0
CTRL2: 0.42	9.0*	-	-	3.8	148.84	-	0.33	4.0	5.0	0
SCC1:0.28-0.38-FA	28.00	5.3	1.5	3.8	151.68	75	0.80	4.0	5.0	2
SCC2:0.32-0.38-FA	29.00	4.2	1.0	3.0	151.84	76	0.30	4.0	5.0	2
SCC3:0.36-0.38-FA	27.50	2.8	1.0	4.3	148.52	81	0.35	4.0	5.5	2
SCC4:0.28-0.42-FA	29.00	5.5	1.5	3.2	150.88	76	0.80	4.0	6.0	2
SCC5:0.32-0.42-FA	28.50	5.4	1.5	3.9	150.40	78	0.35	4.0	5.5	2
SCC6:0.36-0.42-FA	26.00	2.8	0.5	2.7	150.88	69	0.00	4.0	7.5	2
SCC7:0.28-0.46-FA	29.00	5.3	1.5	3.0	151.20	77	0.80	4.0	6.0	2
SCC8:0.32-0.46-FA	29.00	2.7	1.5	4.6	148.00	76	0.35	4.0	6.0	2
SCC9:0.36-0.46-FA	27.75	3.3	1.5	4.7	148.04	74	0.40	4.0	6.0	2
SCC10:0.28-0.42-S	28.00	13.4	1.5	3.0	152.00	76	3.25	6.0	7.5	2
SCC11:0.32-0.42-S	28.00	12.3	1.0	3.4	150.04	76	2.25	6.0	5.5	2
SCC12:0.36-0.42-S	28.00	5.1	1.0	3.8	148.48	83	1.50	6.0	5.5	2
SCC13:0.28-0.46-S	29.00	13.0	1.0	3.6	150.32	76	3.75	6.0	7.0	2
SCC14:0.32-0.46-S	27.00	11.5	1.0	3.9	148.44	76	2.30	6.0	5.5	2
SCC15:0.36-0.46-S	27.75	4.1	2.0	4.8	146.64	76	1.50	6.0	5.5	2
SCC16:0.32-0.42-Ternary	27.00	4.3	1.0	3.3	149.84	71	0.10	6.0	8.5	0
SCC17:0.36-0.42-Ternary	26.50	3.0	1.5	5.3	146.16	71	0.04	6.0	8.5	0
SCC18:0.40-0.42-Ternary	26.50	3.7	1.5	3.8	147.80	73	0.00	7.5	7.0	0
SCC19:0.32-0.46-Ternary	26.50	5.6	0.5	4.1	148.64	72	0.10	6.0	8.5	0
SCC20:0.36-0.46-Ternary	26.00	3.4	1.5	4.2	147.88	72	0.02	6.0	9.0	0
SCC21:0.40-0.46-Ternary	26.00	2.6	0.5	2.5	149.24	74	0.00	10.0	5.0	0

Note: * indicates a conventional-slump. ** indicates that MB AE 90 was used instead of Microair.

Table 4-2: Fresh properties of small-scale prestressed elements

Mixture ID	Slump Flow (in.)	T-50 (sec.)	L-Box (H_2/H_1)	J-Ring (Difference/Rating)	VSI	Total air (%)	Unit Weight (lb/ft^3)
SCC7:0.28-0.46-FA	26.00	3.34	0.50	.75 in./0	1.0	2.4	153.2
SCC9:0.36-0.46-FA	28.50	1.57	0.96	1.25 in./1	2.5	4.5	147.9
SCC13:0.28-0.46-S	31.25	2.93	0.33	2.2 in./2	2.0	1.8	153.8
SCC15:0.36-0.46-S	28.25	2.35	0.92	2.25 in./2	2.5	3.3	147.6

Note: While SCC13:0.28-0.46-S produced a large slump flow of 31.25 in., this mixture had a rapid loss of slump flow over time.

4.1.1 Slump Flow Test Results

4.1.1.1 Slump Flow Results

The slump flow, after approximately 15 minutes of mixing, ranged between 26.0 and 29.0 in. (660 and 735 mm) for Phase I of this project. These results are within the specified range (27 ± 3 inches) that was outlined before the testing began.

4.1.1.2 Discussion of Results

All of the slump flow results have been provided in Table 4-1. The slump flow values cannot be assessed by the *s/agg*, *w/p*, or powder combination alone. The most influential variable affecting the slump flow value was the HRWR admixture dosage. Figure 4-1 shows the required HRWR admixture dosage for each SCC mixture.

On average, the fly ash and slag SCC mixtures (with the same *w/p* and *s/agg*) require approximately the same amount of HRWR admixture at 6.2 and 6.1 oz/cwt respectively. However, for the ternary SCC mixtures to achieve an acceptable slump flow value, the dosage increases to 8.6 oz/cwt for similar *w/p* and *s/agg*. Therefore, the type of SCM has the greatest impact on the amount of HRWR admixture required to achieve an acceptable slump flow. It is important to note that the average slump flow value is highest for the fly ash SCC mixtures at 28.2 in., followed by the slag SCC mixtures at 27.9 in. Even though the ternary SCC mixtures have the highest dosage of HRWR admixture, these SCC mixtures have the lowest average slump flow at 26.5 in.

Other researchers have reported slump flow values ranging from as low as 20 in. (500 mm) (Beaupre, Lacombe, and Khayat 1999) to as high as 29 in. (735 mm) (Ozyildirim and Lane 2003). Khayat (1999) found that a slump flow value of 650 mm (26 in.) was suitable for casting highly congested structural sections. Ozyildirim and Lane (2003) found SCC mixtures with a slump flow range of 23 to 29 in. to be satisfactory. PCI (2003) recommends a slump flow value greater than 22 in. for highly congested elements (Table 2-13). The test results presented above are compatible with these recommended ranges.

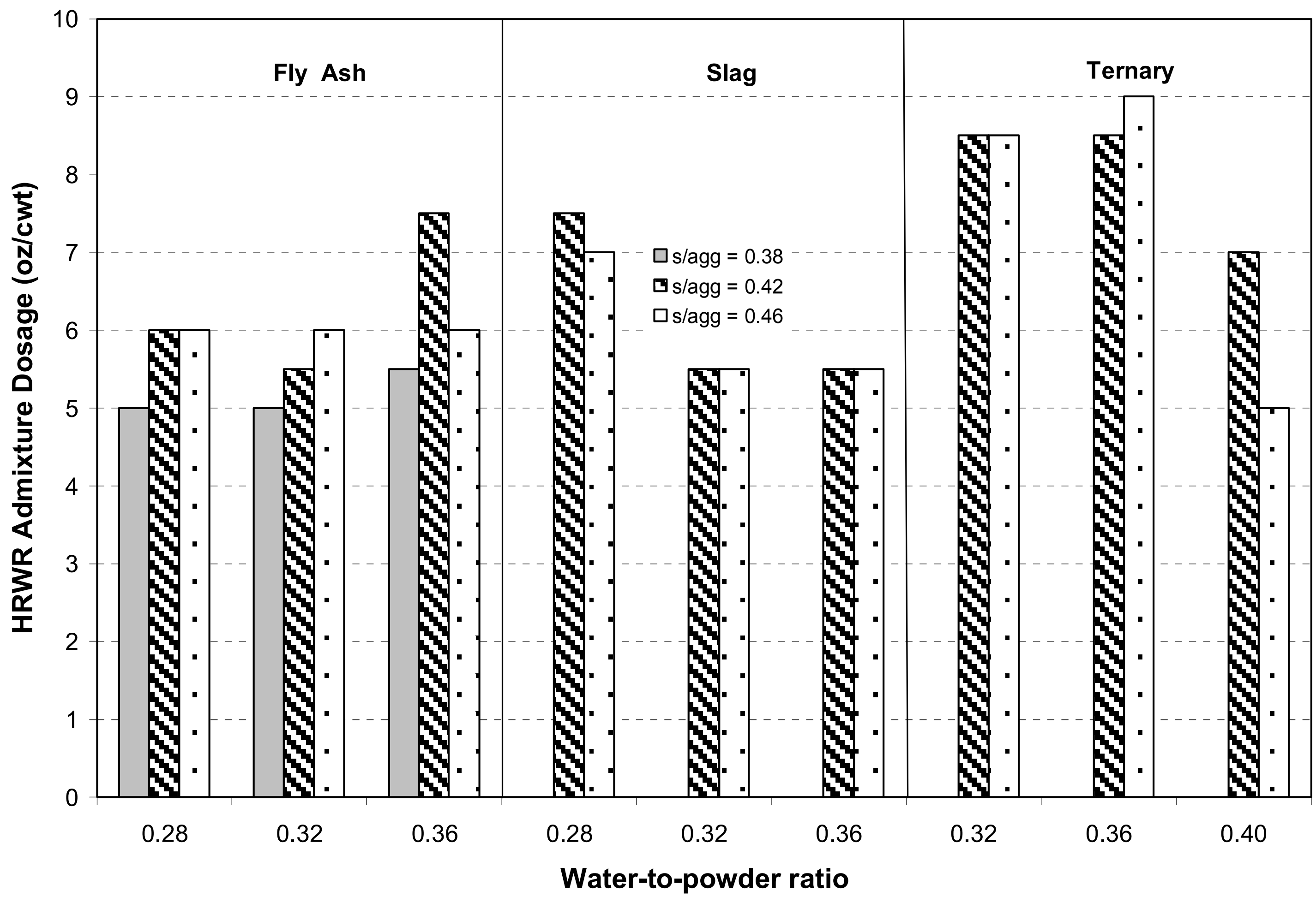

Figure 4-1: Summary of HRWR admixture dosages for the SCC mixtures

4.1.2 T-50

4.1.2.1 T-50 Results

The T-50, taken after approximately 15 minutes of mixing, ranged between 2.6 and 13.4 seconds. A graphical summary of the T-50 results is presented in Figure 4-2.

4.1.2.2 Discussion of Results

Figure 4-2 shows that no fixed trend exists between the T-50 times and the *s/agg* for the fly ash and ternary SCC mixtures. However, for the slag SCC mixtures, the T-50 time decreased as the *s/agg* increased from 0.42 to 0.46 for all *w/p*. From Figure 4-2, it may be seen that the T-50 times generally increase with a decrease in the *w/p*. This is in agrees with the results of previous research (Khayat, Assaad, and Daczko 2004).

Figure 4-2 also shows extremely high T-50 times for the slag SCC mixtures with *w/p* of 0.28 and 0.32. During the mixing process, it was noticed that the slag SCC mixtures possessed a cohesiveness unlike any of the other SCC mixtures. These particular SCC mixtures can best be described as "extremely sticky". This property was unique only to the slag SCC mixtures, and this may have been caused by the very fine GGBF slag particles. It was for this reason that 30% of GGBF slag was used as replacement of cement at the low *w/p* of 0.28. Note that even at a high *w/p* of 0.40, the fine silica fume particles provided a reasonable T-50 for the SCC.

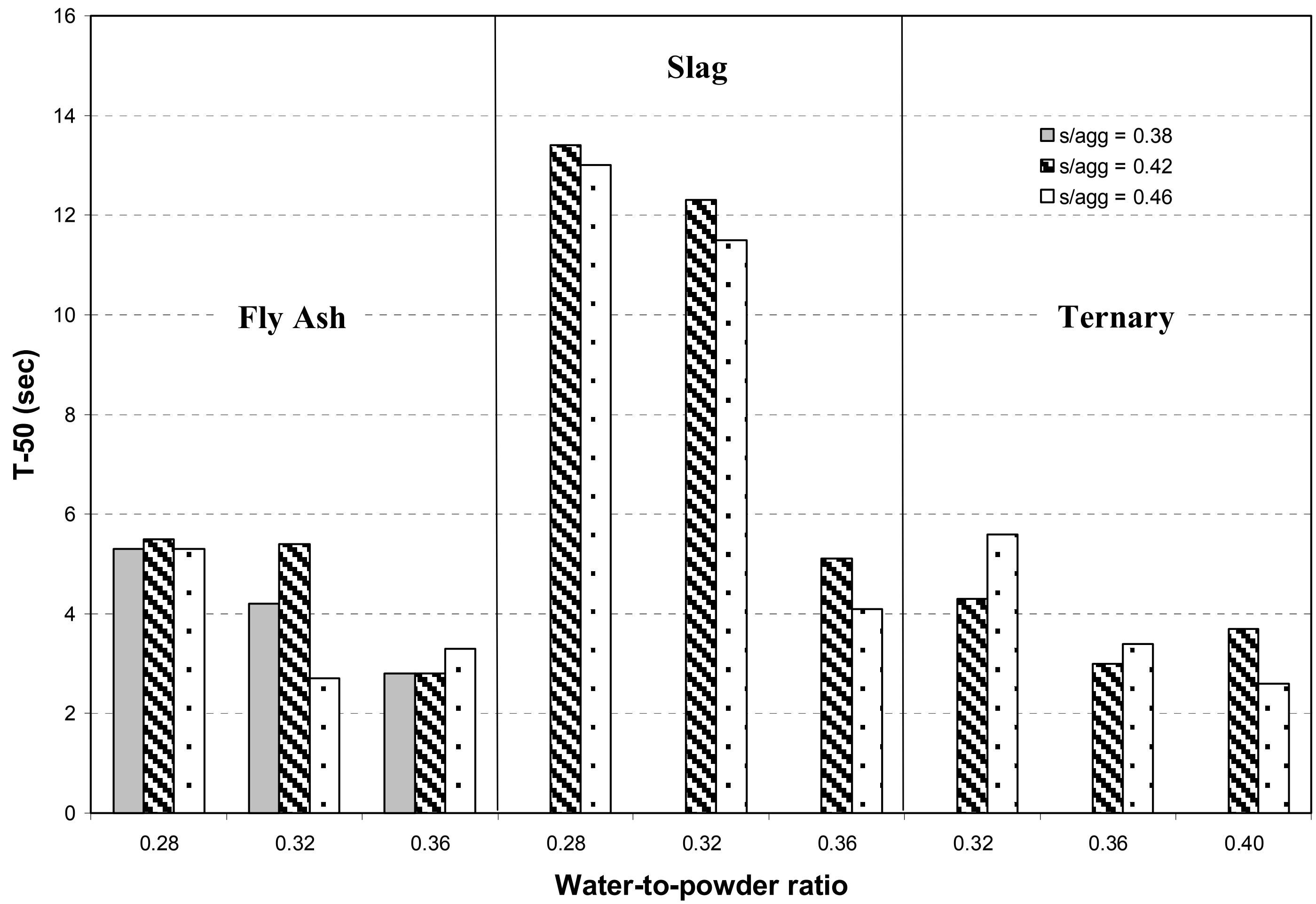

Figure 4-2: Summary of T-50 times

4.1.3 Visual Stability Index (VSI) Test Data

4.1.3.1 VSI Results

Table 4-1 also shows that most of the SCC mixtures of Phase I had a VSI between 1.0 and 1.5. SCC-15 had a VSI of 2.0; however, its other fresh properties were within the required limits stated in Section 3.2.1.1. Although SCC-15 had a VSI of 2.0, its hardened properties were adequate.

4.1.3.2 Discussion of Results

Because most of the SCC mixtures having a VSI of either 1.0 or 1.5, these mixtures should have adequate dynamic stability. Khayat, Assaad, and Daczko (2004) reported a VSI rating ranging from 1.5 to 2.0 and concluded that the VSI is not sufficient for a quantitative estimation of the stability of SCC. The dynamic and static stability of these mixtures must be evaluated under full-scale construction conditions.

4.1.4 Air Content Results

4.1.4.1 Air Content Results

The majority (86%) of the SCC mixtures had air content values that satisfied the specified range of 3 to 5%. The three SCC mixtures that did not fall within this range were reasonably close and satisfied all other fresh and hardened property requirements. The amount of air-entraining admixture required for each mixture is summarized in Figure 4-3. No air-entraining admixture was used in the mixtures for which data are omitted.

4.1.4.2 Discussion of Results

The required amount of air-entraining admixture was significantly affected by the powder type, the dosage of HRWR admixture, and the *w/p*. The *s/agg* had no significant effect on the amount of air-entraining admixture required. From Figure 4-3, for each powder combination, larger dosages of air-entraining admixture were required as the *w/p* was decreased. The use of GGBF slag required much higher dosages of air-entraining admixture.

As previously stated, the specified total air content range for this research was 3 to 5%. Ozyildirim and Lane (2004) had a specified total air content range of 6 ± 2%. Lachemi et al. (2004) reported a total air content ranging from 1.5 to 3.5%. The required air content will vary from state to state. However, the author encountered difficulties in achieving the specified range for this research, which has also troubled other researchers (Ozyildirim and Lane 2004). Increased HRWR admixture dosages generally tended to increase the total air content of the SCC mixtures, and thus required a reduction in air-entraining admixture to meet the target air content. Yet, Ozyildirim and Lane (2004) experienced a drop in total air content as the dosage of HRWR admixture was increased. It may be necessary to widen the specified total air content range to account for the inherent effect of polycarboxylate-based HRWR admixtures on the total air content. The current ALDOT range of 3 to 5% was difficult to satisfy for concrete produced under controlled laboratory conditions. Since the lower limit corresponds to the minimum air content that provides adequate protection against freezing and thawing actions, the upper limit may need to be increased. An upper limit of 8% (PCI 2003), which is typically required in states with severe exposure, should still provide good structural performance provided that the required strength is achieved. A total air content of 3 to 8% should be evaluated with respect to practicality and structural performance.

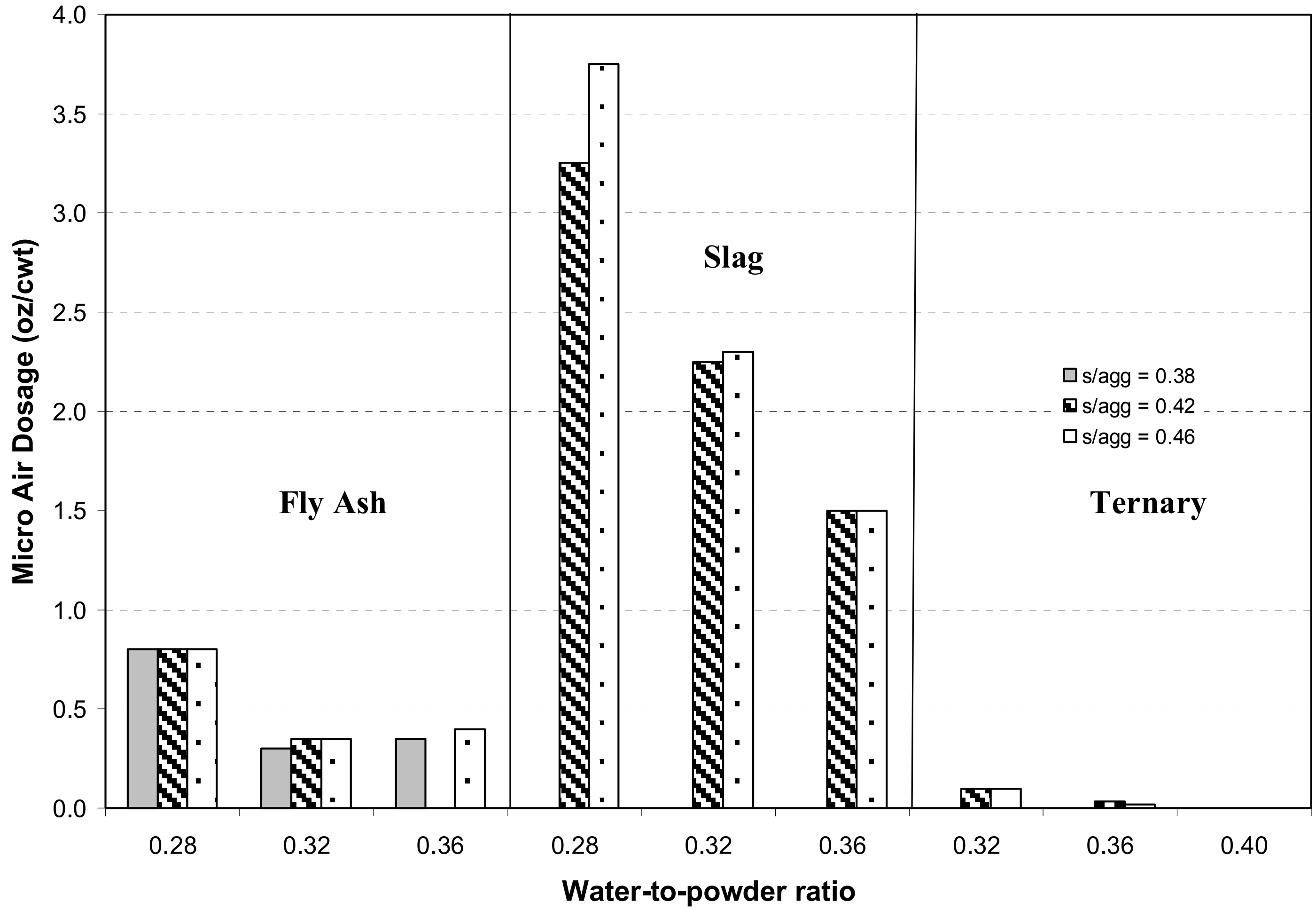

Figure 4-3: Summary of required air-entraining admixture dosage for all SCC mixtures

4.1.5 J-RING

4.1.5.1 Results of J-Ring (Passing Ability)

The J-Ring test was performed for each SCC mixture used to create the small-scale prestressed elements. A summary of these results is presented in Table 4-2. The passing ability (see Section 2.2.3) ranged from 0 to 2.

4.1.5.2 Discussion of Results

The passing ability of SCC13:0.28-0.46-S and SCC15:0.36-0.46-S was a 2.0, which is an indication of "noticeable to extreme blocking" according to ASTM (2004). A passing ability rating of 2.0 indicates that the difference in the slump flow taken with and without the J-Ring is above 2 inches. At this stage, it is uncertain if this rating is an accurate predictor of the passing ability of the SCC. It is recommended to evaluate the passing ability of these SCC mixtures during the construction of congested full-scale prestressed elements.

While the fresh properties of these two SCC mixtures are not ideal, they allow analysis of SCC mixtures that may not have desirable fresh properties. The hardened properties of these mixtures at time of prestress transfer (see Table 4-4) met the requirements specified in Section 3.2.1.2. Slight additional vibration may be required to achieve consolidation of these mixtures in highly congested members, which has also been suggested by Khayat, Assaad, and Daczko (2004).

4.1.6 L-BOX TEST RESULTS

4.1.6.1 L-Box Results (Blocking Ratio)

The L-Box test, like the J-Ring test, was also conducted on each SCC mixture used to create the small-scale prestressed elements. A summary of these results is presented in Table 4-2. The blocking ratio (see Section 2.2.2) ranged from 0.33 to 0.96.

4.1.6.2 Discussion of Results

The closer the blocking ratio gets to 1.0, the better the passing ability of the SCC mixture. According to Petersson (2000), an acceptable value for the blocking ratio is 0.80 or higher. The two SCC mixtures that did not meet this requirement were SCC7:0.28-0.46-FA and SCC13:0.28-0.46-S. SCC7:0.28-0.46-FA met all of the other fresh property requirements except for the total air content, which should not have had a significant impact on its blocking ratio. However, SCC13:0.28-0.46-S had an unacceptable slump flow value and VSI rating which could explain its low blocking ratio.

While these mixtures' fresh properties were not ideal, both SCC7:0.28-0.46-FA and SCC13:0.28-0.46-S had high compressive strength values at prestress transfer. One of the reasons that these mixtures exhibited poor blocking ratios was the amount of time that elapsed before the test was conducted. The L-Box test was performed towards the end of the experiment after the SCC had lost much of its fluidity (the small-scale prestressed elements had been cast by this time). It is the author's opinion that the acceptable blocking ratio prescribed by Petersson (2000) could be lowered or a time constraint should be added to this procedure. An acceptable range for the blocking ratio value needs to be evaluated on full-scale members.

4.1.7 Unit Weight Results

4.1.7.1 Results and Discussion of Unit Weight

The unit weight values, in pounds per cubic foot, for all of the SCC mixtures and both conventional-slump mixtures are given in Table 4-1. The average of all of the SCC mixtures, regardless of *w/p*, *s/agg*, or powder combination, was 149.4 lb/ft^3. The average of the two conventional-slump mixtures was 150.2 lb/ft^3, a difference of less than 1%. The unit weight values for these SCC mixtures are consistent with values commonly used for design purposes.

4.2 MECHANICAL PROPERTIES

The compressive strength and modulus of elasticity results for Phases I and II are summarized in Tables 4-3 and 4-4 respectively. Table 4-3 contains every mixture, including both control mixtures. The 18-hr and 28-day results are presented for the 4 in. x 8 in. cylinders, while the 28 and 56-day results are displayed for the 6 in. x 12 in. cylinders. The compressive strength and modulus of elasticity were measured at 18 hours because this is often the time at which prestress transfer occurs. All results for each cylinder size are summarized in Appendices B and C.

The drying shrinkage results are shown in Tables 4-5 (7-day moist curing period) and 4-6 (28-day moist curing period). These results are for all the SCC mixtures and both control mixtures. The results displayed in Tables 4-5 and 4-6 are for 28 days, 16 weeks, and 32 weeks. All drying shrinkage results are summarized in Appendix D.

The effects of the sand-to-aggregate ratio (*s/agg*), water-to-powder ratio (*w/p*), and powder combination on the compressive strength, modulus of elasticity, and drying shrinkage are discussed in the following sections.

Table 4-3: Compressive strengths and modulus of elasticity results

Mixture ID	4x8 in. Match-Cured Cylinder Results				6x12 in. Moist-Cured Cylinder Results			
	Compressive Strength (psi)		Modulus of Elasticity (ksi)		Compressive Strength (psi)		Modulus of Elasticity (ksi)	
	18 hr	28 day	18 hr	28 day	28 day	56 day	28 day	56 day
CTRL1: 0.37	7,480	10,500	6,100	7,000	10,250	11,190	7,250	7,000
CTRL2: 0.42	6,280	9,550	5,330	6,500	8,850	9,510	7,100	6,500
SCC1:0.28-0.38-FA	9,000	12,410	5,750	6,850	12,510	13,080	7,000	7,150
SCC2:0.32-0.38-FA	7,000	11,760	4,950	7,100	11,090	12,070	7,300	7,150
SCC3:0.36-0.38-FA	5,790	9,220	5,000	6,500	10,150	10,900	6,500	6,700
SCC4:0.28-0.42-FA	8,820	12,700	5,450	7,400	13,600	14,080	7,050	7,400
SCC5:0.32-0.42-FA	7,140	10,490	5,150	6,650	11,580	12,380	7,000	7,600
SCC6:0.36-0.42-FA	5,470	9,110	4,850	6,250	10,330	10,350	6,400	6,900
SCC7:0.28-0.46-FA	8,860	12,520	5,900	6,350	13,300	13,930	7,350	7,900
SCC8:0.32-0.46-FA	7,780	10,970	5,200	6,900	11,550	12,100	6,800	6,850
SCC9:0.36-0.46-FA	5,800	9,280	4,700	5,900	10,060	11,000	6,350	6,650
SCC10:0.28-0.42-S	8,350	10,510	5,870	7,750	11,620	12,540	7,050	7,200
SCC11:0.32-0.42-S	7,610	10,650	5,430	7,000	10,750	11,260	6,950	7,050
SCC12:0.36-0.42-S	6,490	9,740	5,350	6,800	9,880	10,250	6,600	6,800
SCC13:0.28-0.46-S	8,800	11,740	5,750	7,300	11,580	12,290	7,000	7,100
SCC14:0.32-0.46-S	7,090	10,130	5,150	6,600	10,390	10,690	6,500	6,650
SCC15:0.36-0.46-S	5,780	8,610	4,800	6,200	8,960	9,570	7,000	6,650
SCC16:0.32-0.42-Ternary	9,470	11,160	5,600	6,650	12,240	13,390	6,850	6,950
SCC17:0.36-0.42-Ternary	8,310	10,090	5,600	6,200	10,760	12,430	6,550	6,850
SCC18:0.40-0.42-Ternary	6,880	8,840	5,400	6,200	11,020	11,800	6,700	6,800
SCC19:0.32-0.46-Ternary	9,530	11,060	5,700	6,850	12,470	13,160	6,700	7,000
SCC20:0.36-0.46-Ternary	8,320	9,840	5,500	6,100	11,840	12,650	6,700	6,800
SCC21:0.40-0.46-Ternary	7,750	8,600	5,750	6,200	11,630	12,130	6,550	6,750

Table 4-4: Compressive strengths and modulus of elasticity results for small-scale prestressed elements

Mixture ID	4x8 in. Match-Cured Cylinder Results*				6x12 in. Moist-Cured Cylinder Results			
	Compressive Strength (psi)		Modulus of Elasticity (ksi)		Compressive Strength (psi)		Modulus of Elasticity (ksi)	
	18 hr	28 day	18 hr	28 day	28 day	56 day	28 day	56 day
SCC7:0.28-0.46-FA	8,860	12,520	5,900	6,350	13,300	13,930	7,350	7,900
SCC9:0.36-0.46-FA	5,800	9,280	4,700	5,900	10,060	11,000	6,350	6,650
SCC13:0.28-0.46-S	8,800	11,740	5,750	7,300	11,580	12,290	7,000	7,100
SCC15:0.36-0.46-S	5,780	8,610	4,800	6,200	8,960	9,570	7,000	6,650

Note: * These 4 in. x 8 in. cylinders were match-cured to the natural temperature history of 4 in. x 4 in. x 10 ft. prestressed elements that were cured under 68 to 76 °F conditions.

Table 4-5: Drying shrinkage strain (7-day moist curing)

MIXTURE ID	Drying Shrinkage Strain (in./in. x 10^{-6})		
	Duration of Drying		
	28 Days	**16 Weeks**	**32 Weeks**
CTRL1: 0.37	-330	-477	-522
CTRL2: 0.42	-353	-520	-613
SCC1:0.28-0.38-FA	-307	-400	-465
SCC2:0.32-0.38-FA	-297	-382	-443
SCC3:0.36-0.38-FA	-293	-440	-520
SCC4:0.28-0.42-FA	-293	-402	-472
SCC5:0.32-0.42-FA	-343	-432	-497
SCC6:0.36-0.42-FA	-422	-475	-443
SCC7:0.28-0.46-FA	-293	-400	-487
SCC8:0.32-0.46-FA	-357	-482	-545
SCC9:0.36-0.46-FA	-410	-447	-538
SCC10:0.28-0.42-S	-330	-423	-473
SCC11:0.32-0.42-S	-290	-510	-485
SCC12:0.36-0.42-S	-327	-415	-535
SCC13:0.28-0.46-S	-290	-420	-497
SCC14:0.32-0.46-S	-347	-500	-530
SCC15:0.36-0.46-S	-280	-457	-530
SCC16:0.32-0.42-Ternary	-372	-418	
SCC17:0.36-0.42-Ternary	-410	-445	
SCC18:0.40-0.42-Ternary	-398	-415	
SCC19:0.32-0.46-Ternary	-377	-460	
SCC20:0.36-0.46-Ternary	-437	-480	
SCC21:0.40-0.46-Ternary	-373	-373	

Table 4-6: Drying shrinkage strain (28-day moist-cured)

MIXTURE ID	Drying Shrinkage Strain (in./in. x 10^{-6})		
	Duration of Drying		
	28 Days	**16 Weeks**	**32 Weeks**
CTRL1: 0.37	-260	-400	-483
CTRL2: 0.42	-300	-447	-518
SCC1:0.28-0.38-FA	-183	-287	-370
SCC2:0.32-0.38-FA	-237	-373	-427
SCC3:0.36-0.38-FA	-277	-413	-497
SCC4:0.28-0.42-FA	-273	-348	-403
SCC5:0.32-0.42-FA	-263	-337	-455
SCC6:0.36-0.42-FA	-270	-380	-365
SCC7:0.28-0.46-FA	-220	-312	-363
SCC8:0.32-0.46-FA	-233	-382	-447
SCC9:0.36-0.46-FA	-290	-405	-490
SCC10:0.28-0.42-S	-198	-315	-345
SCC11:0.32-0.42-S	-258	-358	-427
SCC12:0.36-0.42-S	-242	-420	-478
SCC13:0.28-0.46-S	-197	-298	-330
SCC14:0.32-0.46-S	-250	-413	-380
SCC15:0.36-0.46-S	-233	-438	-468
SCC16:0.32-0.42-Ternary	-282	-292	
SCC17:0.36-0.42-Ternary	-222	-265	
SCC18:0.40-0.42-Ternary	-260	-288	
SCC19:0.32-0.46-Ternary	-272	-287	
SCC20:0.36-0.46-Ternary	-237	-258	
SCC21:0.40-0.46-Ternary	Bad Reading	-237	

4.2.1 Compressive Strength

The 18-hour compressive strengths (f'_{ci}) for SCC mixtures summarized in Table 4-3 vary between 5,470 and 9,530 psi (38 and 66 MPa), which slightly exceeds the target range of 5,000 to 9,000 psi (34 and 62 MPa). The two control mixtures had f'_{ci} values of 6,280 and 7,480 psi (43 and 52 MPa).

4.2.1.1 Effects of Sand-to-Aggregate Ratio

The effect of the *s/agg* on f'_{ci} for all three powder combinations is evaluated in Figures 4-4 through 4-6. From these figures, it may be concluded that when the *w/p* is held constant, the *s/agg* has little to no effect on f'_{ci}. The effect of *s/agg* on long-term (56-day) compressive strengths for all three powder combinations is evaluated in Figures 4-7 through 4-9. The 56-day compressive strength is not affected by the *s/agg*. While all of the 0.42 *s/agg* slag mixtures have higher 56-day compressive strengths than the 0.46 *s/agg* for the slag mixtures, the strengths are very comparable (< 7% difference). The effects of the *s/agg* on the 28-day compressive strength are evaluated in Appendix B. As was the case for the 56-day strengths, the *s/agg* has little to no effect on 28-day compressive strengths obtained from either the 4 in. x 8 in. or 6 in. x 12 in. cylinders.

As stated by Neville (1996), the strength of concrete is mostly affected by the *w/p*. The size and shape of the aggregates will affect the strength, but a constant fine and coarse aggregate were used in every SCC mixture. Some literature reviewed for this report documented influence by the *s/agg* on the drying shrinkage and modulus of elasticity (Bonen and Shah 2003; Su et al. 2002). However, no relationship between the *s/agg* and the compressive strength was reported.

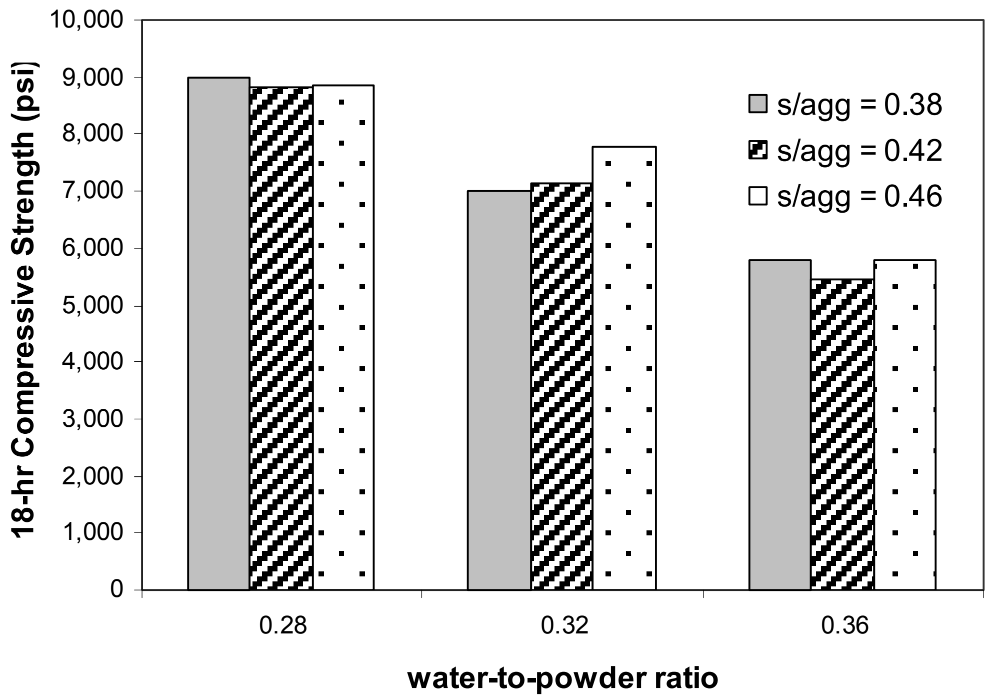

Figure 4-4: Effect of *s/agg* on the 18-hr compressive strength for fly ash mixtures

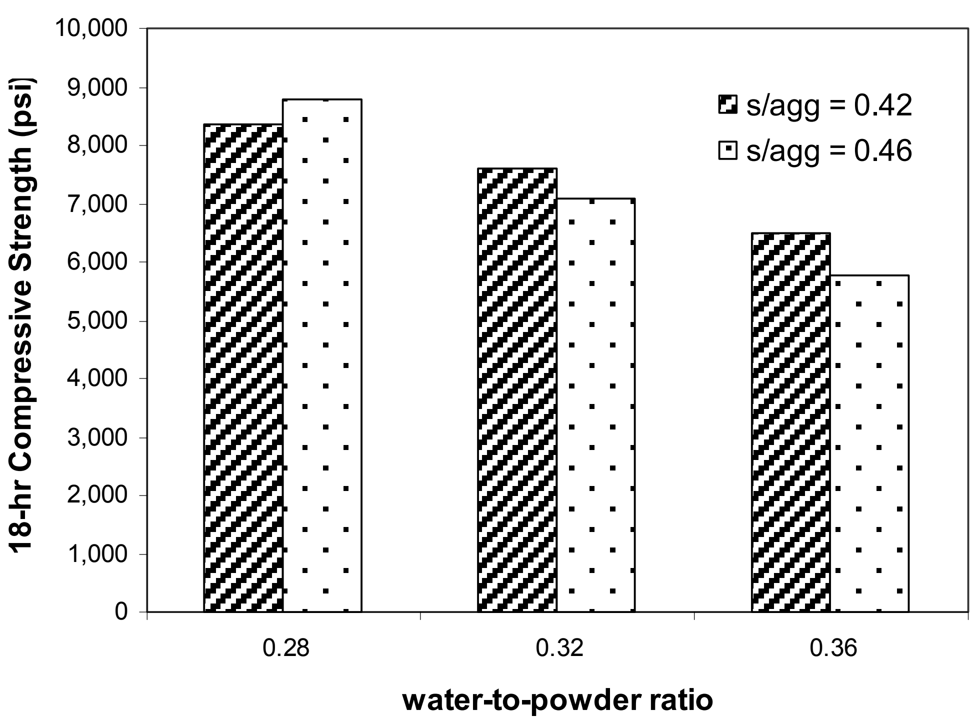

Figure 4-5: Effect of *s/agg* on the 18-hr compressive strength for slag mixtures

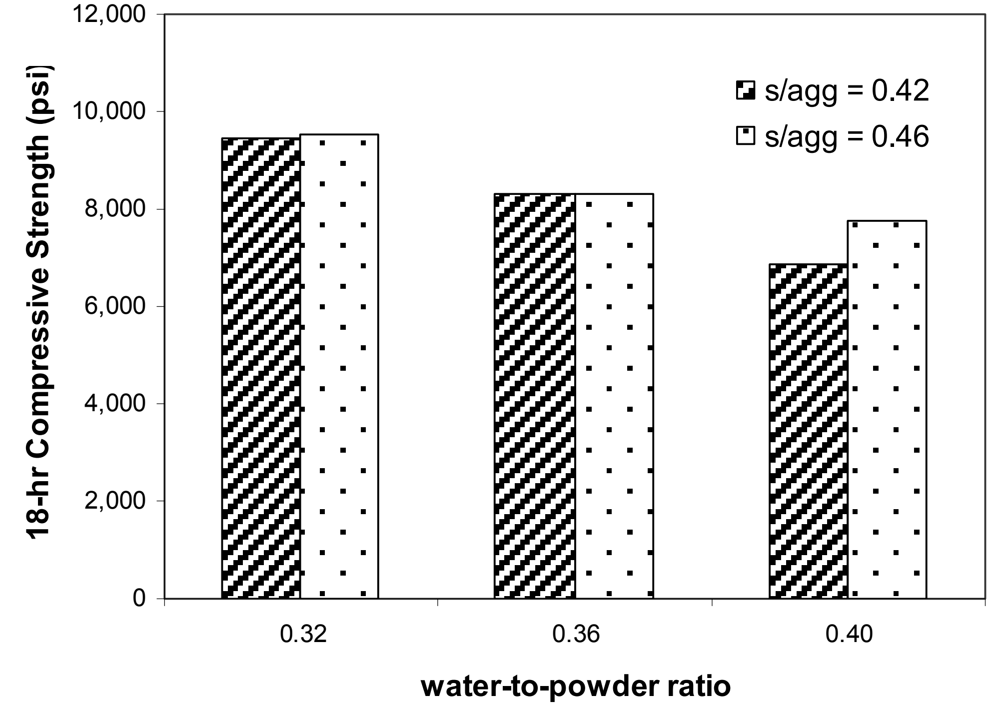

Figure 4-6: Effect of *s/agg* on the 18-hr compressive strength for ternary mixtures

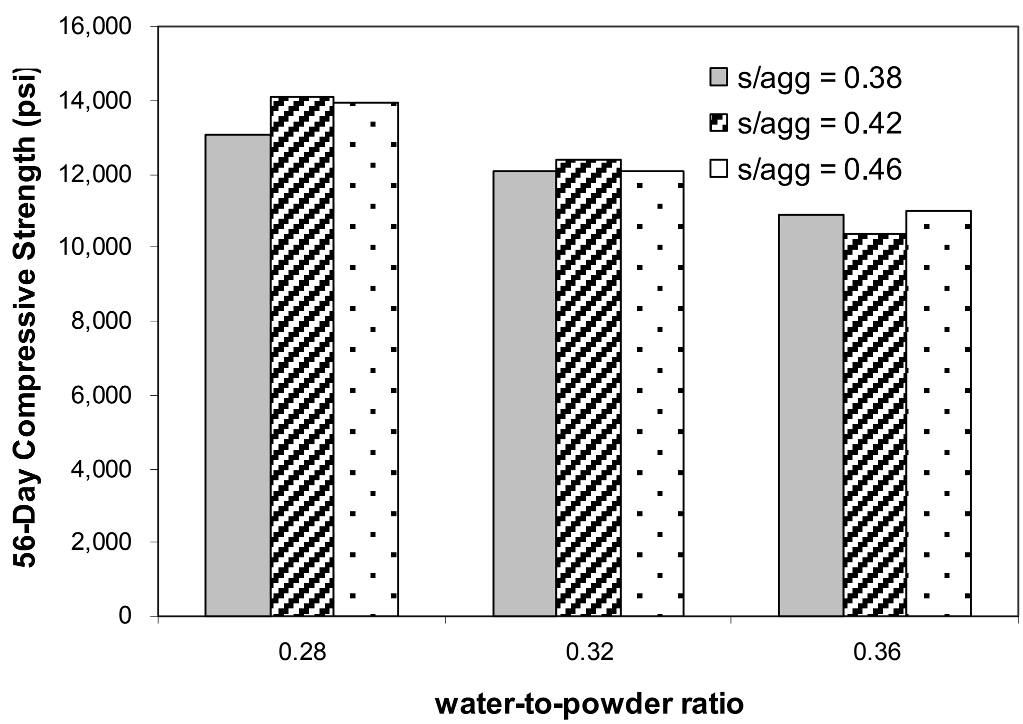

Figure 4-7: Effect of *s/agg* on the 56-day compressive strength for fly ash mixtures

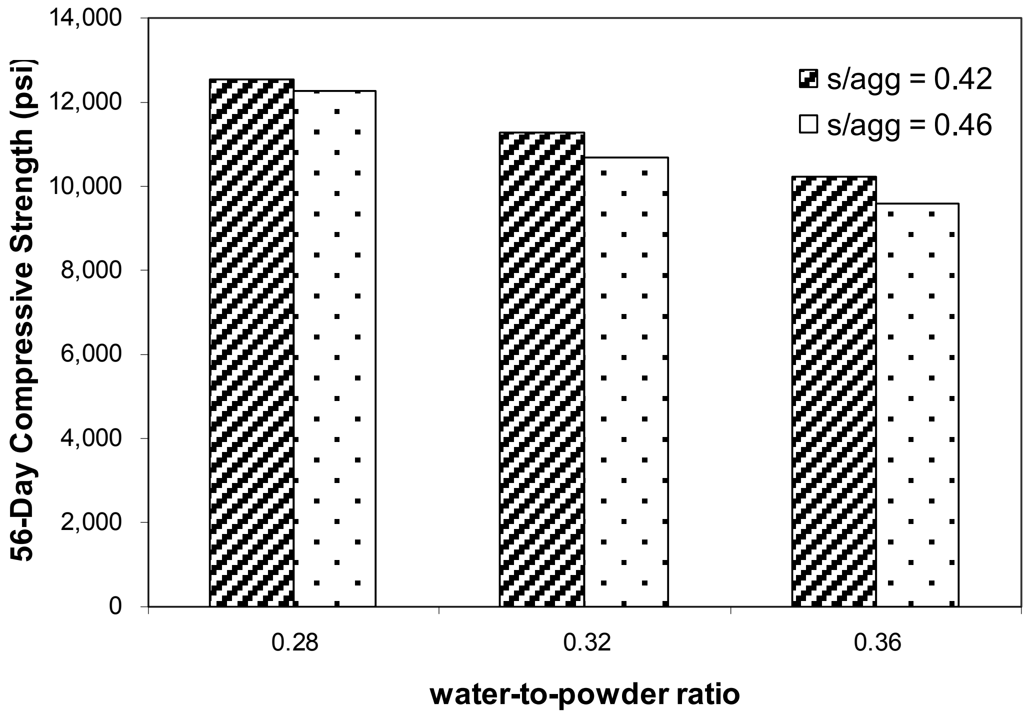

Figure 4-8: Effect of *s/agg* on the 56-day compressive strength for slag mixtures

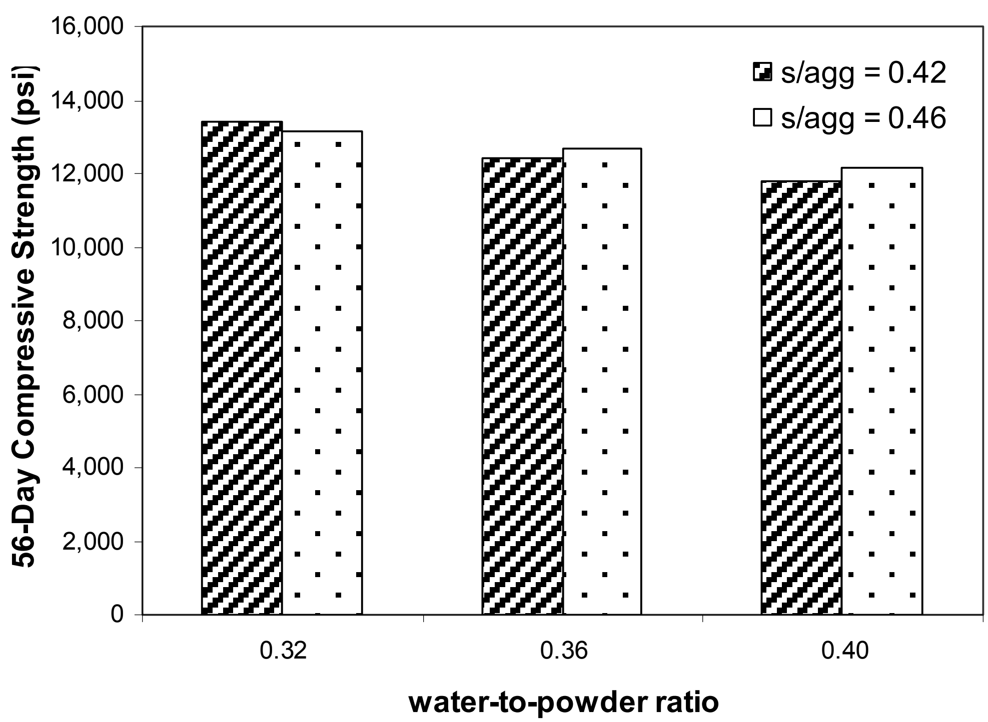

Figure 4-9: Effect of *s/agg* on the 56-day compressive strength for ternary mixtures

4.2.1.2 Effects of Water-to-Powder Ratio

The effect of the *w/p* on f'_{ci} for all three powder combinations is evaluated in Figures 4-10 through 4-12. For all *s/agg*, f'_{ci} increases as the *w/p* decreases. This is in agreement with trends associated with conventional-slump concrete. The effect of *w/p* on long-term (56-day) compressive strengths for all three powder combinations is evaluated in Figures 4-13 through 4-15. The 56-day compressive strength increases as the *w/p* decreases for all *s/agg*. Not shown in Chapter 4 are the 28-day evaluations of the *w/p* on f'_c. These results are reported in Appendix B. The compressive strength increases as the *w/p* decreases for all *s/agg* at 28 days with two exceptions. Mixture SCC10:0.28-0.42-S has a slightly lower f'_c than Mixture SCC11:0.32-0.42-S for the 4 in. x 8 in. cylinders. Mixture SCC17:0.36-0.42-Ternary has a lower f'_c than Mixture SCC18:0.40-0.42-Ternary for the 6 in. x 12 in. cylinders. These two anomalies are unexplainable. Other than the two abnormalities mentioned, these results are as expected for conventional-slump concrete, because the compressive strength is inversely proportional to the *w/p* (Neville 1996).

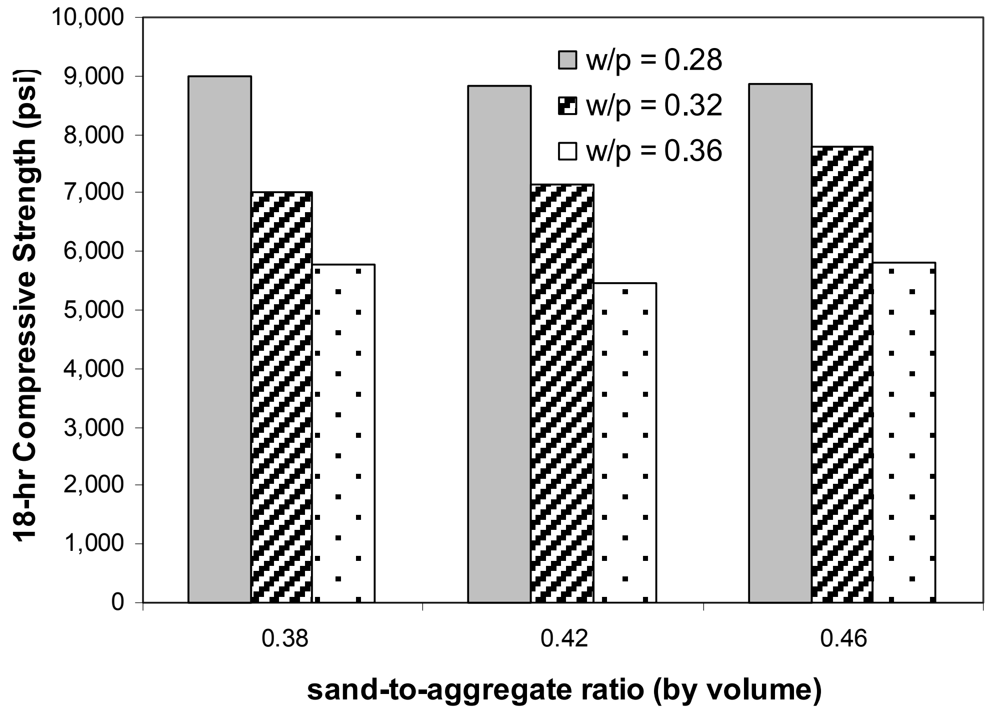

Figure 4-10: Effect of *w/p* on the 18-hr compressive strength for fly ash mixtures

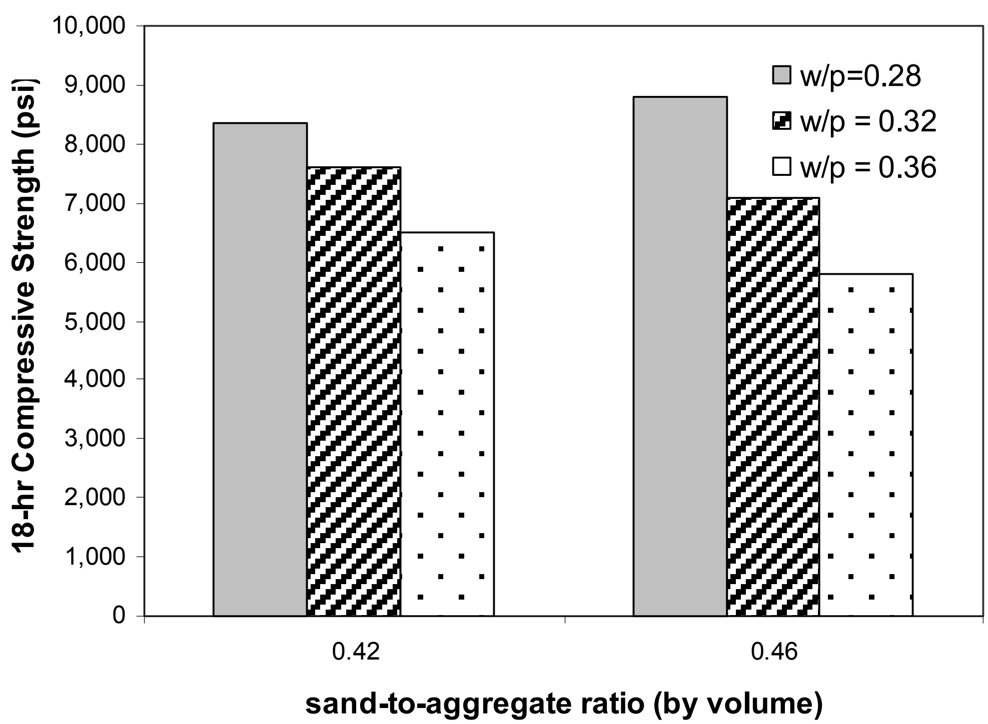

Figure 4-11: Effect of *w/p* on the 18-hr compressive strength for slag mixtures

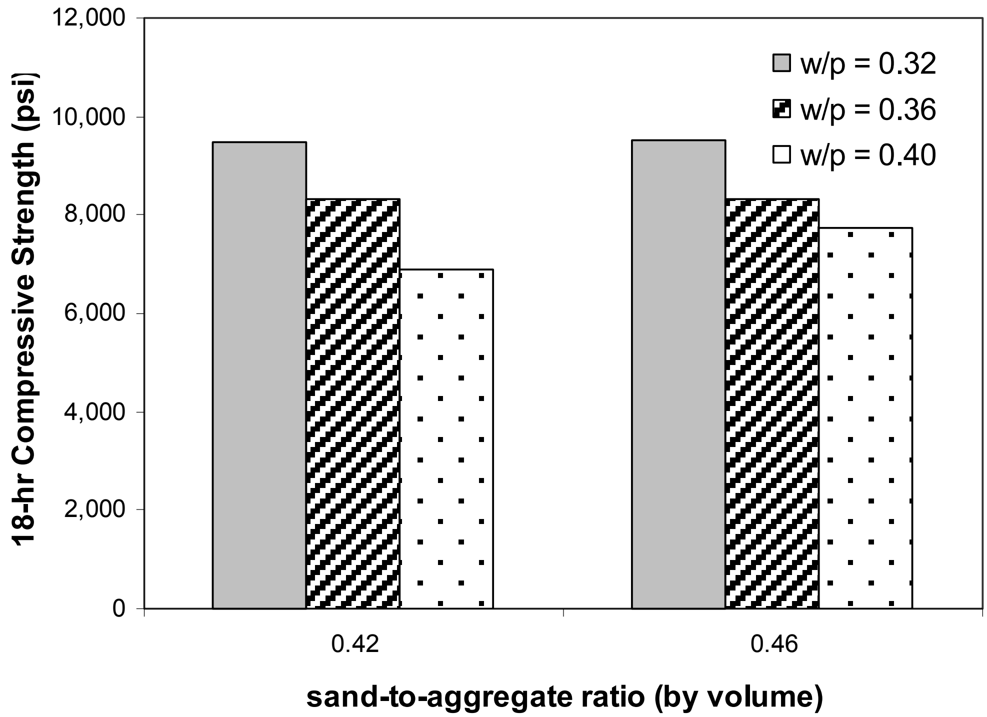

Figure 4-12: Effect of *w/p* on the 18-hr compressive strength for ternary mixtures

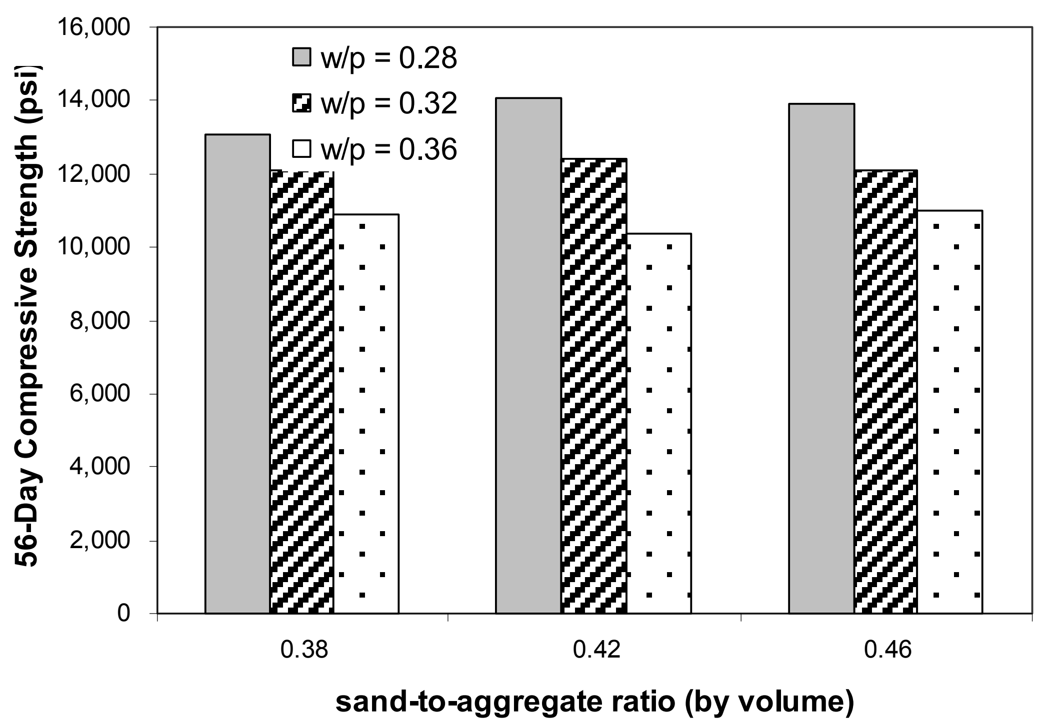

Figure 4-13: Effect of *w/p* on the 56-day compressive strength for fly ash mixtures

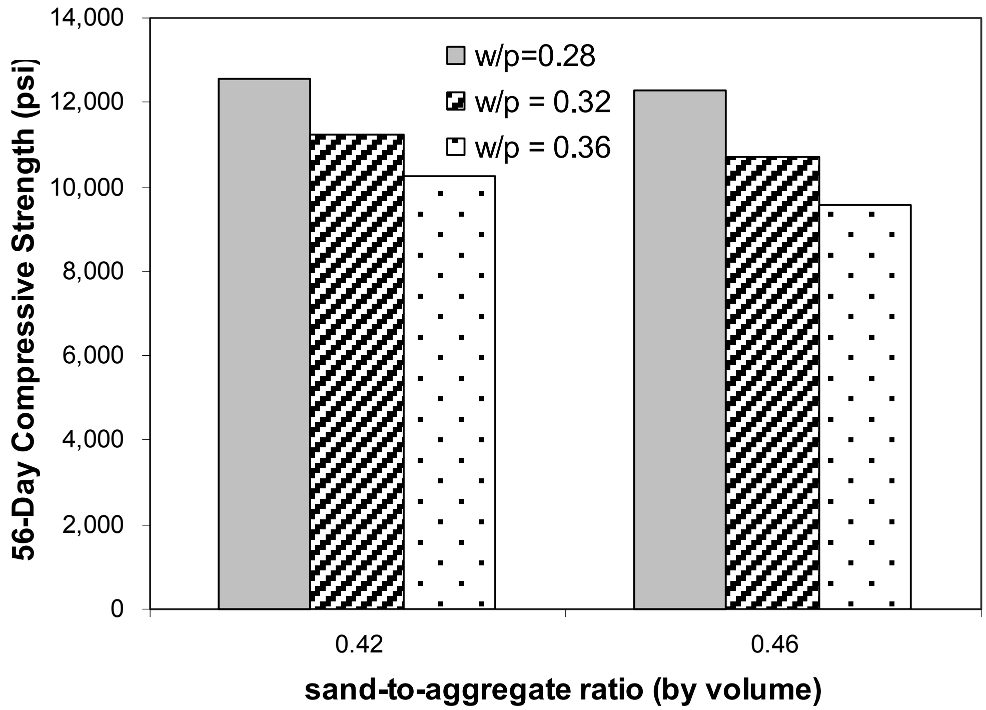

Figure 4-14: Effect of *w/p* on the 56-day compressive strength for slag mixtures

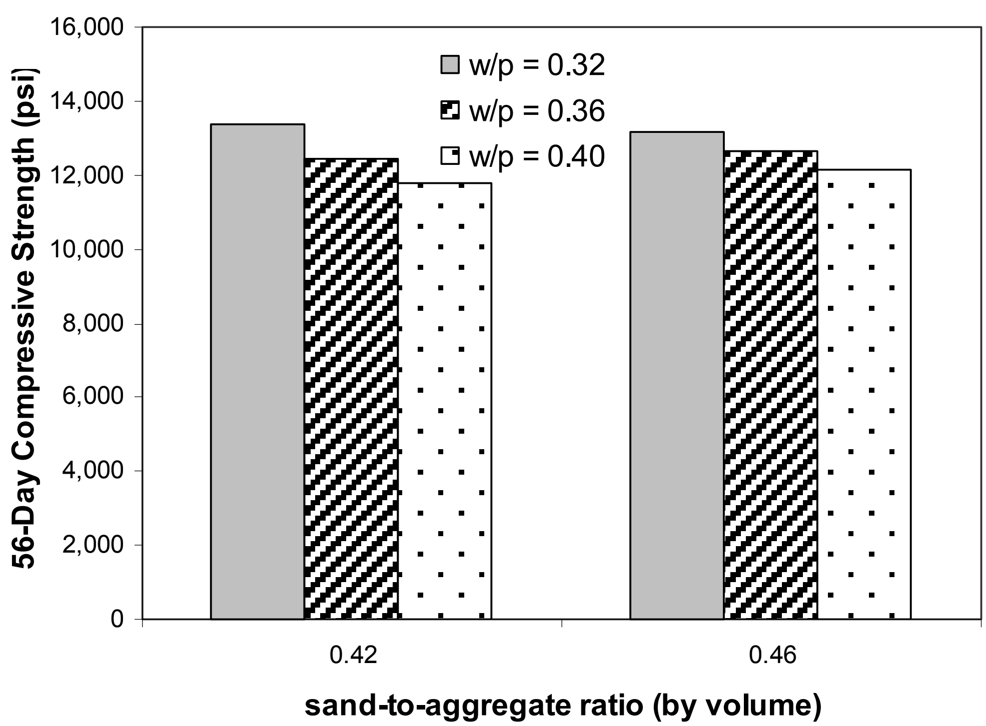

Figure 4-15: Effect of *w/p* on the 56-day compressive strength for ternary mixtures

4.2.1.3 Effects of Powder Combinations

The effects of different powder combinations on the 18-hour compressive strengths (f'_{ci}) and 56-day compressive strengths are illustrated in Figures 4-16 and 4-17 respectively. All 21 SCC mixtures are presented in each of these figures. To evaluate the effects of the different powders on the compressive strengths of the SCC mixtures, the effects of powder(s) were analyzed by comparing similar mixtures only, even though it was determined that the *s/agg* had no effect on SCC's compressive strength.

At 18 hours, the ternary mixtures had a much higher f'_{ci} than their counterparts made with the same *w/p* and *s/agg*. Comparing the slag mixtures to the fly ash mixtures, it may be seen that similar f'_{ci} levels are obtained. SCC11:0.32-0.42-S has a higher f'_{ci} than SCC5:0.32-0.42-FA, but SCC8:0.32-0.46-FA has a higher f'_{ci} than SCC14:0.32-0.46-S. SCC12:0.36-0.42-S has a higher f'_{ci} than SCC6:0.36-0.42-FA, while SCC15:0.36-0.46-S and SCC9:0.36-0.46-FA have equivalent f'_{ci}. The total air content and dosage of HRWR admixture were evaluated for these mixtures, but they had no apparent effect on relative strength. The introduction of 8% silica fume to the SCC mixtures that contained only Type III cement and Class C fly ash significantly increased f'_{ci}. This observation agrees with the findings of Mindess, Young, and Darwin (2003), which stated that silica fume increases early strength gain.

The long-term (56-day) compressive strength results are presented in Figure 4-17. Again, at equal *w/p*, the ternary mixtures have a higher 56-day compressive strength than the other two powder combinations. However, the fly ash mixtures have a higher 56-day compressive strength than the slag mixtures. While neither fly ash nor GGBF slag mixtures seemed to have an early strength gain advantage, Figure 4-17 shows that the fly ash mixtures reach a greater long-term strength than the slag mixtures of similar *w/p*. Since the mixtures in question do not contain the same amount of SCMs (refer to Table 3-1), one could argue that the lack of Type III cement is the reason for the difference. However, at an identical replacement level of 30%, the same pattern holds true when evaluating the two powder combinations at a *w/p* of 0.28 and *s/agg* of 0.42 and 0.46.

4.2.1.4 Behavior of SCC Versus Conventional-Slump Concrete

Comparison of the control mixtures' f'_{ci} versus those of the SCC mixtures can be seen in Figure 4-16. At a *w/p* of 0.36, f'_{ci} values of the fly ash and slag SCC mixtures were significantly less (24% on average) than that of the control mixture made with a *w/c* of 0.37 (CTRL1:0.37). However, at a *w/p* of 0.32, f'_{ci} values of the fly ash and slag SCC mixtures were approximately the same as for CTRL1:0.37. Therefore, replacing Type III cement with high dosages of Class C fly ash or GGBF Grade 120 slag will decrease the f'_{ci} of SCC mixtures. Higher f'_{ci} values can be obtained by using a decreased water-to-powder ratio. The effect of *w/p* on f'_{ci} of the ternary SCC mixtures matches that obtained for the two control mixtures.

Comparison of the control mixtures' 56-day f'_c versus those of the SCC mixtures can be seen in Figure 4-17. At a *w/p* of 0.36, 56-day f'_c values for the fly ash and slag SCC mixtures were lower than that of CTRL1:0.37 by an average of 4% and 13% respectively. At a *w/p* of 0.32, the slag SCC mixtures had strengths approximately equal to CTRL1:0.37. All of the ternary SCC mixtures had higher f'_c values than CTRL1:0.37 at 56 days. All of the SCC mixtures exhibited higher 56-day f'_c values than CTRL2:0.42.

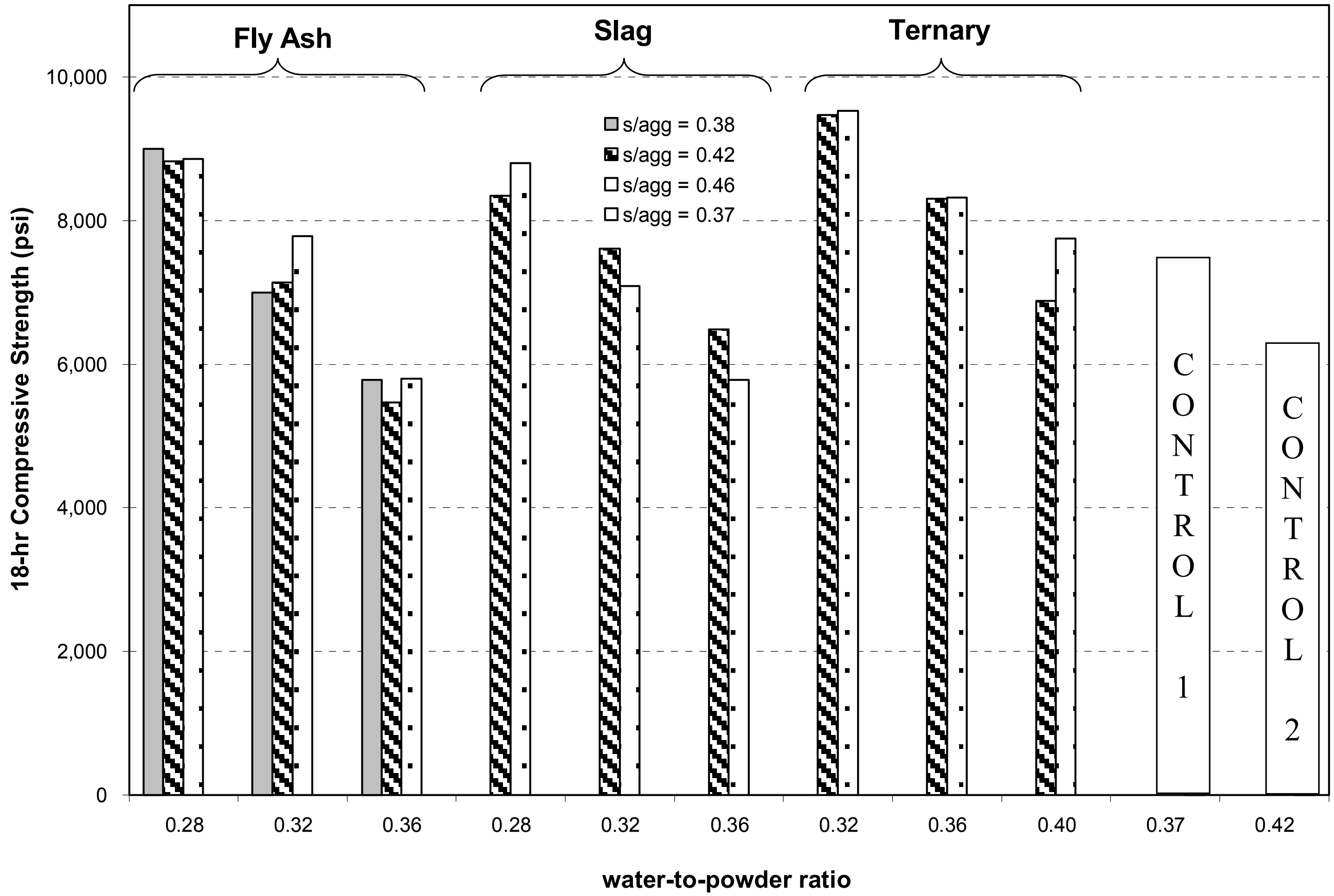

Figure 4-16: Effect of different powder combinations on the 18-hr compressive strengths

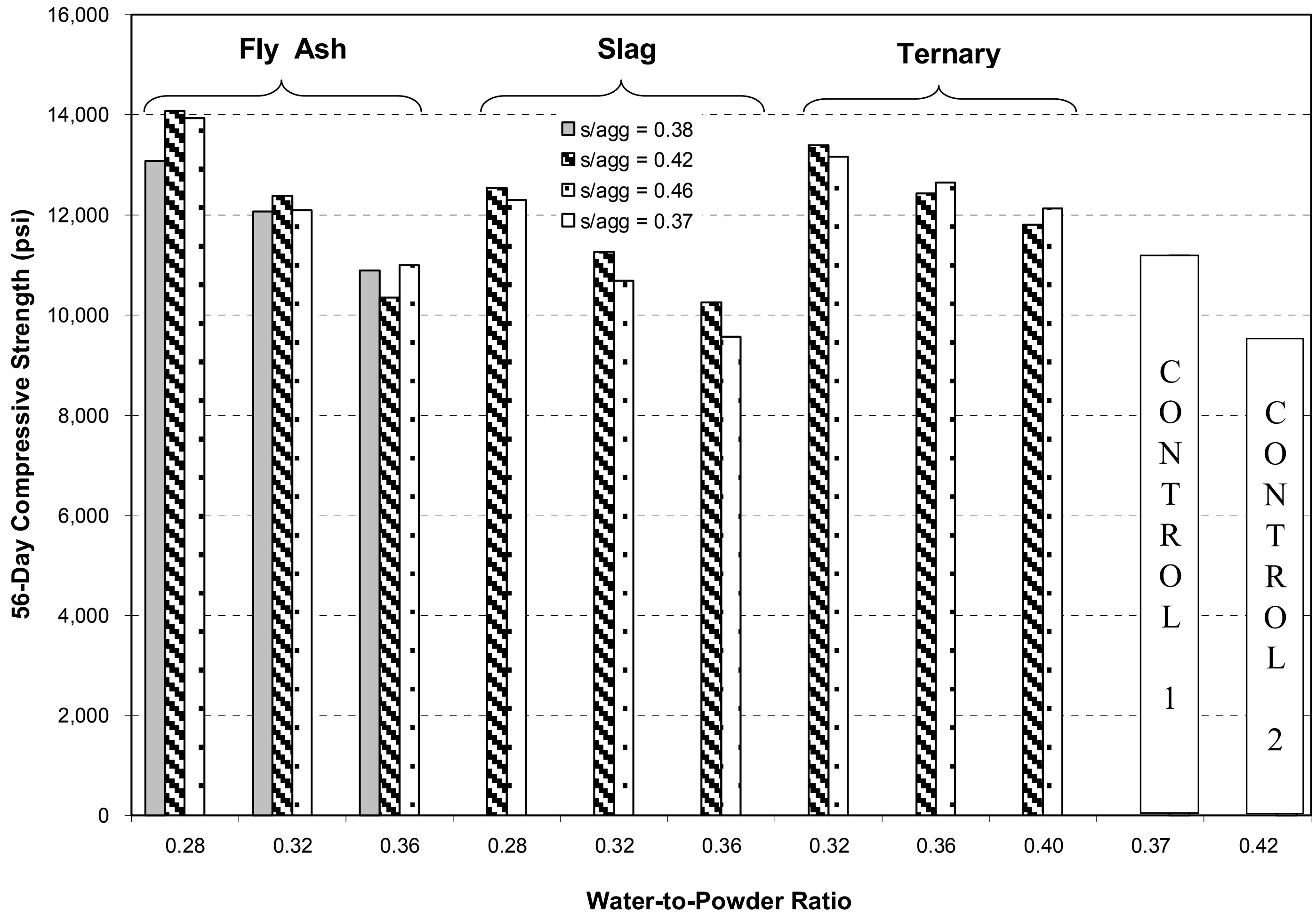

Figure 4-17: Effect of different powder combinations on the 56-day compressive strengths

4.2.1.5 Compressive Strength Gain With Respect to Time

The compressive strength gain with respect to time is presented in Figures 4-18 and 4-19. In both figures, all powder combinations are presented and have been grouped according to their *w/p* since the *w/p* has more influence on strength than the *s/agg*. The control mixtures' strength gains have also been shown for comparison purposes.

The compressive strength gain (in percent) of the 28-day compressive strength relative to the 18-hour compressive strength for the match-cured 4 in. x 8 in. cylinders is presented in Figure 4-18. From Figure 4-18, one can see that the strength gain increases as the *w/p* increases for all mixtures. Among the three types of powder systems used to make the SCC mixtures, the fly ash mixtures experienced the most strength gain from 18 hours to 28 days, followed by the slag SCC mixtures, and then the ternary SCC mixtures. At a *w/p* of 0.36, both the slag and fly ash SCC mixtures experienced a greater strength gain than CTRL1:0.37.

The compressive strength gain (in percent) of the 56-day compressive strength relative to the 3-day compressive strength for the 6 in. x 12 in. moist-cured cylinders is presented in Figure 4-19. As with the match-cured cylinders, the moist-cured cylinders' strength gain increases with increasing *w/p* for all mixtures, except the control mixtures. Both control mixtures had a 35% increase in strength from 3 days to 56 days. All of the SCC mixtures had higher strength gain at similar *w/p* than the control mixtures. The ternary SCC mixtures had the largest gain in strength, followed by the slag mixtures, and then the fly ash mixtures.

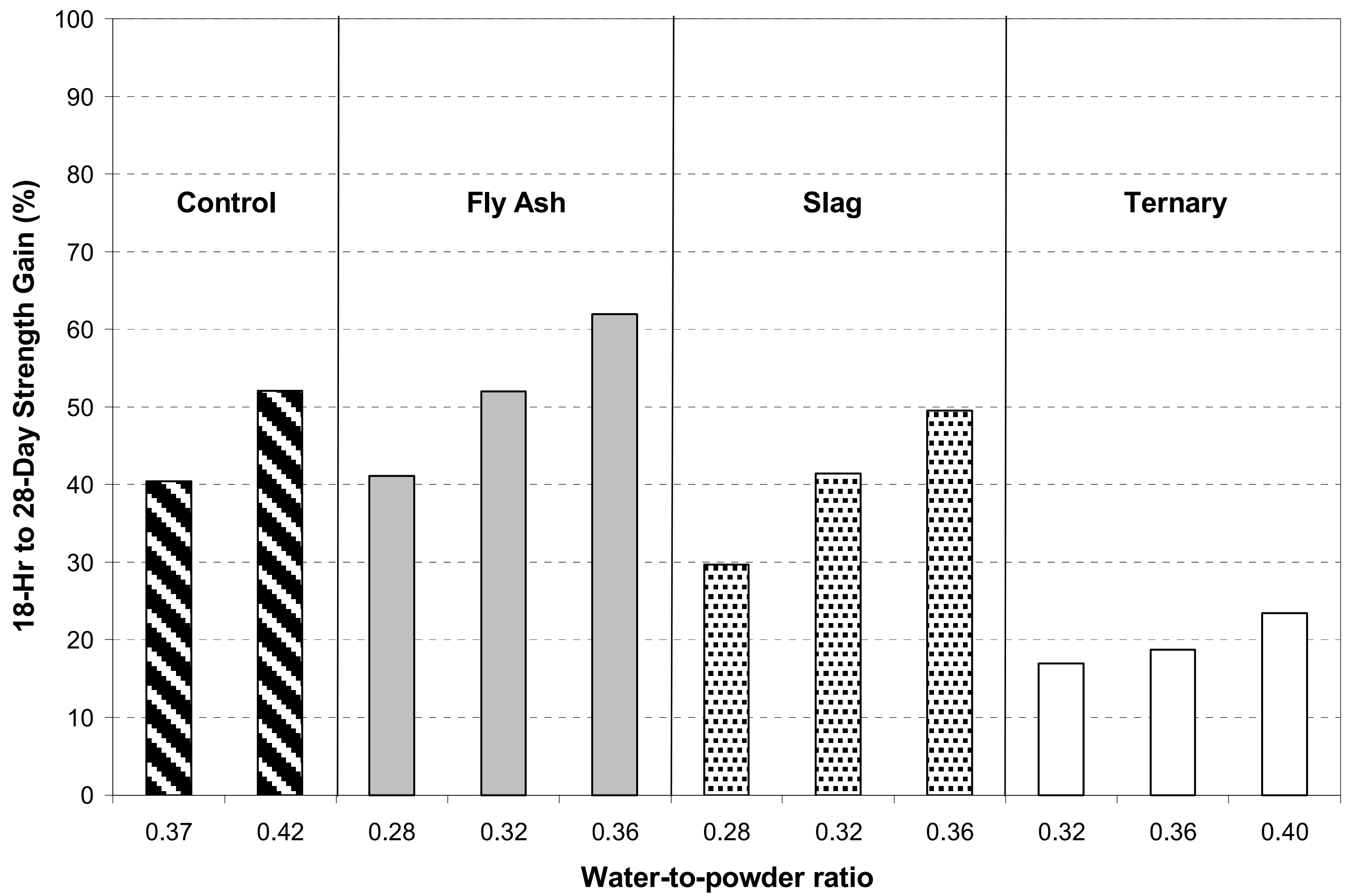

Figure 4-18: 18-hr to 28-day strength gain (%) for match-cured cylinders

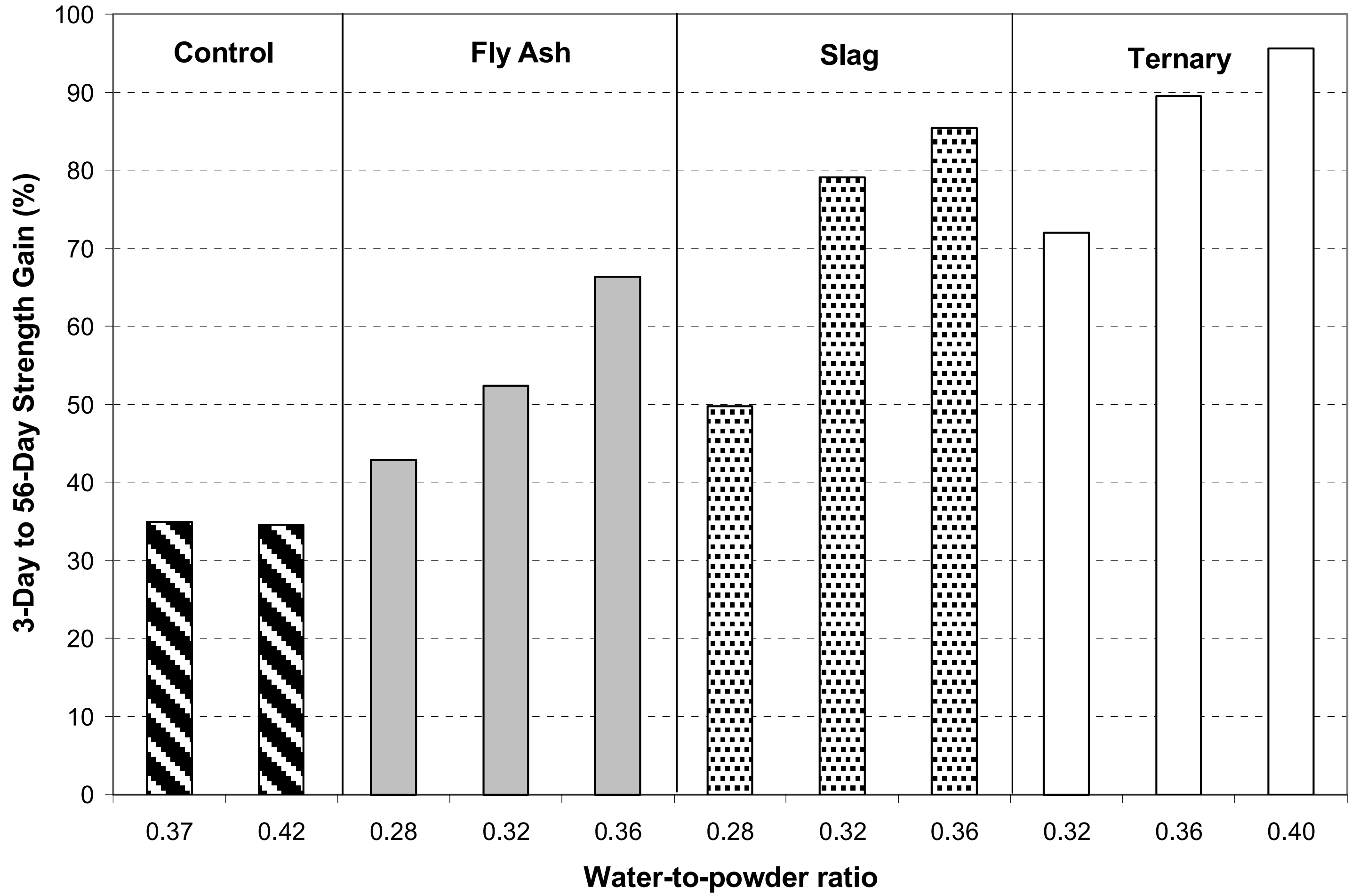

Figure 4-19: 3-day to 56-day strength gain (%) for moist-cured cylinders

4.2.2 MODULUS OF ELASTICITY

The modulus of elasticity (E_c) results are summarized in Table 4-3. The 18-hour modulus of elasticity (E_{ci}) values of the SCC mixtures varied between 4,700 and 5,900 ksi, while the two control mixtures had E_{ci} values of 5,330 and 6,100 ksi. There was no specified requirement for E_{ci}.

4.2.2.1 Effects of Sand-to-Aggregate Ratio

The effect of the *s/agg* on E_{ci} is seen for all three powder combinations in Figures 4-20 through 4-22. It can be seen from Figures 4-20 and 4-22 that the *s/agg* has no distinct effect on E_{ci} for the fly ash and ternary SCC mixtures. From Figure 4-21, it appears that the *s/agg* has a small effect on E_{ci} for the slag SCC mixtures. The slag mixtures with a *s/agg* of 0.46 have a 2 to 12% lower E_{ci} than the mixtures with a *s/agg* of 0.42.

The effect of the *s/agg* on the long-term (56 -day) E_c is presented in Figures 4-23 through 4-25 for all three powder combinations. The *s/agg* has no distinct effect on fly ash or ternary SCC mixtures. As previously mentioned, the *s/agg* seemed to have a small effect on E_{ci} of the slag SCC mixtures. However, Figure 4-24 shows that the effect of the *s/agg* on these slag SCC mixtures decreases with time. At 18 hours, the greatest difference between the two *s/agg* was 12%; however, at 56 days this difference was reduced to 6%.

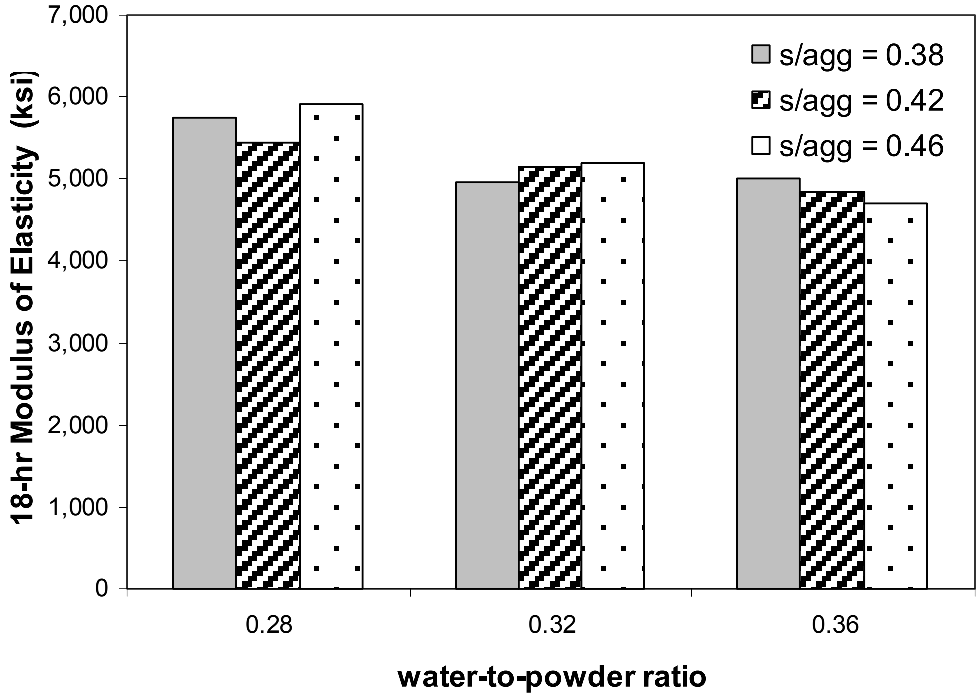

Figure 4-20: Effect of *s/agg* on the 18-hr modulus of elasticity for fly ash mixtures

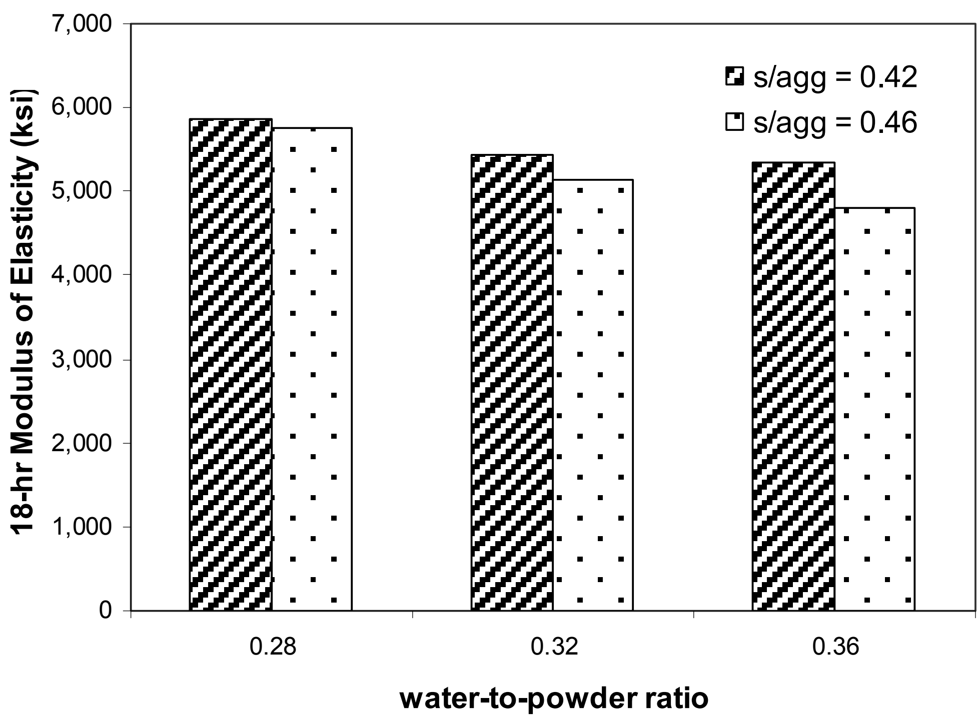

Figure 4-21: Effect of *s/agg* on the 18-hr modulus of elasticity for slag mixtures

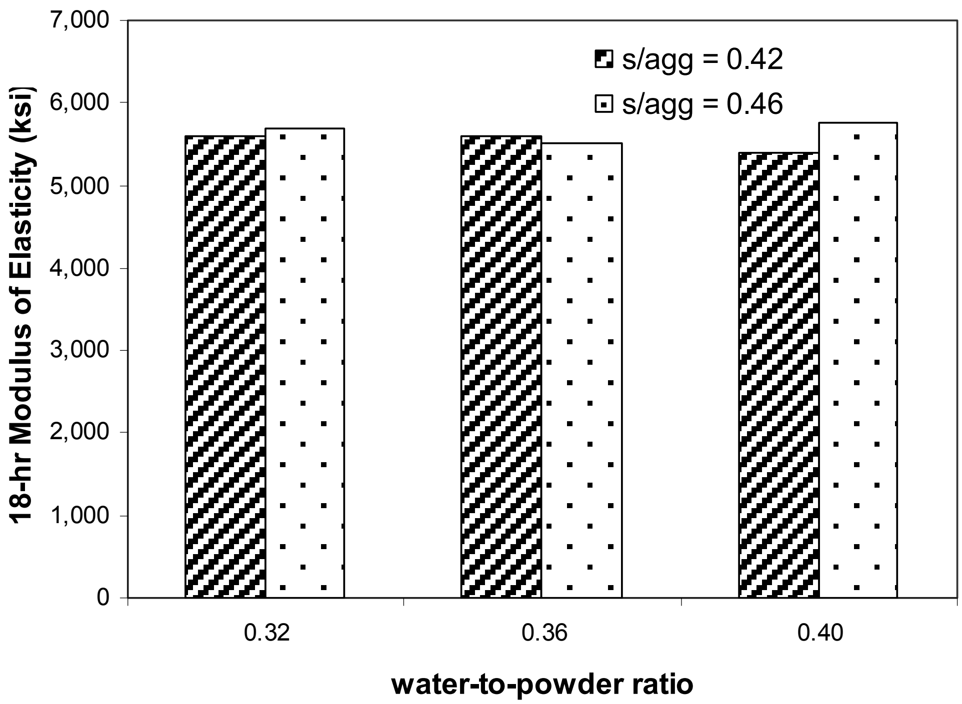

Figure 4-22: Effect of *s/agg* on the 18-hr modulus of elasticity for ternary mixtures

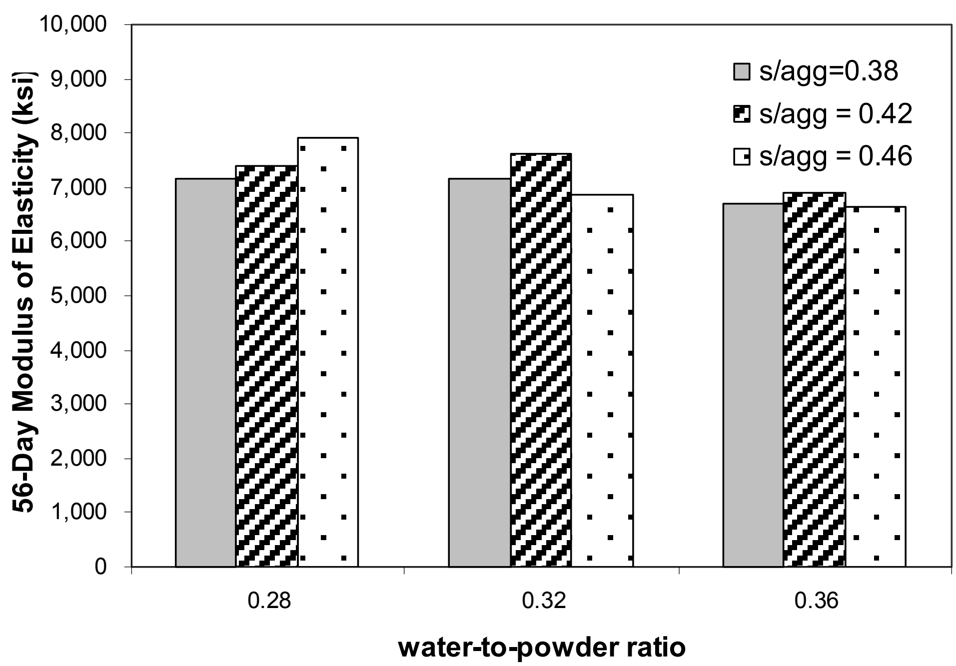

Figure 4-23: Effect of *s/agg* on the 56-day modulus of elasticity for fly ash mixtures

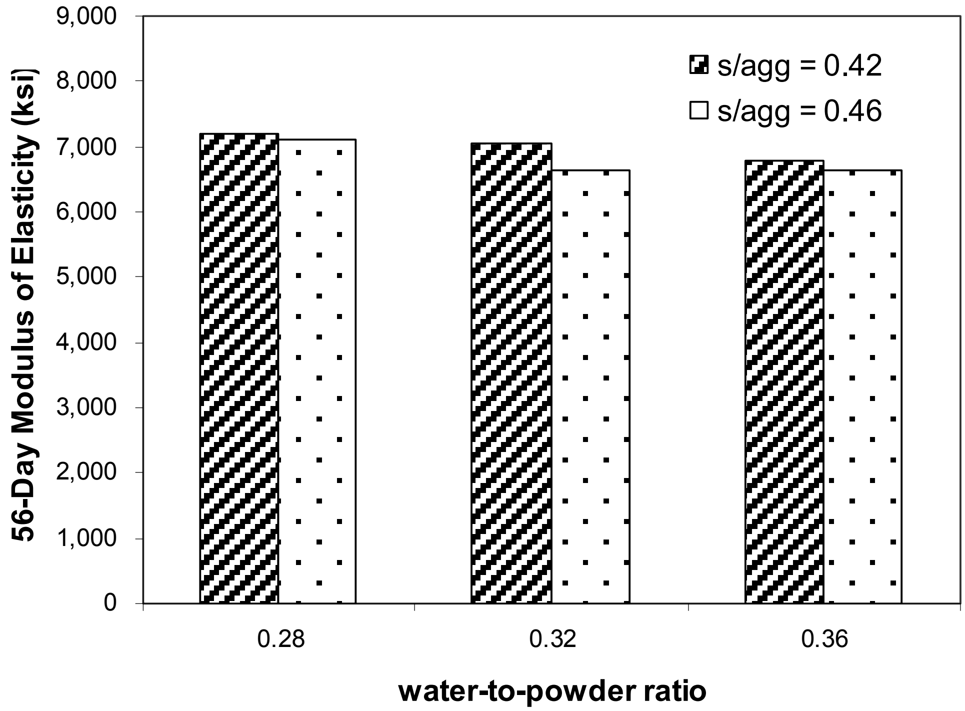

Figure 4-24: Effect of *s/agg* on the 56-day modulus of elasticity for slag mixtures

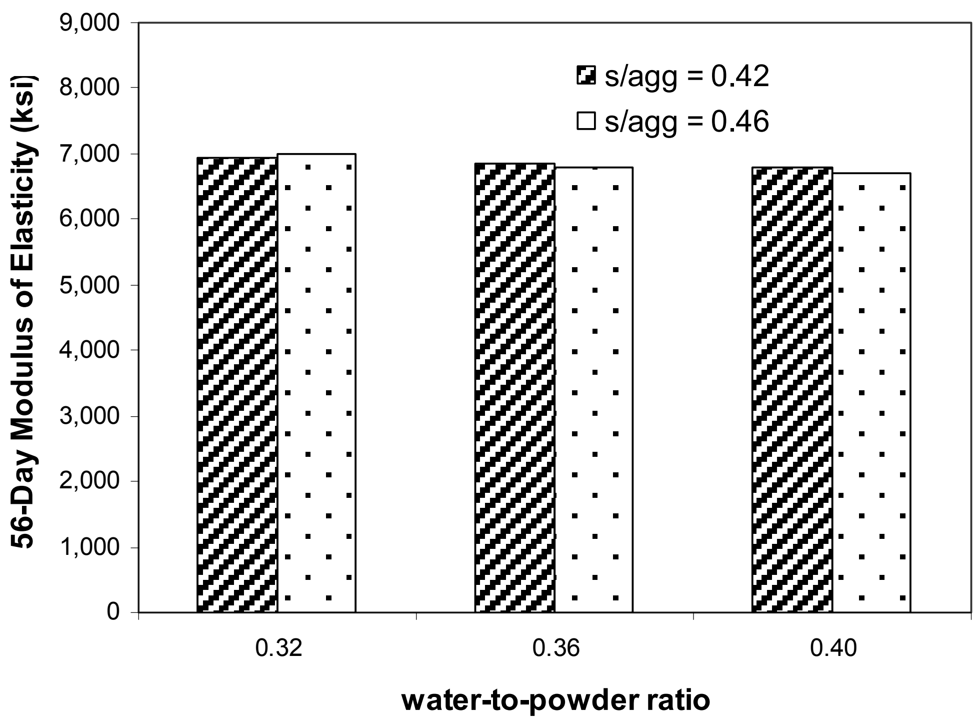

Figure 4-25: Effect of *s/agg* on the 56-day modulus of elasticity for ternary mixtures

Not shown in Chapter 4 are the 28-day evaluations of the *s/agg* on E_c. These results can be found in Appendix C. The same observations regarding the effect of the *s/agg* on E_{ci} hold true for the match-cured specimens at 28 days. However, for the 28-day moist-cured cylinders, the *s/agg* has no noticeable effect on E_c for any of the powder combinations.

These findings are in agreement with those of Su et al. (2002). Su et al. (2002) concluded that when the fine and coarse aggregate have comparable elastic moduli, and the total volume of aggregate is held constant, the sand-to-aggregate ratio does not significantly affect the modulus of elasticity of the concrete. In this case, the total volume of aggregate remained fairly constant (62 to 64% by volume).

4.2.2.2 Effects of Water-to-Powder Ratio

The effect of the *w/p* on E_{ci} for all three powder combinations is illustrated in Figures 4-26 through 4-28. Generally, E_{ci} decreases with an increase in *w/p* for the fly ash and slag SCC mixtures. The *w/p* has no effect on E_{ci} for the ternary mixtures. The effect of the *w/p* on the long-term E_c is shown in Figures 4-29 through 4-31. There is no consistent relationship between the *w/p* and E_c for any of the powder combinations at 56 days.

Not shown in Chapter 4 are the 28-day evaluations of the *w/p* on E_c. This is shown in Appendix C. For the match-cured 28-day cylinders, the *w/p* has no effect on E_c for the fly ash SCC mixtures, while the slag SCC mixtures' E_c continued to increase with decreasing *w/p*. The 28-day E_c for the ternary SCC mixtures is highest at the lowest *w/p* (0.32), but E_c is comparable at *w/p* of 0.42 and 0.46. There is no reliable relationship between any of the 28-day moist-cured cylinders' E_c and the *w/p*.

As Mindess, Young, and Darwin (2003) state, the modulus of elasticity is related to the compressive strength, and thus factors that affect the compressive strength will similarly influence E_c. Since the compressive strength decreases as the w/p increases, this could explain why E_c had a slight tendency to decrease with an increasing *w/p* in some cases.

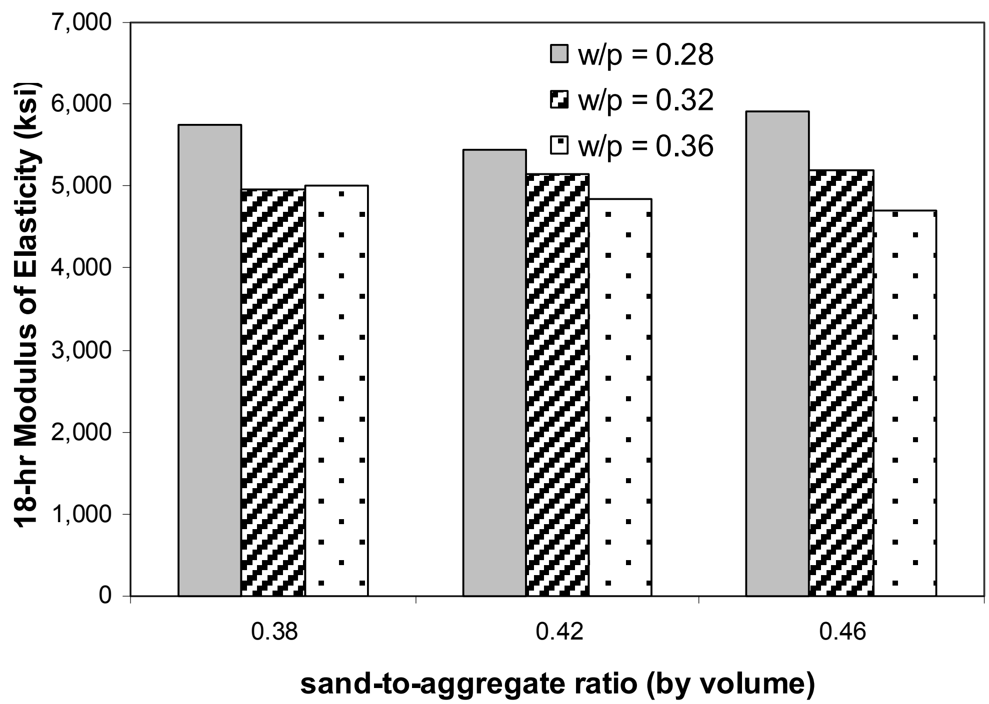

Figure 4-26: Effect of *w/p* on the 18-hr modulus of elasticity for fly ash mixtures

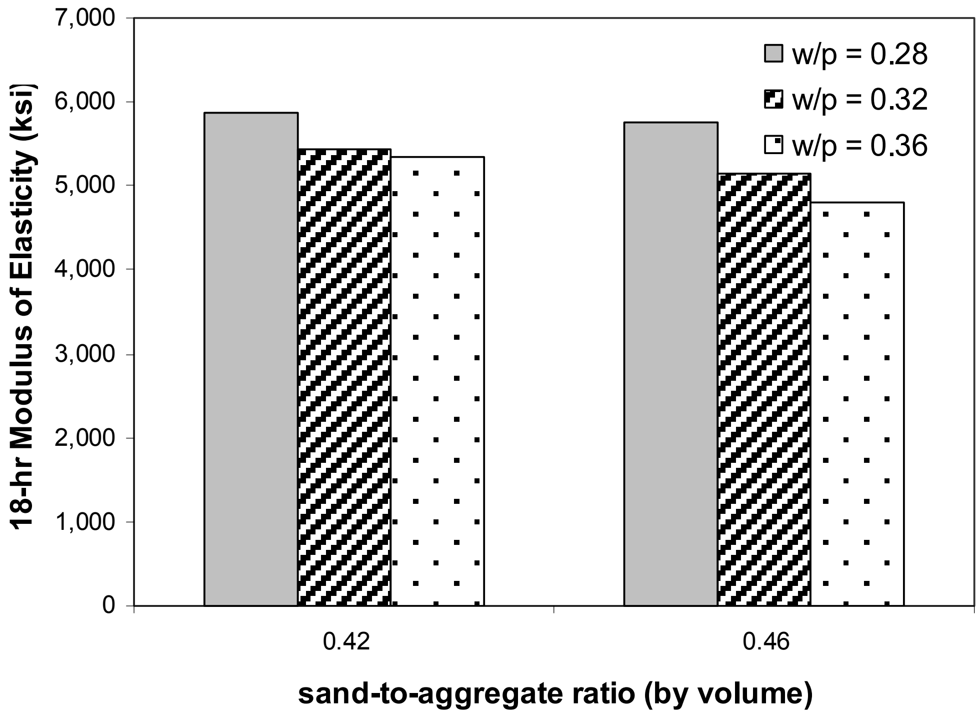

Figure 4-27: Effect of *w/p* on the 18-hr modulus of elasticity for slag mixtures

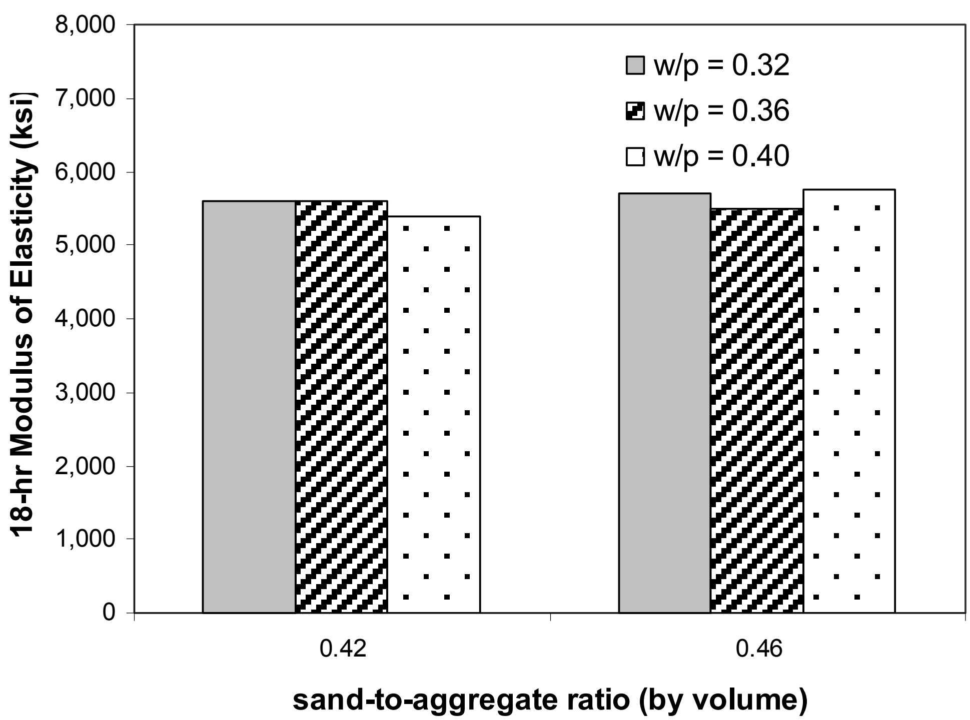

Figure 4-28: Effect of *w/p* on the 18-hr modulus of elasticity for ternary mixtures

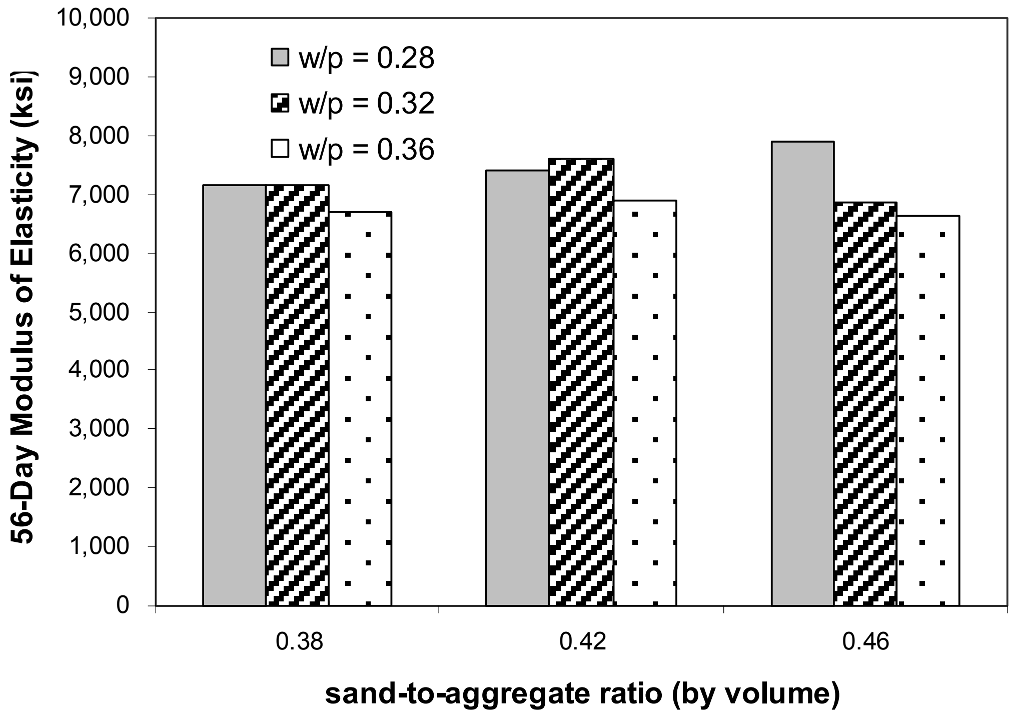

Figure 4-29: Effect of *w/p* on the 56-day modulus of elasticity for fly ash mixtures

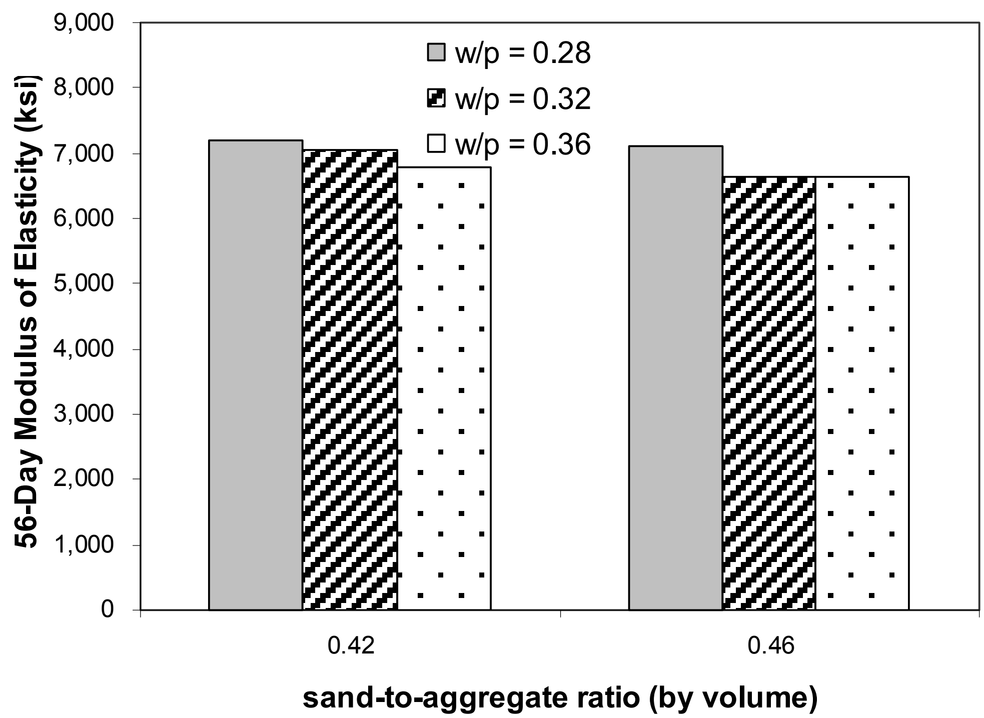

Figure 4-30: Effect of *w/p* on the 56-day modulus of elasticity for slag mixtures

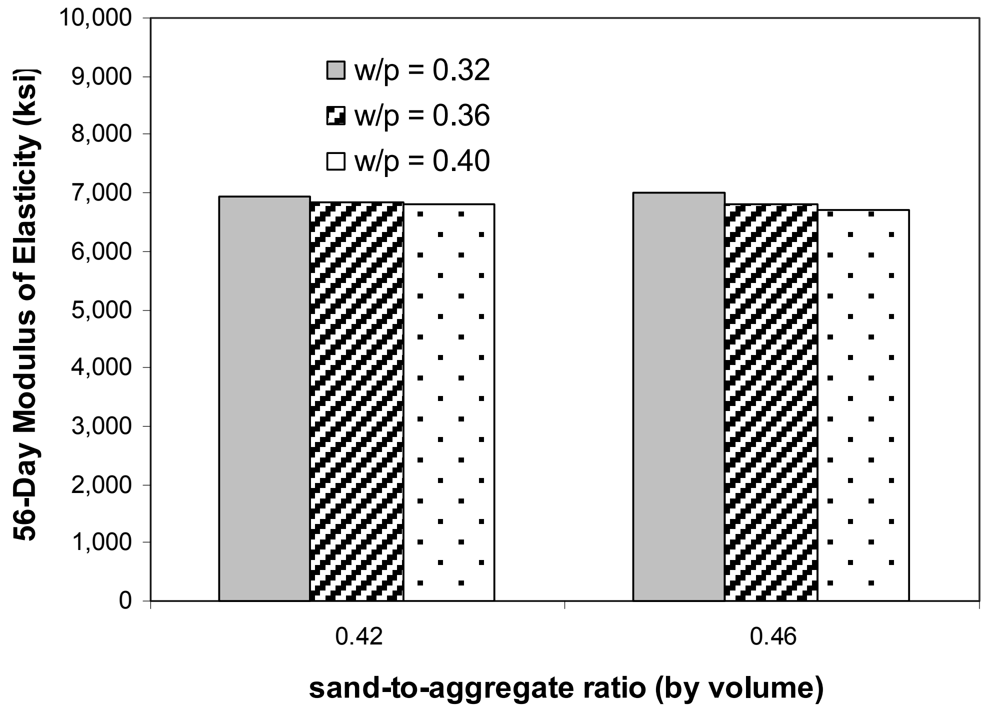

Figure 4-31: Effect of *w/p* on the 56-day modulus of elasticity for ternary mixtures

4.2.2.3 Effects of Powder Combinations

The effects of different powder combinations on the 18-hour E_{ci} and 56-day E_c are illustrated in Figures 4-32 and 4-33 respectively. While all 21 SCC mixtures are presented in each of these figures, the only constants common to all three powder combinations are *w/p* of 0.32 and 0.36 and *s/agg* of 0.42 and 0.46. Therefore, to evaluate the effects that the different powders had on the modulus of elasticity of the SCC mixtures, mixtures of similar *w/p* and *s/agg* should be compared.

The ternary SCC mixtures have a higher E_{ci} than both the fly ash and slag SCC mixtures. On average, the slag SCC mixtures have a slightly higher E_{ci} than the fly ash SCC mixtures by approximately 4%. The different powder combinations have no significant effect on the long-term (56-day) E_c. The long-term E_c is within 3% (on average) for all three powder combinations.

The effects of the different powder combinations on the 28-day E_c are shown in Appendix C. The powder combinations had no effect on the 28-day E_c.

4.2.2.4 Behavior of SCC Versus Conventional-Slump Concrete

The E_{ci} of the control mixtures versus the E_{ci} of these SCC mixtures is shown in Figure 4-32. The 18-hr modulus of elasticity (E_{ci}) for all of the SCC mixtures with a *w/p* of 0.36 is less than the E_{ci} of the control mixture made with a *w/c* of 0.37 (CTRL1:0.37) by 19% on average. However, at a *w/p* of 0.28, E_{ci} of the fly ash and slag SCC mixtures are of the same order of magnitude as CTRL1:0.37. The ternary SCC mixtures with a *w/p* of 0.40 have a higher E_{ci} than the control mixture with a *w/c* of 0.42 (CTRL2:0.42) by 5% on average. The E_{ci} of the control mixtures, like the fly ash and slag SCC mixtures, decreases with an increase in *w/p*.

When comparing the control mixtures to any of the SCC mixtures with comparable strengths, the control mixtures have a higher E_{ci}. This may be due to the slightly higher volume of aggregate in the control mixtures (Bonen and Shah 2003). However, the fact that the 56-day E_c value of the CTRL1:0.37 mixture is comparable to the 56-day E_c of SCC mixtures of equal strength may indicate that the high dosage of fly ash or GGBF slag may be the cause. These SCMs take time to react, and this could explain the relative difference in E_c values from 18 hours to 56 days.

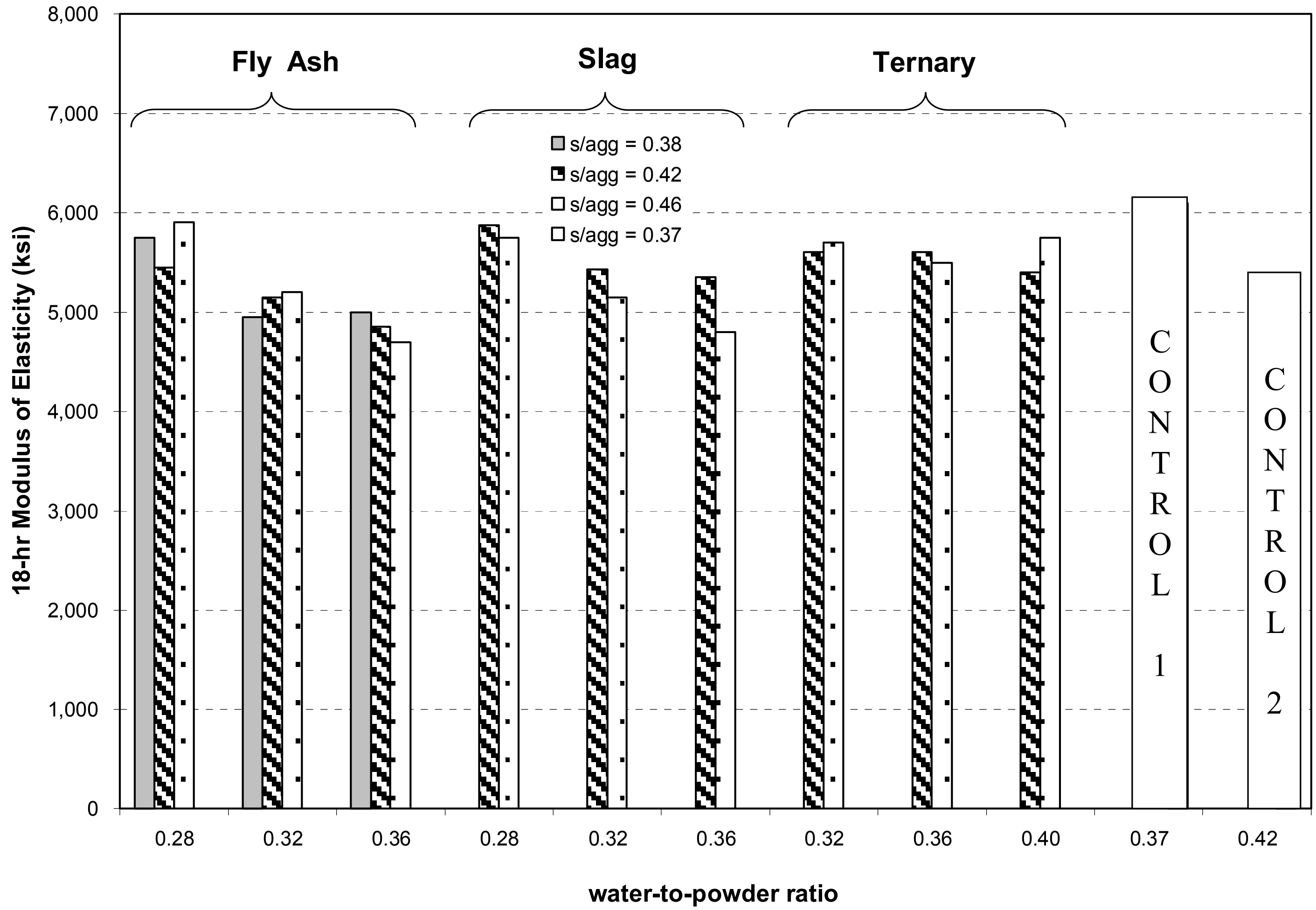

Figure 4-32: Effect of different powder combinations on the 18-hr modulus of elasticity

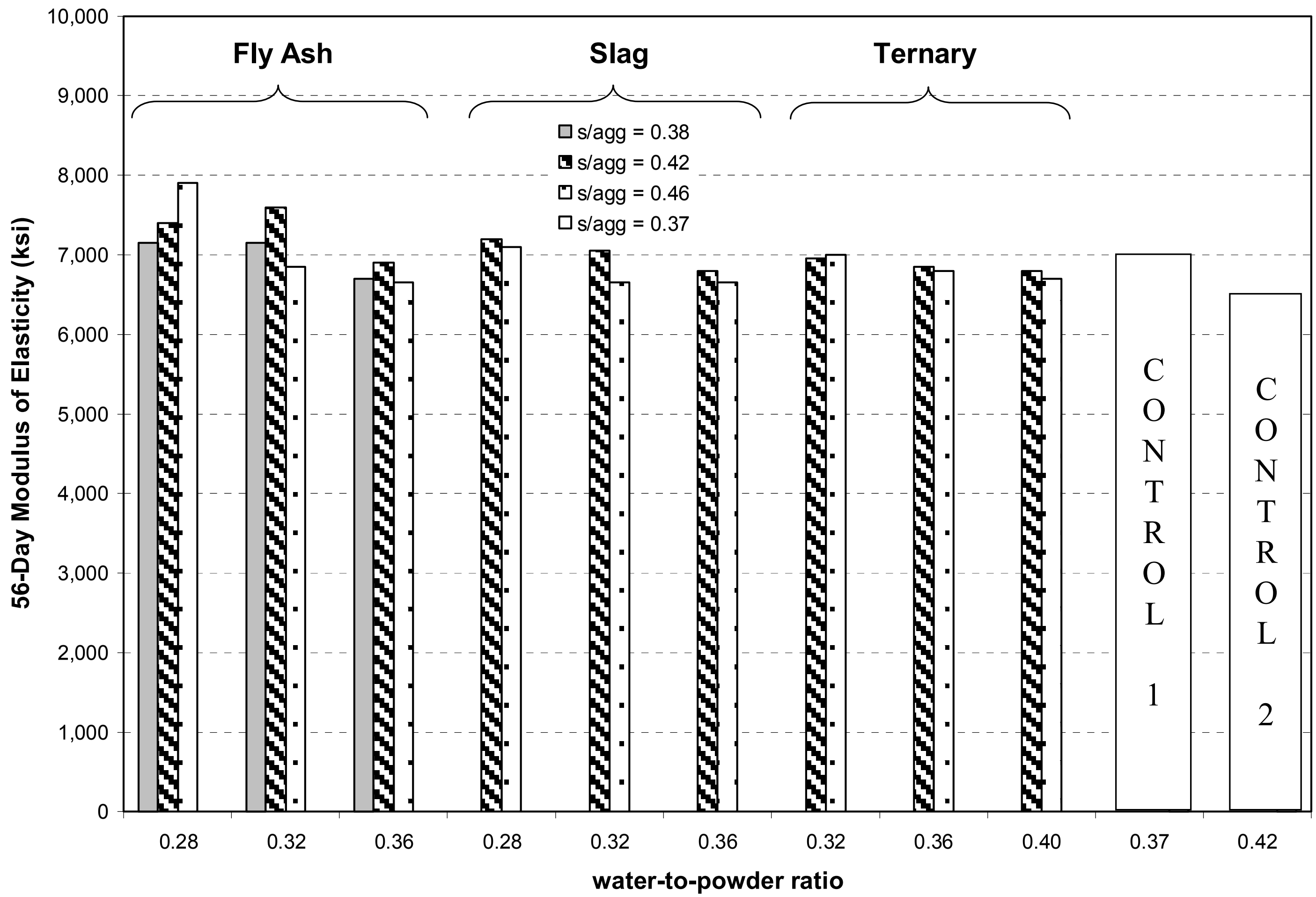

Figure 4-33: Effect of different powder combinations on the 56-day modulus of elasticity

4.2.2.5 Measured E_c versus Predicted E_c

The modulus of elasticity was estimated using Equation 2-2 (AASHTO LRFD 2004; ACI 318 2005) to determine if the E_c values obtained for the SCC mixtures correspond to the behavior of conventional-slump concrete. Every SCC mixture's E_c, collected at all ages, is presented in Figure 4-34 versus that estimated by the AASHTO LRFD formulation. If Equation 2-2 provides a perfect estimate of all the measured E_c values, then all of the data points would fall on the 45° line of equality. If the points are above the 45° line of equality, then the AASHTO LRFD formulation overestimates the E_c, but if the data points fall below the 45° line of equality, then the AASHTO LRFD formulation underestimates E_c. The AASHTO LRFD formulation generally underestimates E_c of the SCC mixtures; however, the majority of the errors fall within the 0% and -10% range. The measured E_c values of these SCC mixtures slightly exceed what one would estimate with the AASHTO LRFD E_c formulation.

Equation 2-3 (ACI 363 1997) was also used to predict E_c. This equation was formulated for high-strength concretes, and it is valid for concretes ranging from 3,000 to 12,000 psi (ACI 363 1997). Every SCC mixture's E_c, collected at all of the different ages, is presented in Figure 4-35 versus that estimated by the ACI 363 formulation. If Equation 2-3 provides a perfect estimate of all the measured E_c values, then all of the data points would fall on the 45° line of equality. If data points are above the 45° line of equality, then the ACI 363 formulation overestimates the E_c, but if the data points fall below the 45° line of equality, then the ACI 363 formulation underestimates E_c. The majority of the Ec estimates have errors within the -10% to -25% range. The ACI 363 formulation underestimates E_c on a higher order of magnitude than the AASHTO LRFD formulation. In some instances, the ACI 363 formulation underestimates E_c by more than 25%. Generally, the E_c values of these SCC mixtures significantly exceed what one would estimate with the ACI 363 formulation.

Overall, the E_c values obtained for the SCC mixtures are in reasonable agreement with the elastic stiffness assumed during the design of conventional-slump concrete structures. Summaries for the measured E_c versus the estimated E_c, for both AASHTO LRFD and ACI 363, are provided in Appendix C and have been categorized by their concrete age.

4.2.3 DRYING SHRINKAGE

As stated previously, the drying shrinkage strain (ε_{SH}) data presented in Tables 4-5 and 4-6 are for all of the SCC mixtures and both control mixtures. Out of the 21 SCC mixtures made for this research, only the fly ash and slag SCC mixtures have drying shrinkage data through 32 weeks at the time of this document's development, while the ternary SCC mixtures have drying shrinkage data through 16 weeks. Therefore, the reader should pay close attention to the results of Sections 4.2.4.1 through 4.2.4.3 as the analysis of the specimens will reflect different long-term drying shrinkage ages.

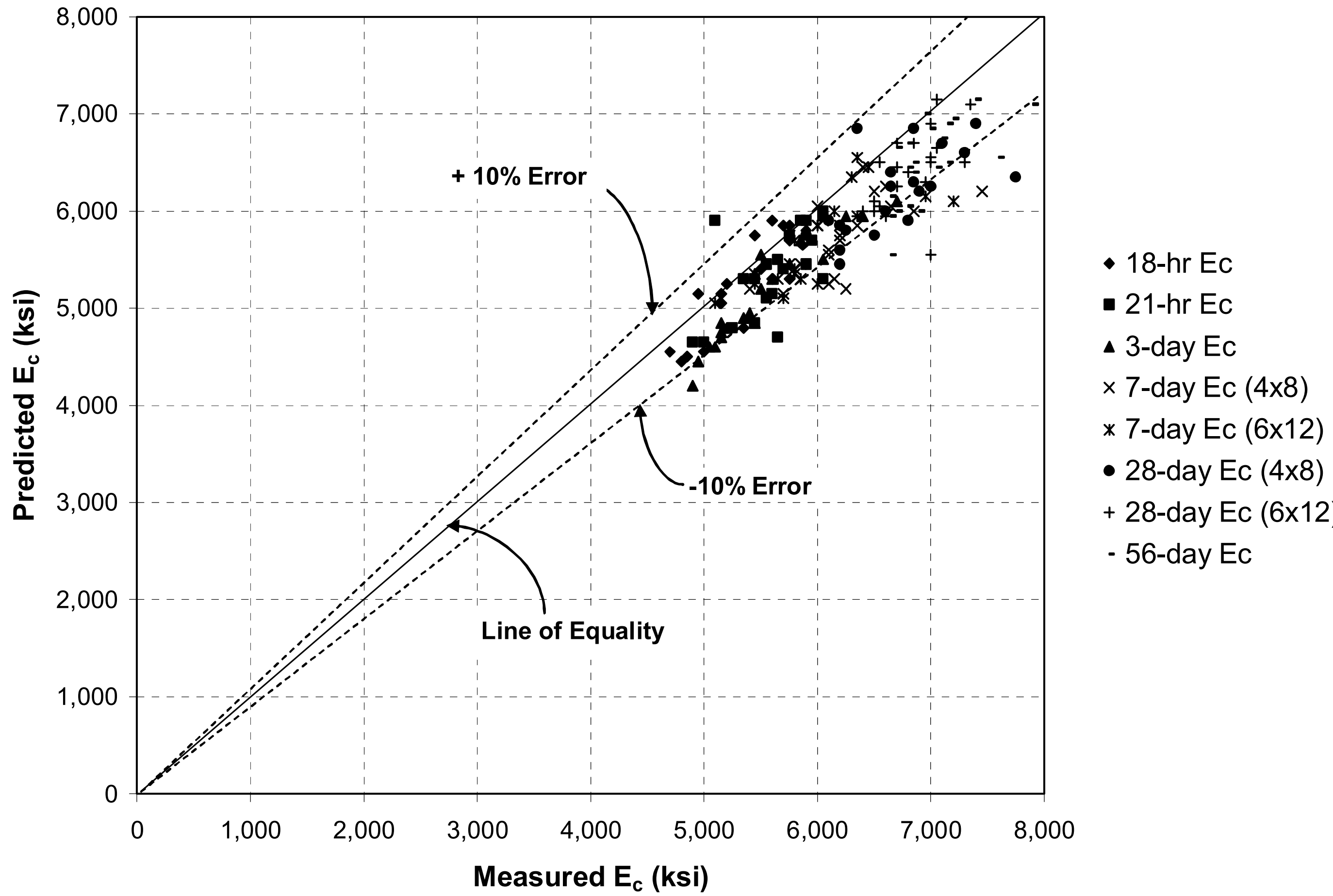

Figure 4-34: AASHTO LRFD estimate of the modulus of elasticity

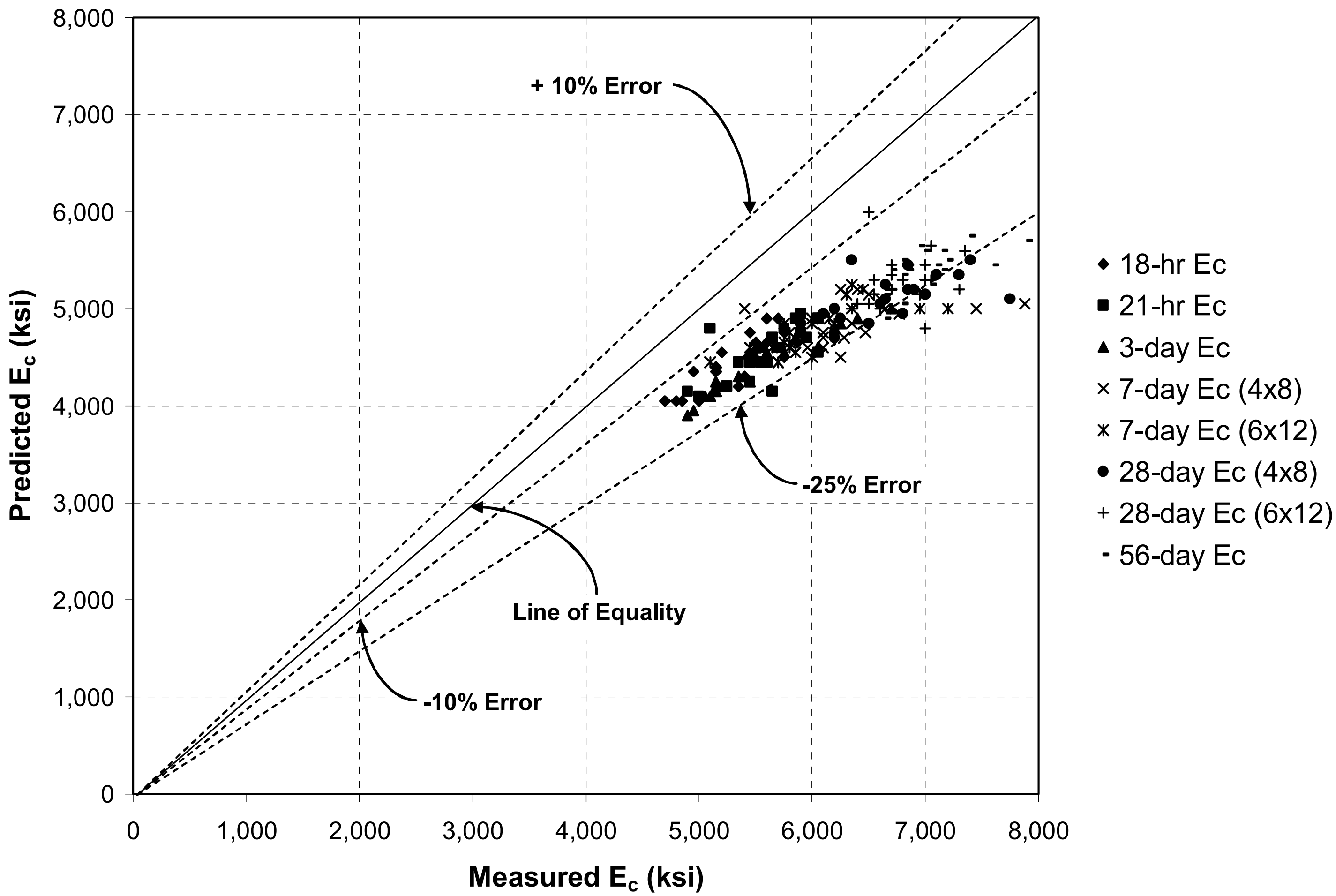

Figure 4-35: ACI 363 estimate of the modulus of elasticity

The drying shrinkage of the specimens that have been moist-cured for seven days are most representative of actual prestressed girders, because 24 hours of steam curing at elevated temperatures is approximately equal to seven days of moist curing at room temperature. Since the long-term shrinkage (relative to early-age shrinkage) has the most impact on prestress losses and camber development in beams, the magnitude of the shrinkage at its greatest age (for 7-day moist-cured specimens) will be the focus of this discussion. The 16-week ε_{SH} of the SCC mixtures varied between 373 and 510 microstrain while the two control mixtures had a 16-week ε_{SH} range of 477 and 520 microstrain.

All of the drying shrinkage data, including that for the specimens that were moist-cured for 28 days, not presented in Chapter 4 is summarized in Appendix D.

4.2.3.2 Effects of Sand-to-Aggregate Ratio

The effect of the *s/agg* on the long-term drying shrinkage for all three powder combinations is evaluated in Figures 4-36 through 4-38. There is no fixed trend in the change in 32-week (or 16-week for ternary SCC mixtures) ε_{SH} relative to a change in *s/agg*. In Figure 4-36, when the *w/p* is held constant at 0.32, the 32-week ε_{SH} increases 23% as the *s/agg* increases from 0.38 to 0.46. However, at *w/p* of 0.28 and 0.36, the *s/agg* has no discernable trend on the 32-week ε_{SH} for the fly ash SCC mixtures. In Figure 4-37, the ε_{SH} of the slag SCC mixtures is evaluated, and at *w/p* of 0.28 and 0.32, the 32-week ε_{SH} increases as the *s/agg* increases from 0.42 to 0.46. The *s/agg* has no significant effect on the 32-week ε_{SH} when the *w/p* is 0.36. For the ternary SCC mixtures, the 16-week ε_{SH} increases as the *s/agg* increases from 0.42 to 0.46 for *w/p* of 0.32 and 0.36 as shown in Figure 4-38. However, the 16-week ε_{SH} decreases when the *s/agg* increases from 0.42 to 0.46 for a *w/p* of 0.40.

The effects of the *s/agg* on the 16 and 32-week ε_{SH} for specimens moist-cured for 28 days are presented in Appendix D. The *s/agg* had no significant effect on the long-term ε_{SH} for any of the SCC mixtures.

Some of the data reported in Figures 4-36 through 4-38 agrees with the statement made by ACI Committee 209 (1997) and research conducted by Attiogbe, See, and Daczko (2003) that the shrinkage will increase with an increase in the *s/agg*, but this is not true in every instance. Generally, only small changes in the long-term shrinkage occurred when the sand-to-aggregate ratio was changed.

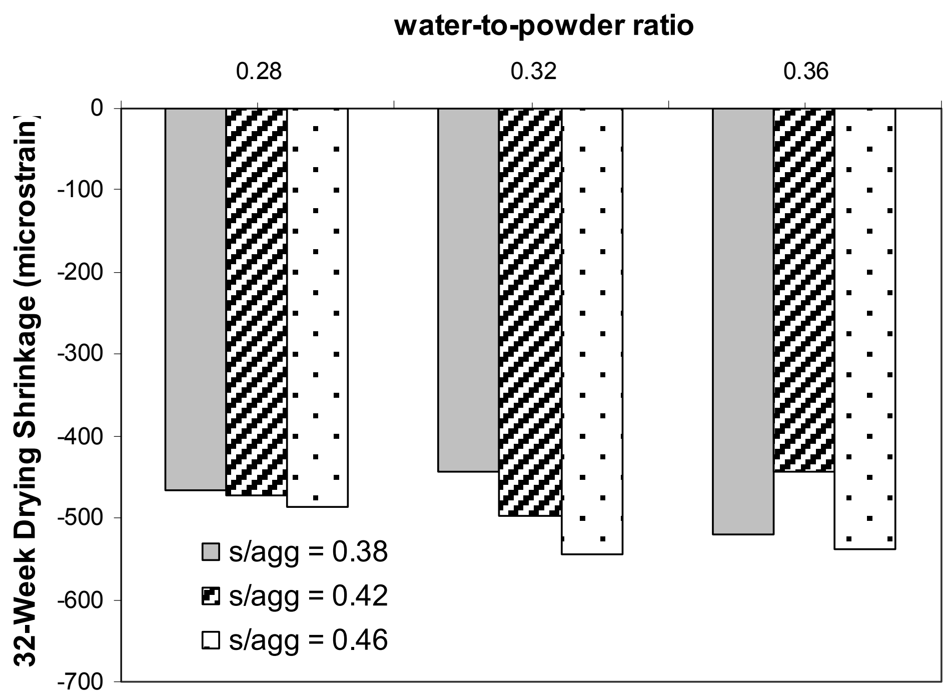

Figure 4-36: Effect of *s/agg* on the *32*-week drying shrinkage for fly ash mixtures

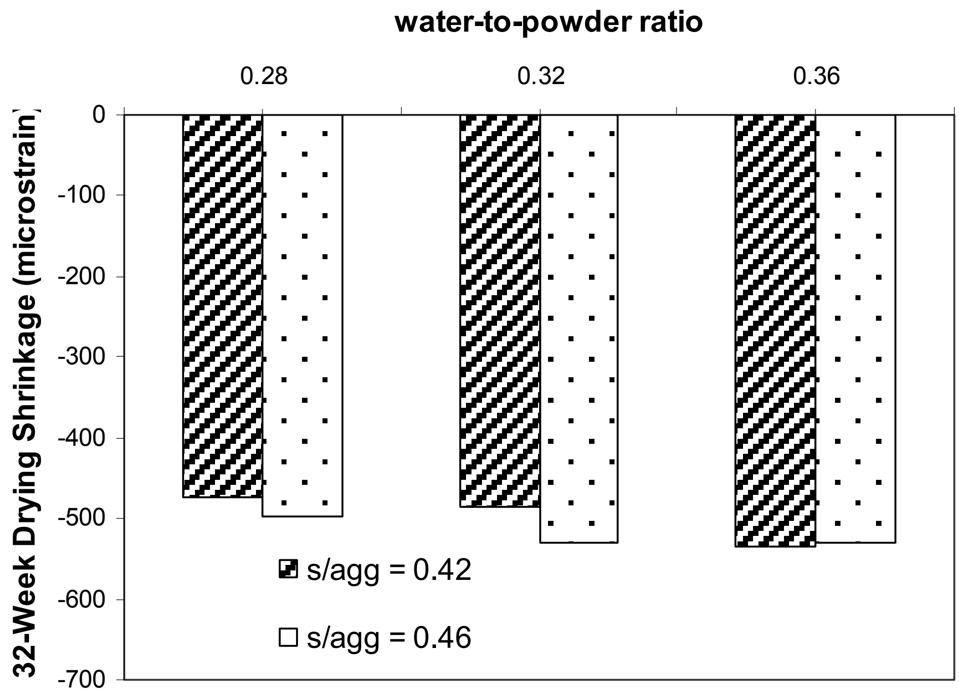

Figure 4-37: Effect of *s/agg* on the *32*-week drying shrinkage for slag mixtures

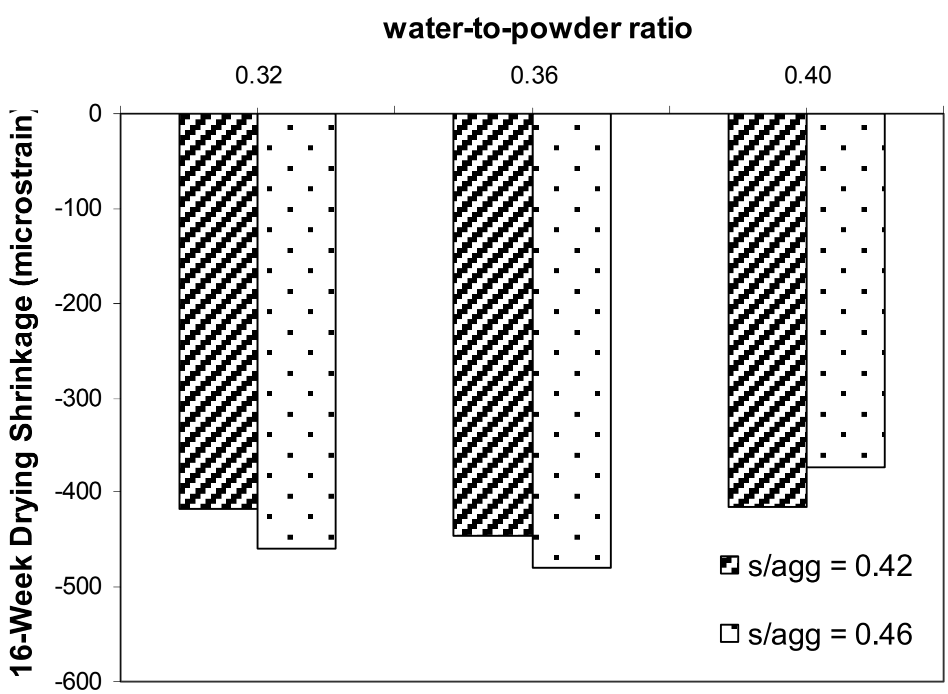

Figure 4-38: Effect of *s/agg* on the *16*-week drying shrinkage for ternary mixtures

4.2.3.3 Effects of Water-to-Powder Ratio

The effect of the *w/p* on the long-term drying shrinkage for all three powder combinations is illustrated in Figures 4-39 through 4-41. For the fly ash SCC mixtures, shown in Figure 4-39, the *w/p* has no effect on the 32-week ε_{SH} when the *s/agg* is held constant. The effect of the *w/p* on the 32-week ε_{SH} for slag SCC mixtures is presented in Figure 4-40. At a *s/agg* of 0.42, the 32-week ε_{SH} increases 13% as the *w/p* increases from 0.28 to 0.36. At a *s/agg* of 0.46, the 32-week ε_{SH} increases 6% as the *w/p* increases from 0.28 to 0.32, but remains the same as the *w/p* increases from 0.32 to 0.36. For the ternary SCC mixtures shown in Figure 4-41, the *w/p* has no reliable effect on the 16-week ε_{SH} when the *s/agg* is held constant.

The effects of the *w/p* on the 16- and 32-week ε_{SH} for specimens moist-cured for 28 days are presented in Appendix D. For the specimens that were moist-cured for 28 days, there is no fixed trend in the change in 32-week (or 16-week for ternary SCC mixtures) ε_{SH} relative to a change in *w/p* at constant *s/agg*. At *s/agg* of 0.38 and 0.46, the 32-week ε_{SH} increases as the *w/p* increases, but at a *s/agg* of 0.42, the *w/p* has no effect on the 32-week ε_{SH} for the fly ash SCC mixtures. At *s/agg* of 0.42 and 0.46, the 32-week ε_{SH} increases 39% and 42% respectively as the *w/p* increases from 0.28 to 0.36 for the slag SCC mixtures. The *w/p* has no effect on the ternary SCC mixtures for a *s/agg* of 0.42, but at a *s/agg* of 0.46, the 16-week ε_{SH} *decreases* as the *w/p* increases.

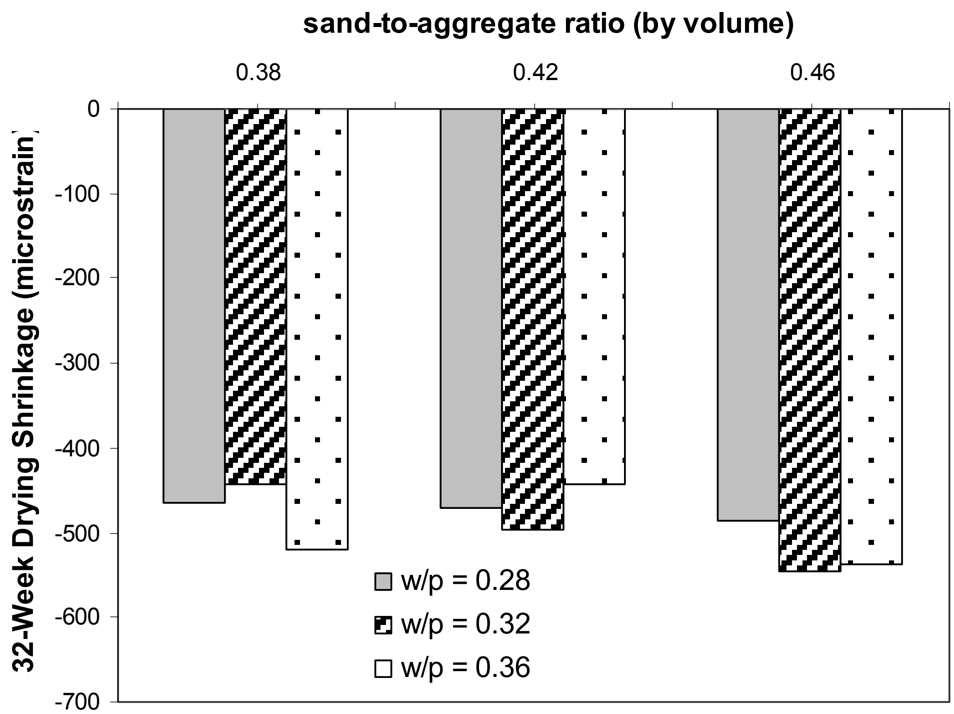

Figure 4-39: Effect of *w/p* on the *32*-week drying shrinkage for fly ash mixtures

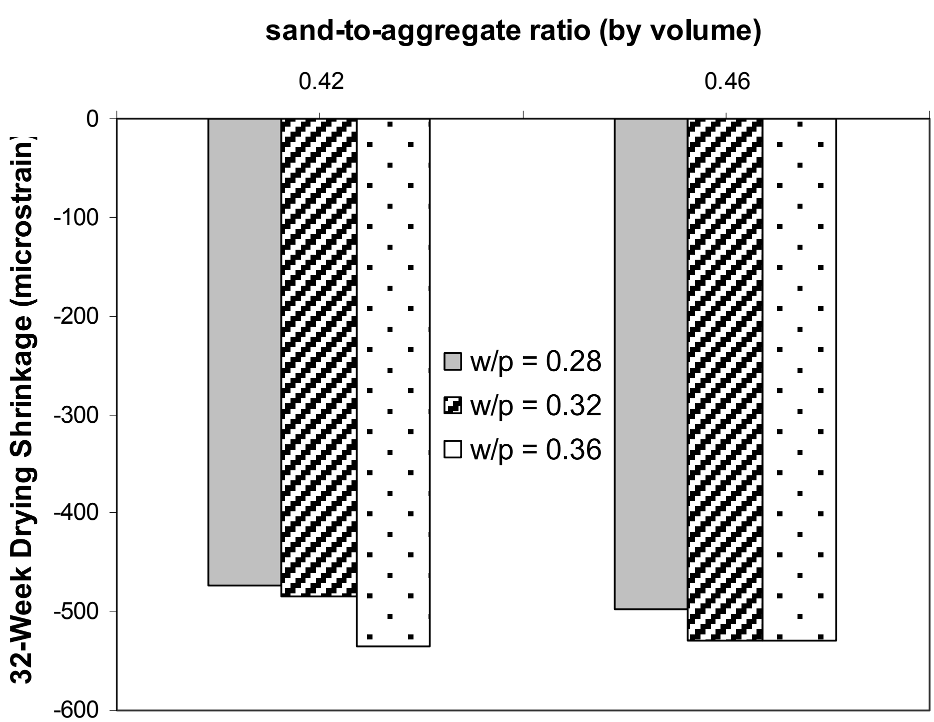

Figure 4-40: Effect of *w/p* on the *32*-week drying shrinkage for slag mixtures

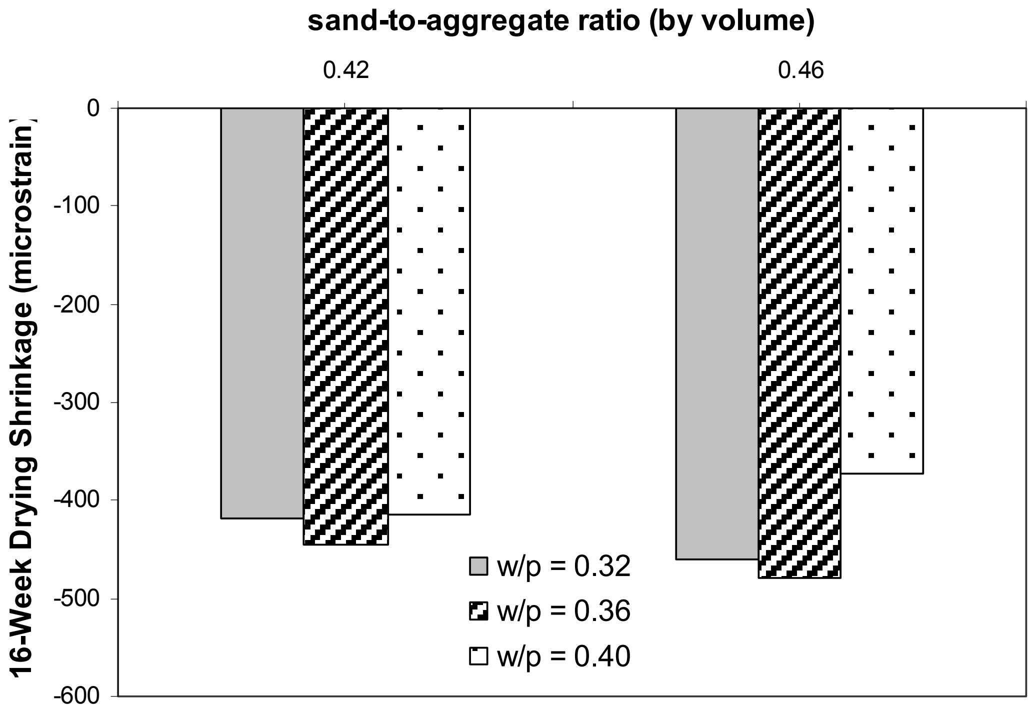

Figure 4-41: Effect of *w/p* on the *16*-week drying shrinkage for ternary mixtures

4.2.3.4 Effects of Powder Combinations

The effects of different powder combinations on the long-term ε_{SH} can be evaluated in Figure 4-42. Due to the fact that not all 21 SCC mixtures have 32-week ε_{SH} data available at this time, the effects of the powder combinations relative to the 16-week (7-day moist-cured) ε_{SH} are analyzed. Even though all 21 SCC mixtures are shown in Figure 4-42, the only constants associated with all three powder combinations are *w/p* of 0.32 and 0.36 and *s/agg* of 0.42 and 0.46. Therefore, to assess the effects the different powders had on the 16-week ε_{SH} of the SCC mixtures, the author determined the powder(s)' effects by comparing the ε_{SH} of mixtures with similar *w/p* and *s/agg*.

When averaging the 16-week ε_{SH} for all three powder combinations with the same constants (*w/p* of 0.32 and 0.36 and *s/agg* of 0.42 and 0.46), the slag SCC mixtures exhibited the most amount of drying shrinkage, although the difference was minimal. On average, the slag SCC mixtures had 3% more ε_{SH} than the fly ash SCC mixtures and 4% more ε_{SH} than the ternary SCC mixtures on average. Since this is such a small amount, these differences are negligible.

The analysis of the effect the powder combinations had on the 16-week ε_{SH} data, where the specimens were moist-cured for 28 days can be found in Appendix D. The 28-day moist-cured results were the same as the 7-day moist-cured results, except that they were more pronounced, especially when comparing the ε_{SH} of the ternary SCC mixtures to the ε_{SH} of the slag SCC mixtures. One possible reason for this extreme result is that the ternary SCC mixtures contain silica fume, which greatly enhances the early-age strength. Because the curing period was increased from 7 days to 28 days, the strength of the ternary SCC mixtures' paste became much stronger enabling the mixture to possess a greater shrinkage resistance. The slag SCC mixtures had 8% more ε_{SH} than the fly ash SCC mixtures and 48% more ε_{SH} than the ternary SCC mixtures on average.

4.2.3.5 Behavior of SCC versus Conventional-Slump Concrete

The following analyses are illustrated in Figure 4-42. The 16-week ε_{SH} for all SCC mixtures is on the same order of magnitude or less than both control mixtures. The same can be said when comparing the available 32-week ε_{SH} for fly ash and slag SCC mixtures to the 32-week ε_{SH} collected for the control mixtures. When examining SCC mixtures with a *w/p* of 0.36 and a *s/agg* of 0.38 to CTRL1:0.37, which has a *w/p* of 0.37 and a *s/agg* of 0.37, the SCC mixtures exhibited a similar long-term ε_{SH} for the same curing conditions. Attiogbe, See, and Daczko (2003) noticed similar results when comparing the drying shrinkage of their SCC mixtures to that of conventional-slump concrete. From these results, excessive drying shrinkage is not expected for members constructed with the SCC mixtures used in this study.

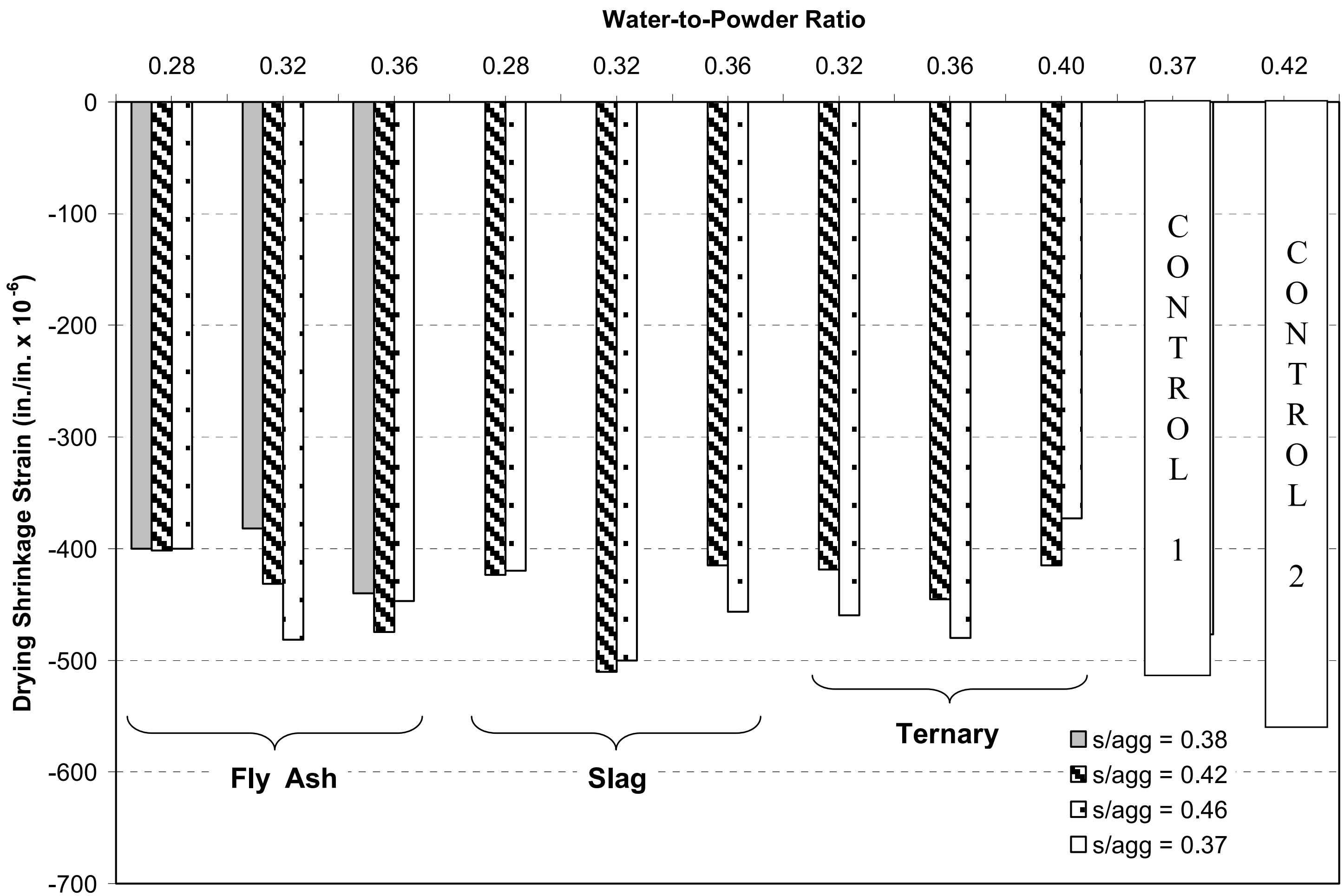

Figure 4-42: Effects of different powder combinations on the *16*-week drying shrinkage

4.2.3.6 Drying Shrinkage Comparison to ACI 209, AASHTO LRFD, and NCHRP 496 Estimates

To determine whether ε_{SH} values obtained for the SCC mixtures evaluated for this research correspond to behavior currently assumed during design, the ε_{SH} values are compared to those estimated by ACI 209 (1997), AASHTO LRFD (2004), and NCHRP 496 (Tadros et al. 2003). All three of these methods are discussed in Sections 2.7.2.1 through 2.7.2.3. Since some of the parameters in these methods are not directly applicable for SCC, assumptions were made:

- In Equation 2-9, the slump correction factor for the ACI 209 procedure was computed using the wet slump before any chemical admixtures were added to the mixture. This approach was used since the ACI 209 procedure was developed before the use of water-reducing admixtures. This approach yields the lowest and most conservative shrinkage estimate from the ACI 209 procedure.
- In Equation 2-10, the cement content was interpreted as the total cementitious content (cement plus SCMs). This is a conservative interpretation because it will give the lowest estimate of ε_{SH}.

As stated in AASHTO LRFD (2004), it is expected that "large concrete members may undergo substantially less shrinkage than that measured by laboratory testing of small specimens of the same concrete". Thus, it is expected that if the shrinkage estimates from using these procedures are of the same order of magnitude as those measured, then the shrinkage of full-scale members should be less than or equal to those estimated by these procedures.

Comparisons of the measured ε_{SH} to the estimated ε_{SH} by the three procedures are summarized in Figures 4-43 through 4-45 for all mixtures moist-cured for seven days. From Figure 4-43, it may be seen that the ACI 209 procedure underestimates the drying shrinkage at 7 and 14 days for all SCC and conventional-slump mixtures. At later ages of 56 and 112 days, the measured ε_{SH} values correspond reasonably well to those estimated by ACI 209.

AASHTO LRFD only provides a single drying shrinkage strain at each age for all the mixtures tested in this study. In Figure 4-44 it may be seen that the AASHTO LRFD procedure underestimates the drying shrinkage at 7 days for all SCC and conventional-slump mixtures. At later ages of 56 and 112 days, the ε_{SH} values estimated by AASHTO LRFD are more than the measured ε_{SH} for the SCC and conventional-slump mixtures.

In Figure 4-45, it may be seen that the NCHRP 496 procedure significantly underestimates the drying shrinkage for all mixtures at 7, 14, and 28 days. For this research, NCHRP 496 underestimates ε_{SH} more than 90% of the time. However, at later ages of 56 and 112 days, NCHRP 496 underestimates the majority of the mixtures within 0% to -20%.

In Appendix D, the measured ε_{SH} for 28-day moist-cured specimens is compared against ε_{SH} estimated using ACI 209 and AASHTO LRFD. For specimens that have been moist-cured for 28 days, ACI 209 gives a more reliable estimate of ε_{SH} at 7, 14, and 28 days than it does for 7-day moist-cured specimens. However, ACI 209 overestimates ε_{SH} at 56 and 112 days. AASHTO LRFD overestimates all of the SCC and conventional-slump mixtures at 28, 56, and 112 days between 20% and 80% when moist-cured for a period of 28 days.

Also shown in Appendix D is each individual mixture's shrinkage progression over time compared to the conventional-slump mixtures and the ACI 209 and NCHRP 496 procedures. Since the AASHTO LRFD estimate over time is the same for each mixture, this procedure is shown with corresponding powder combinations.

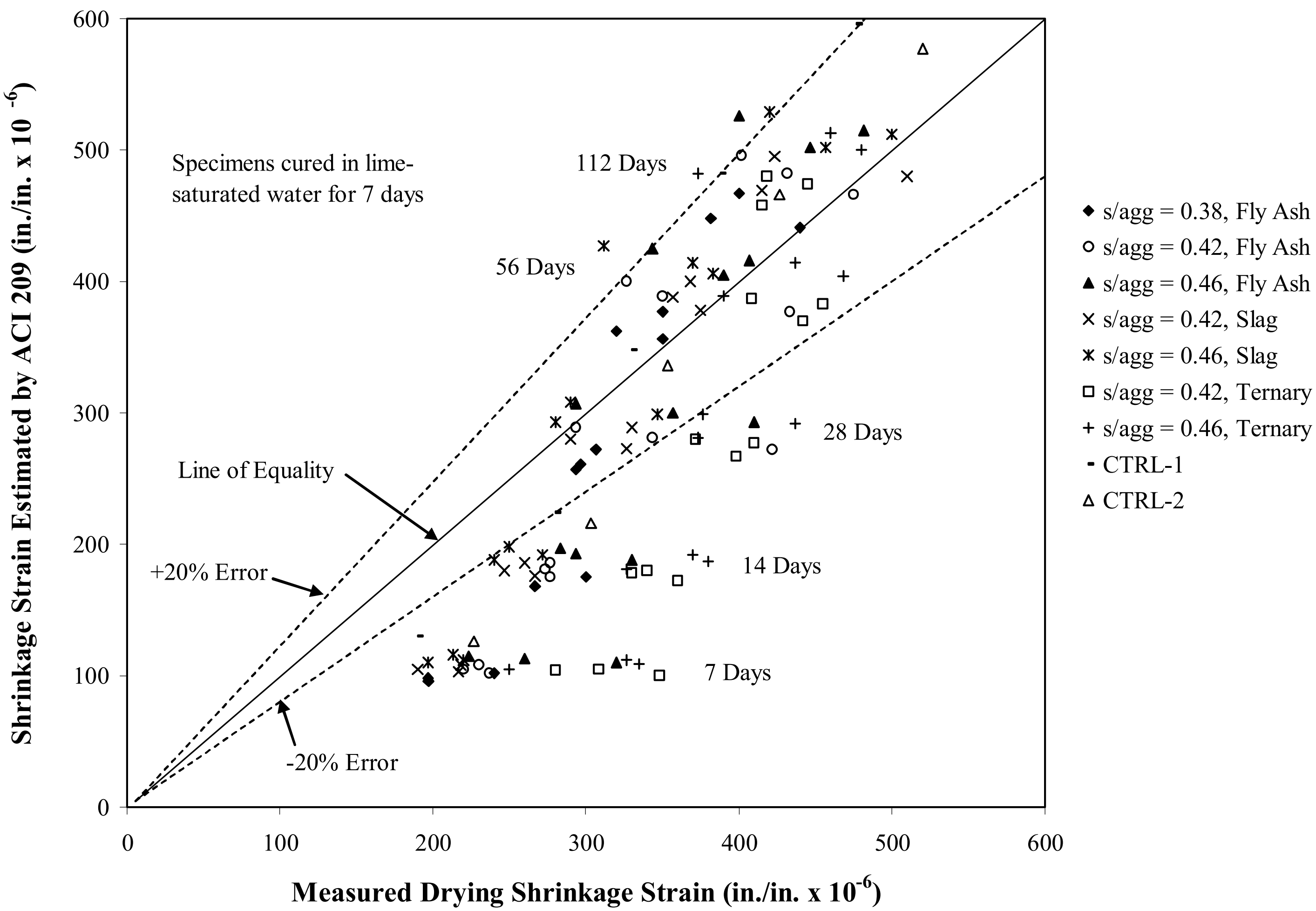

Figure 4-43: Measured versus estimated drying shrinkage strain using the ACI 209 procedure

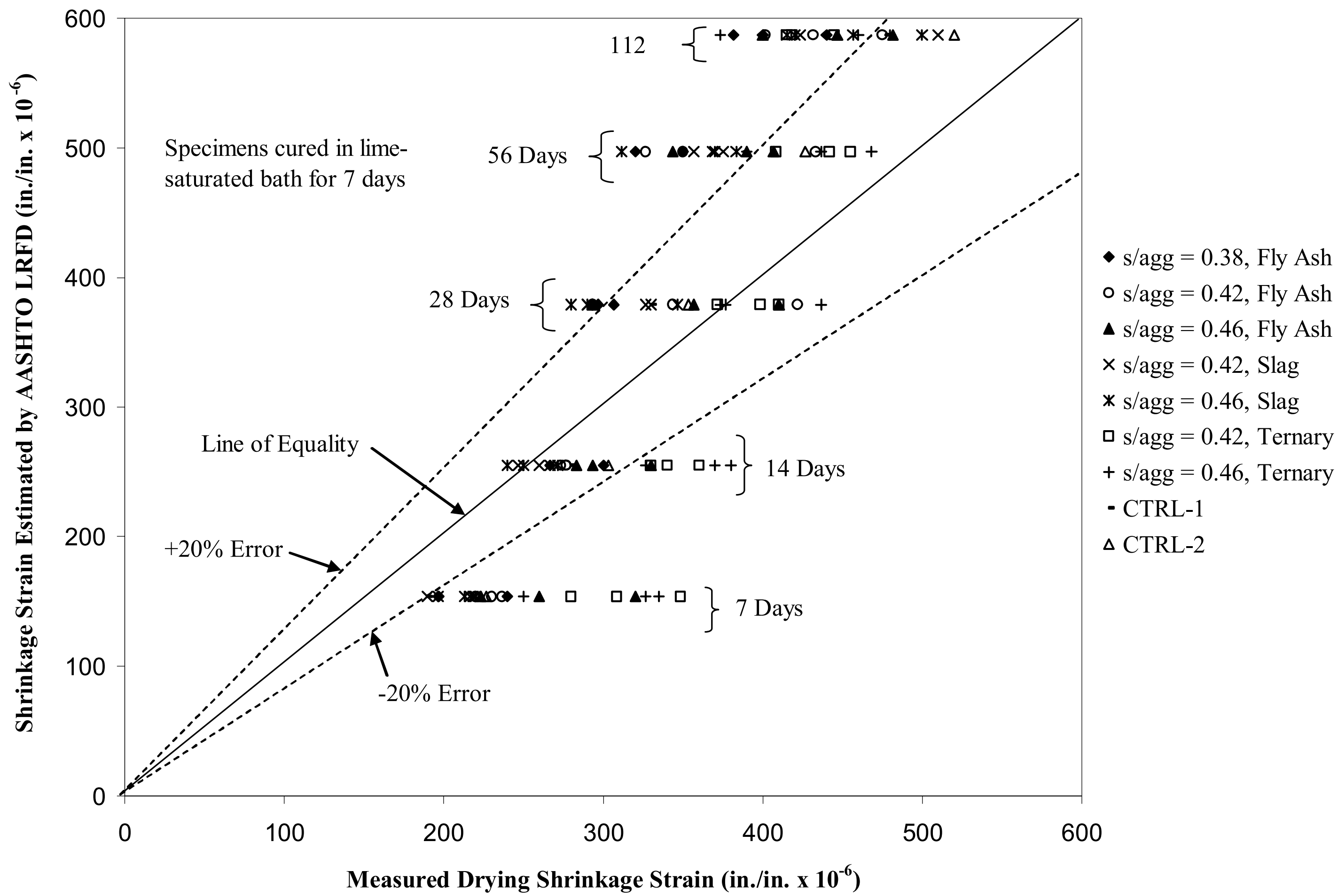

Figure 4-44: Measured versus estimated drying shrinkage strain using the AASHTO LRFD procedure

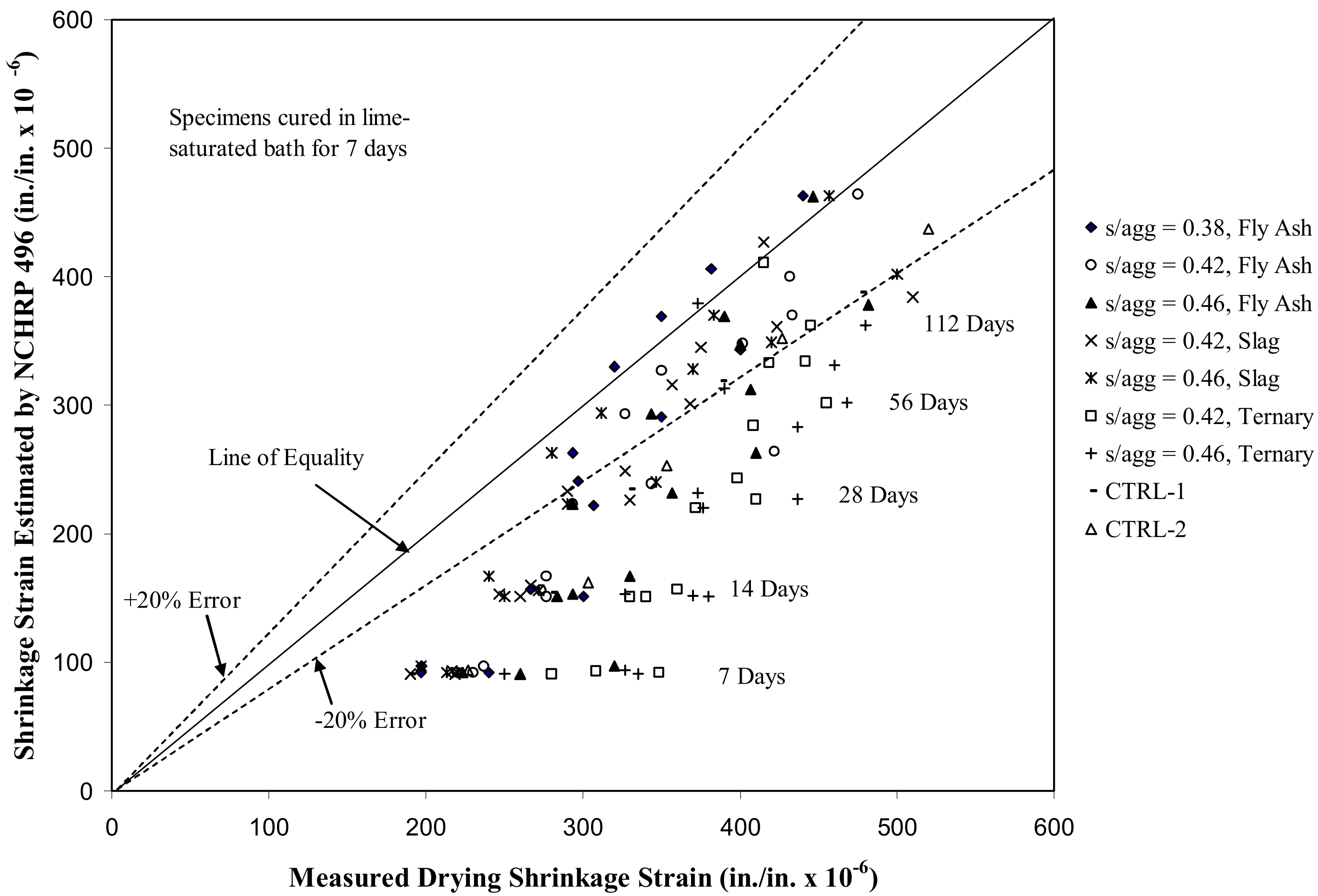

Figure 4-45: Measured versus estimated drying shrinkage strain using the NCHRP 496 procedure

4.3 SUMMARY OF RESULTS

4.3.1 SUMMARY OF FRESH PROPERTIES

From this research, the following conclusions can be made about the fresh properties of SCC:

- A slump flow value in the range of 24 to 30 in. can be easily achieved with a polycarboxylate HRWR admixture. Mixtures within this slump flow range should possess satisfactory fluidity to fill the forms of prestressed girders.
- The type of supplementary cementitious material (SCM) used in each SCC mixture had a significant effect on the dosage of HRWR admixture required to achieve the desired slump flow. On average, the fly ash and GGBF slag mixtures required the same amount of HRWR admixture. The ternary SCC mixtures required 25% more HRWR admixture to achieve the target slump flow values.
- In general, T-50 times will increase with a decrease in the water-to-powder ratio.
- The GGBF slag mixtures had much higher T-50 times than any of the other mixtures.
- A SCC mixture having a VSI of 2.0 or less should be adequate, but the dynamic and static stability of such SCC mixtures should be evaluated during placement of full-scale, prestressed specimens. The VSI alone is not enough to judge the stability of a SCC mixture.
- The total air content seemed to increase as the dosage of HRWR admixture increased.

- As the w/p decreased, the required dosage of AEA increased.
- SCC mixtures containing GGBF slag required larger dosages of AEA than SCC mixtures containing Class C fly ash and silica fume.
- Due to the inherent effects of polycarboxylate-based HRWR admixtures on the total air content, a total air content ranging from 3 to 8% may be more practical and still provide good structural performance.

4.3.2 Summary of Mechanical Properties

From this research, the following conclusions can be made about the hardened properties of SCC:

- It is possible to attain compressive strength values at prestress transfer that exceed 9,000 psi when the SCC has been match-cured to follow a time-temperature profile typical of a prestressed plant.
- The strength at prestress transfer ranged between 5,470 and 9,530 psi for the SCC mixtures.
- Like conventional-slump concrete, the most influential factor on the compressive strength is the water-to-powder ratio. As the water-to-powder ratio decreases, the compressive strength increases.
- Replacing Type III cement with Class C fly ash or Grade 120 GGBF slag will result in lower early-age compressive strengths for similar water-to-powder ratios.
- When the water-to-powder ratio is held constant, the sand-to-aggregate ratio has little to no effect on the early-age or long-term compressive strengths.

- When the various SCC mixtures were exposed to the elevated temperatures associated with the time-temperature profile (Figure 3-9), the fly ash SCC mixtures experienced the greatest strength gain from 18 hours to 28 days, followed by the slag SCC mixtures, and then the ternary SCC mixtures. At a water-to-powder ratio of 0.36, both the slag and fly ash SCC mixtures experienced a greater strength gain than CTRL1:0.37.
- When the various SCC mixtures were moist-cured, the ternary SCC mixtures had the largest gain in strength from 3 days to 56 days, followed by the slag SCC mixtures, and then the fly ash SCC mixtures. All of the SCC mixtures had higher strength gain from 3 days to 56 days at similar water-to-powder ratios than the control mixtures.
- The incorporation of silica fume in the ternary SCC mixtures yields higher early-age and long-term compressive strengths than the Class C fly ash and GGBF slag mixtures.
- All SCC mixtures had lower 18-hour moduli of elasticity (E_{ci}) than the control mixture with a water-to-powder ratio of 0.37.
- The sand-to-aggregate ratio has no distinct effect on E_{ci} of the fly ash and silica fume SCC mixtures. The GGBF slag mixtures with a sand-to-aggregate ratio of 0.46 have a 2 to 12% lower E_{ci} than the mixtures with a sand-to-aggregate ratio of 0.42.
- Generally, the modulus of elasticity at prestress transfer (E_{ci}) decreased as the water-to-powder ratio increased for the fly ash and slag SCC mixtures. The

water-to-powder ratio had no discernable effect on E_{ci} for the ternary SCC mixtures.

- The modulus of elasticity values can be affected by the type of supplementary cementitious material used in each mixture. SCC mixtures created with large dosages of GGBF slag and Class C fly ash experience lower modulus values at 18 hours relative to their modulus values at 56 days because these supplementary cementitious materials take time to react.
- Moduli of elasticity (E_c) values obtained from these SCC mixtures slightly exceed (on average) what one would estimate with the AASHTO LRFD formulation. E_c values obtained for the SCC mixtures are in reasonable agreement with the elastic stiffness assumed during the design of conventional-slump concrete.
- An increase in the sand-to-aggregate ratio from 0.38 to 0.46 had no significant effect on the long-term drying shrinkage strain for the SCC mixtures considered.
- The 112-day drying shrinkage strains for all the SCC mixtures are of the same order of magnitude or less than the 112-day drying shrinkage strains measured for the control mixtures.
- The ACI 209 procedure underestimates the drying shrinkage at 7 and 14 days for all SCC and conventional-slump mixtures. However, at later ages of 56 and 112 days, the measured drying shrinkage strain values correspond reasonably well to those estimated by ACI 209.

- The AASHTO LRFD procedure underestimates the early-age drying shrinkage for all SCC and conventional-slump mixtures. At later ages of 56 and 112 days, the drying shrinkage strain values estimated by AASHTO LRFD are more than the measured values for all of the SCC and conventional-slump mixtures.
- The NCHRP 496 procedure significantly underestimates the measured drying shrinkage strain for all of the SCC and conventional-slump mixtures at 7, 14, and 28 days. At later ages of 56 and 112 days, the NCHRP 496 procedure underestimates the majority of the SCC mixtures and both control mixtures within 0% to -20%.

CHAPTER 5

CONCLUSIONS AND RECOMMENDATIONS

5.1 SUMMARY OF LABORATORY WORK

In total, 21 SCC mixtures and two conventional-slump mixtures were developed for this project. The SCC mixtures varied in the type and amounts of constituents. One type of cement (Type III) and three types of supplementary cementing materials (Class C fly ash, GGBF slag, and silica fume), with different replacement percentages, were used to formulate various powder combinations. Four different water-to-powder ratios and three different sand-to-aggregate ratios were evaluated for various SCC mixtures. All of the mixtures' compressive strengths, moduli of elasticity, and drying shrinkage strain were tested at early and long-term ages to examine the effects of these variables. With each SCC and conventional-slump mixture, eight 4 in. x 8 in. cylinders were cured at elevated temperatures representative of prestressing plants in the southeastern United States.

For each mixture of SCC, the slump flow, VSI, T-50, and total air content were determined. The modulus of elasticity test was conducted on 6 in. x 12 in. cylinders and 4 in. x 8 in. cylinders according to ASTM C 469 (2002), while the compressive strength was determined for 6 in. x 12 in. cylinders and 4 in. x 8 in. cylinders according to AASHTO T 22 (2003). Shrinkage prisms were made, and the change in drying shrinkage was measured in accordance with AASHTO T 160 (2003).

5.2 CONCLUSIONS

5.2.1 SCC FRESH PROPERTIES

From this research, the following conclusions can be made about SCC's fresh properties:

1. SCC has three fresh property requirements: adequate filling ability, adequate passing ability, and adequate resistance to segregation.
2. A slump flow value in the range of 24 to 30 in. can be easily achieved with a polycarboxylate HRWR admixture. Mixtures within this slump flow range will likely possess satisfactory fluidity to fill the forms of prestressed girders.
3. The type of supplementary cementitious material (SCM) used in each SCC mixture had a significant effect on the dosage of HRWR admixture required to achieve the desired slump flow. On average, the fly ash and GGBF slag mixtures required the same amount of HRWR admixture. The ternary SCC mixtures required 25% more HRWR admixture to achieve the target slump flow values.
4. In general, T-50 times will increase with a decrease in the water-to-powder ratio.
5. The GGBF slag mixtures had much higher T-50 times than any of the other mixtures.
6. For the stated slump flow range, a T-50 value ranging from 2 to 8 seconds should be acceptable.
7. A SCC mixture having a VSI of 2.0 or less should be adequate, but the VSI alone is not adequate for judging the stability of a SCC mixture.

5.2.2 SCC Hardened Properties

From this research, the following conclusions can be made about SCC's hardened properties:

1. It is possible to attain compressive strength values at prestress transfer that exceed 9,000 psi when the SCC has been match-cured to follow a time-temperature profile typical of a prestressed plant.
2. The strength at prestress transfer ranged between 5,470 and 9,530 psi for the SCC mixtures.
3. Like conventional-slump concrete, the most influential factor on the compressive strength is the water-to-powder ratio. As the water-to-powder ratio decreases, the compressive strength increases.
4. Replacing Type III cement with Class C fly ash or Grade 120 GGBF slag will result in lower early-age compressive strengths at similar water-to-powder ratios.
5. When the water-to-powder ratio is held constant, the sand-to-aggregate ratio has little to no effect on the early-age or long-term compressive strengths.
6. When the various SCC mixtures were exposed to the elevated temperatures associated with the time-temperature profile (Figure 3-9), the fly ash SCC mixtures experienced the greatest strength gain from 18 hours to 28 days, followed by the slag SCC mixtures, and then the ternary SCC mixtures. At a water-to-powder ratio of 0.36, both the slag and fly ash SCC mixtures experienced a greater strength gain than CTRL1:0.37.

7. When the various SCC mixtures were moist-cured, the ternary SCC mixtures had the largest gain in strength from 3 days to 56 days, followed by the slag SCC mixtures, and then the fly ash SCC mixtures. All of the SCC mixtures had higher strength gain from 3 days to 56 days at similar water-to-powder ratios than the control mixtures.
8. The incorporation of silica fume in the ternary SCC mixtures yields higher early-age and long-term compressive strengths than the Class C fly ash and GGBF slag mixtures.
9. All SCC mixtures had lower 18-hour moduli of elasticity (E_{ci}) than the control mixture with a water-to-powder ratio of 0.37.
10. The sand-to-aggregate ratio has no distinct effect on E_{ci} of the fly ash and silica fume SCC mixtures. The GGBF slag mixtures with a sand-to-aggregate ratio of 0.46 have a 2 to 12% lower E_{ci} than the mixtures with a sand-to-aggregate ratio of 0.42.
11. Generally, the modulus of elasticity at prestress transfer (E_{ci}) decreased as the water-to-powder ratio increased for the fly ash and slag SCC mixtures. The water-to-powder ratio had no discernable effect on E_{ci} for the ternary SCC mixtures.
12. The modulus of elasticity values can be affected by the type of supplementary cementitious material used in each mixture. SCC mixtures created with large dosages of GGBF slag and Class C fly ash experience lower modulus values at 18 hours relative to their modulus values at 56 days because these supplementary cementitious materials take time to react.

13. Moduli of elasticity (E_c) values obtained from these SCC mixtures slightly exceed (on average) what one would estimate with the AASHTO LRFD formulation. E_c values obtained for the SCC mixtures are in reasonable agreement with the elastic stiffness assumed during the design of conventional-slump concrete.
14. An increase in the sand-to-aggregate ratio from 0.38 to 0.46 had no significant effect on the long-term drying shrinkage strain for the SCC mixtures considered.
15. The 112-day drying shrinkage strains for all the SCC mixtures are of the same order of magnitude or less than the 112-day drying shrinkage strains measured for the control mixtures.
16. The ACI 209 procedure underestimates the drying shrinkage at 7 and 14 days for all SCC and conventional-slump mixtures. However, at later ages of 56 and 112 days, the measured drying shrinkage strain values correspond reasonably well to those predicted by ACI 209. The NCHRP 496 and AASHTO LRFD procedures provided poor estimates of the drying shrinkage strain.
17. Excessive drying shrinkage is not expected for full-scale members constructed with the SCC mixtures used in this study.

5.2.3 Production, Quality Assurance, and Quality Control of SCC

The following conclusions about production, quality assurance, and quality control can be made from this research:

1. Because there are a variety of different constituents, mixture proportions, and mixing procedures, trial batches should be produced to assess both the fresh and hardened states of the SCC mixture before its use in full-scale applications.
2. The use of a HRWR admixture based on polycarboxylate chemistry is a necessity for every SCC mixture.
3. The L-Box test should be conducted as early as possible. If this test is run towards the end of placement, the blocking ratio may not be representative of the actual SCC mixture.
4. In order to use this product, the total air content range must be increased to account for the inherent effect of the polycarboxylate-based HRWR admixtures. It is anticipate that keeping the lower total air limit at 3% and widening the total air content range will not affect the performance of the concrete as long as it meets the strength requirements.
5. Conducting the slump flow test, J-Ring test, and inspecting the slump flow patty and mixer (VSI) are sufficient tests to assess whether or not a SCC mixture has acceptable SCC characteristics.

5.3 RECOMMENDATIONS FOR FUTURE RESEARCH

Before the implementation of SCC, further research needs to be performed. The following recommendations can be made based on the research stated in this report:

- Several types of methods are available for the transportation and placement of SCC (see Sections 2.6.1.3 and 2.6.1.4). These methods need to be investigated to see which methods are most efficient.
- The effects of a higher air content on the practicality of SCC production and its structural performance need to be investigated.
- Further research is required to evaluate the creep behavior of these SCC mixtures.
- Full-scale prestressed elements with realistic reinforcement congestion need to be fabricated to evaluate the performance of these SCC mixtures.

The testing of these SCC mixtures' creep behavior is ongoing, and the testing of full-scale prestressed elements is planned. With the creation of the full-scale prestressed elements, many aspects of SCC that could not be investigated in Phases I and II should be investigated, such as

- The lateral pressure that SCC exerts on the formwork.
- An acceptable tolerance for the passing ability (J-Ring) and the blocking ratio (L-Box) of these SCC mixtures.
- The dynamic and static stability of SCC mixtures in full-scale prestressed elements.
- Effects of moderate mechanical vibration (if needed) on the stability of the SCC mixture.
- Effects of creep and shrinkage of SCC on the behavior of full-scale prestressed elements.

5.4 RECOMMENDATIONS FOR IMPLEMENTATION

The following recommendations are made toward the implementation of SCC in the prestressed/precast industry:

- Specifications need to be developed for the slump flow test, the L-Box test, the J-Ring test, the VSI, and the T-50, including tolerance levels for specific applications.
- After the acceptance of the above specifications, the concrete producer should decide the conditions/terms of acceptance of a SCC batch and actions to take if the mixture is rejected before mixing begins.
- Industry personnel need to be properly trained and certified in order to correctly evaluate SCC.
- *Satisfactory* performance of the fresh and hardened properties of SCC used in the full-scale prestressed elements needs to be established before full-scale implementation is recommended.

REFERENCES

AASHTO M 43. 2003. “Sizes of Aggregate for Road and Bridge Construction”. In *Standard Specifications for Transportation Materials and Methods of Sampling and Testing.* Washington, DC: American Association of State Highway and Transportation Officials.

AASHTO M 6. 2003. “Fine Aggregate for Portland Cement Concrete”. In *Standard Specifications for Transportation Materials and Methods of Sampling and Testing.* Washington, DC: American Association of State Highway and Transportation Officials.

AASHTO T 119. 2003. “Slump of Hydraulic-Cement Concrete”. In *Standard Specifications for Transportation Materials and Methods of Sampling and Testing.* Washington, DC: American Association of State Highway and Transportation Officials.

AASHTO T 121. 2003. “Mass per Cubic Meter (Cubic Foot), Yield, and Air Content (Gravimetric) of Concrete”. In *Standard Specifications for Transportation Materials and Methods of Sampling and Testing.* Washington, DC: American Association of State Highway and Transportation Officials.

AASHTO T 126. 2003. "Making and Curing Concrete Test Specimens in the Laboratory". In *Standard Specifications for Transportation Materials and Methods of Sampling and Testing.* Washington, DC: American Association of State Highway and Transportation Officials.

AASHTO T 160. 2003. "Length Change of Hardened Hydraulic Cement Mortar and Concrete". In *Standard Specifications for Transportation Materials and Methods of Sampling and Testing.* Washington, DC: American Association of State Highway and Transportation Officials.

AASHTO T 22. 2003. "Compressive Strength of Cylindrical Concrete Specimens". In *Standard Specifications for Transportation Materials and Methods of Sampling and Testing.* Washington, DC: American Association of State Highway and Transportation Officials.

AASHTO T 309. 2003. "Temperature of Freshly Mixed Portland Cement Concrete". In *Standard Specifications for Transportation Materials and Methods of Sampling and Testing.* Washington, DC: American Association of State Highway and Transportation Officials.

ACI 116. 2000. "Cement and Concrete Technology (ACI 116R)". In *ACI Manual of Concrete Practice 2001: Part 1*. Farmington Hills, Michigan: American Concrete Institute, 116R-1-116R-73.

ACI 209. 1997. "Prediction of Creep, Shrinkage, and Temperature Effects in concrete Structures (ACI 209R)". In *ACI Manual of Concrete Practice 2001: Part 1*. Farmington Hills, Michigan: American Concrete Institute, 209R-1-209R-47.

ACI 232. 1996. “Use of Fly Ash in Concrete (ACI 232R)”. In *ACI Manual of Concrete Practice 2001: Part 1*. Farmington Hills, Michigan: American Concrete Institute, 232.2R-1-232.2R-34.

ACI 233. 2000. “Ground Granulated Blast-Furnace Slag as a Cementitious Constituent in Concrete (ACI 233R)”. In *ACI Manual of Concrete Practice 2001: Part 1*. Farmington Hills, Michigan: American Concrete Institute, 233R-1-233R-18.

ACI 234. 2000. “Guide for the Use of Silica Fume in Concrete (ACI 234R)”. In *ACI Manual of Concrete Practice 2001: Part 1*. Farmington Hills, Michigan: American Concrete Institute, 234R-1-234R-51.

ACI 318. 2002. “Building Code Requirements for Structural Concrete (ACI 318R)”. In *ACI Manual of Concrete Practice 2002: Part 3*. Farmington Hills, Michigan: American Concrete Institute, 318R-1-318R-439

ACI 363. 1997. “State-of-the-Art Report on High-Strength Concrete (ACI 363R)”. In *ACI Manual of Concrete Practice 2001: Part 1*. Farmington Hills, Michigan: American Concrete Institute, 363R-1-363R-55.

ALDOT. 2002. “Structural Portland Cement Concrete”. In *Standard Specifications for Highway Construction.* Montgomery, Alabama: Alabama Department of Transportation, 5-1-5-9

Ambroise, J. and J. Pera. 2003. Design of Self-Leveling Concrete. In *First North American Conference on the Design and Use of Self-Consolidating Concrete 12-13 November 2002*, ed. S. Shah, J. Daczko, and J. Lingscheit, 89-94. Addison, Illinois: Hanley-Wood.

Assaad, J., K. H. Khayat, and J. Daczko. 2004. Evaluation of Static Stability of Self-Consolidating Concrete. *ACI Materials Journal* 101, no. 3: 207-215.

ASTM C 469. 1998. Standard Test Method for Static Modulus of Elasticity and Poisson's Ratio Strength of Concrete in Compression. *Annual Book of ASTM Standards* 1998. Section 04, V. 4.02: Concrete and Aggregates.

ASTM Draft. 2004. Standard Test Method for Passing Ability of Self-Consolidating Concrete by J-Ring and Slump ConeStandard Specification for Concrete Aggregates. *Annual Book of ASTM Standards* 2002. Section 04, V. 4.02: Concrete and Aggregates.

Beaupre, D., P. Lacombe, and K. H. Khayat. 1999. Laboratory Investigation of Rheological Properties and Scaling Resistance of Air Entrained Self-Consolidating Concrete. *Materials and Structures* 32 (April): 235-240.

Berke, N. S., C. R. Cornman, A. A. Jeknavorian, and G. F. Knight. 2003. "The Effective Use of Superplasticizers and Viscosity Modifying Agents in Self-Consolidating Concrete". In *First North American Conference on the Design and Use of Self-Consolidating Concrete 12-13 November 2002*, ed. S. Shah, J. Daczko, and J. Lingscheit. Addison, Illinois: Hanley-Wood, 165-169.

Bilodeau, A. and G. G. Carette. 1989. "Resistance of Condensed Silica Fume Concrete to the Combined Action of Freezing and Thawing Cycling and De-Icing Salts". In *Fly Ash, Silica Fume, Slag, and Natural Pozzolans in Concrete: Proceedings Third International Conference. Trondheim, Norway, 1989,* ed. V. M. Malhotra. Detroit, Michigan: American Concrete Institute, 945-970.

Bonen, D. and S. Shah. 2004. "The Effects of Formulation on the Properties of Self-Consolidating Concrete". In *Concrete Science and Engineering: A Tribute to Arnon Bentur: Proceedings of the International RILEM Symposium,* ed. K. Kovler, J. Marchand, S. Mindess, and J. Weiss. Cachan Cedex, France: RILEM Publications, 43-56.

Bury, M. A. and B. J. Christensen. 2003. "The Role of Innovative Chemical Admixtures in Producing Self-Consolidating Concrete". In *First North American Conference on the Design and Use of Self-Consolidating Concrete 12-13 November 2002*, ed. S. Shah, J. Daczko, and J. Lingscheit. Addison, Illinois: Hanley-Wood, 137-140.

Bury, M. A. and E. Buhler. 2003. "Methods and Techniques for Placing Self-Consolidating Concrete-An Overview of Field Experiences in North American Applications". In *First North American Conference on the Design and Use of Self-Consolidating Concrete 12-13 November 2002*, ed. S. Shah, J. Daczko, and J. Lingscheit. Addison, Illinois: Hanley-Wood, 253-257.

Degussa Admixtures, Inc. 2004. Master Builders Admixture Systems. Viewed 10 September 2005. http://www.masterbuilders.com

Domone, P. 2000. "Mix Design". In *State-of-the-Art Report (23) of RILEM Technical Committee 174-SCC*, ed. A. Skarendahl and O. Petersson. Cachan Cedex, France: RILEM Publications, 49-56.

Emborg, M. 1999. "Rheology Tests for Self-Compacting Concrete-How Useful are they for the Design of Concrete Mix for Full Scale Production?". In *Self-Compacting Concrete*: *Proceedings of the First International RILEM Symposium*, ed. A. Skarendahl and O. Petersson. Cachan Cedex, France: RILEM Publications, 95-105.

Fang, W., C. Jianxiong, and Y. Changhui. 1999. “Studies on Self-Compacting High Performance Concrete With high Volume Mineral Additives”. In *Self-Compacting Concrete*: *Proceedings of the First International RILEM Symposium*, ed. A. Skarendahl and O. Petersson. Cachan Cedex, France: RILEM Publications, 569-578.

Felekoglu, B., M. Y. Yardimci, and B. Baradan. 2003. “A Comparative Study on the Use of Mineral and Chemical Types of Viscosity Enhancers in Self-Compacting Concrete”. In *Self-Compacting Concrete*: *Proceedings of the Third International RILEM Symposium,* ed. O. Wallevik and I. Nielsson. Bagneux, France: RILEM Publications, 446-456.

Ghezal, A., K. H. Khayat, and D. Beaupre. 2003. Development of Self-Consolidating Concrete With Low Binder Content and Minerals Additives. In *First North American Conference on the Design and Use of Self-Consolidating Concrete 12-13 November 2002*, ed. S. Shah, J. Daczko, and J. Lingscheit, 75-80. Addison, Illinois: Hanley-Wood.

Hindy, E. E., B. Miao, O. Chaallal, and P. C. Aitcin. 2001. Drying Shrinkage of Ready-Mixed High-Performance Concrete. *ACI Materials Journal* 91, no. 3: 300-305.

Huo, X. S., N. Al-Omaishi, and M. K. Tadros. 2001. Creep, Shrinkage, and Modulus of Elasticity of High Performance Concrete. *ACI Materials Journal* 98, no. 6: 440-449.

Khayat, K and J. Daczko. 2003. “The Holistic Approach to Self-Consolidating Concrete”. In *First North American Conference on the Design and Use of Self-Consolidating Concrete 12-13 November 2002*, ed. S. Shah, J. Daczko, and J. Lingscheit. Addison, Illinois: Hanley-Wood, 9-14.

Khayat, K. H. 1995. Frost Durability of Concrete Containing Viscosity Modifying Admixtures. *ACI Materials Journal* 92, no. 6: 625-633.

Khayat, K. H. 1999. Workability, Testing, and Performance of Self-Consolidating Concrete. *ACI Materials Journal* 96, no. 3: 346-353.

Khayat, K. H. and J. Assaad. 2002. Air-Void Stability in Self-Consolidating Concrete. *ACI Materials Journal* 96, no. 4: 408-417.

Khayat, K. H., A. Ghezal, and M. S. Hadriche. 1999. Factorial Design Model for Proportioning Self-Consolidating Concrete. *Materials and Structures* 32 (November): 679-686.

Khayat, K. H., J. Assaad, and H. Mesbah. 2003. "Variations of Formwork Pressure of Self-Consolidating Concrete—Effect of Section Width and Casting Rate". In *First North American Conference on the Design and Use of Self-Consolidating Concrete 12-13 November 2002*, ed. S. Shah, J. Daczko, and J. Lingscheit. Addison, Illinois: Hanley-Wood, 267-272.

Khayat, K., C. Hu, and H. Monty. 1999. "Stability of Self-Consolidating Concrete, Advantages, and Potential Applications". In *Self-Compacting Concrete*: *Proceedings of the First International RILEM Symposium*, ed. A. Skarendahl and O. Petersson. Cachan Cedex, France: RILEM Publications, 143-152.

Khayat, K., J. Assaad, and J. Daczko. 2004. Comparison of Field-Oriented Test Methods to Assess Dynamic Stability of Self-Consolidating Concrete. *ACI Materials Journal* 101, no. 2: 168-172.

Lachemi, M., K. M. A. Hossain, V. Lambros, P. C. Nkinamubanzi, and N. Bouzoubaa. 2004. Self-Consolidating Concrete Incorporating New Viscosity Modifying Admixtures. *Cement and Concrete Research* 34 (June): 917-926.

Mindess, S., J. F. Young, and D. Darwin. 2003. *Concrete*, 2nd edition. Upper Saddle River, New Jersey: Prentice Hall.

Naaman, A. E. 2004. *Prestressed Concrete Analysis and Design,* 2nd edition. Ann Arbor, Michigan: Techno Press.

National Cooperative Highway Research Program (NCHRP). 2005. Project 18-12: Self-Consolidating Concrete for Precast, Prestressed Concrete Bridge Elements. Viewed 17 October 2005. http://www4.trb.org/trb/crp.nsf/e7bcd526f5af4a2c8525672f006245fa/303c9198458cdf7685256d0b00655844?OpenDocument

Neville, A. M. 1996. *Properties of Concrete*, 4th edition. New York, New York: John Wiley & Sons, Inc.

Okamura, H. and M. Ouchi. 1999. "Self-Compacting Concrete. Development, Present Use and Future". In *Self-Compacting Concrete*: *Proceedings of the First International RILEM Symposium,* ed. A. Skarendahl and O. Petersson. Cachan Cedex, France: RILEM Publications, 3-14.

Ozyildirim, C. and D. S. Lane. 2003. Final Report. Evaluation of Self-Consolidating Concrete. *Virginia Transportation Research Council* (June). Charlottesville, Virginia: Commonwealth of Virginia.

Persson, B. 2001. A Comparison Between Mechanical Properties of Self-Compacting Concrete and the Corresponding Properties of Normal Concrete. *Cement and Concrete Research* 31 (February): 193-198.

Petersson, O. 2000. "L-Shape Box Test". In *State-of-the-Art Report (23) of RILEM Technical Committee 174-SCC*, ed. A. Skarendahl and O. Petersson. Cachan Cedex, France: RILEM Publications, 126-128.

Petersson, O. and P. Billberg. 1999. "Investigation on Blocking of Self-Compacting Concrete With Different Maximum Aggregate Size and Use of Viscosity Agent Instead of Filler". In *Self-Compacting Concrete*: *Proceedings of the First International RILEM Symposium,* ed. A. Skarendahl and O. Petersson. Cachan Cedex, France: RILEM Publications, 333-344.

Philleo, R. E. 1989. "Slag or Other Supplementary Materials?". In *Fly Ash, Silica Fume, Slag, and Natural Pozzolans in Concrete: Proceedings Third International Conference. Trondheim, Norway, 1989,* ed. V. M. Malhotra. Detroit, Michigan: American Concrete Institute, 1197-1207.

Precast/Prestressed Concrete Institute (PCI). 2003. *Interim Guidelines for the Use of Self-Consolidating Concrete in Precast/Prestressed Concrete Institute Member Plants*, 1st edition. Chicago, Illinois: Precast/Prestressed Concrete Institute.

Ramsburg, P. 2003. The SCC Test: Inverted or Upright. *Concrete Producer* 21, no. 7: 34-38.

Skarendahl, A. 2000a. "Definitions". In *Self-Compacting Concrete. State-of-the-Art Report (23) of RILEM Technical Committee 174-SCC*, ed. A. Skarendahl and O. Petersson. Cachan Cedex, France: RILEM Publications, 3-5.

Skarendahl, A. 2000b. "Development Objectives". In *Self-Compacting Concrete. State-of-the-Art Report (23) of RILEM Technical Committee 174-SCC*, ed. A. Skarendahl and O. Petersson. Cachan Cedex, France: RILEM Publications, 9-13.

Skarendahl, A. 2000c. "Early Age and Hardened Properties". In *Self-Compacting Concrete*. *State-of-the-Art Report (23) of RILEM Technical Committee 174-SCC*, ed. A. Skarendahl and O. Petersson. Cachan Cedex, France: RILEM Publications 43-46.

Sonebi, M. 2004. Medium Strength Self-Compacting Concrete Containing Fly Ash: Modelling Using Factorial Experimental Plans. *Cement and Concrete Research* 34 (July): 1199-1208.

Sonebi, M. and P. J. M. Bartos. 2002. Filling Ability and Plastic Settlement of Self-Compacting Concrete. *Materials and Structures* 35 (September-October): 462-469.

Su, J. K., S. W. Cho, C. C. Yang, and R. Huang. 2002. Effect of Sand Ratio on the Elastic Modulus of Self-Compacting Concrete. *Journal of Marine Science and Technology* 10, no.1: 8-13.

Sugamata, T., Y. Edamatsu, and M. Ouchi. 2003. "A Study of Particle Dispersing Retention Effect of Polycarboxylate-Based Superplasticizers". In *Self-Compacting Concrete*: *Proceedings of the Third International RILEM Symposium,* ed. O. Wallevik and I. Nielsson. Bagneux, France: RILEM Publications, 420-431.

Tadros, M. K., N. Al-Omaishi, S. J. Seguirant, and J. G. Gallt. 2003. *NCHRP Report 496. Prestress Losses in Pretensioned High-Strength Concrete Bridge Girders*. Washington, DC: Transportation Research Board.

Takada, K. 2000. “Placement”. In *Self-Compacting Concrete*. *State-of-the-Art Report (23) of RILEM Technical Committee 174-SCC*, ed. A. Skarendahl and O. Petersson. Cachan Cedex, France: RILEM Publications, 79-87.

Takada, K. and S. Tangtermsirikul. 2000. “Testing of Fresh Concrete”. In *Self-Compacting Concrete*. *State-of-the-Art Report (23) of RILEM Technical Committee 174-SCC*, ed. A. Skarendahl and O. Petersson. Cachan Cedex, France: RILEM Publications, 25-39.

Tangtermsirikul, S. and K. Khayat. 2000. “Fresh Concrete Properties”. In *State-of-the-Art Report (23) of RILEM Technical Committee 174-SCC*, ed. A. Skarendahl and O. Petersson. Cachan Cedex, France: RILEM Publications, 17-22.

Tragargh, J. 1999. “Microstructural Features and Related Properties of Self-Compacting Concrete”. In *Self-Compacting Concrete*: *Proceedings of the First International RILEM Symposium*, ed. A. Skarendahl and O. Petersson. Cachan Cedex, France: RILEM Publications, 175-186.

APPENDICES

APPENDIX A

TEST PROCEDURES FOR FRESH PROPERTIES

A.1 SLUMP FLOW TEST

A.1.1 APPARATUS

- Mold- A mold in the shape of a truncated cone that conforms to the specifications of AASHTO T 119 (2003). This piece of equipment is commonly referred to as the slump cone and is shown in Figure 3-3. (PCI 2003)
- Base Plate- A plate that is made of a non-absorbing material, such as plexy glass or steel. The plate needs to be at least 28 inches square and have a central circle marking the placement of the slump cone. A further concentric circle with a 20 inch diameter must also be marked to assist in recording the T-50. This can also be referred to as the slump table. (PCI 2003)
- Trowel
- Scoop
- Tape Measure
- Stop Watch

A.1.2 PROCEDURE

Approximately six liters of SCC is required to perform the test, sampled normally. After moistening the inside of the slump cone and the base plate, align the slump cone with the circle in the center of the base plate. Make sure that the base plate is on a flat surface.

Next, fill the slump cone with the scoop. No tamping is required. Strike off excess concrete with a trowel and remove any SCC that may have fallen on the slump table. Carefully lift the slump cone in a continuous vertical motion until all of the concrete has flowed out of the slump cone. (PCI 2003)

A.2 L-BOX TEST

A.2.1 APPARATUS

- L-Box made from a stiff non-absorbing material, see Figure 2-11
- Trowel
- Scoop
- Stopwatch

A.2.2 PROCEDURE

Approximately 14 liters of normally sampled SCC will be required to perform the test. Find a level, firm spot on the ground. Moisten the inside of the L-Box and remove any excess water. Before pouring any concrete into the apparatus, check to make sure that the gate will open and close without any hindrances. Next, fill the vertical section of the apparatus with concrete, level off the top of the vertical section, and allow the concrete to stand for approximately 1 minute to allow for any segregation. No tamping or rodding is required. Lift the moveable gate to allow the concrete to flow into the horizontal section. Record the H_2 and H_1 measurements so that the blocking ratio can be calculated. The entire test needs to be performed within 5 minutes. (PCI 2003)

A.3 J-RING TEST

A.3.1 APPARATUS

- J-Ring made from steel or equivalent material, see Figure 2-12
- Mold- A mold that conforms to the description provided in AASHTO T 119 (2003), with the exception that the foot pieces can be removed for the upright position. This is the same mold that is used for the slump flow test. (ASTM Draft 2004)
- Base Plate- A base plate with the same properties as that prescribed in the slump flow test with the exception of a minimum diameter of 36 inches (ASTM Draft 2004). There should also be feet attached to the four corners of the base plate to provide clearance after the J-Ring has been attached. The feet can be made out of the same material as the plate itsel. Plate should remain level at all times.
- Tamping Rod- A round, straight steel rod approximately 24 inches in length and having a diameter of 5/8 inch. Ends of rod should be rounded to a hemispherical tip. (ASTM Draft 2004)

A.3.2 PROCEDURE

After securing a flat surface to perform the test, dampen the base plate and the inside of the mold. Place the mold on the base plate concentric with the J-Ring. If the upright method is being performed, one operator needs to hold the mold down until it is ready to be lifted. Next, fill the mold in one lift with the normally sampled concrete. Use the tamping rod to level the top of the mold by means of a screeding and rolling motion. Remove any concrete that may have fallen on the base plate. Raise the mold a distance of 9 ± 3 inches in 3 ± 1 seconds with a steady upward motion with no lateral or torsional movement. The entire test should not exceed 2 ½ minutes. (ASTM Draft 2004)

Note: The slump flow test should be performed just prior to the J-Ring test or immediately after. Often times, it is in the interest of the operator(s) to have two slump tables to reduce the time required to perform this test.

APPENDIX B

SUMMARY OF COMPRESSIVE STRENGTH RESULTS

B.1 MATCH-CURED CYLINDERS (4 IN. X 8 IN.)

The following figures are the results from specimens that were match-cured to the time-temperature profile shown in Figure 3-7:

- Figures B-1 through B-3
- Figures B-7 through B-9
- Figure B-13

In the description of each of these figures, {4x8} is a reminder to the reader that the specimens were 4 in. x 8 in. match-cured specimens.

B.2 MOIST-CURED CYLINDERS (6 IN. X 12 IN.)

The following figures are the results from specimens that were moist-cured according to AASHTO T 126 (2003):

- Figures B-4 through B-6
- Figures B-10 through B-12
- Figure B-14

In the description of each of these figures, {6x12} is a reminder to the reader that the specimens were 4 in. x 8 in. match-cured specimens.

Table B-1: Complete summary of compressive strength results

Mixture ID	4x8 in. Match-Cured Cylinder Results Compressive Strength (psi)				6x12 in. Moist-Cured Cylinder Results Compressive Strength (psi)			
	18 hr	21 hr	7 day	28 day	3 day	7 day	28 day	56 day
CTRL1: 0.37	7,480	7,880	9,700	10,500	8,290	8,880	10,250	11,190
CTRL2: 0.42	6,280	6,310	7,940	9,550	7,070	7,670	8,850	9,510
SCC1:0.28-0.38-FA	9,000	9,110	10,970	12,410	9,330	10,660	12,510	13,080
SCC2:0.32-0.38-FA	7,000	7,430	9,540	11,760	8,140	9,450	11,090	12,070
SCC3:0.36-0.38-FA	5,790	6,490	7,500	9,220	6,570	8,020	10,150	10,900
SCC4:0.28-0.42-FA	8,820	9,410	10,520	12,700	9,540	11,390	13,600	14,080
SCC5:0.32-0.42-FA	7,140	7,530	9,220	10,490	7,960	9,250	11,580	12,380
SCC6:0.36-0.42-FA	5,470	5,750	7,150	9,110	6,150	7,800	10,330	10,350
SCC7:0.28-0.46-FA	8,860	9,580	10,950	12,520	9,890	11,060	13,300	13,930
SCC8:0.32-0.46-FA	7,780	7,930	10,050	10,970	7,890	9,290	11,550	12,100
SCC9:0.36-0.46-FA	5,800	6,100	7,650	9,280	6,670	7,990	10,060	11,000
SCC10:0.28-0.42-S	8,350	8,470	10,020	10,510	8,480	9,950	11,620	12,540
SCC11:0.32-0.42-S	7,610	8,120	8,930	10,650	6,310	8,850	10,750	11,260
SCC12:0.36-0.42-S	6,490	6,650	8,610	9,740	5,520	7,660	9,880	10,250
SCC13:0.28-0.46-S	8,800	8,950	9,950	11,740	8,110	10,020	11,580	12,290
SCC14:0.32-0.46-S	7,090	7,430	8,850	10,130	5,950	8,350	10,390	10,690
SCC15:0.36-0.46-S	5,780	6,290	8,060	8,610	5,170	7,360	8,960	9,570
SCC16:0.32-0.42-Ternary	9,470	9,480	10,270	11,160	7,880	9,370	12,240	13,390
SCC17:0.36-0.42-Ternary	8,310	8,790	8,860	10,090	6,470	8,140	10,760	12,430
SCC18:0.40-0.42-Ternary	6,880	7,420	8,190	8,840	5,960	7,410	11,020	11,800
SCC19:0.32-0.46-Ternary	9,530	9,700	10,700	11,060	7,560	9,620	12,470	13,160
SCC20:0.36-0.46-Ternary	8,320	8,570	9,680	9,840	6,770	8,260	11,840	12,650
SCC21:0.40-0.46-Ternary	7,750	8,000	8,470	8,600	6,280	7,830	11,630	12,130

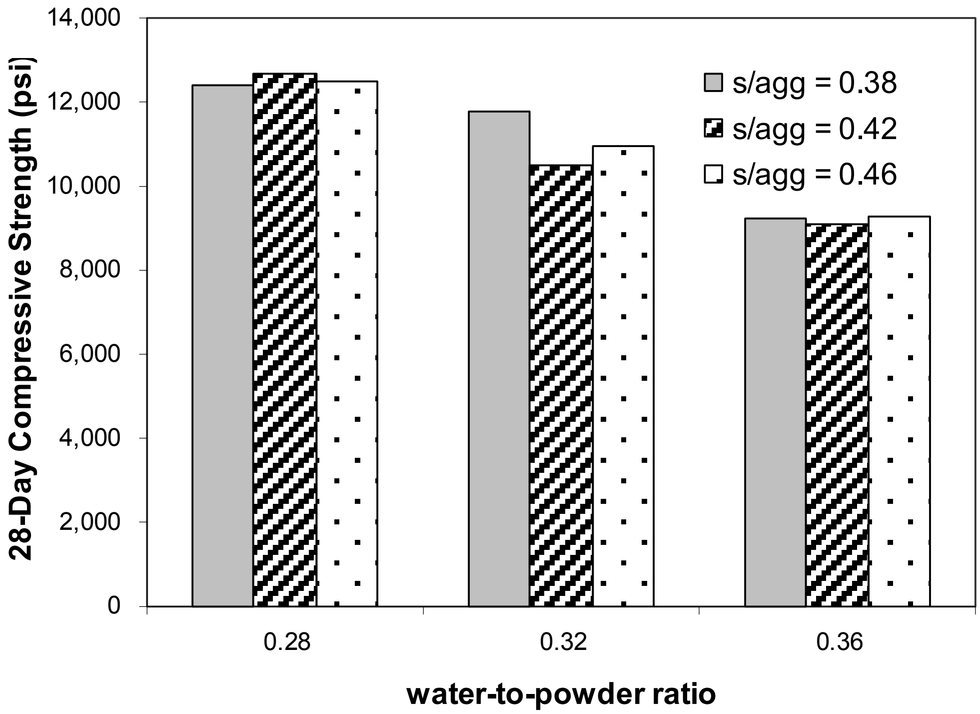

Figure B-1: Effect of *s/agg* on 28-day compressive strength for fly ash mixtures {4x8}

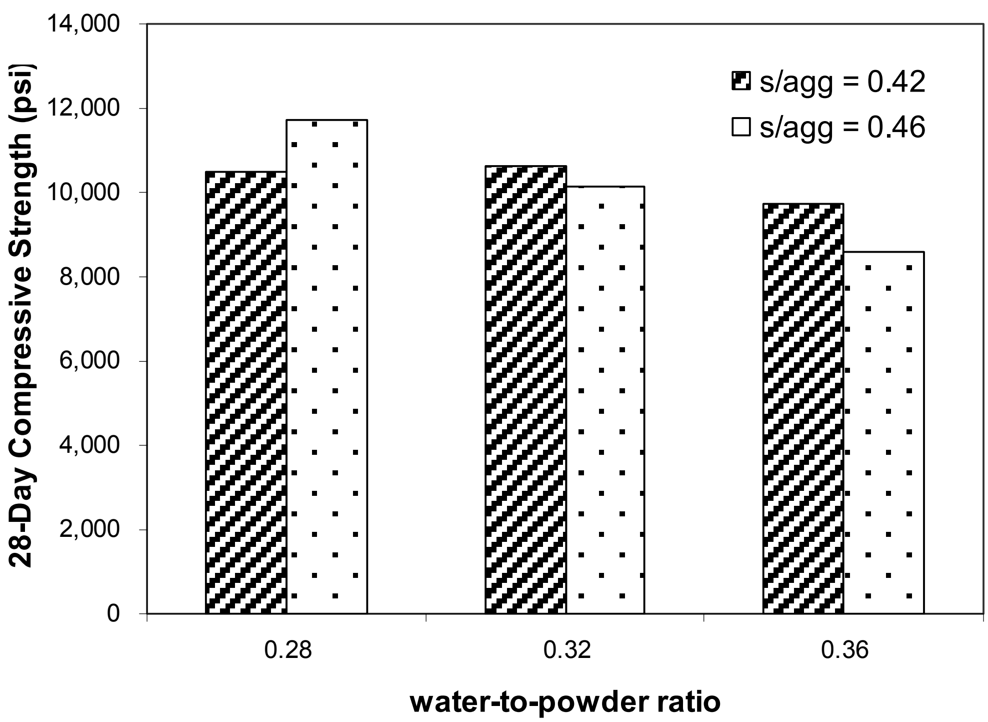

Figure B-2: Effect of *s/agg* on 28-day compressive strength for slag mixtures {4x8}

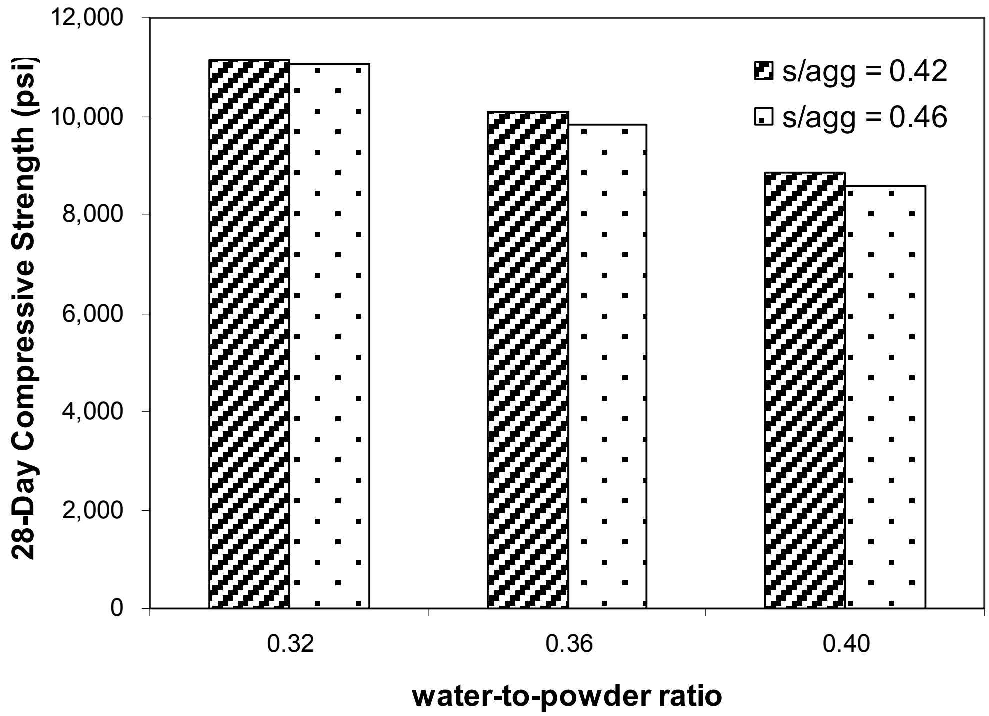

Figure B-3: Effect of *s/agg* on 28-day compressive strength for ternary mixtures {4x8}

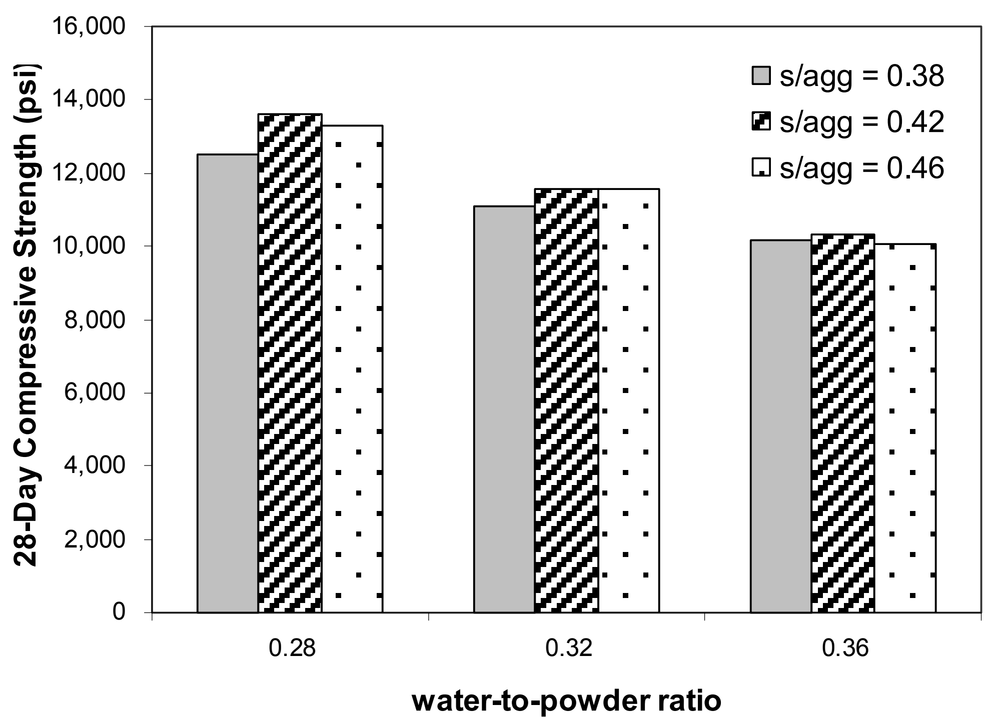

Figure B-4: Effect of *s/agg* on 28-day compressive strength for fly ash mixtures {6x12}

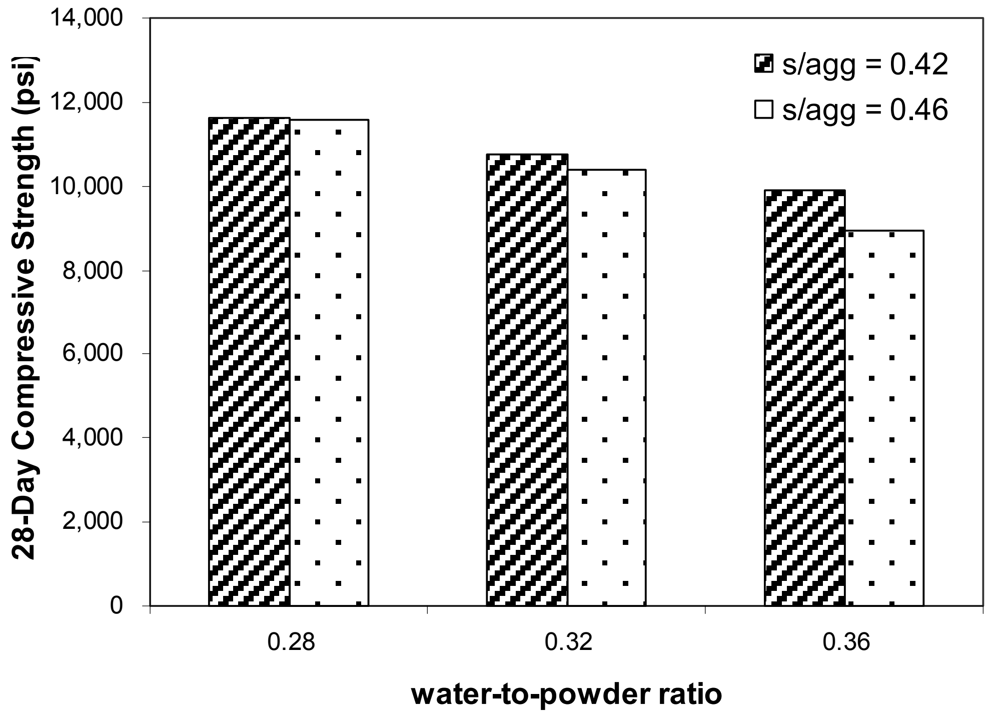

Figure B-5: Effect of *s/agg* on 28-day compressive strength for slag mixtures {6x12}

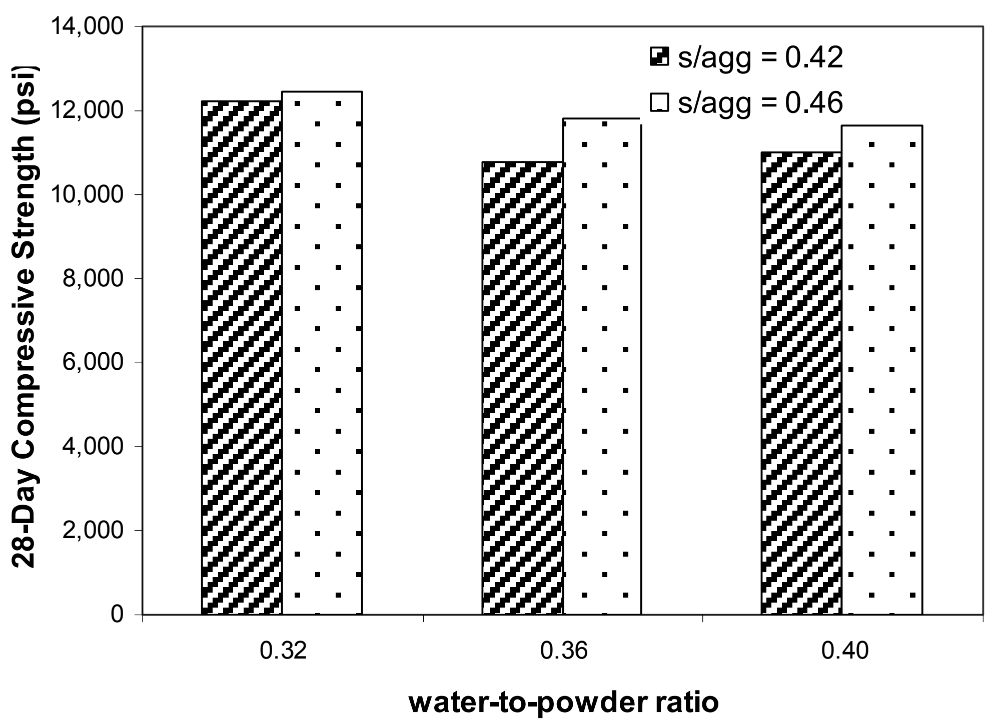

Figure B-6: Effect of *s/agg* on 28-day compressive strength for ternary mixtures {6x12}

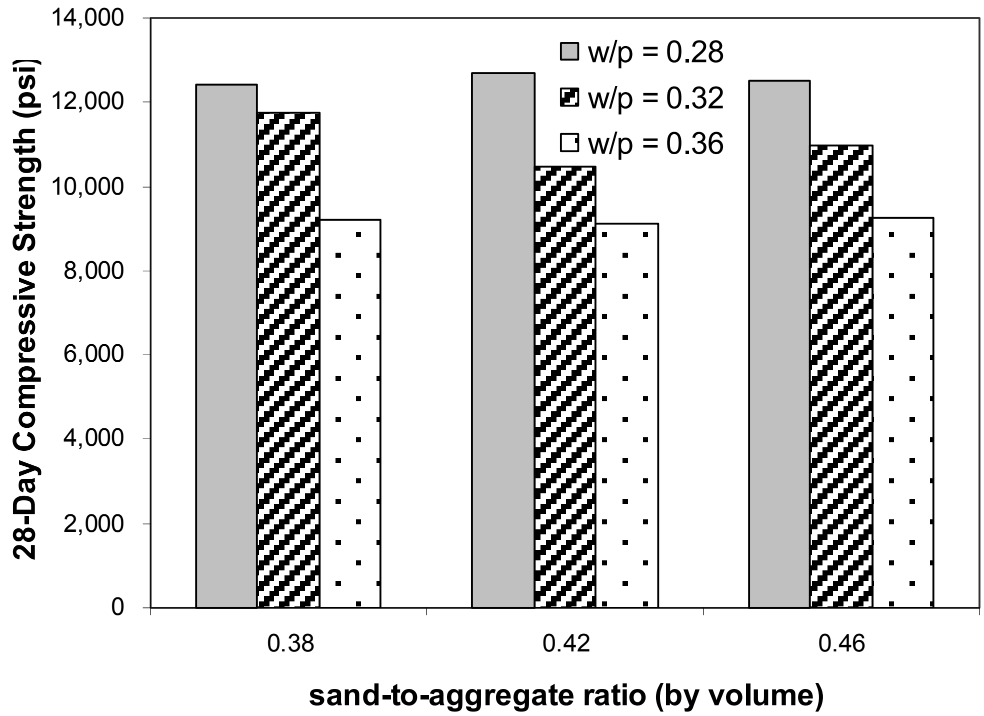

Figure B-7: Effect of *w/p* on 28-day compressive strength for fly ash mixtures {4x8}

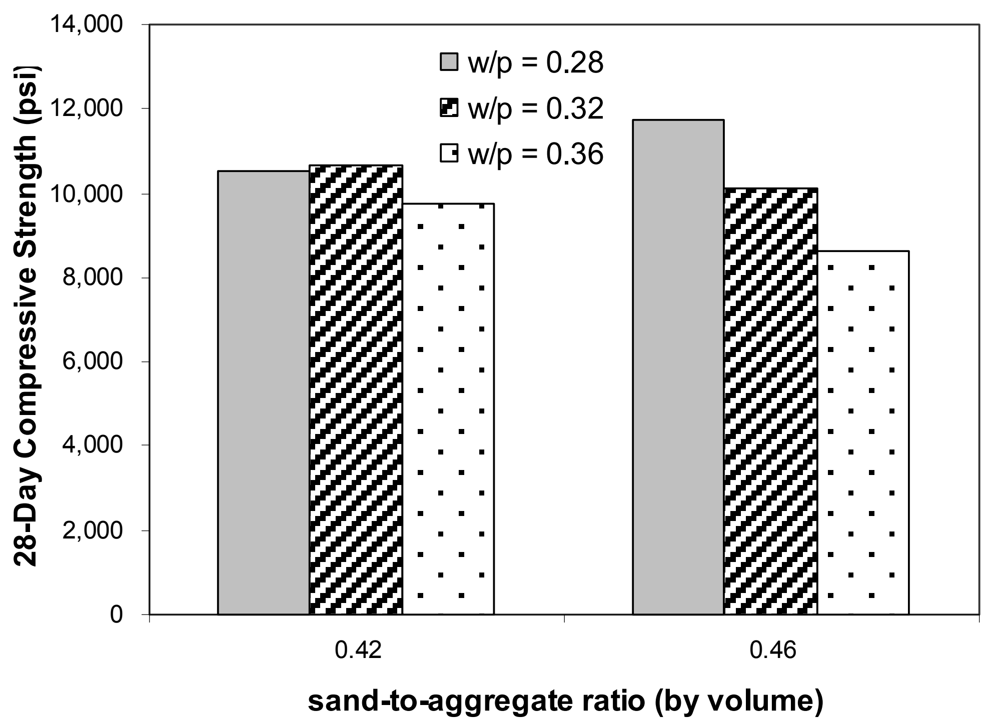

Figure B-8: Effect of *w/p* on 28-day compressive strength for slag mixtures {4x8}

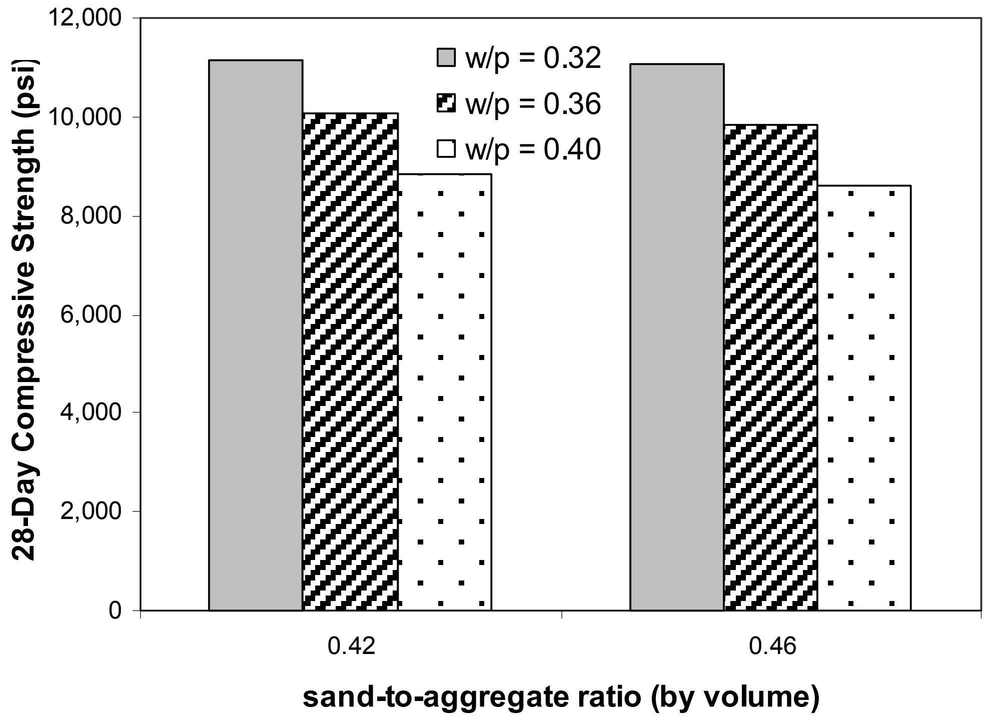

Figure B-9: Effect of *w/p* on 28-day compressive strength for ternary mixtures {4x8}

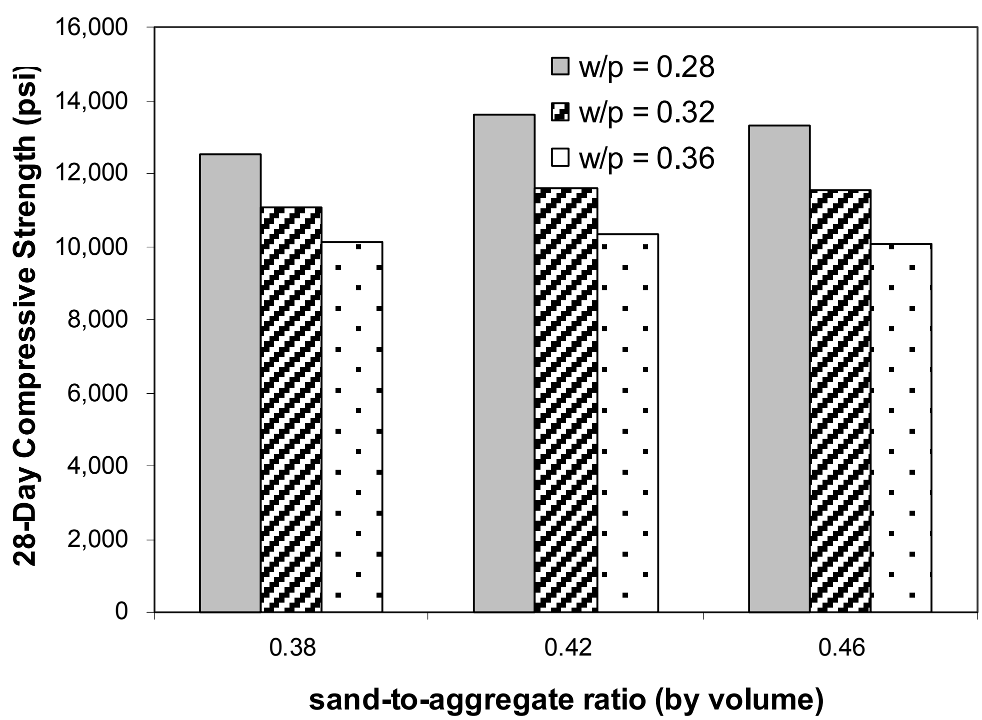

Figure B-10: Effect of *w/p* on 28-day compressive strength for fly ash mixtures {6x12}

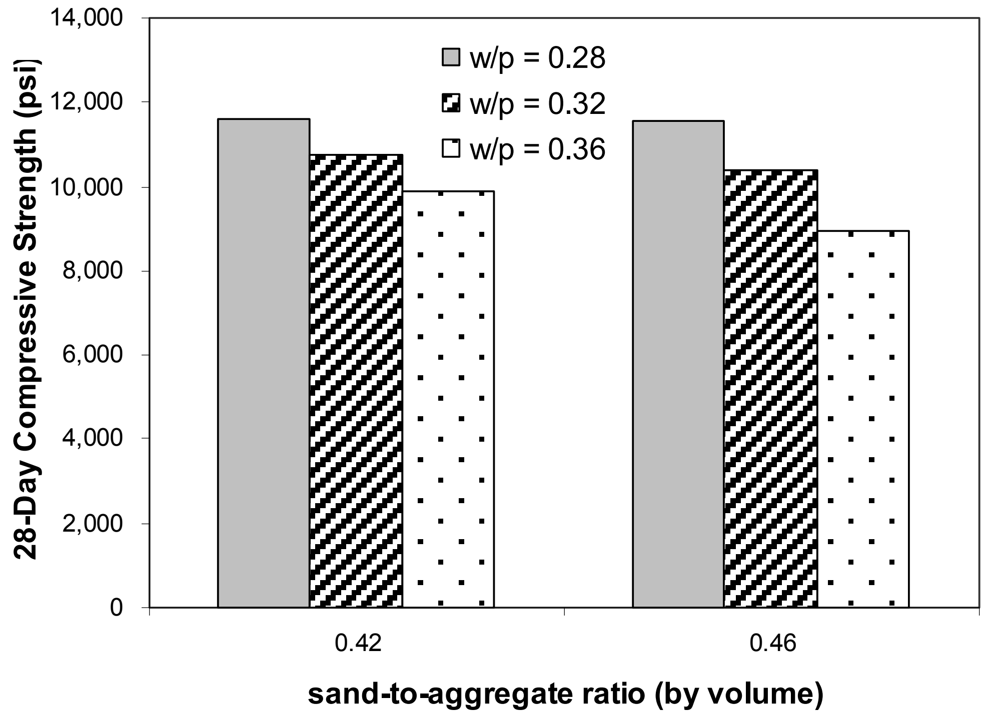

Figure B-11: Effect of *w/p* on 28-day compressive strength for slag mixtures {6x12}

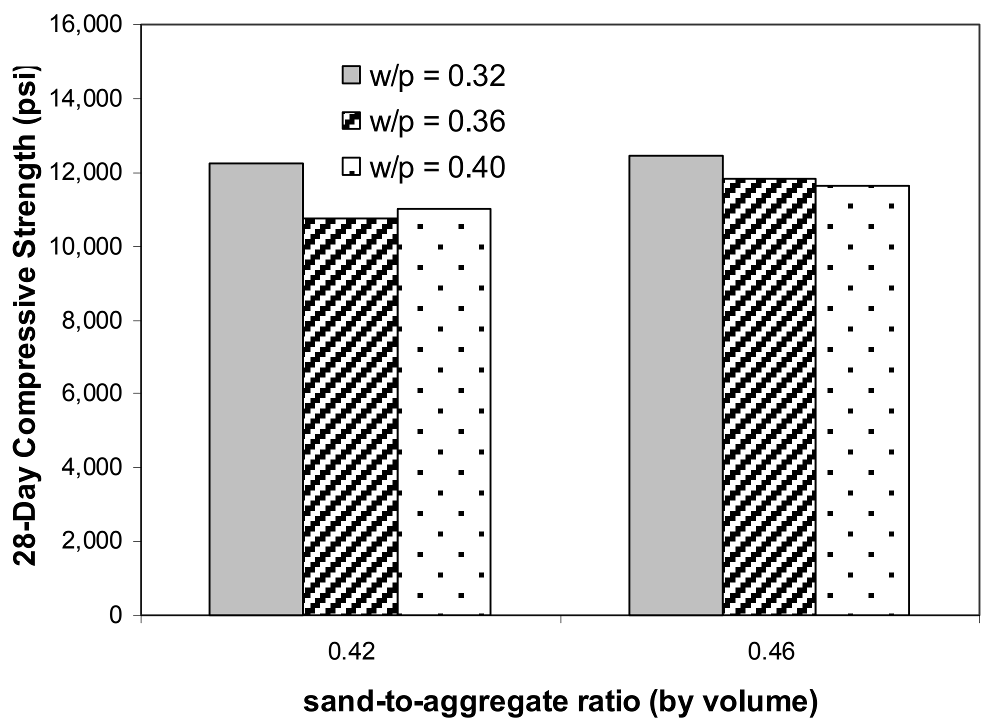

Figure B-12: Effect of *w/p* on 28-day compressive strength for ternary mixtures {6x12}

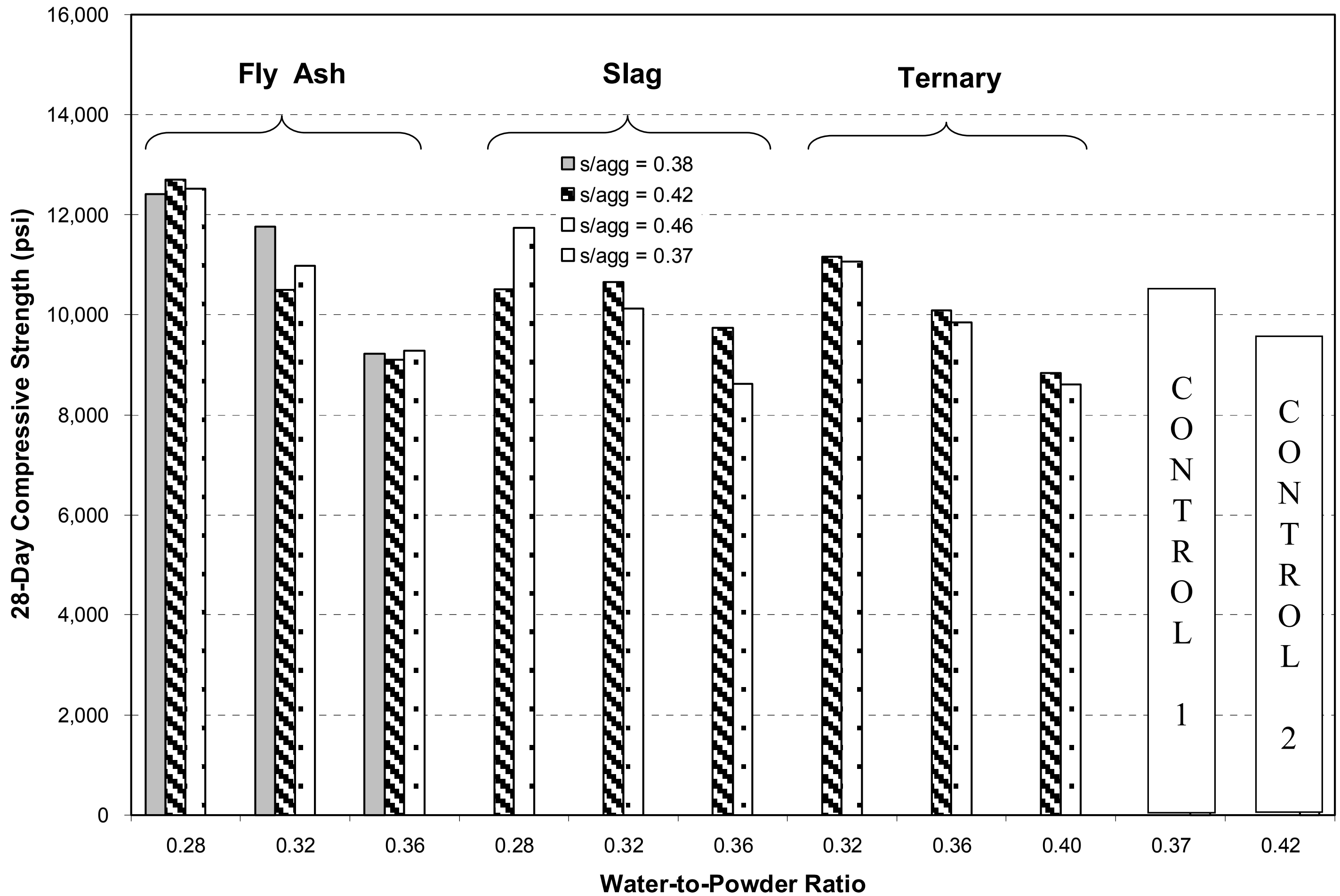

Figure B-13: Effect of different powder combinations on the 28-day compressive strength {4x8}

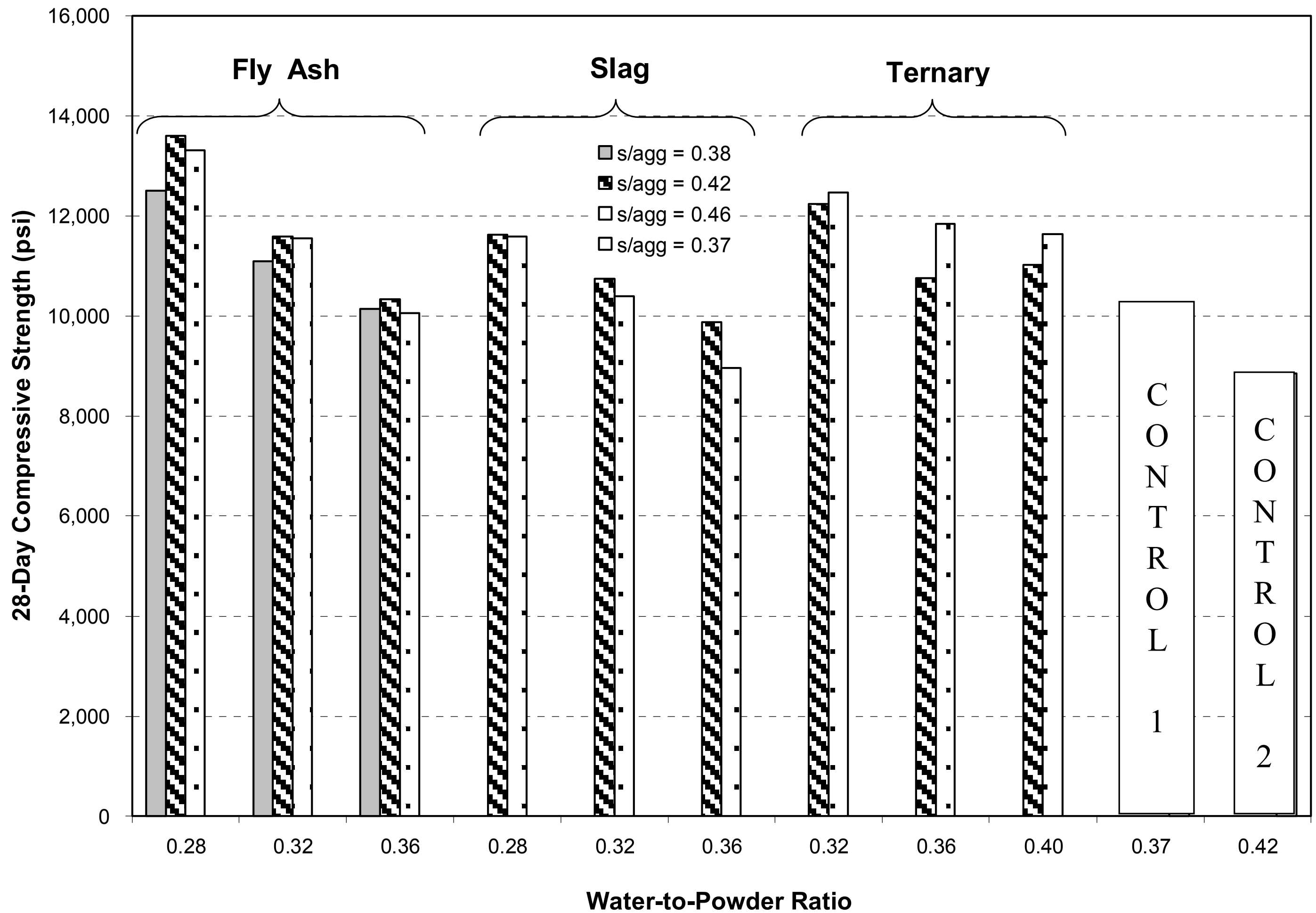

Figure B-14: Effect of different powder combinations on the 28-day compressive strength {6x12}

APPENDIX C

SUMMARY OF MODULUS OF ELASTICITY RESULTS

C.1 MATCH-CURED CYLINDERS (4 IN. X 8 IN.)

The following figures are the results from specimens that were match-cured to the time-temperature profile shown in Figure 3-7:

- Figures C-1 through C-3
- Figures C-7 through C-9
- Figure C-13
- Figures C-15, C-16, C-18, C-20

In the description of each of these figures, {4x8} is a reminder to the reader that the specimens were 4 in. x 8 in. match-cured specimens.

C.2 MOIST-CURED CYLINDERS (6 IN. X 12 IN.)

The following figures are the results from specimens that were moist-cured according to AASHTO T 126 (2003):

- Figures C-4 through C-6
- Figures C-10 through C-12
- Figure C-14
- Figures C-17, C-19, C-21, C-22

In the description of each of these figures, {6x12} is a reminder to the reader that the specimens were 4 in. x 8 in. match-cured specimens.

Table C-1: Complete summary of modulus of elasticity results

Mixture ID	4x8 in. Match-Cured Cylinder Results Modulus of Elasticity Results (ksi)				6x12 in. Moist-Cured Cylinder Results Modulus of Elasticity Results (ksi)			
	18 hr	21 hr	7 day	28 day	3 day	7 day	28 day	56 day
CTRL1: 0.37	6,100	5,750	6,250	6,850	7,350	7,000	7,250	7,000
CTRL2: 0.42	5,330	5,300	5,950	6,650	6,150	6,500	7,100	6,500
SCC1:0.28-0.38-FA	5,750	5,100	6,250	6,400	6,300	6,848	7,000	7,150
SCC2:0.32-0.38-FA	4,950	5,450	5,500	6,000	6,150	7,100	7,300	7,150
SCC3:0.36-0.38-FA	5,000	5,250	5,450	5,700	5,450	6,500	6,500	6,700
SCC4:0.28-0.42-FA	5,450	6,050	6,400	6,600	6,350	7,400	7,050	7,400
SCC5:0.32-0.42-FA	5,150	5,350	5,750	6,350	6,200	6,650	7,000	7,600
SCC6:0.36-0.42-FA	4,850	5,100	5,450	5,850	5,650	6,250	6,400	6,900
SCC7:0.28-0.46-FA	5,900	6,050	6,700	6,250	6,450	6,350	7,350	7,900
SCC8:0.32-0.46-FA	5,200	6,050	5,600	6,350	5,750	6,900	6,800	6,850
SCC9:0.36-0.46-FA	4,700	5,000	5,150	5,400	5,650	5,900	6,350	6,650
SCC10:0.28-0.42-S	5,870	5,950	5,850	7,450	6,950	7,750	7,050	7,200
SCC11:0.32-0.42-S	5,430	5,550	5,200	6,200	5,800	7,000	6,950	7,050
SCC12:0.36-0.42-S	5,350	5,450	4,950	6,100	6,000	6,800	6,600	6,800
SCC13:0.28-0.46-S	5,750	5,750	6,050	6,650	7,200	7,300	7,000	7,100
SCC14:0.32-0.46-S	5,150	5,600	5,100	6,100	5,750	6,600	6,500	6,650
SCC15:0.36-0.46-S	4,800	4,900	4,900	6,100	5,100	6,200	7,000	6,650
SCC16:0.32-0.42-Ternary	5,600	5,850	5,450	6,850	6,000	6,650	6,850	6,950
SCC17:0.36-0.42-Ternary	5,600	5,900	5,150	6,200	5,450	6,200	6,550	6,850
SCC18:0.40-0.42-Ternary	5,400	5,550	5,050	6,150	5,700	6,200	6,700	6,800
SCC19:0.32-0.46-Ternary	5,700	5,900	5,500	6,500	6,000	6,850	6,700	7,000
SCC20:0.36-0.46-Ternary	5,500	5,650	5,350	6,050	5,800	6,100	6,700	6,800
SCC21:0.40-0.46-Ternary	5,750	5,700	5,150	5,850	5,850	6,200	6,550	6,700

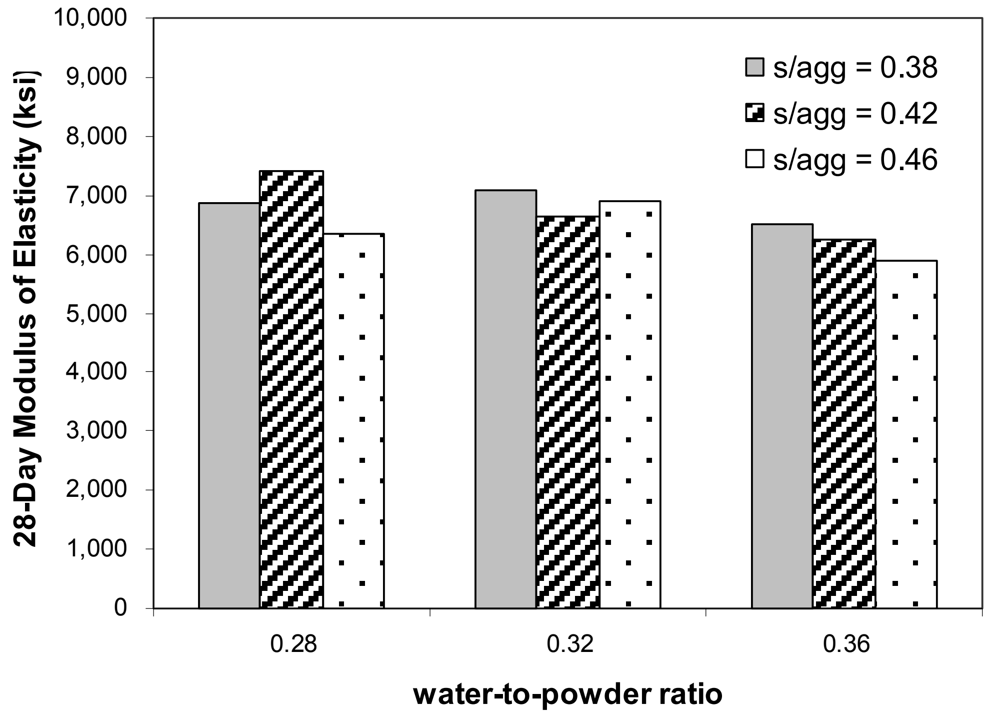

Figure C-1: Effect of *s/agg* on the 28-day modulus of elasticity for fly ash mixtures {4x8}

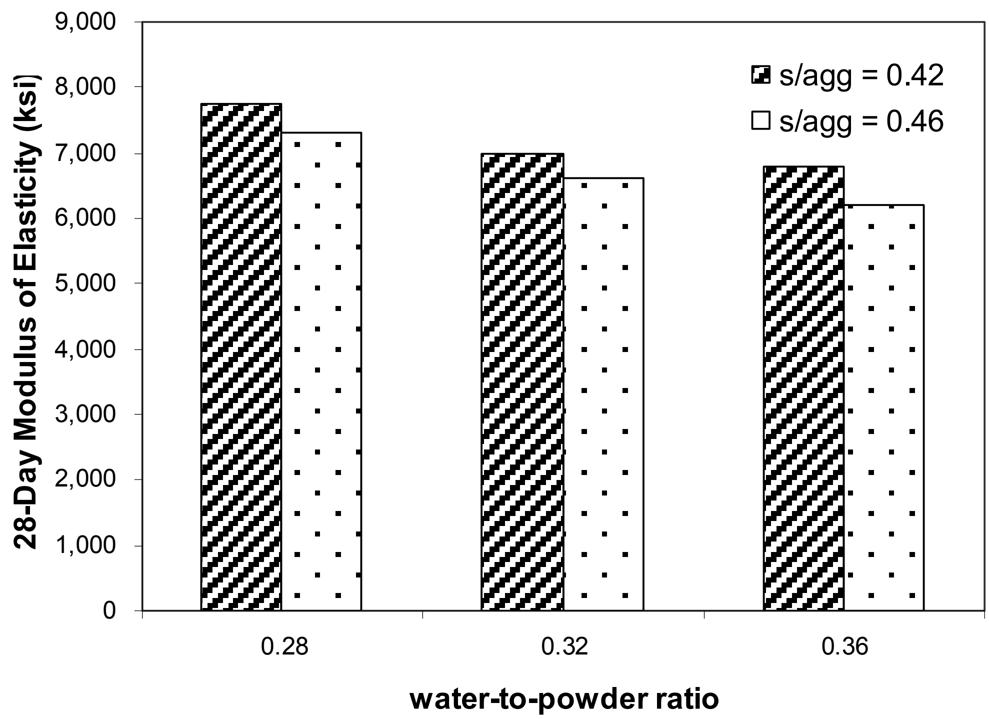

Figure C-2: Effect of *s/agg* on the 28-day modulus of elasticity for slag mixtures {4x8}

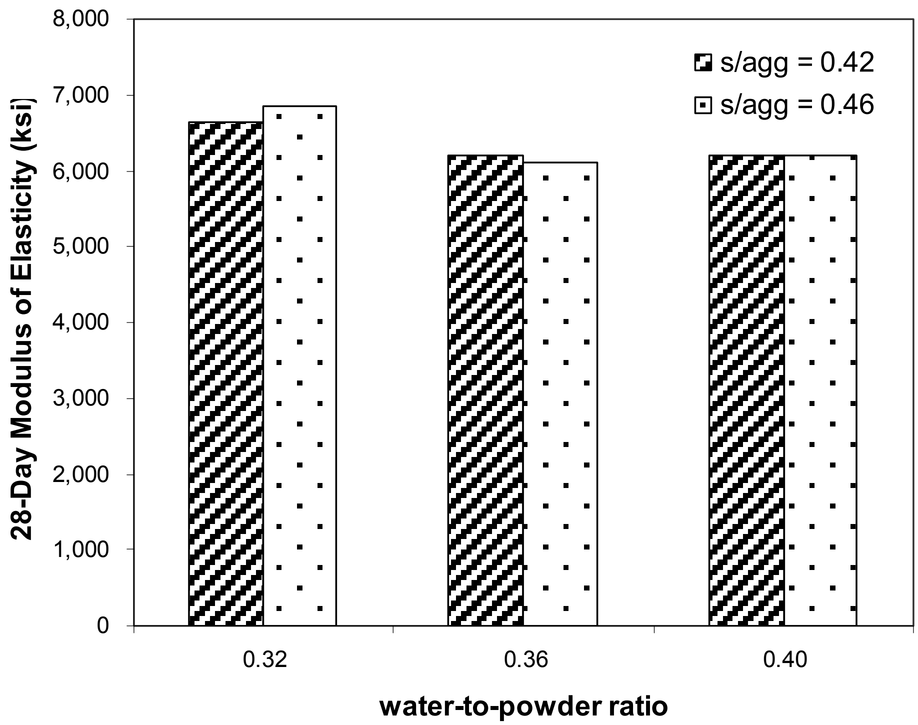

Figure C-3: Effect of *s/agg* on the 28-day modulus of elasticity for ternary mixtures {4x8}

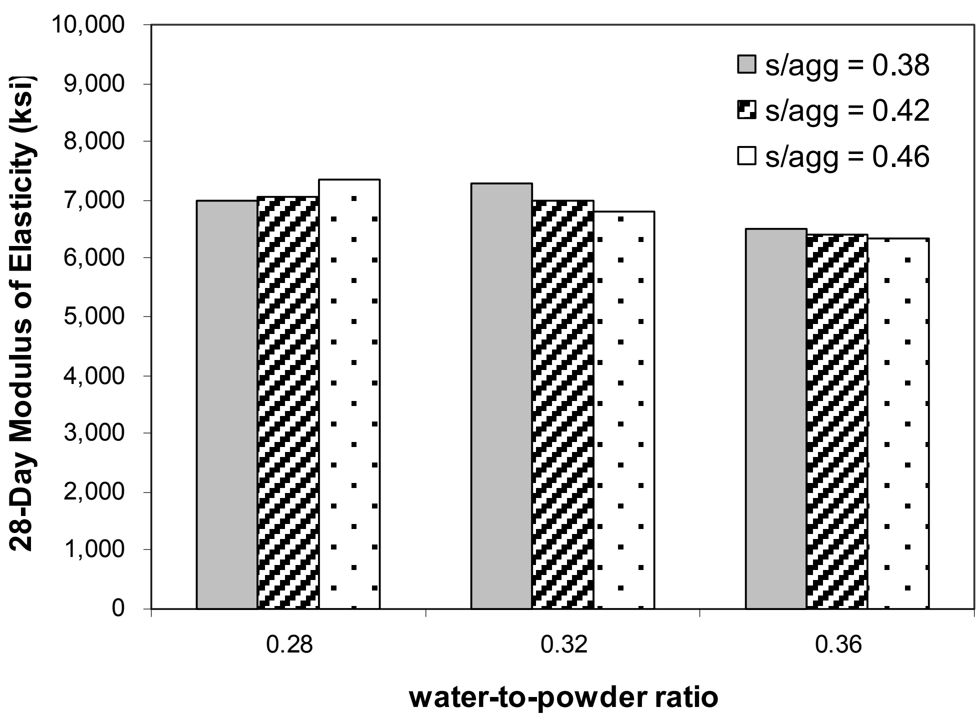

Figure C-4: Effect of *s/agg* on the 28-day modulus of elasticity for fly ash mixtures {6x12}

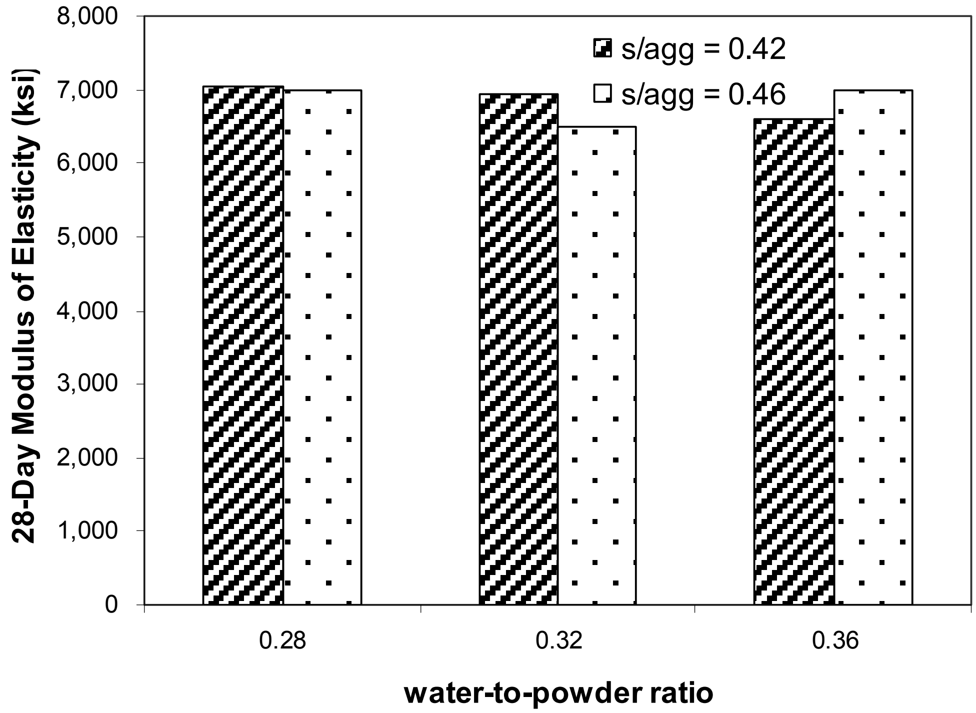

Figure C-5: Effect of *s/agg* on the 28-day modulus of elasticity for slag mixtures {6x12}

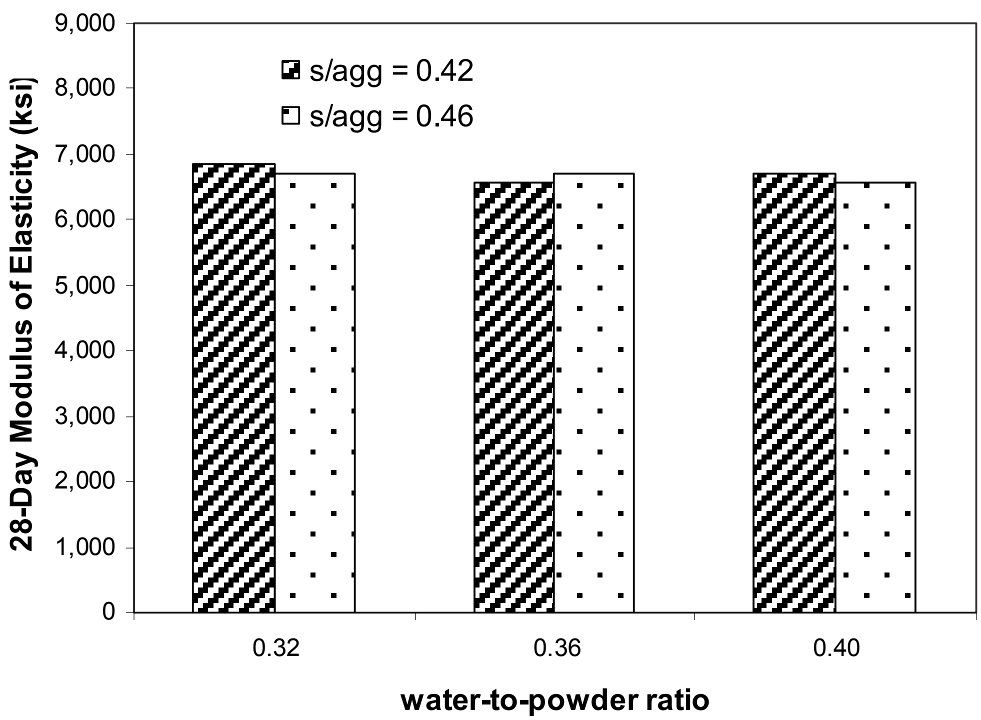

Figure C-6: Effect of *s/agg* on the 28-day modulus of elasticity for ternary mixtures {6x12}

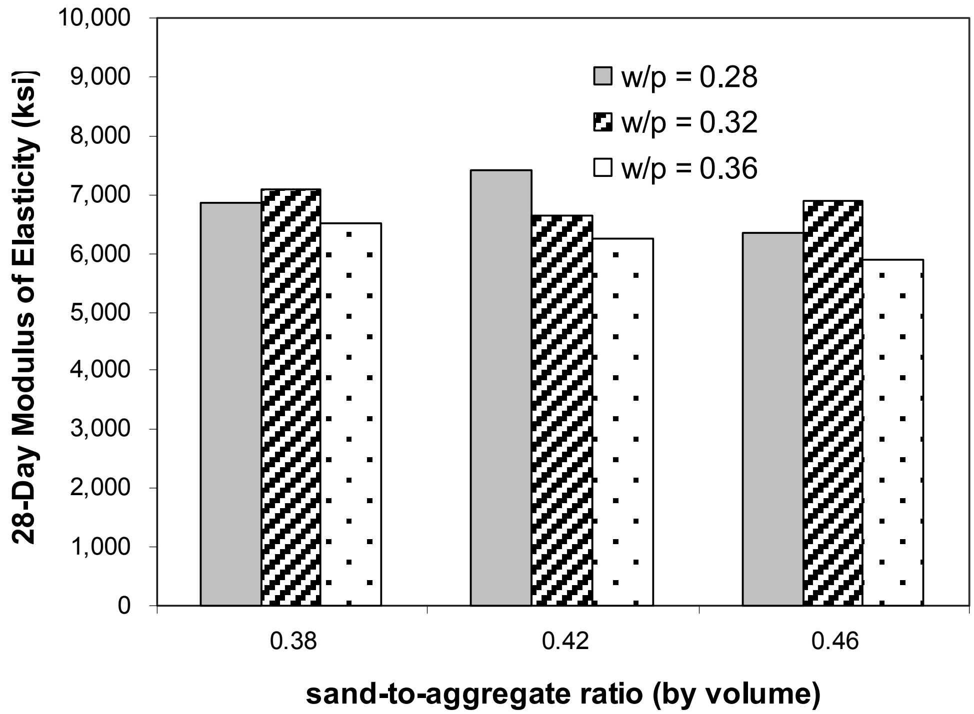

Figure C-7: Effect of *w/p* on the 28-day modulus of elasticity for fly ash mixtures {4x8}

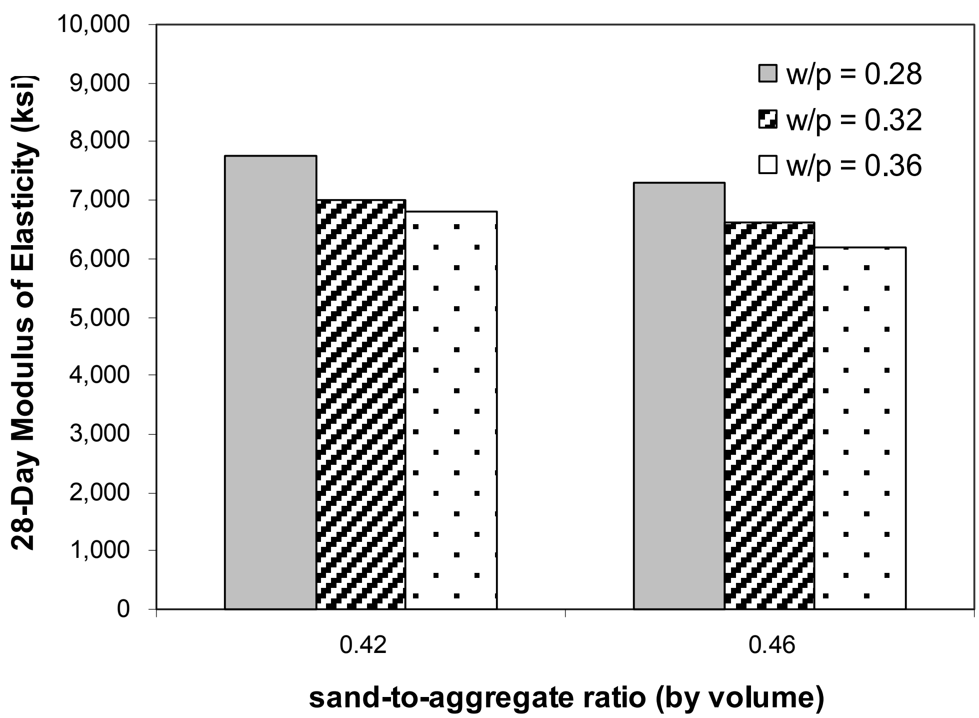

Figure C-8: Effect of *w/p* on the 28-day modulus of elasticity for slag mixtures {4x8}

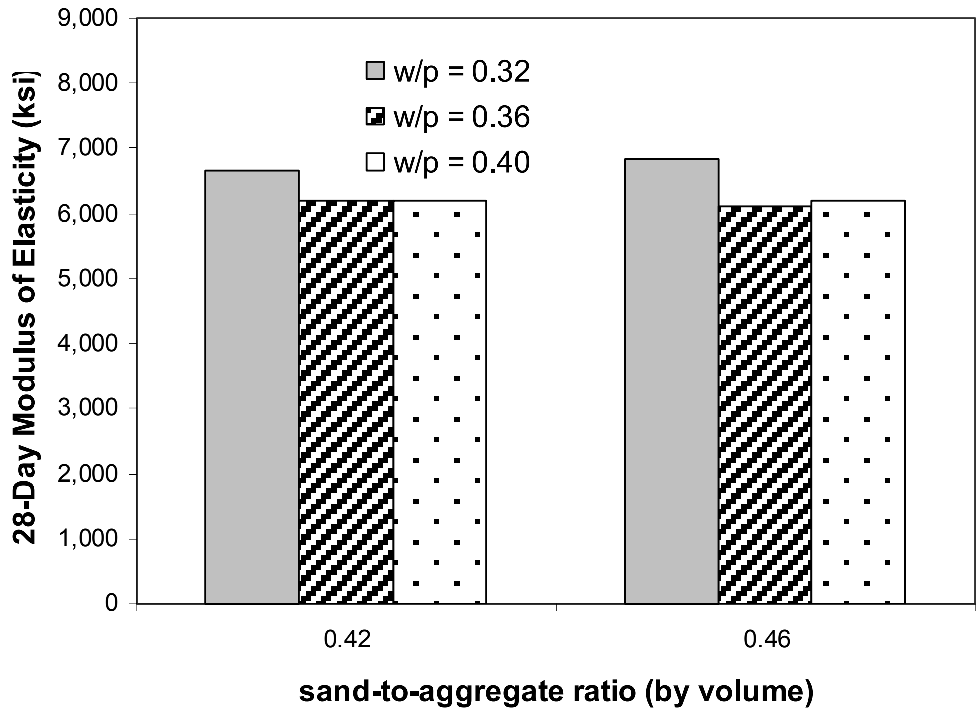

Figure C-9: Effect of *w/p* on the 28-day modulus of elasticity for ternary mixtures {4x8}

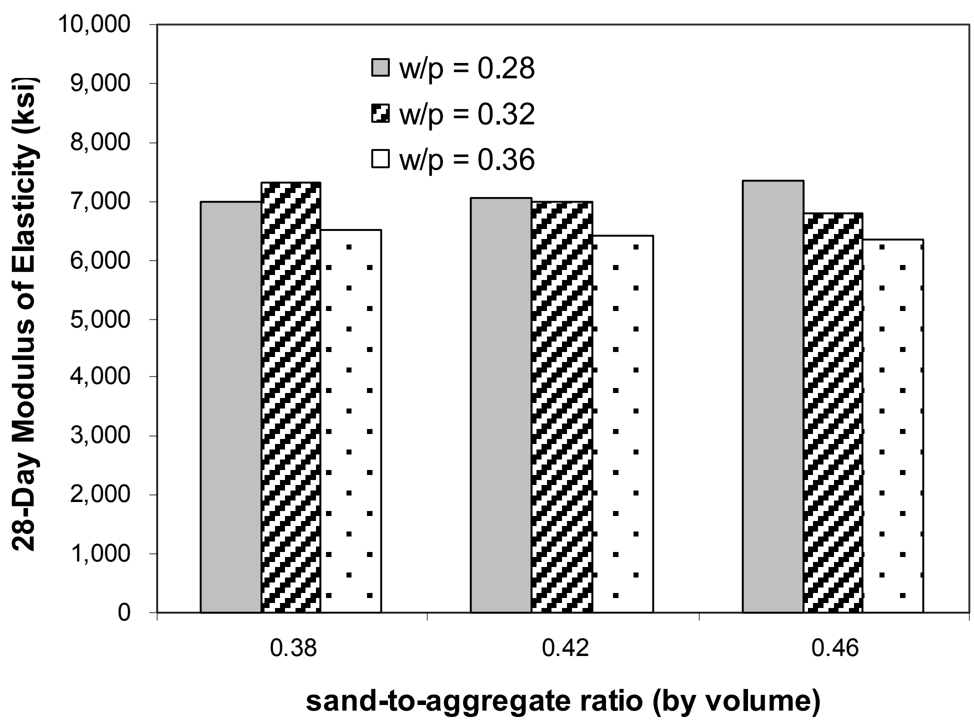

Figure C-10: Effect of *w/p* on the 28-day modulus of elasticity for fly ash mixtures {6x12}

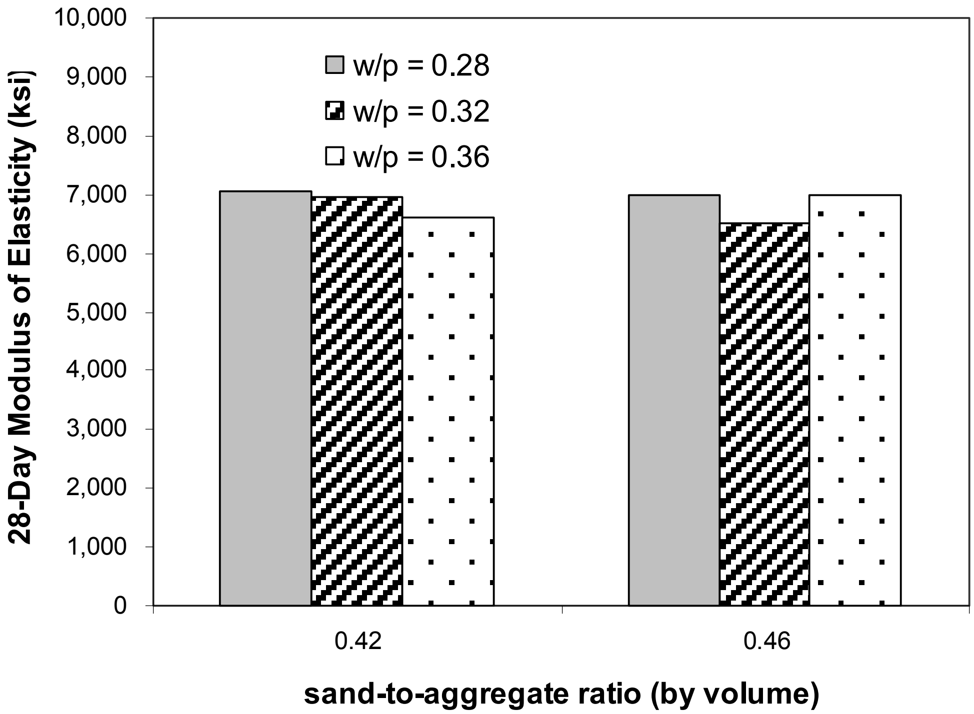

Figure C-11: Effect of *w/p* on the 28-day modulus of elasticity for slag mixtures {6x12}

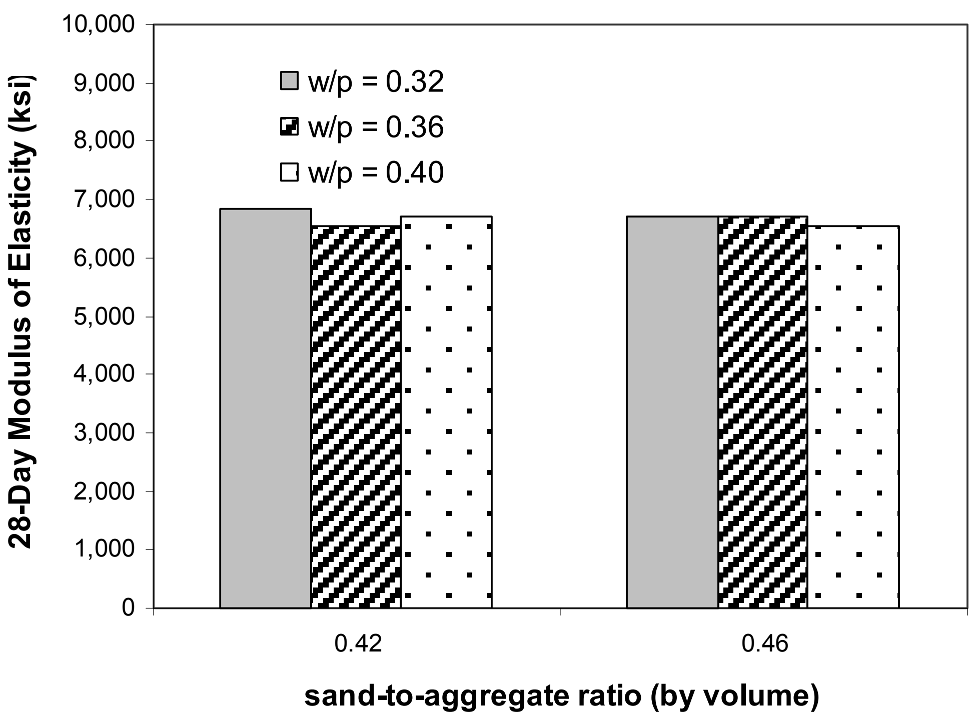

Figure C-12: Effect of *w/p* on the 28-day modulus of elasticity for ternary mixtures {6x12}

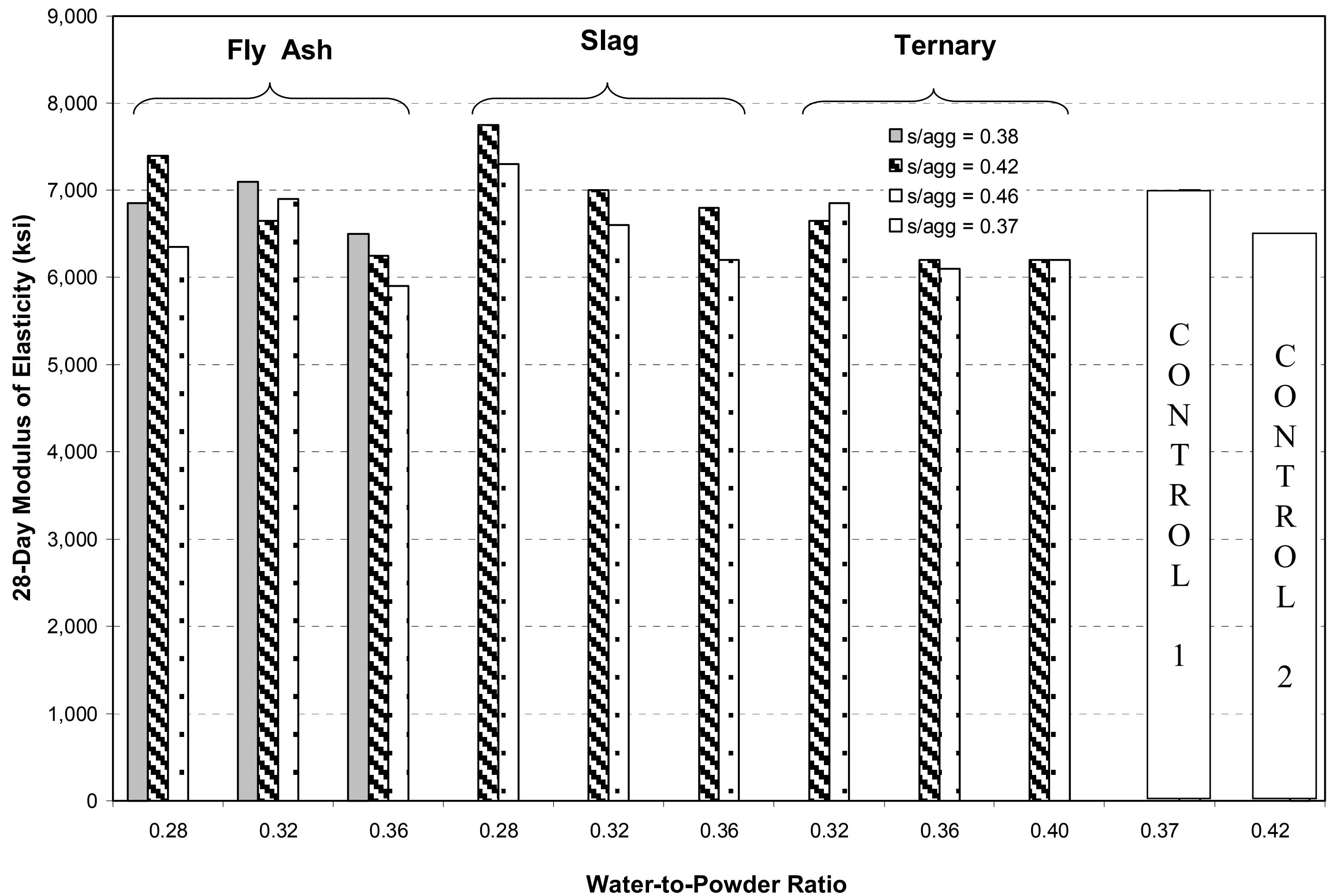

Figure C-13: Effect of different powder combinations on the 28-day modulus of elasticity {4x8}

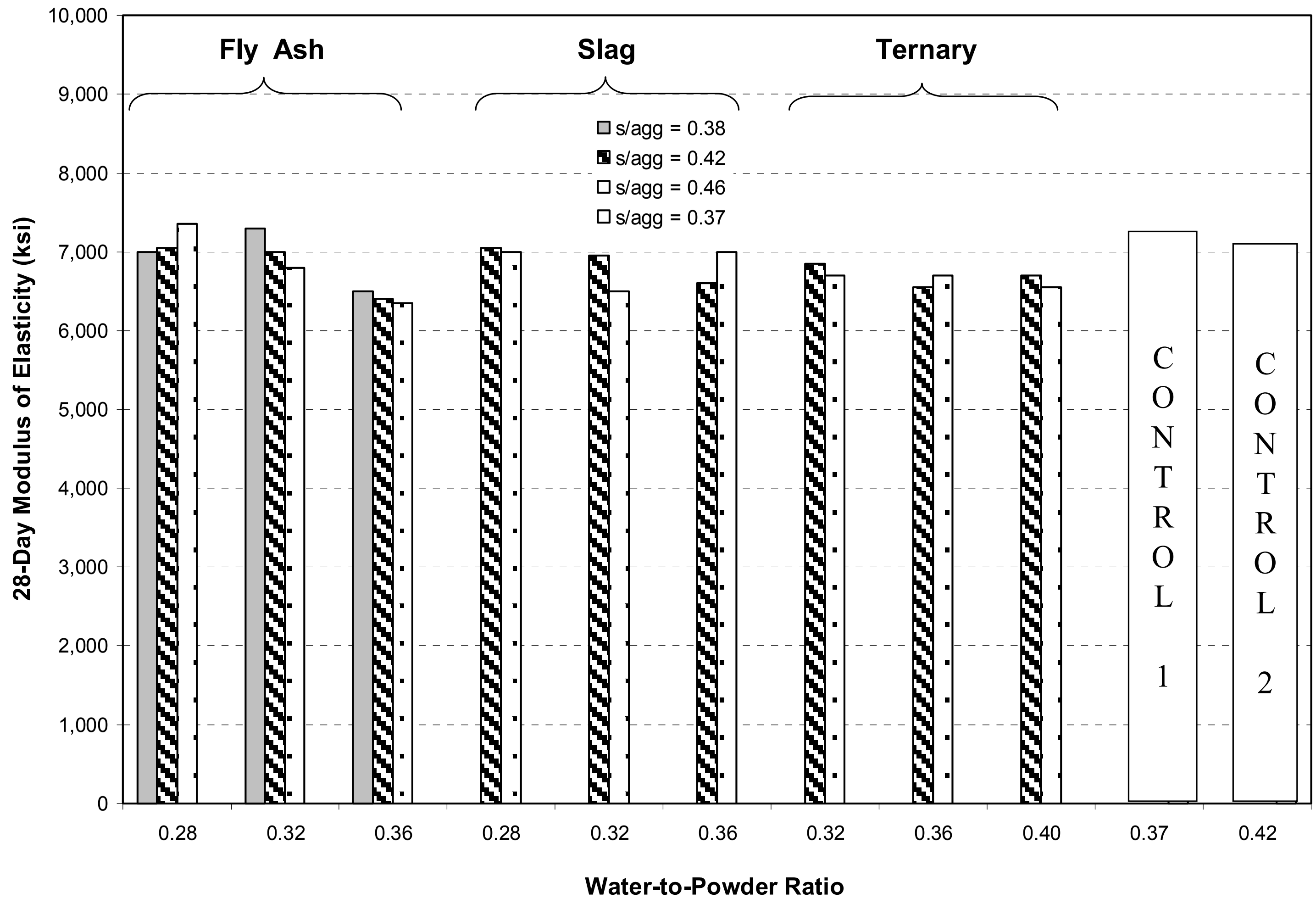

Figure C-14: Effect of different powder combinations on the 28-day modulus of elasticity {6x12}

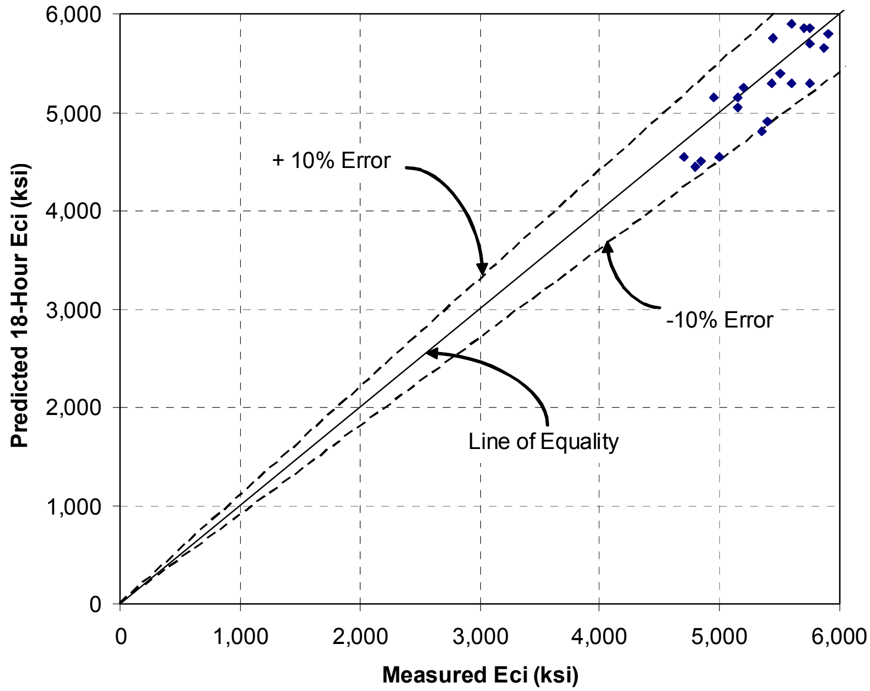

Figure C-15: AASHTO LRFD prediction of the 18-hour modulus of elasticity {4x8}

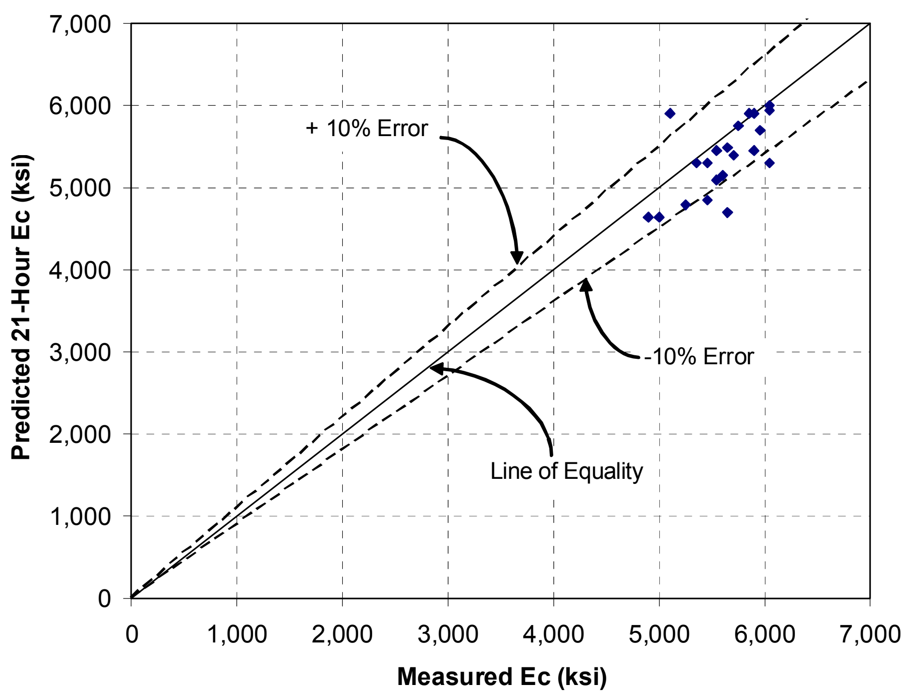

Figure C-16: AASHTO LRFD prediction of the 21-hour modulus of elasticity {4x8}

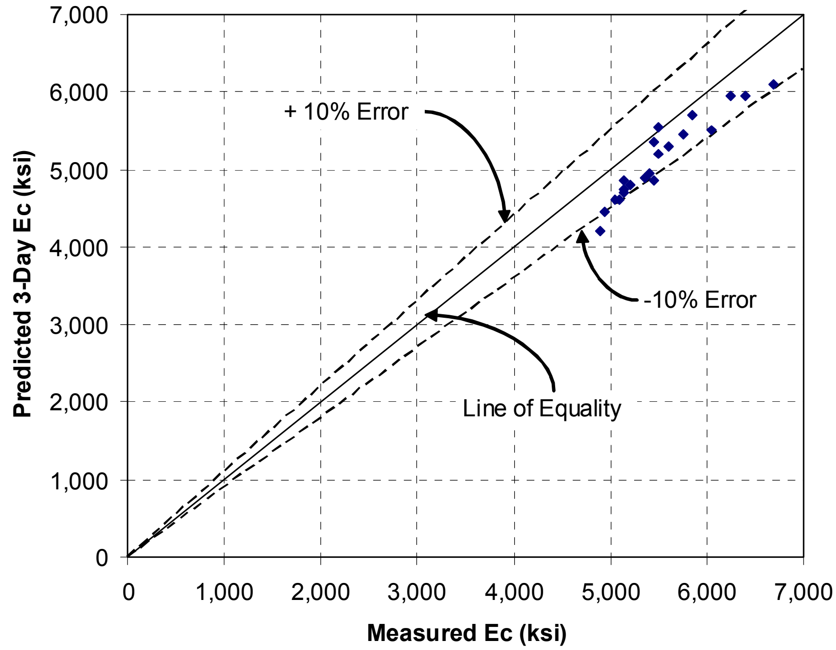

Figure C-17: AASHTO LRFD prediction of the 3-day modulus of elasticity {6x12}

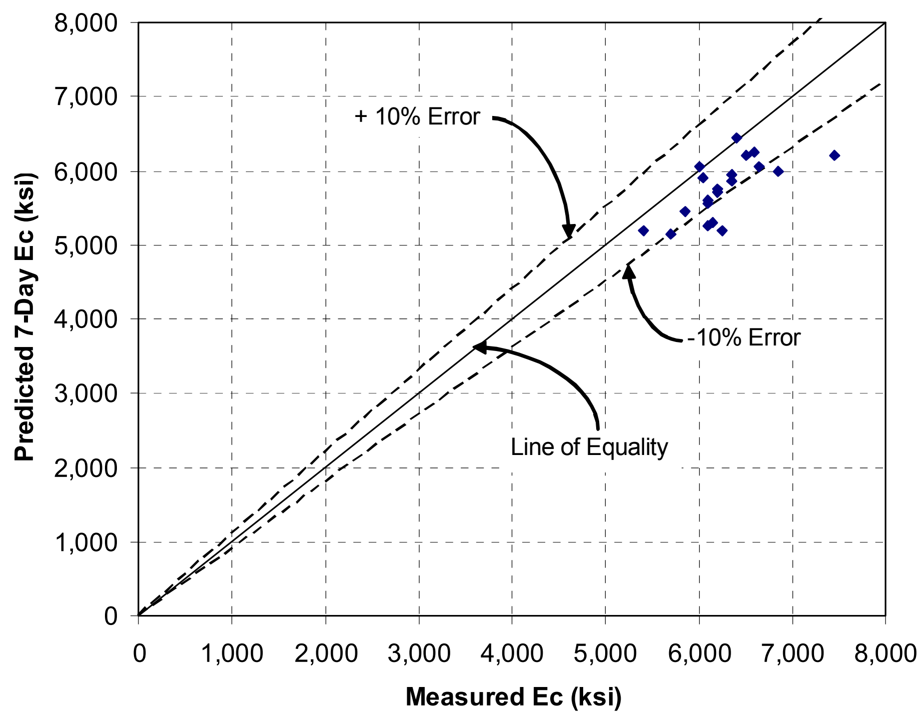

Figure C-18: AASHTO LRFD prediction of the 7-day modulus of elasticity {4x8}

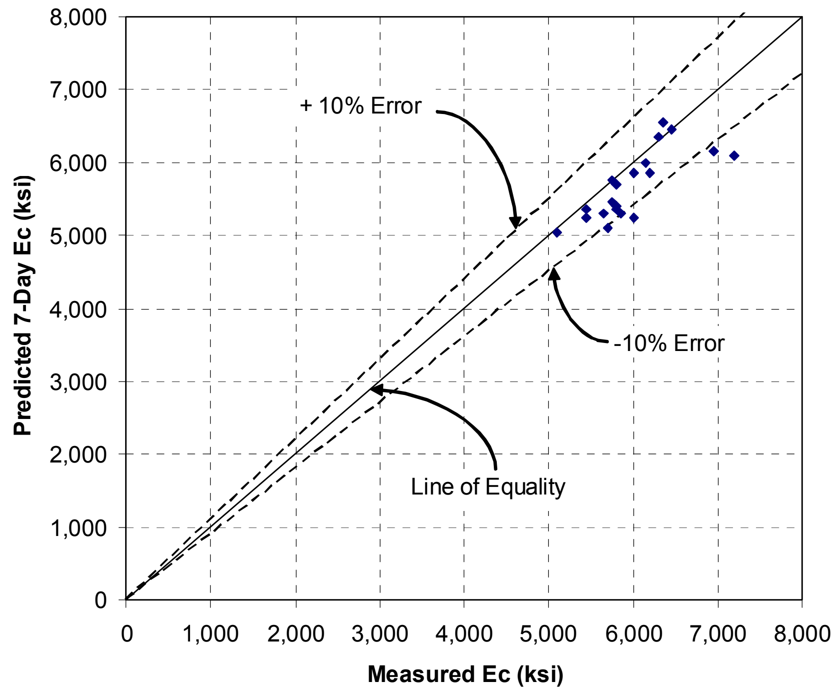

Figure C-19: AASHTO LRFD prediction of the 7-day modulus of elasticity {6x12}

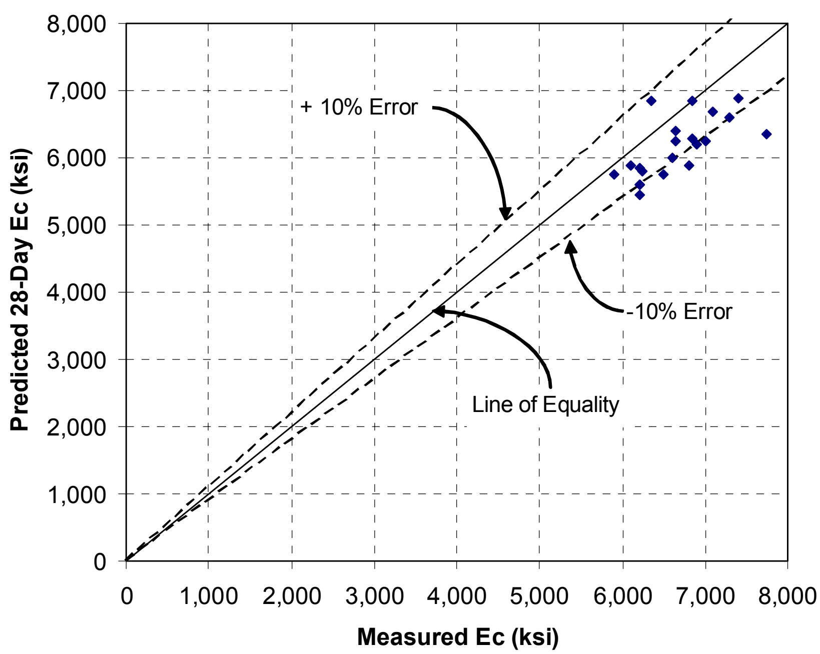

Figure C-20: AASHTO LRFD prediction of the 28-day modulus of elasticity {4x8}

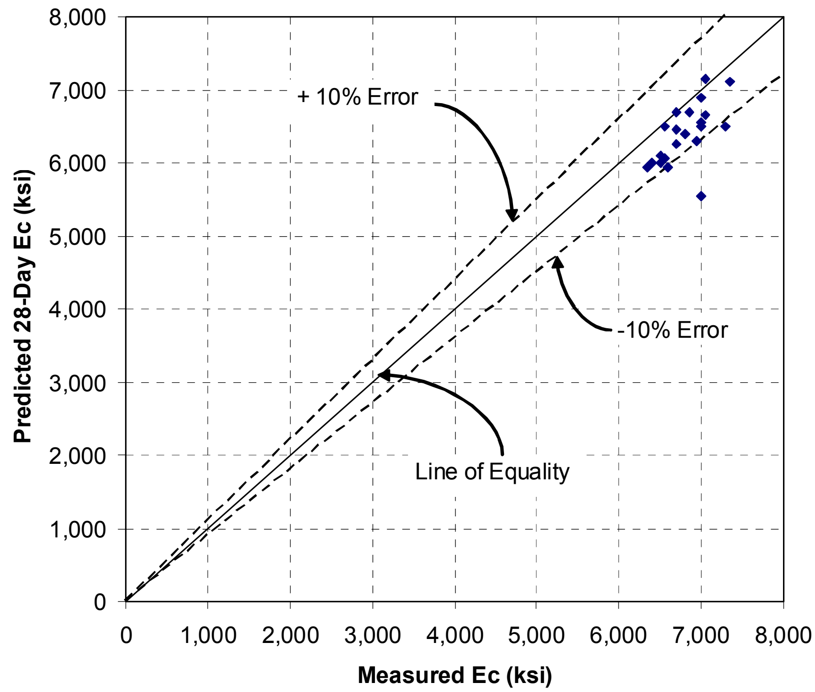

Figure C-21: AASHTO LRFD prediction of the 28-day modulus of elasticity {6x12}

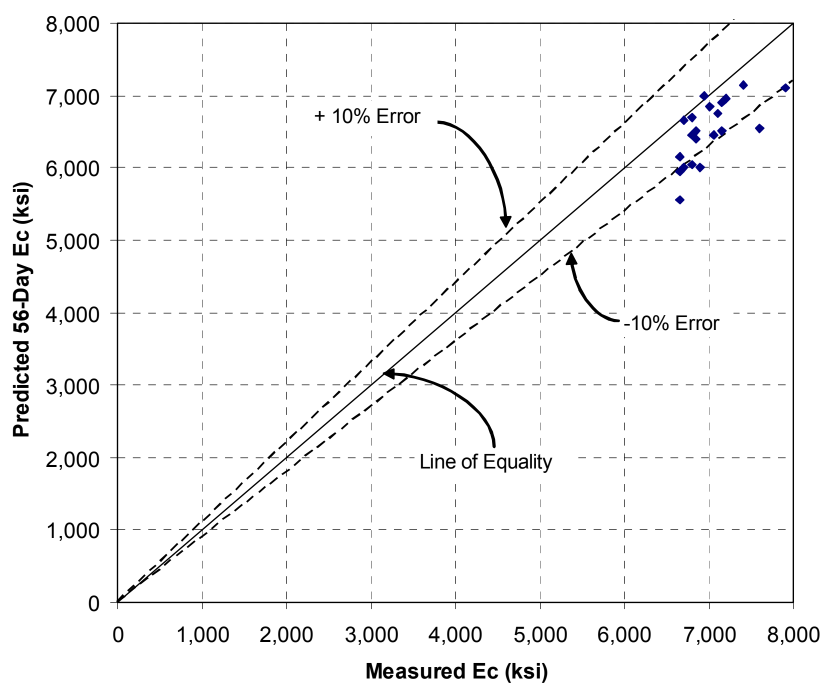

Figure C-22: AASHTO LRFD prediction of the 56-day modulus of elasticity {6x12}

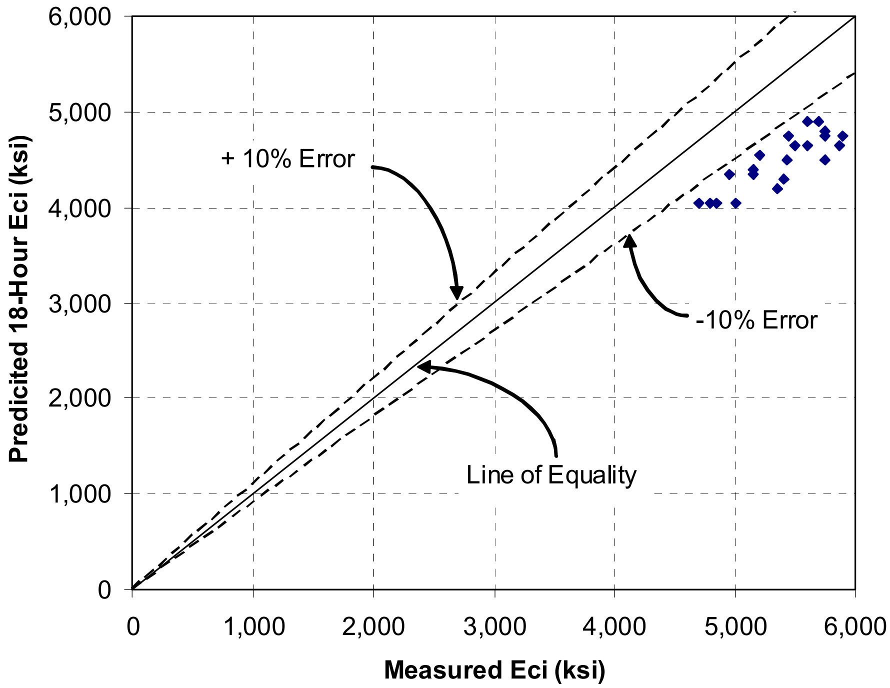

Figure C-23: ACI 363 prediction of the 18-hour modulus of elasticity {4x8}

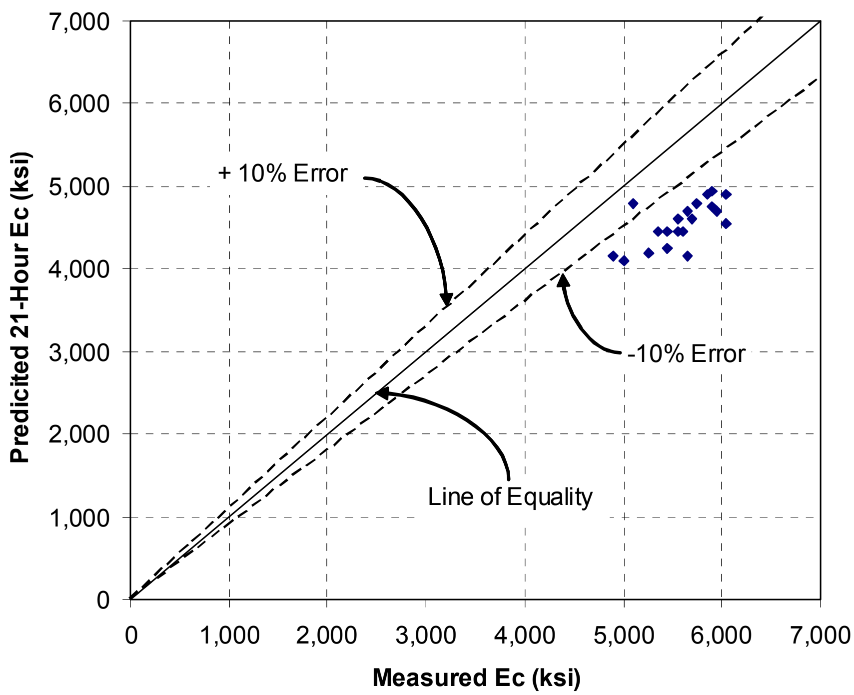

Figure C-24: ACI 363 prediction of the 21-hour modulus of elasticity {4x8}

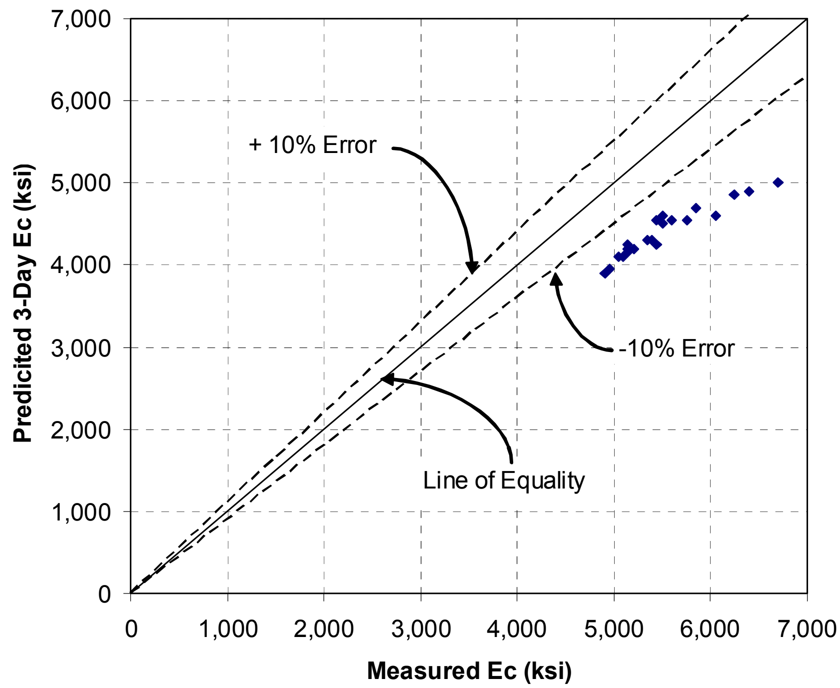

Figure C-25: ACI 363 prediction of the 3-day modulus of elasticity {6x12}

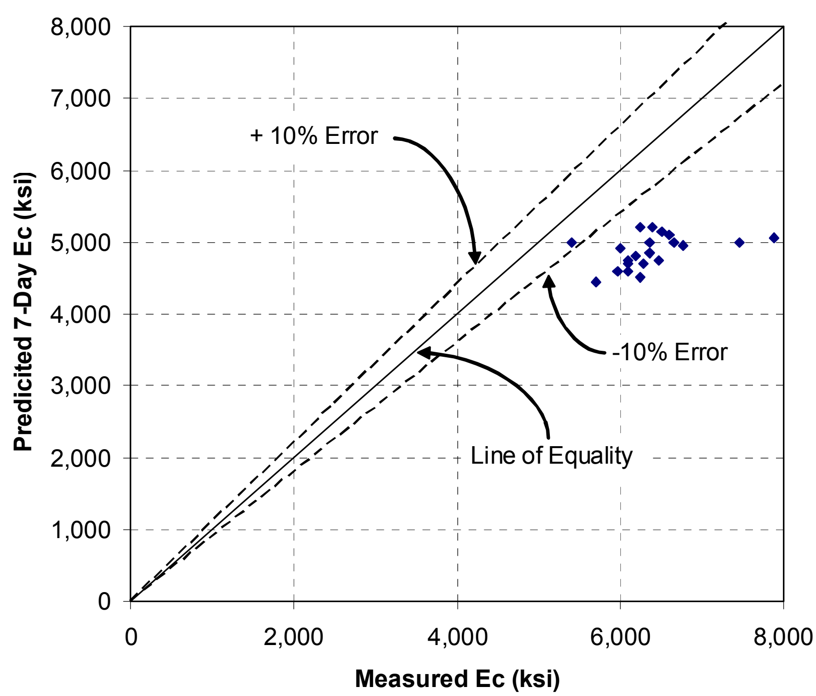

Figure C-26: ACI 363 prediction of the 7-day modulus of elasticity {4x8}

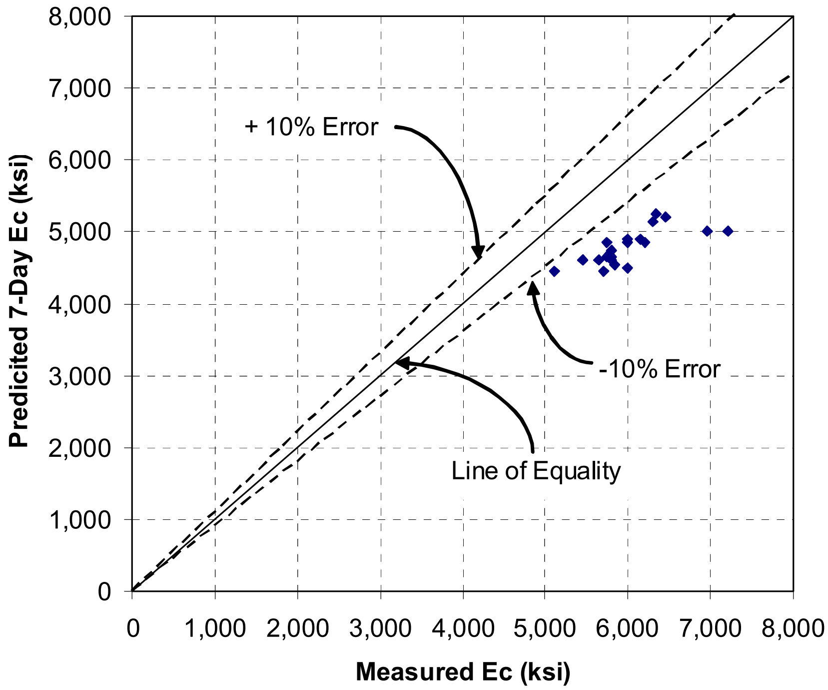

Figure C-27: ACI 363 prediction of the 7-day modulus of elasticity {6x12}

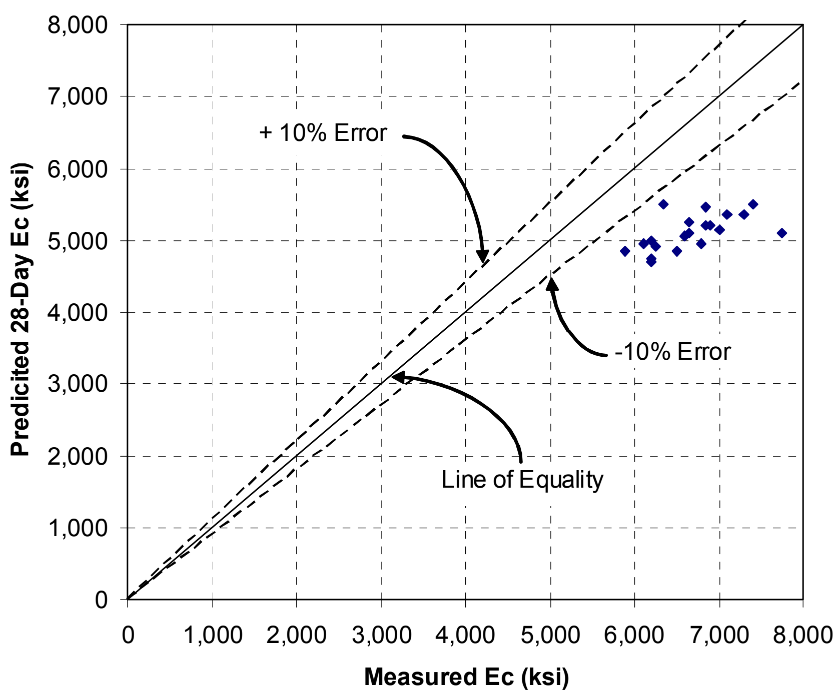

Figure C-28: ACI 363 prediction of the 28-day modulus of elasticity {4x8}

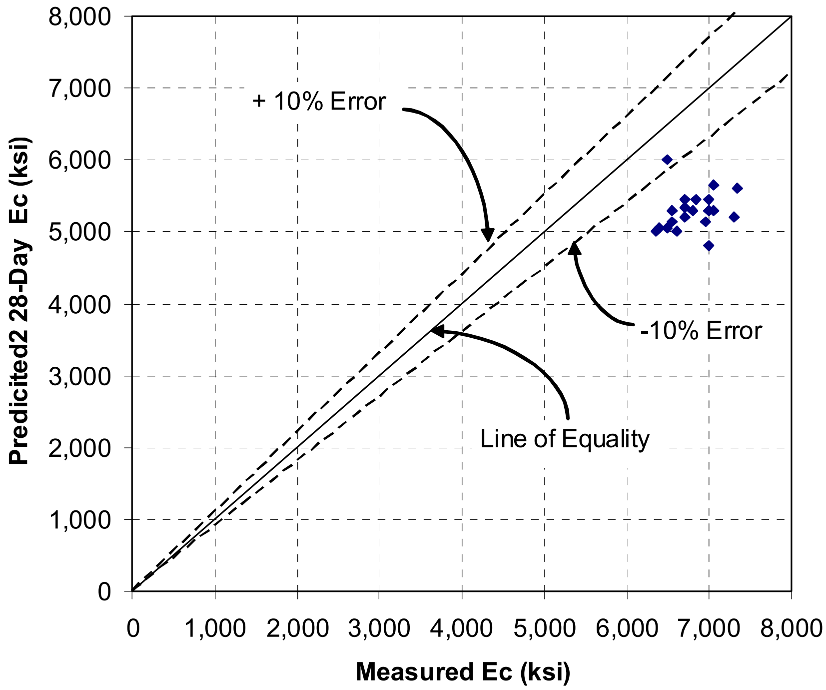

Figure C-29: ACI 363 prediction of the 28-day modulus of elasticity {6x12}

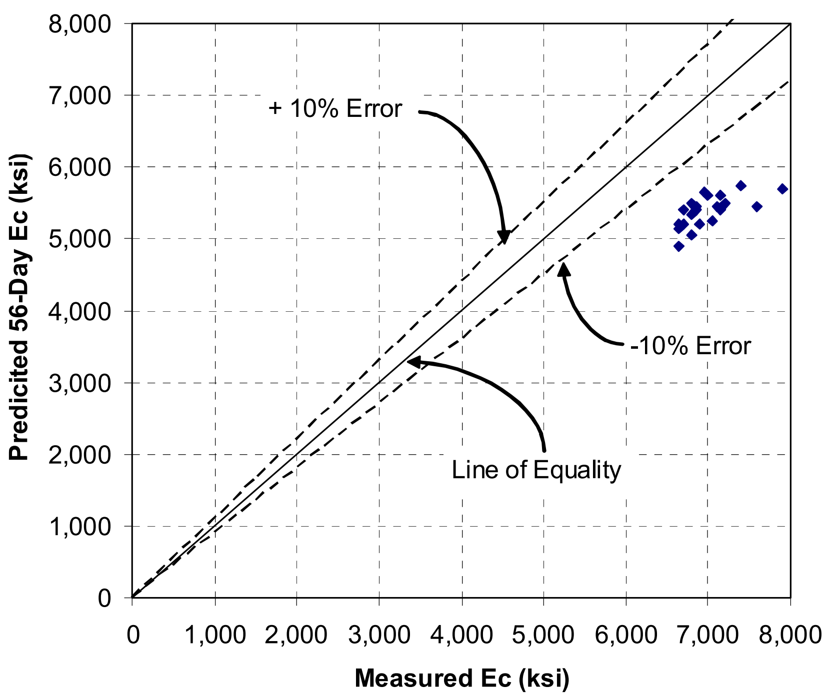

Figure C-30: ACI 363 prediction of the 56-day modulus of elasticity {6x12}

APPENDIX D

SUMMARY OF DRYING SHRINKAGE STRAIN RESULTS

Appendix D contains a summary of the drying shrinkage strain results. The analyses of these figures were discussed in Chapter 4. The curing period for each figure is outlined in Sections D.1 and D.2. Appendix D contains the effects of the *s/agg*, *w/p*, and powder combinations on the long-term drying shrinkage as well as the shrinkage development over time.

D.1 7-DAY MOIST-CURED PRISMS

The following figures are for specimens that were moist-cured in lime-saturated water for 7 days:

- Table D-1
- Figures D-11 through D-19
- Figures D-29 through D-31

In the description of each of these figures, {7} is a reminder to the reader of the curing duration unless stated otherwise.

D.2 28-DAY MOIST-CURED PRISMS

The following figures are for specimens that were moist-cured in lime-saturated water for 28 days:

- Table D-2

- Figures D-1 through D-10
- Figures D-20 through D-28
- Figures D-32 through D-34

In the description of each of these figures, {28} is a reminder to the reader of the curing duration unless stated otherwise.

Table D-1: Summary of drying shrinkage for all mixtures {7}. Results not available for ternary SCC mixtures.

MIXTURE ID	Drying Shrinkage Strain (in./in. x 10^{-6})				
	Duration of Drying				
	7 Days	**14 Days**	**28 Days**	**16 Weeks**	**32 Weeks**
CTRL1: 0.37	-190	-280	-330	-477	-522
CTRL2: 0.42	-227	-303	-353	-520	-613
SCC1:0.28-0.38-FA	-240	-300	-307	-400	-465
SCC2:0.32-0.38-FA	-197	-267	-297	-382	-443
SCC3:0.36-0.38-FA	-197	-293*	-293	-440	-520
SCC4:0.28-0.42-FA	-230	-277	-293	-402	-472
SCC5:0.32-0.42-FA	-220	-273	-343	-432	-497
SCC6:0.36-0.42-FA	-237	-277	-422	-475	-443
SCC7:0.28-0.46-FA	-223	-283	-293	-400	-487
SCC8:0.32-0.46-FA	-260	-293	-357	-482	-545
SCC9:0.36-0.46-FA	-320	-330	-410	-447	-538
SCC10:0.28-0.42-S	-218	-260	-330	-423	-473
SCC11:0.32-0.42-S	-190	-247	-290	-510	-485
SCC12:0.36-0.42-S	-217	-267	-327	-415	-535
SCC13:0.28-0.46-S	-213	-250	-290	-420	-497
SCC14:0.32-0.46-S	-220	-272	-347	-500	-530
SCC15:0.36-0.46-S	-197	-240	-280	-457	-530
SCC16:0.32-0.42-Ternary	-308	-340	-372	-418	
SCC17:0.36-0.42-Ternary	-280	-330	-410	-445	
SCC18:0.40-0.42-Ternary	-348	-360	-398	-415	
SCC19:0.32-0.46-Ternary	-327	-370	-377	-460	
SCC20:0.36-0.46-Ternary	-335	-380	-437	-480	
SCC21:0.40-0.46-Ternary	-250	-327	-373	-373	

Table D-2: Summary of drying shrinkage for all mixtures {28}. Results not available for ternary SCC mixtures.

MIXTURE ID	Drying Shrinkage Strain (in./in. x 10^{-6})				
	Duration of Drying				
	7 Days	**14 Days**	**28 Days**	**16 Weeks**	**32 Weeks**
CTRL1: 0.37	-160	-220	-260	-400	-483
CTRL2: 0.42	-167	-247	-300	-447	-518
SCC1:0.28-0.38-FA	-190	-170	-183	-287	-370
SCC2:0.32-0.38-FA	-153	-203	-237	-373	-427
SCC3:0.36-0.38-FA	-180	-247	-277	-413	-497
SCC4:0.28-0.42-FA	-190	-213	-273	-348	-403
SCC5:0.32-0.42-FA	-157	-200	-263	-337	-455
SCC6:0.36-0.42-FA	-205	-255	-270	-380	-365
SCC7:0.28-0.46-FA	-120	-170	-220	-312	-363
SCC8:0.32-0.46-FA	-147	-190	-233	-382	-447
SCC9:0.36-0.46-FA	-233	-273	-290	-405	-490
SCC10:0.28-0.42-S	-128	-160	-198	-315	-345
SCC11:0.32-0.42-S	-147	-212	-258	-358	-427
SCC12:0.36-0.42-S	-143	-173	-242	-420	-478
SCC13:0.28-0.46-S	-103	-130	-197	-298	-330
SCC14:0.32-0.46-S	-157	-198	-250	-413	-380
SCC15:0.36-0.46-S	-103	-172	-233	-438	-468
SCC16:0.32-0.42-Ternary	-160	-187	-282	-292	
SCC17:0.36-0.42-Ternary	-142	-192	-222	-265	
SCC18:0.40-0.42-Ternary	-143	-207	-260	-288	
SCC19:0.32-0.46-Ternary	-143	-190	-272	-287	
SCC20:0.36-0.46-Ternary	-135	-178	-237	-258	
SCC21:0.40-0.46-Ternary	-110	-168	Bad Reading	-237	

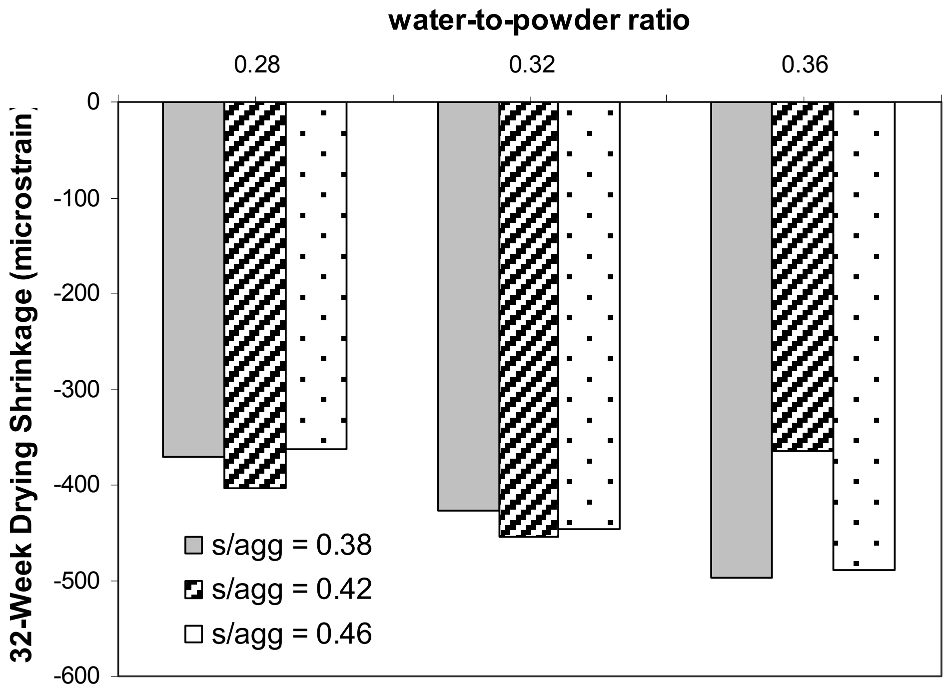

Figure D-1: Effect of *s/agg* on *32*-week drying shrinkage for fly ash mixtures {28}

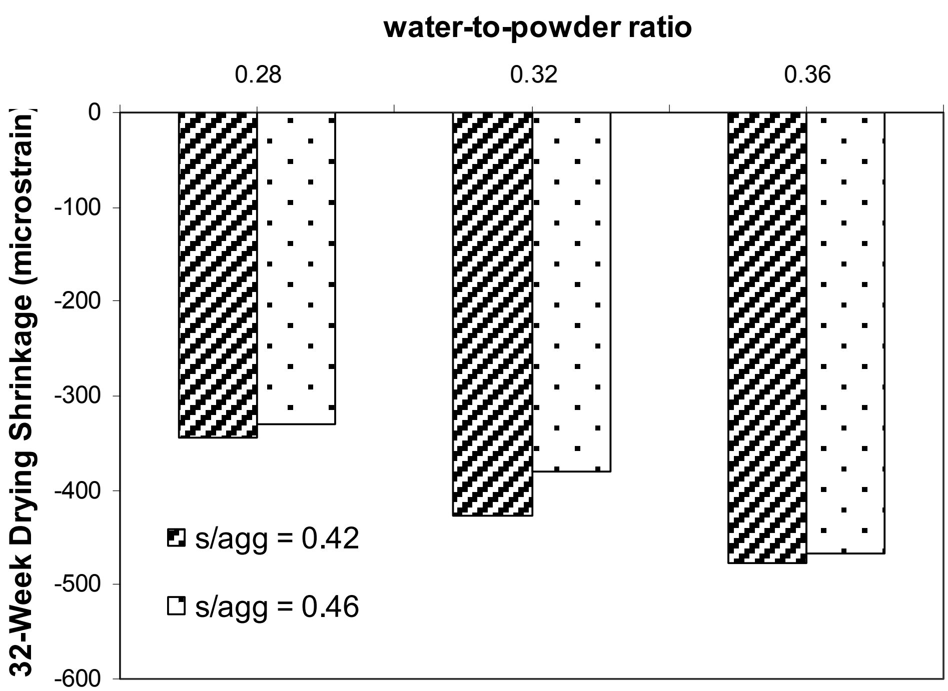

Figure D-2: Effect of *s/agg* on *32*-week drying shrinkage for slag mixtures {28}

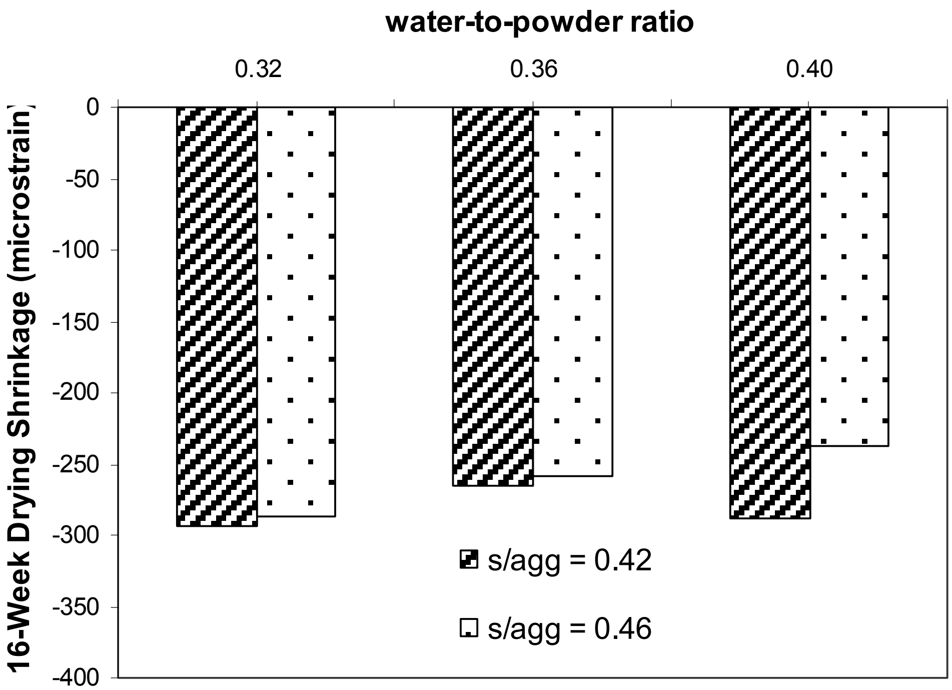

Figure D-3: Effect of *s/agg* on *16*-week drying shrinkage for ternary mixtures {28}

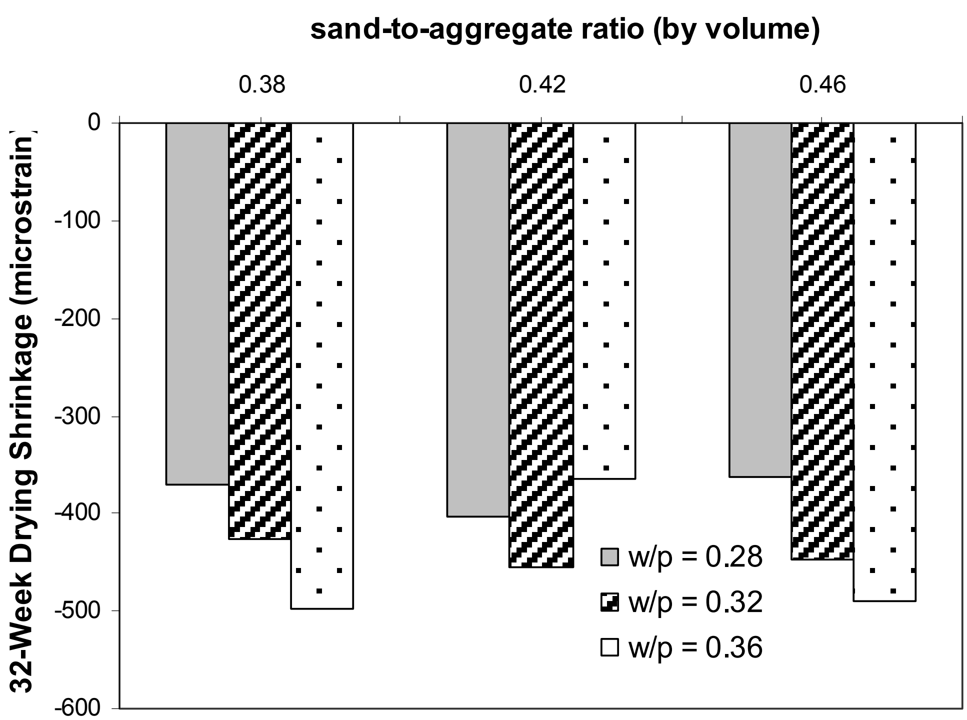

Figure D-4: Effect of *w/p* on *32*-week drying shrinkage for fly ash mixtures {28}

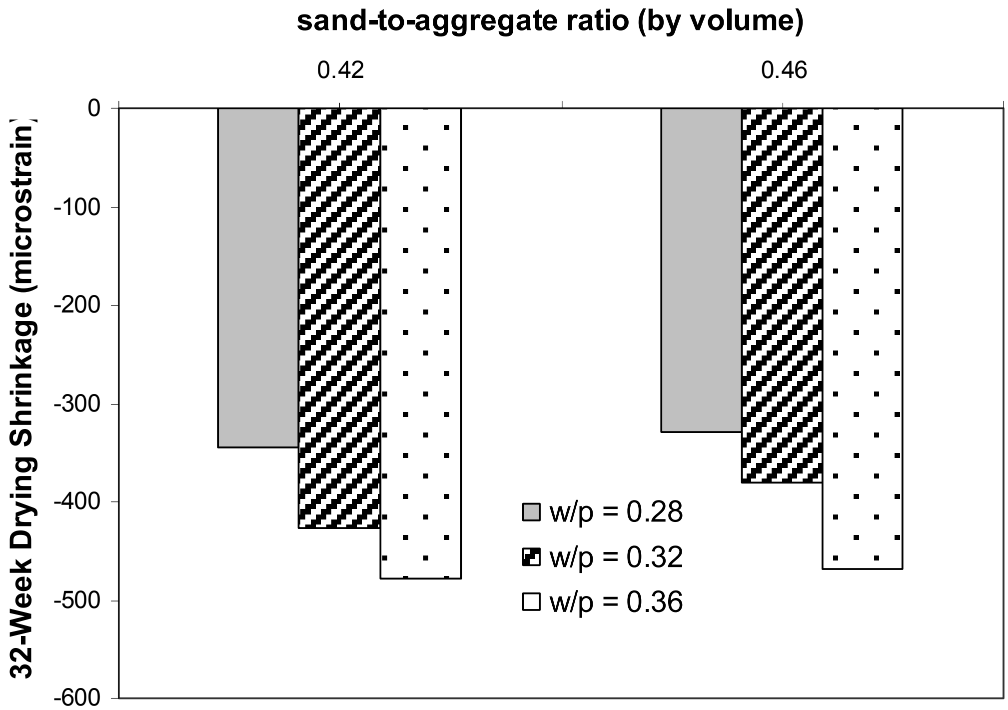

Figure D-5: Effect of *w/p* on *32*-week drying shrinkage for slag mixtures {28}

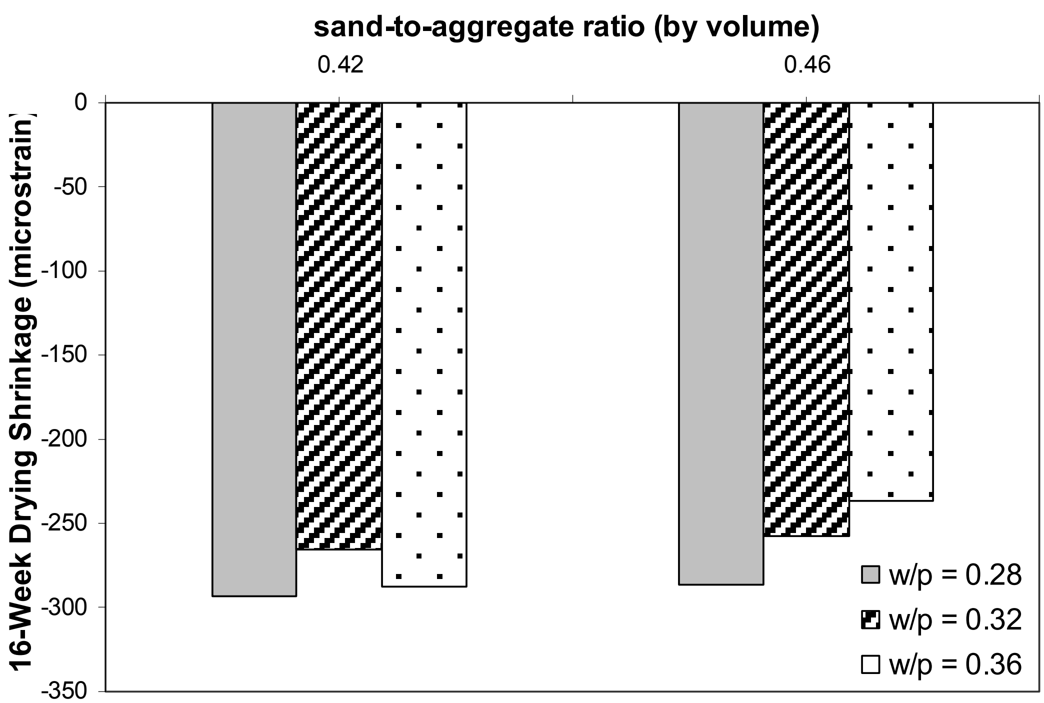

Figure D-6: Effect of *w/p* on *16*-week drying shrinkage for ternary mixtures {28}

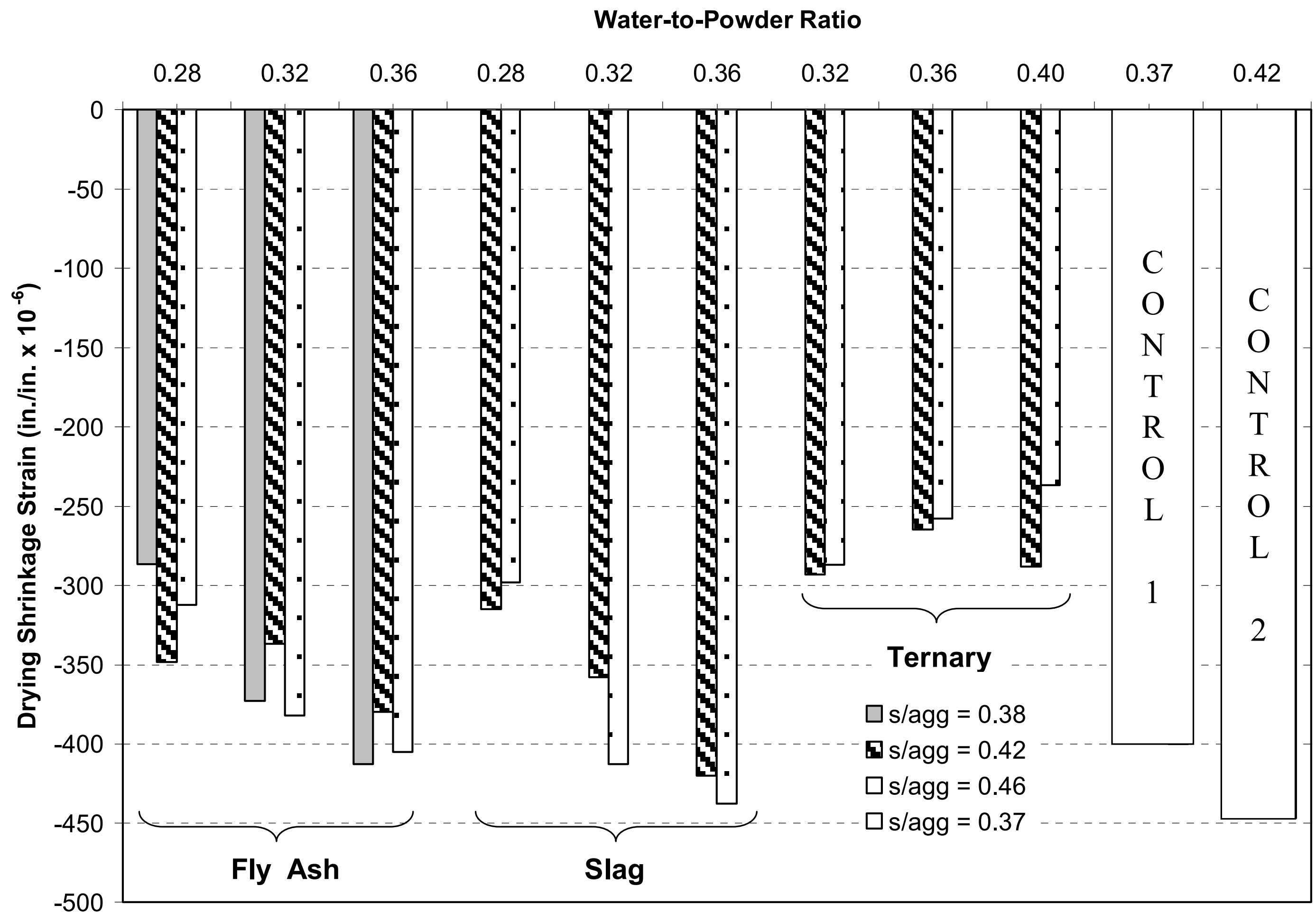

Figure D-7: Effects of different powder combinations on *16*-week drying shrinkage {28}

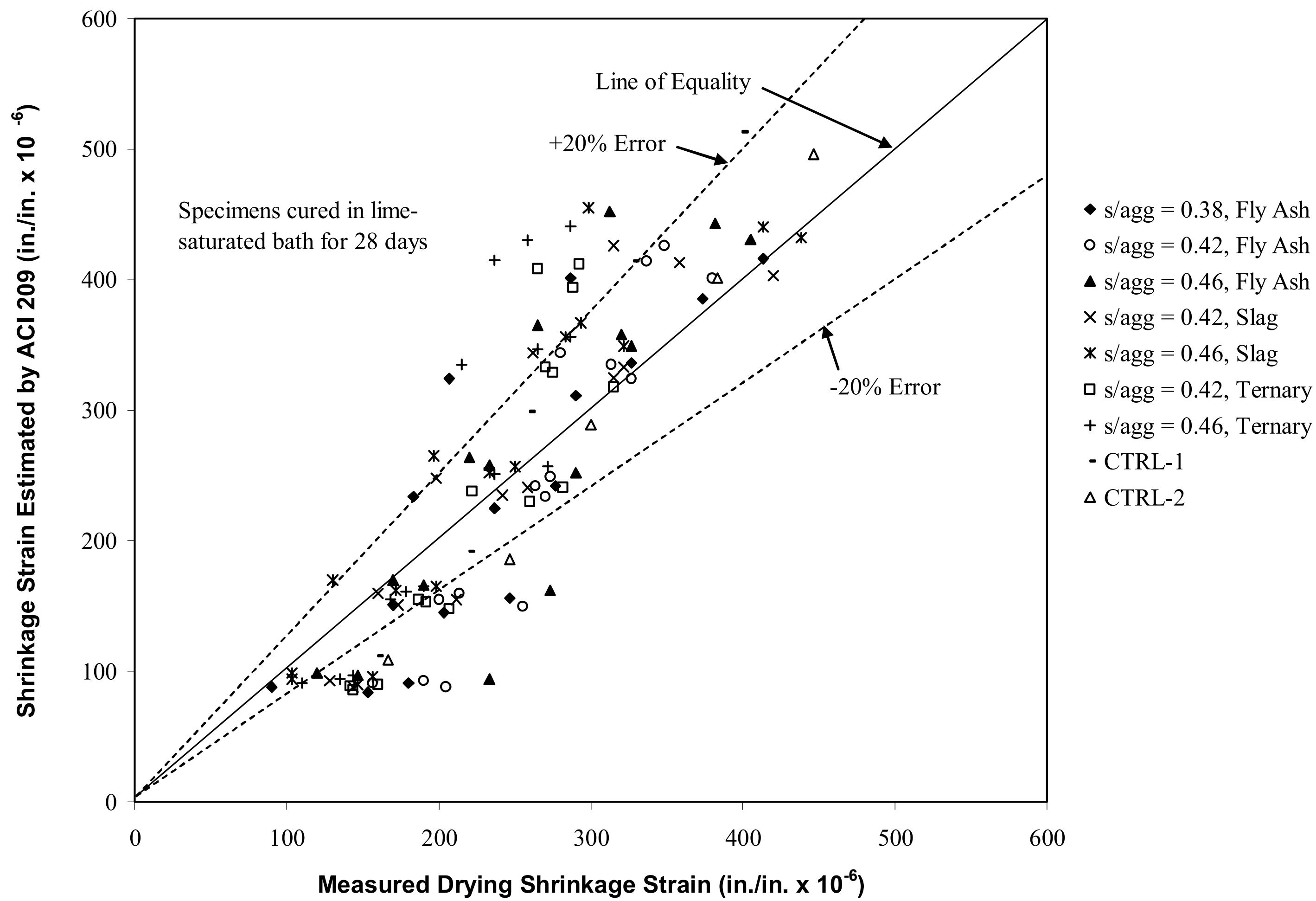

Figure D-8: Measured versus estimated drying shrinkage strain using the ACI 209 procedure

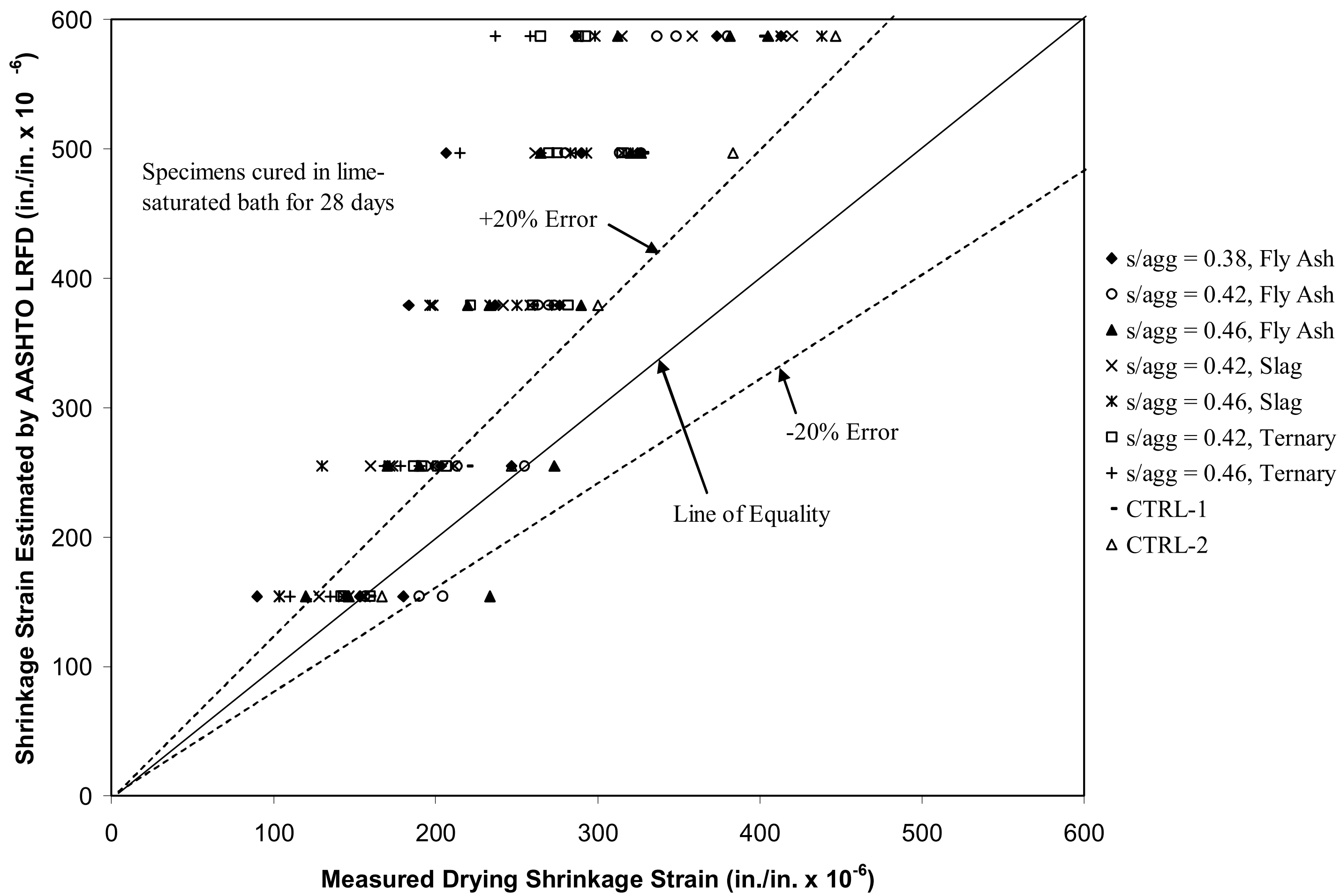

Figure D-9: Measured versus estimated drying shrinkage strain using the AASHTO LRFD procedure

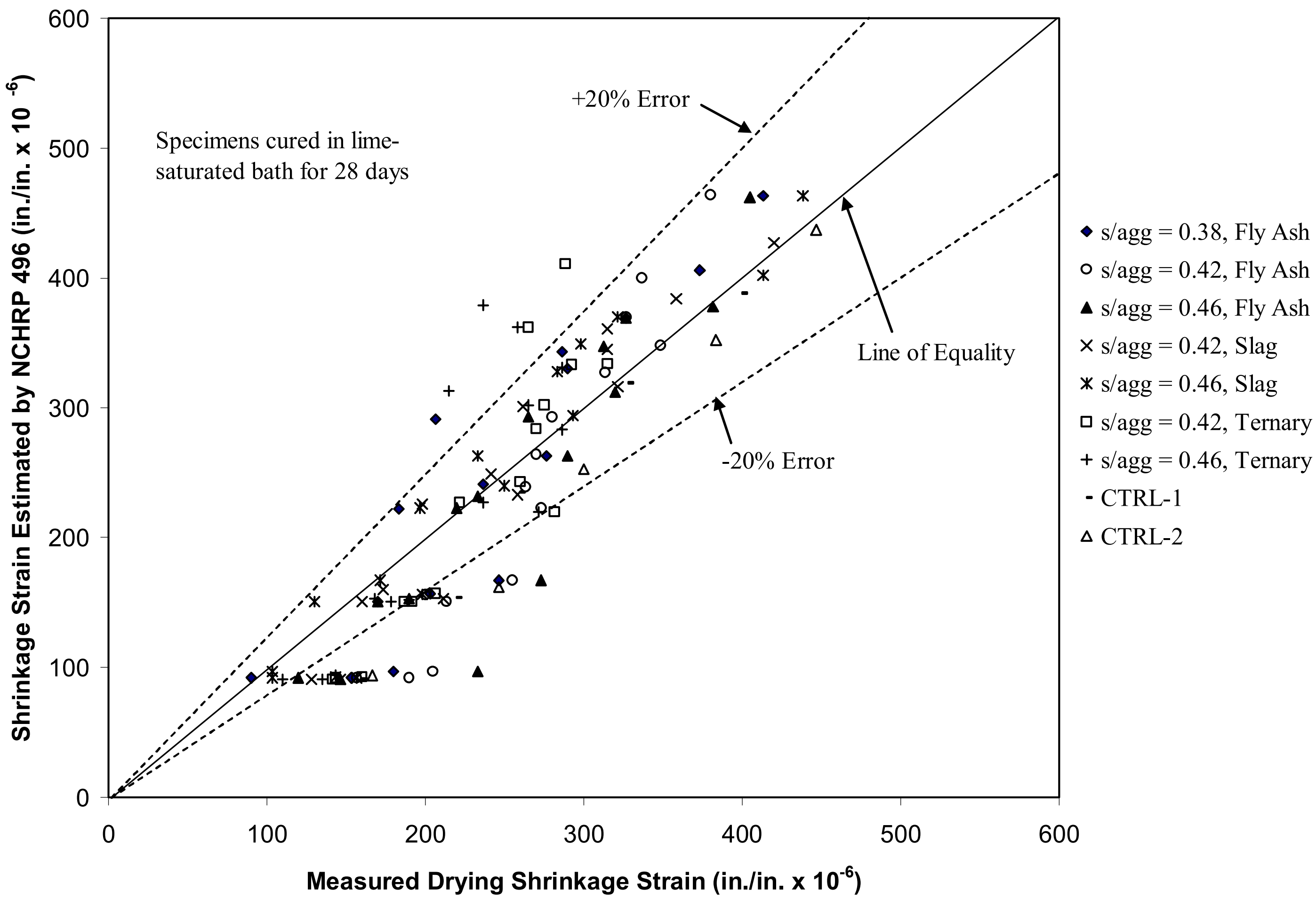

Figure D-10: Measured versus estimated drying shrinkage strain using the NCHRP 496 procedure

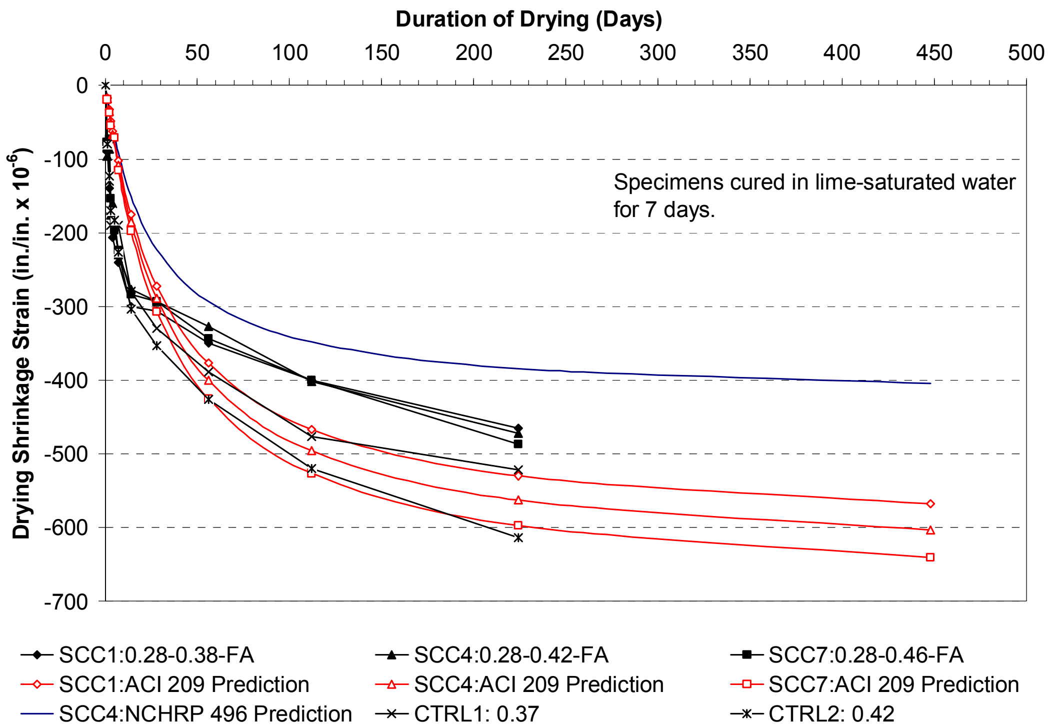

Figure D-11: Shrinkage development of fly ash mixtures with a *w/p* of 0.28

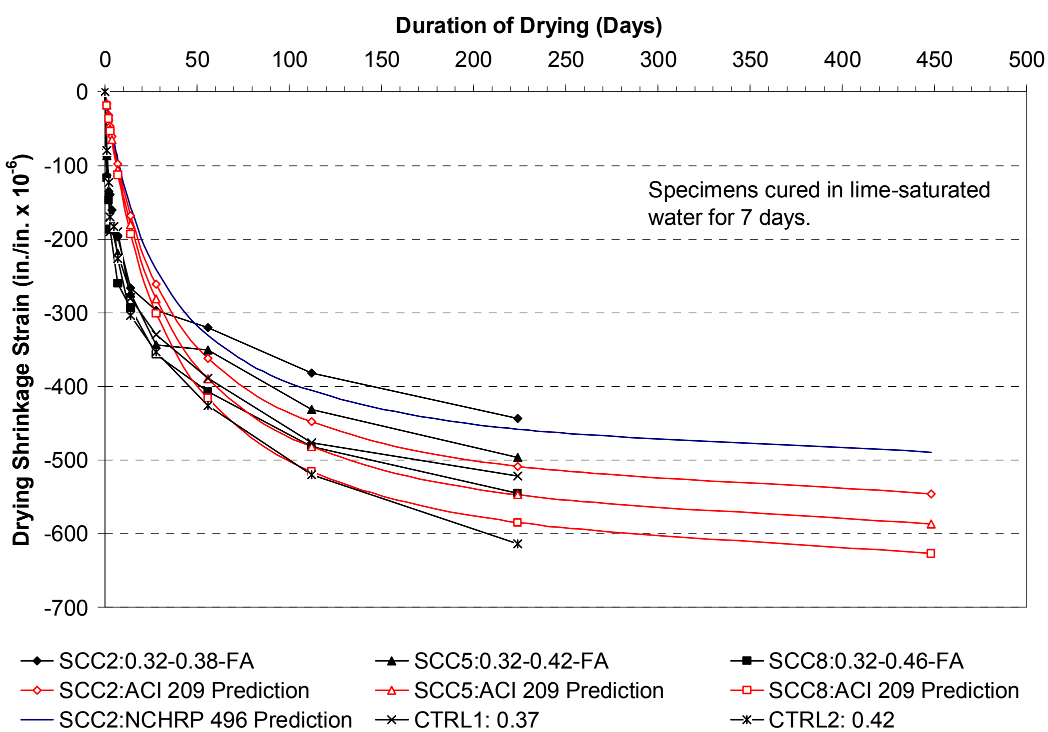

Figure D-12: Shrinkage development of fly ash mixtures with a *w/p* of 0.32

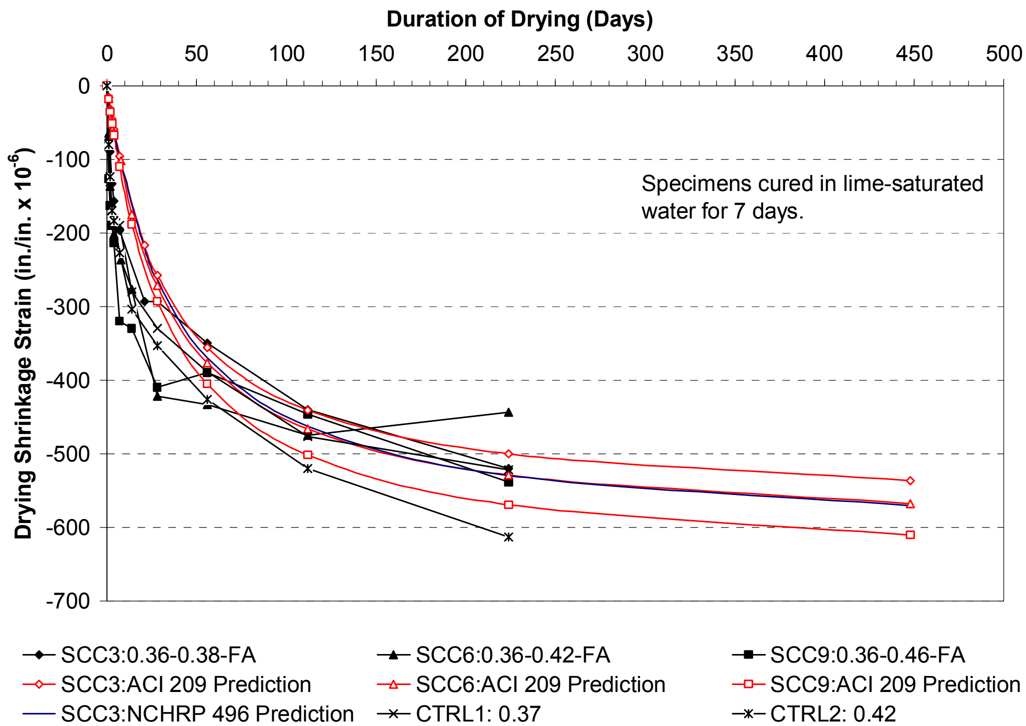

Figure D-13: Shrinkage development of fly ash mixtures with a *w/p* of 0.36

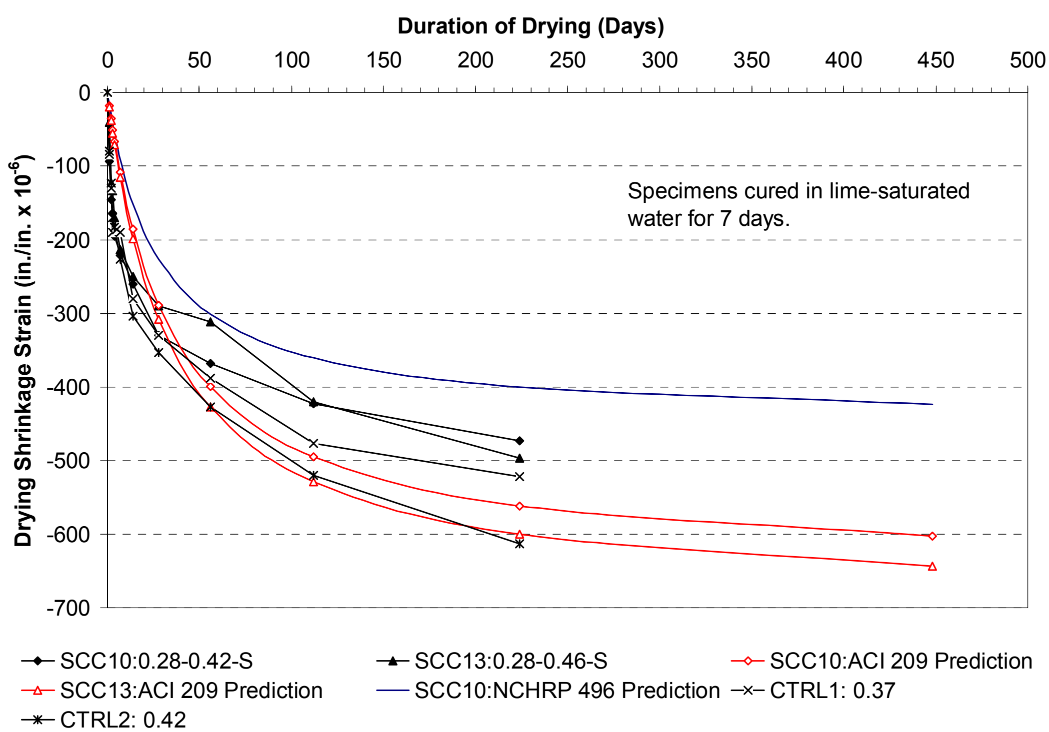

Figure D-14: Shrinkage development of slag mixtures with a *w/p* of 0.28

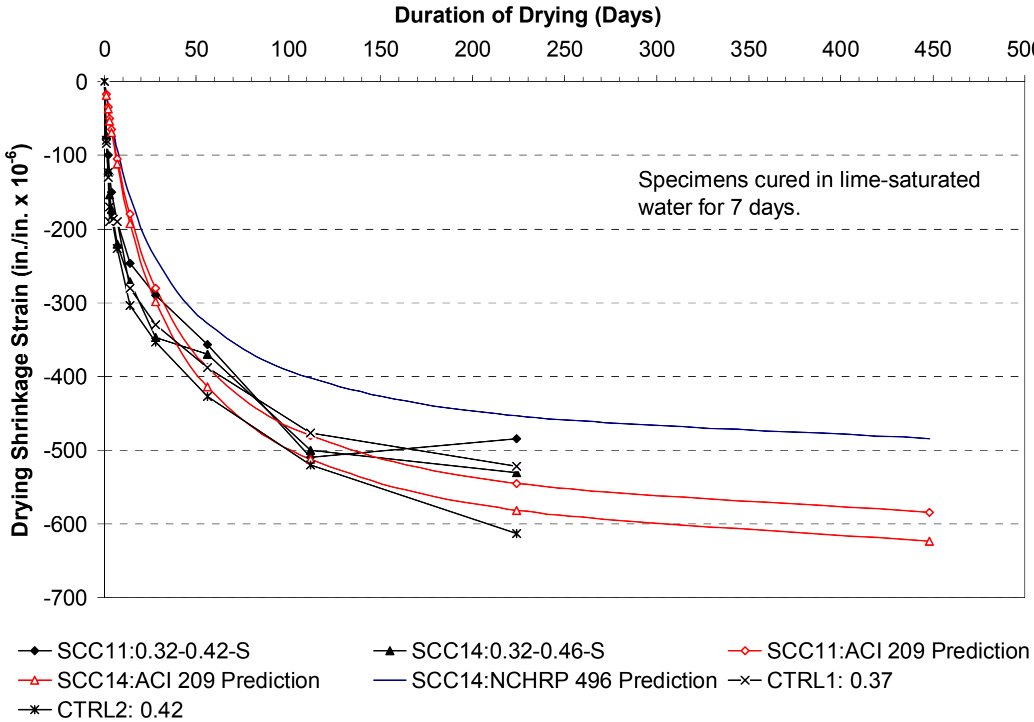

Figure D-15: Shrinkage development of slag mixtures with a *w/p* of 0.32

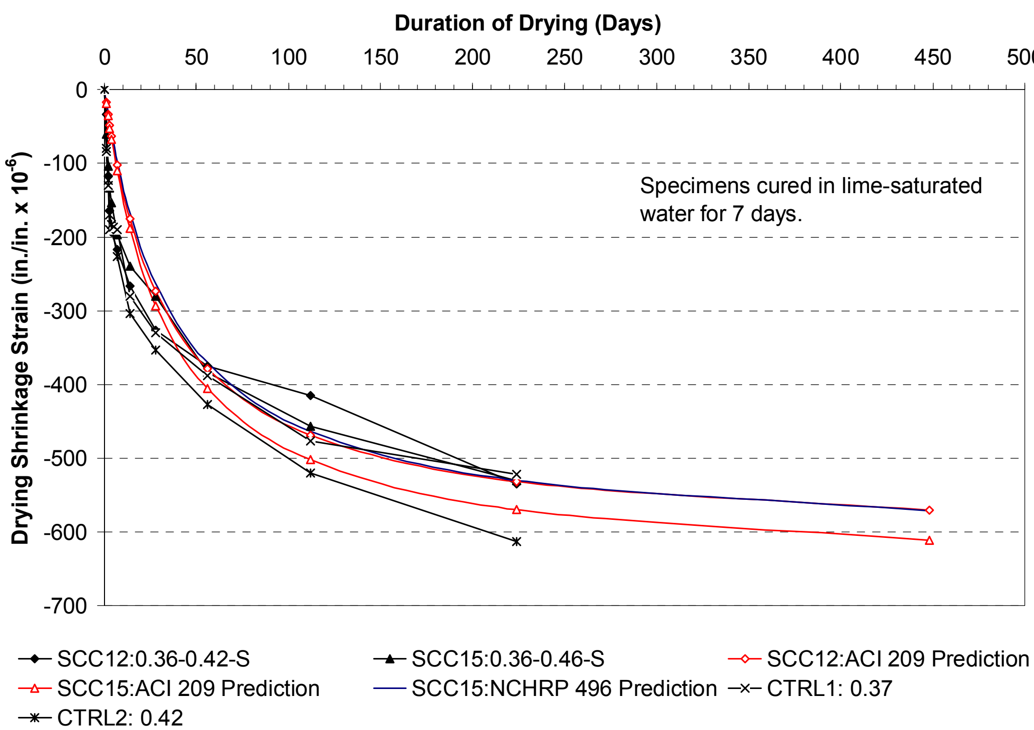

Figure D-16: Shrinkage development of slag mixtures with a *w/p* of 0.36

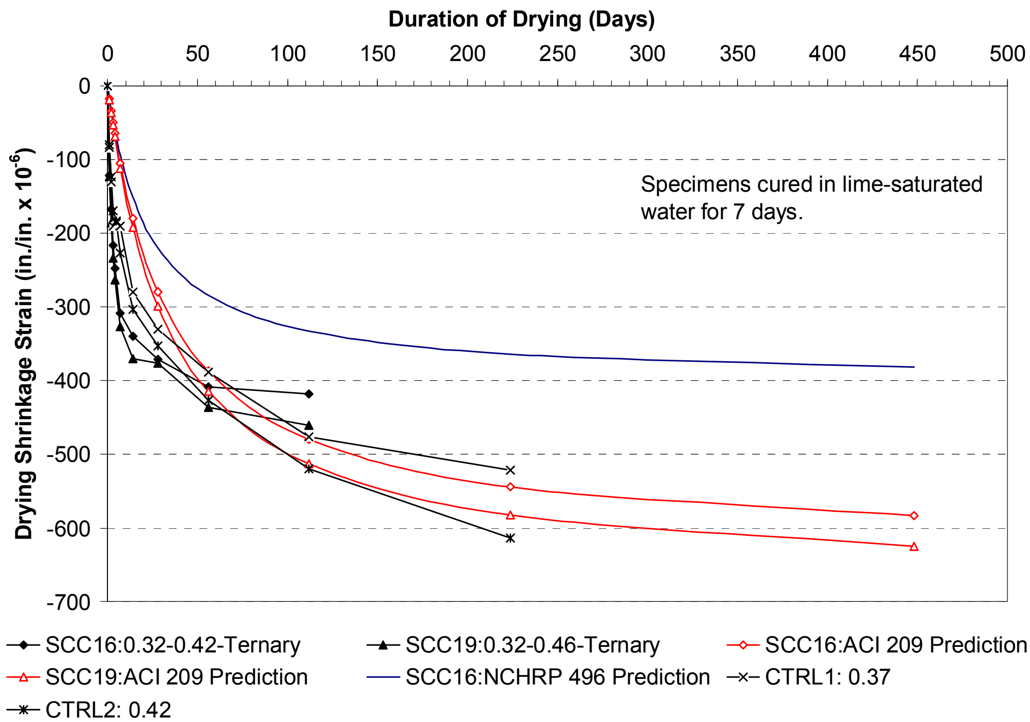

Figure D-17: Shrinkage development of ternary mixtures with a *w/p* of 0.32

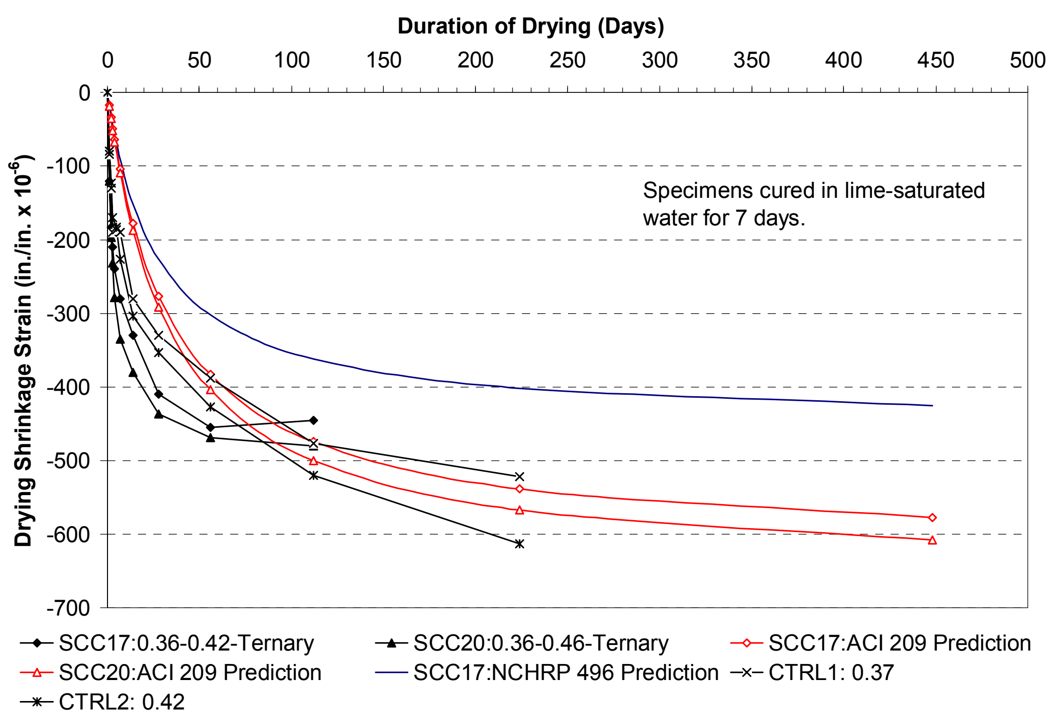

Figure D-18: Shrinkage development of ternary mixtures with a *w/p* of 0.36

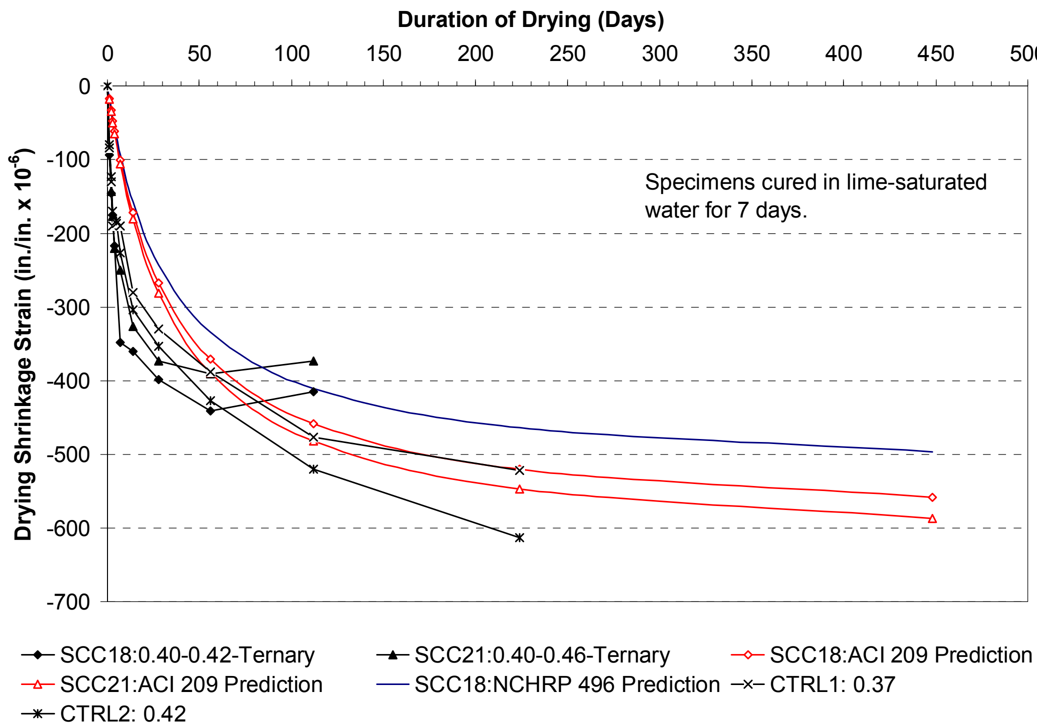

Figure D-19: Shrinkage development of ternary mixtures with a *w/p* of 0.40

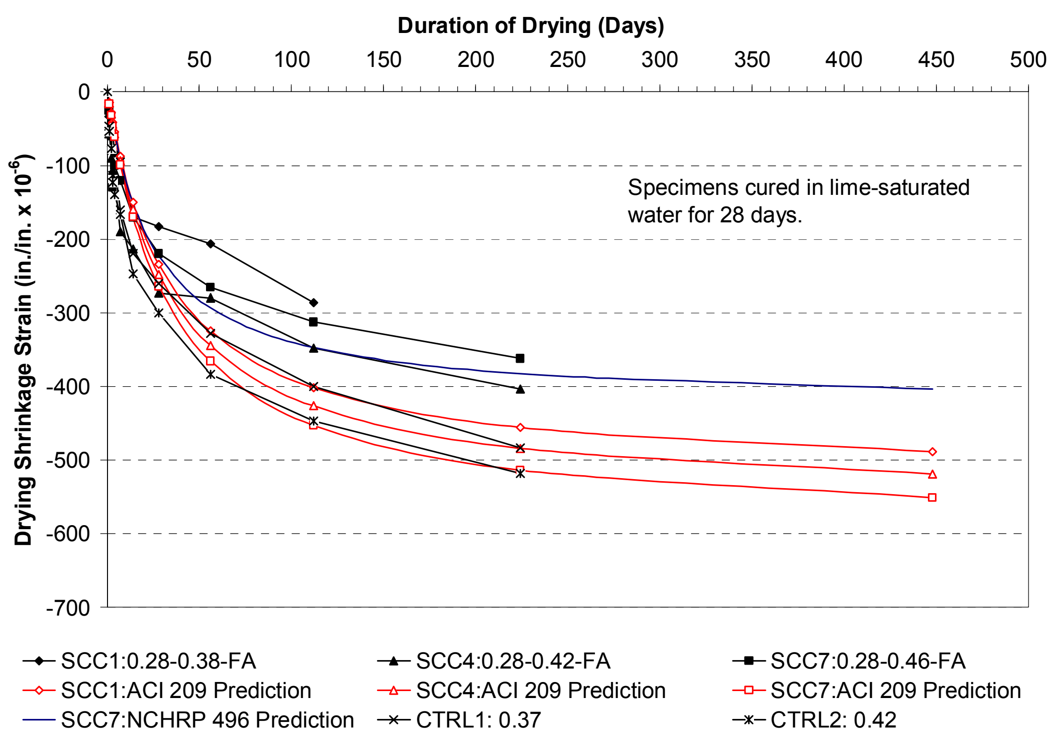

Figure D-20: Shrinkage development of fly ash mixtures with a *w/p* of 0.28

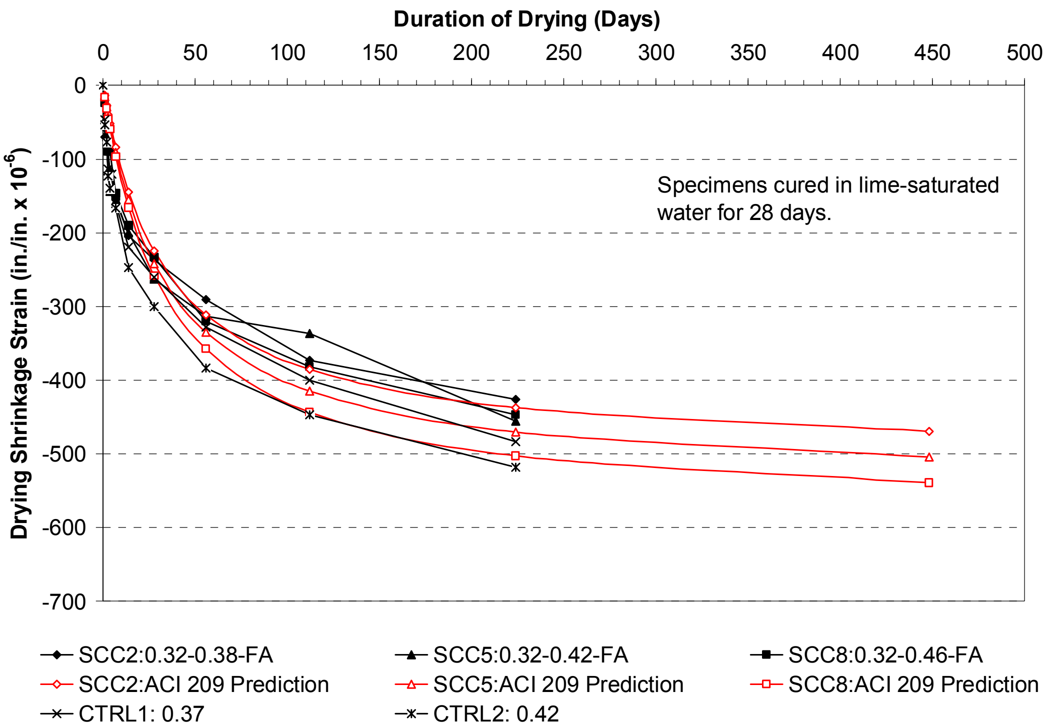

Figure D-21: Shrinkage development of fly ash mixtures with a *w/p* of 0.32

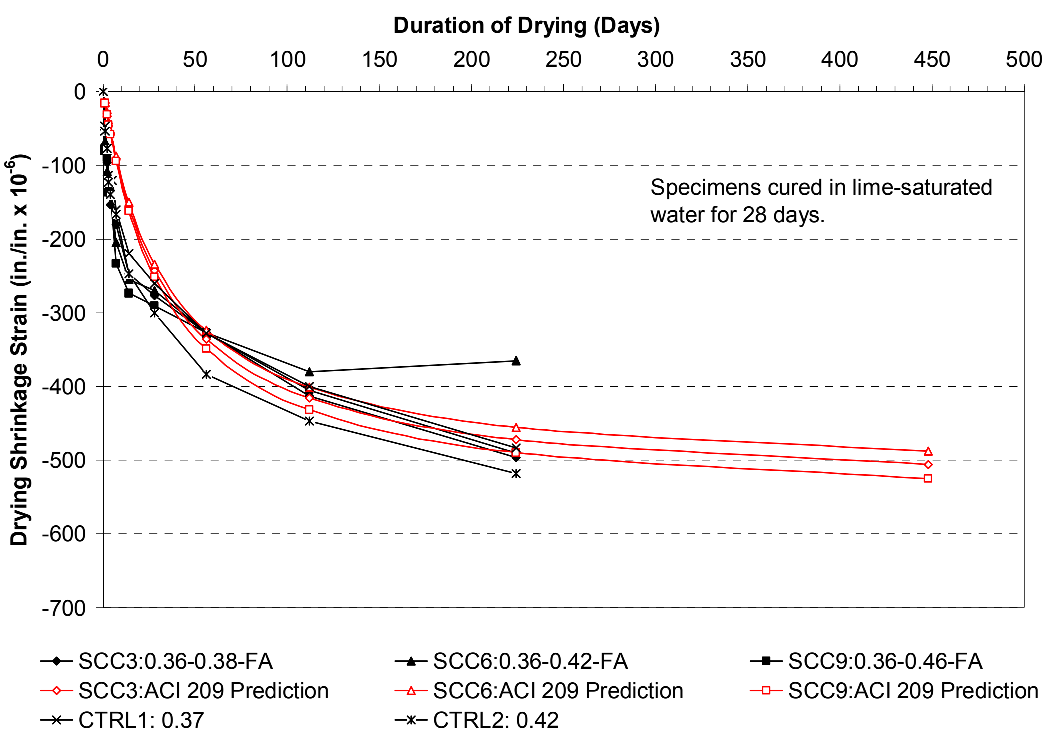

Figure D-22: Shrinkage development of fly ash mixtures with a *w/p* of 0.36

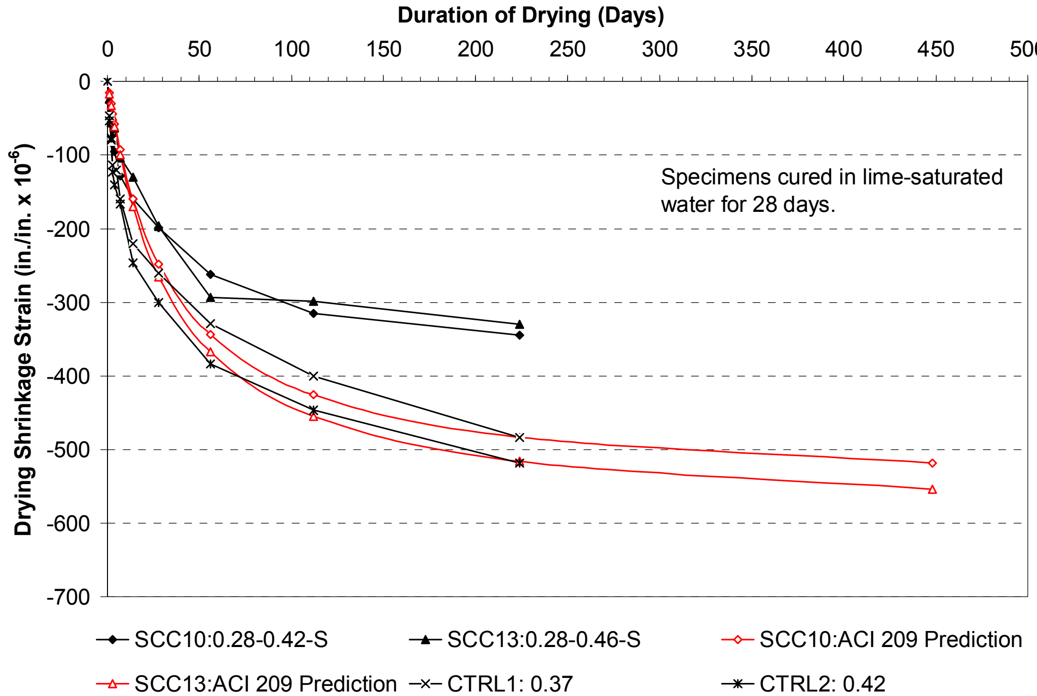

Figure D-23: Shrinkage development of slag mixtures with a *w/p* of 0.28

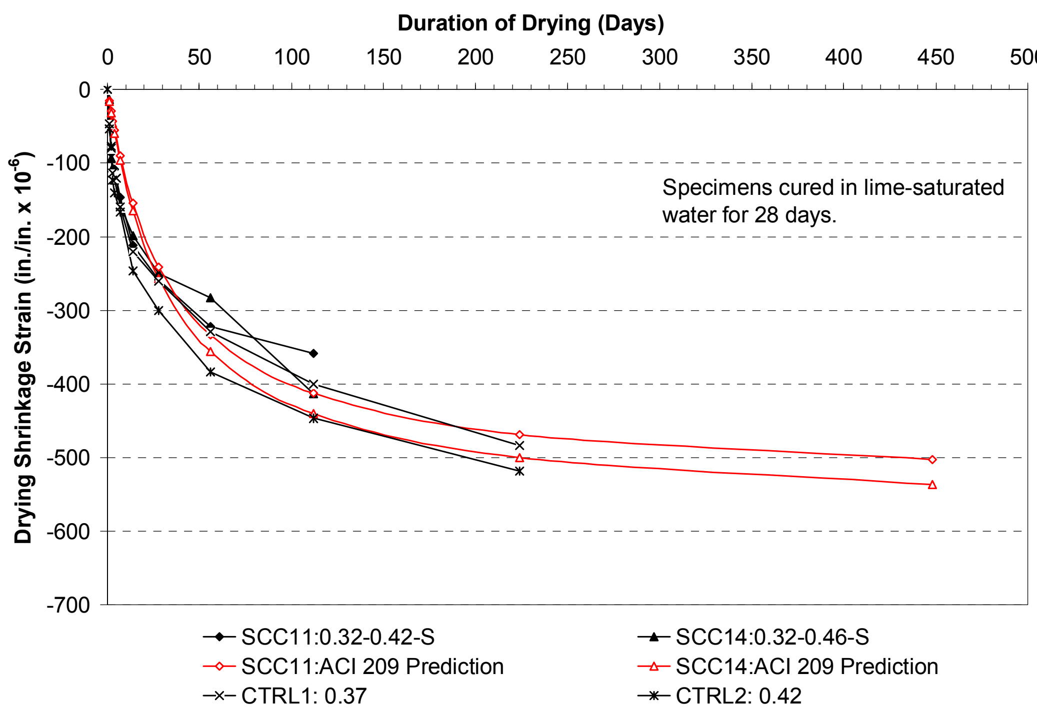

Figure D-24: Shrinkage development of slag mixtures with a *w/p* of 0.32

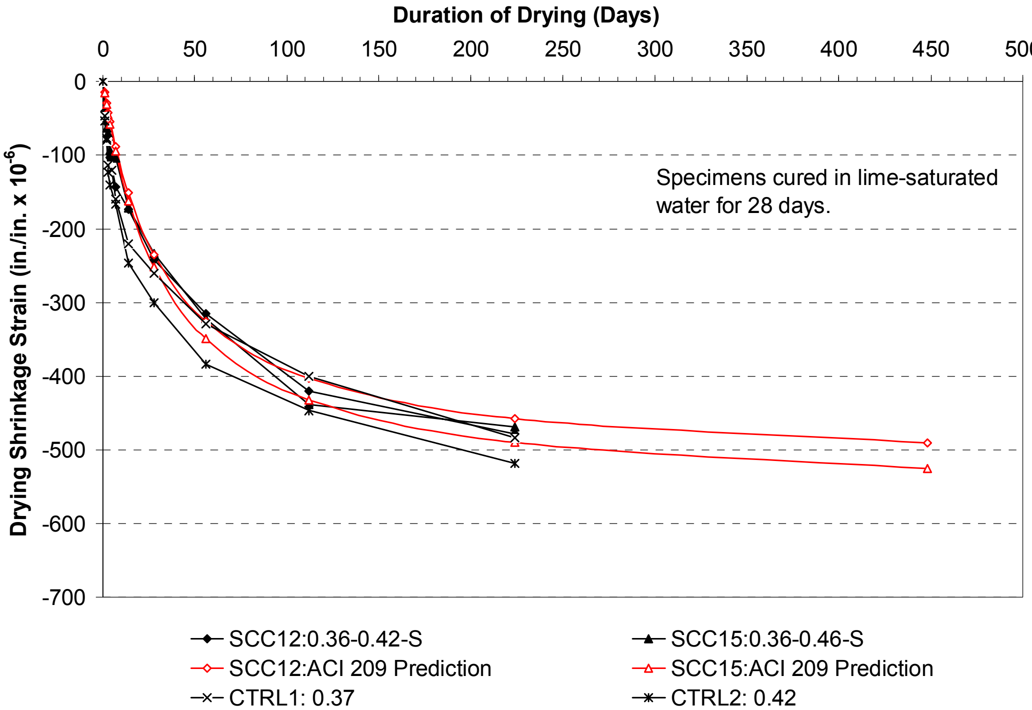

Figure D-25: Shrinkage development of slag mixtures with a *w/p* of 0.36

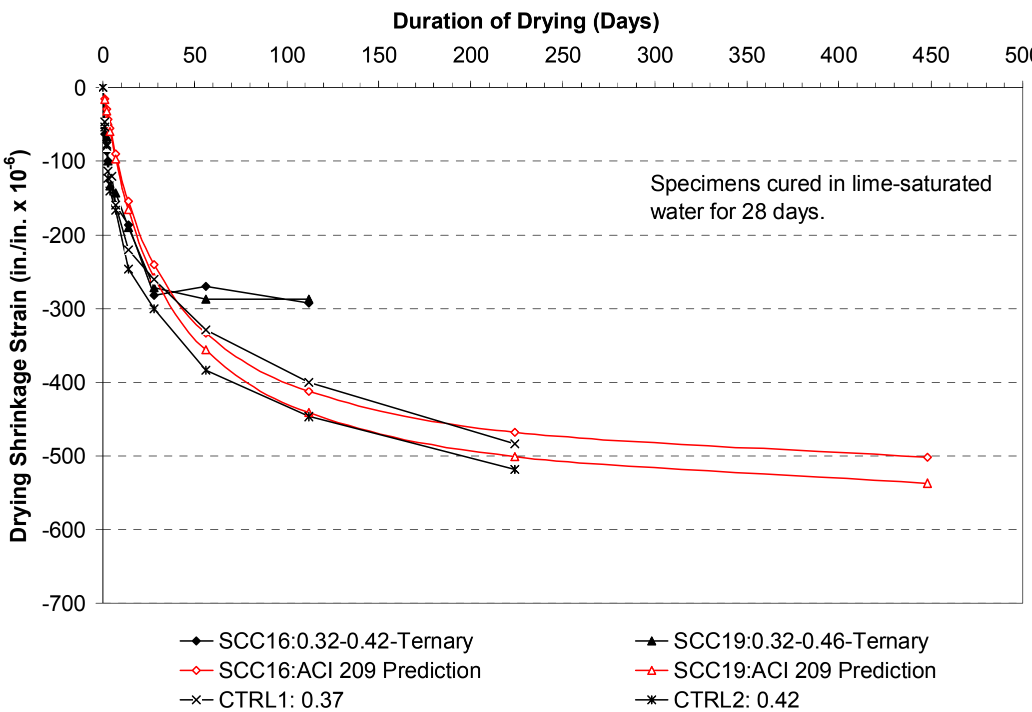

Figure D-26: Shrinkage development of ternary mixtures with a *w/p* of 0.32

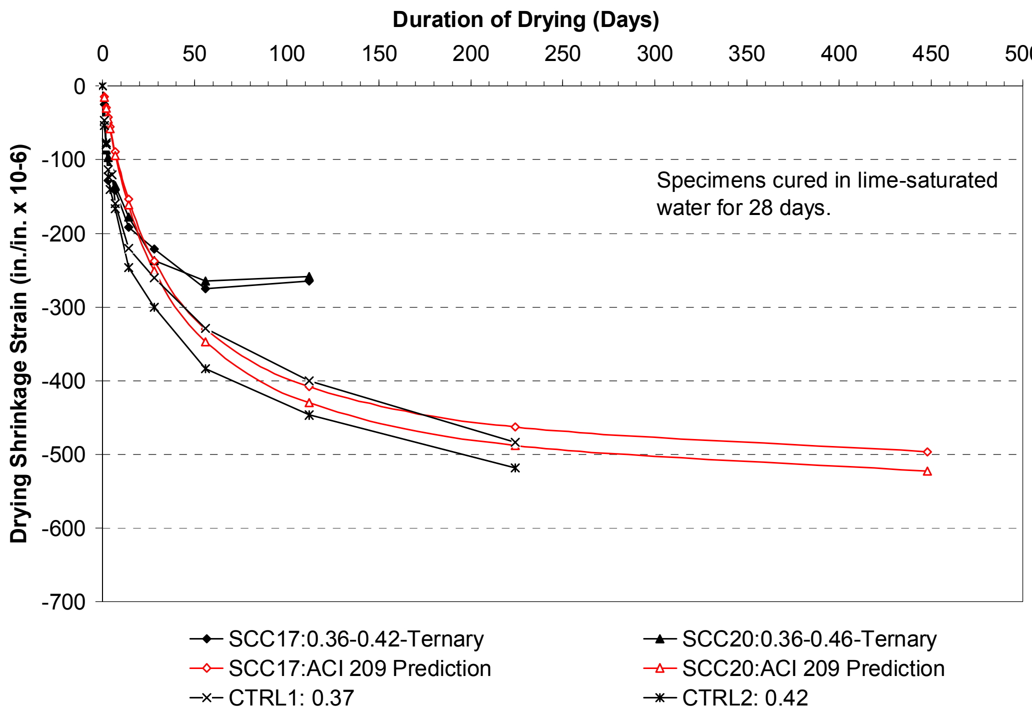

Figure D-27: Shrinkage development of ternary mixtures with a *w/p* of 0.36

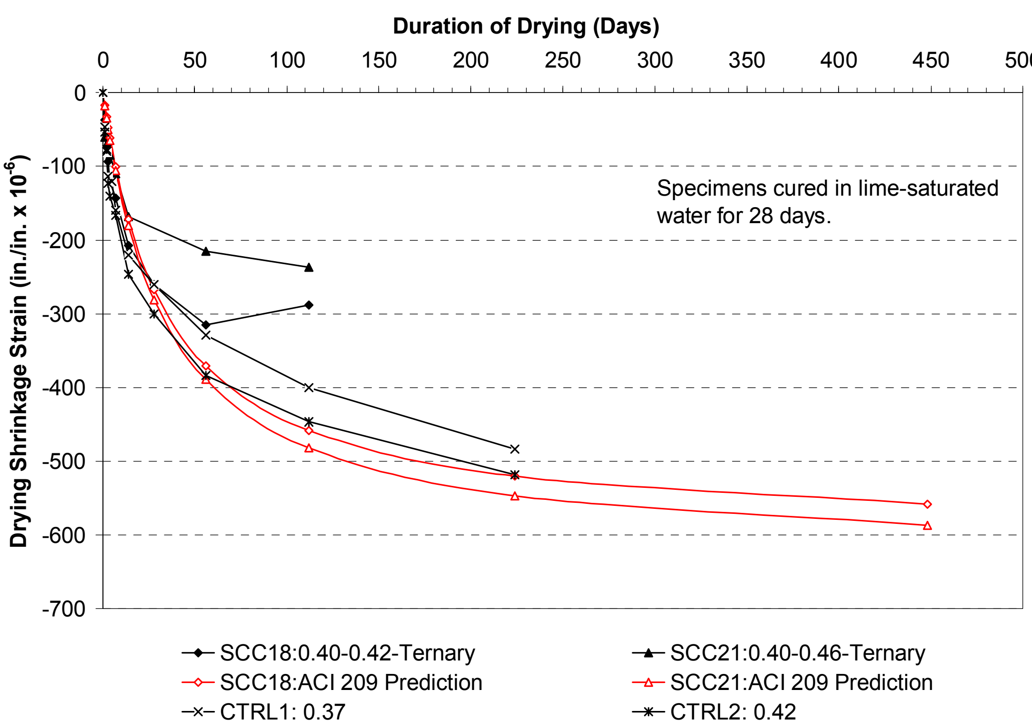

Figure D-28: Shrinkage development of ternary mixtures with a *w/p* of 0.40

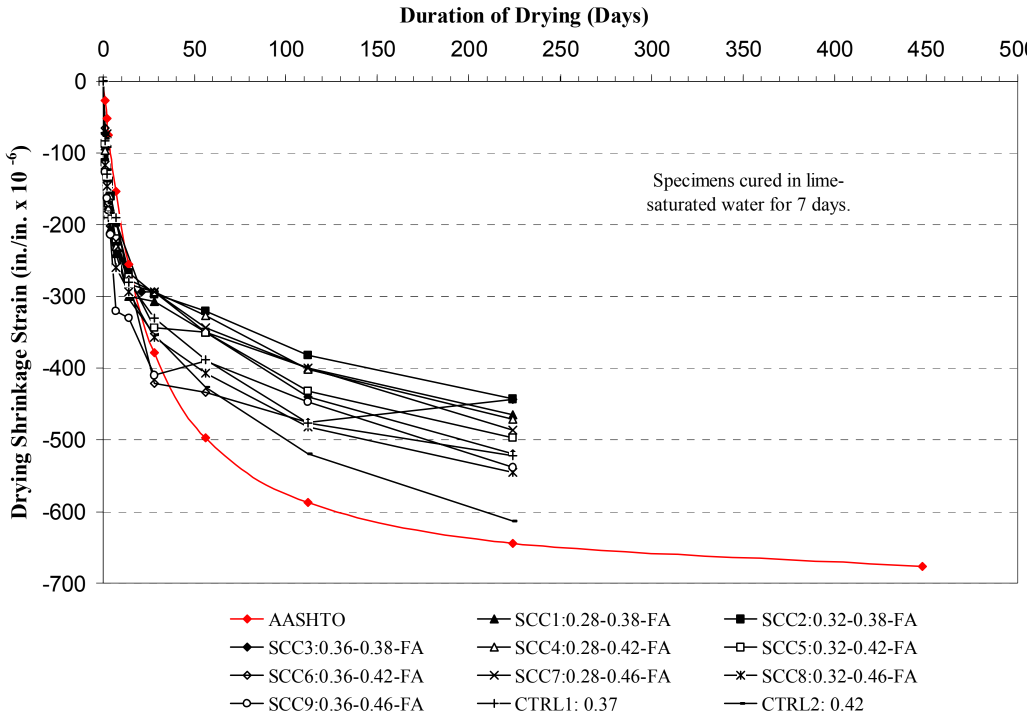

Figure D-29: Shrinkage development of fly ash mixtures versus AASHTO prediction

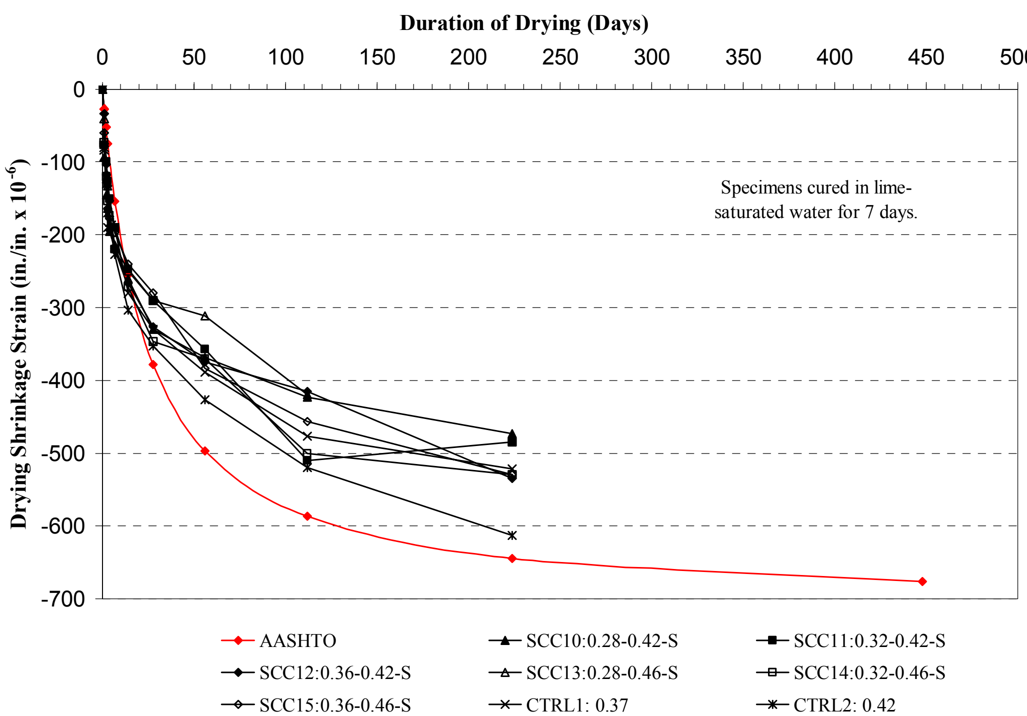

Figure D-30: Shrinkage development of slag mixtures versus AASHTO prediction

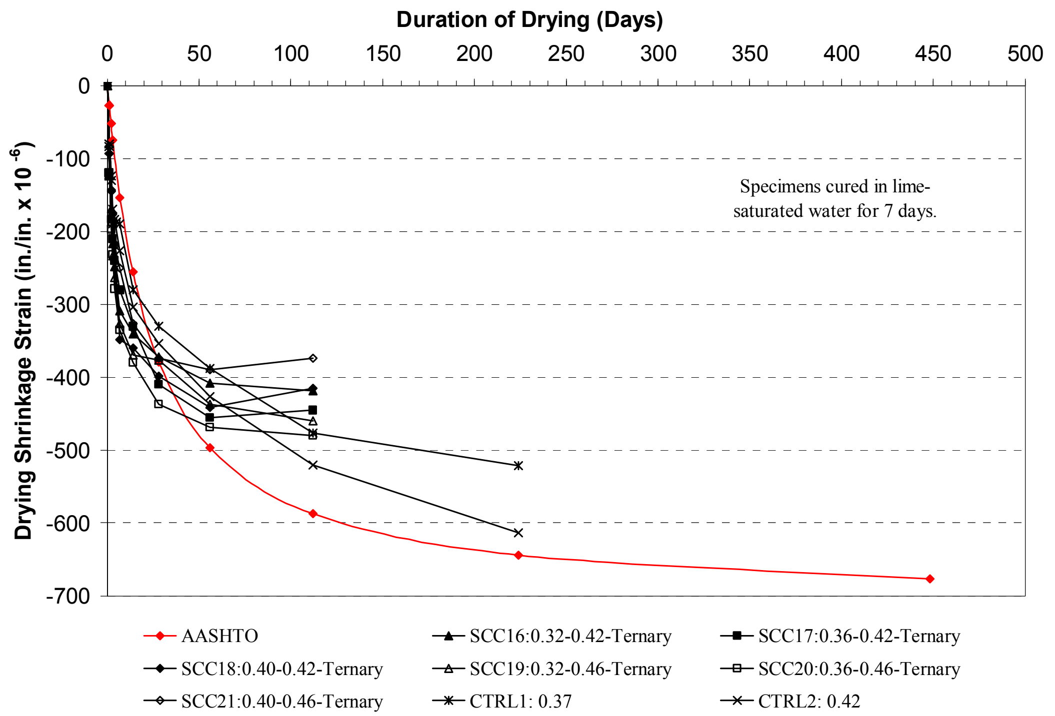

Figure D-31: Shrinkage development of ternary mixtures versus AASHTO prediction

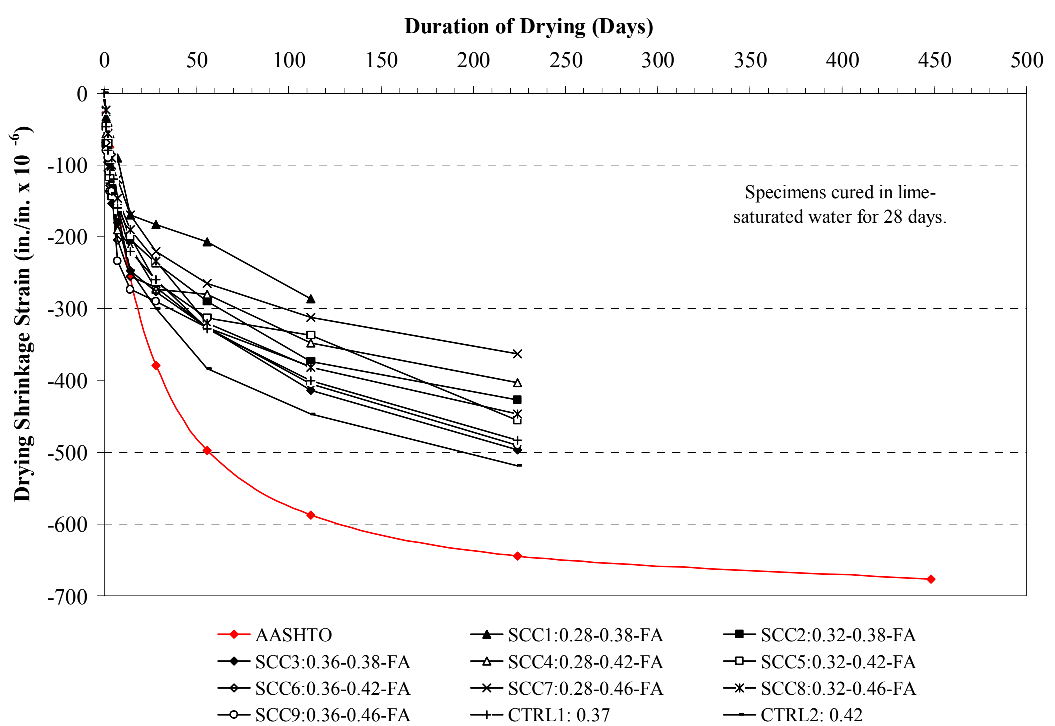

Figure D-32: Shrinkage development of fly ash mixtures versus AASHTO prediction

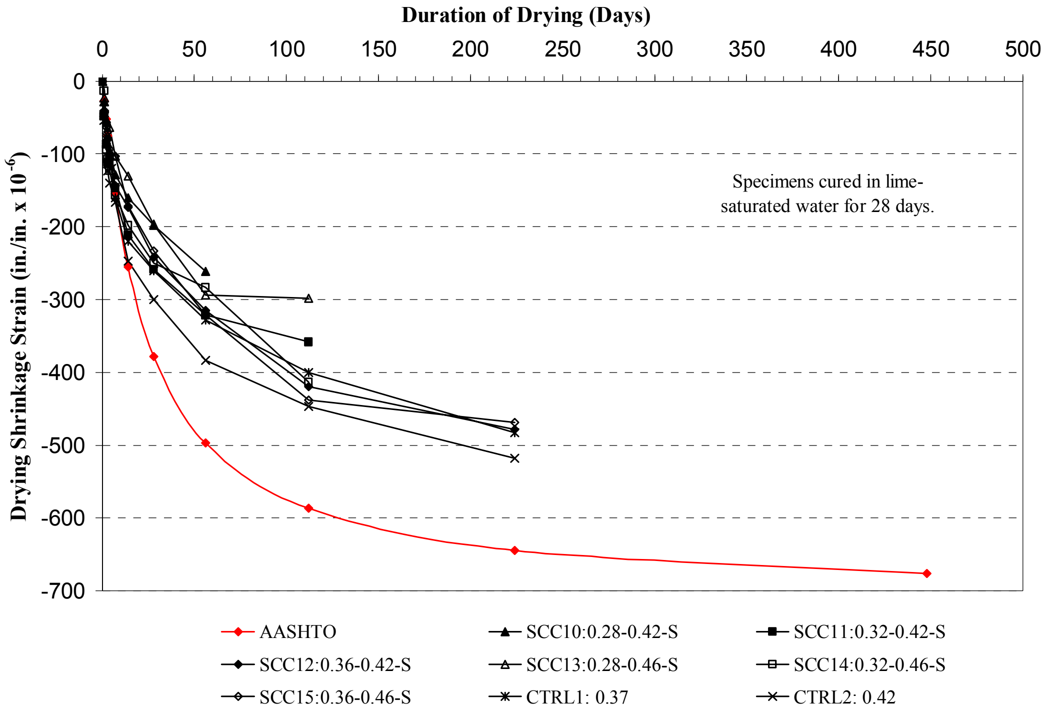

Figure D-33: Shrinkage development of slag mixtures versus AASHTO prediction

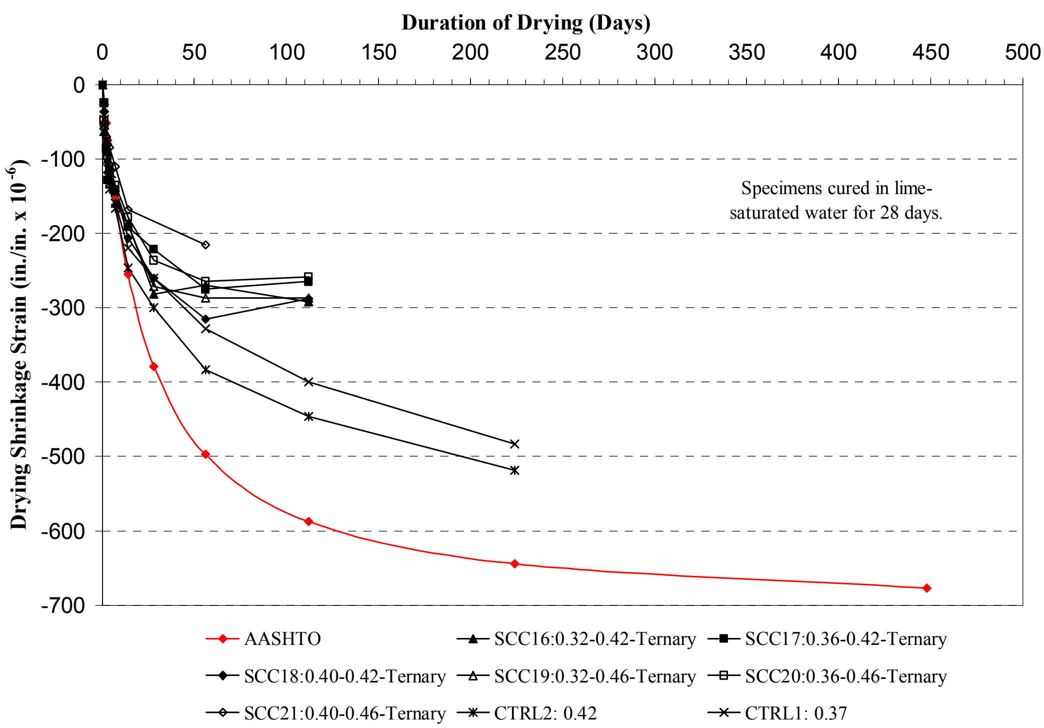

Figure D-34: Shrinkage development of ternary mixtures versus AASHTO prediction